DETECTION OF AEROBIC BACTERIAL ENDOSPORES: FROM AIR SAMPLING, STERILIZATION VALIDATION TO ASTROBIOLOGY

Thesis by

Pun To (Douglas) Yung

In Partial Fulfillment of the Requirements

for the Degree of

Doctor of Philosophy

California Institute of Technology

Pasadena, California

2008

(Defended May 9, 2008)

Acknowledgment

I would like to express my deepest gratitude to my thesis adviser, Dr. Adrian Ponce, for his guidance and support. It is due to his scholastic guidance and encouragement that ultimately made this work possible. I appreciate the time and attention of my committee members: Professor Morteza Gharib, Professor Scott Fraser, and Professor Changhuei Yang. Given their busy schedules, it has been kind of them to play a role in my course of study.

I owe my gratitude to all members of the Ponce Group who have made this dissertation possible, and because of them my graduate experience has been one that I will cherish forever. Elizabeth Lester has kindly introduced me to techniques in microbiology. Alan Fung has taught me principles in mechanical engineering and instrument design. I have enjoyed working with Elizabeth Lester, Alan Fung, Morgan Cable, Hannah Shafaat and Wanwan Yang. I would like express thanks to my summer undergraduate mentees, Wilson Sung, Christine Tarleton, and William Fan, who have contributed important pieces to my thesis work. I would like to acknowledge the other individuals who have contributed to the completion of this thesis: Dr. James Kirby, Dr. Xenia Amashukeli, Dr. Christine Pelletier, Raymond Lam, Dr. Michael Kempf, Michael Lee, Dr. Fei Chen, Dr. Anita Fisher, Dr. Steve Monacos, Dr. Stephanie Connon, and Dr. Donald Obenhuber.

I appreciate the support from the many reliable staff members working at JPL and Caltech, including Stacey Klinger, Robert Downer, Icy Ma, Steve Gould, Lillian Kremar, Joe Drew, Cora Carriedo, and Carlos Hernandez. Last but not least, I have to thank Linda Scott for being the most efficient professional in bioengineering. I would like to thank

Ray Pini, Amir Ettehdieh and Universal Detection Technology for helpful discussions. I thank Fei Chen for her help in a preliminary vaporized hydrogen peroxide experiment and access to the spacecraft assembly clean room. I thank Steris Corporation for preparing vaporized hydrogen peroxide treated-endospore strips.

I am also indebted to my friends and family for their continuous support, love and patience. Particularly, I would like to express my heartfelt gratitude to Jerry Ruiz and Karen Chan. I warmly appreciate the encouragement from Dr. Stephen Shum and Dr. James Tong from high school, college, to graduate school.

“The most beautiful and most profound emotion we can experience is the sensation of the mystical. It is the source of all true science. He to whom the emotion is a stranger, who can no longer wonder and stand rapt in awe, is as good as dead.”

Albert Einstein

Abstract

Bacterial endospores are formed in genera such as *Bacillus* and *Clostridium* in times of incipient stresses. Derivative of their remarkable resistance and ubiquity, endospores are delivery vehicles for anthrax attack, biological indicators for checking sterilization efficacy, and candidates for *Panspermia* and potential extraterrestrial life, thereby underscoring the significance of their rapid detection. In this thesis project, spectroscopy and microscopy methods are studied to measure the release of a unique constituent, dipicolinic acid (DPA), *via* germination as a proxy for endospore viability. In particular, a luminescence time-gated microscopy technique (called microscopy endospore viability assay, acronym: μEVA) has been developed to enumerate germination-capable aerobic endospores rapidly based on energy transfer from DPA to terbium ions doped on a solid matrix upon UV excitation. The distinctive emission and millisecond lifetime enable time-resolved imaging to achieve a sensitivity of one endospore.

Effective air sampling of endospores is crucial in view of the potential catastrophe caused by the dissemination of airborne anthrax endospores. Based on time-gated spectroscopy of terbium-DPA luminescence, the Anthrax Smoke Detector has been built to provide real-time surveillance of air quality for timely mitigation and decontamination. This technology also finds application in the monitoring of airborne endospore bioburden as an indicator of total biomass in a closed spacecraft system in order to safeguard the health of astronauts.

Sterilization validation is of prime concern in the medical field and planetary protection to prevent cross-contaminations among patients and planets. μEVA has yielded faster and comparable results compared with the culture-based NASA standard assay in

assessing surface endospore bioburden on spacecraft materials and clean rooms surfaces. The current analysis time has been expedited from 3 days to within an hour in compliance with planetary protection requirements imposed on landers and probes designed for life detection missions.

From the perspective of astrobiology, endospores are time capsules preserving geological history and may exist as dormant lives in analogous extraterrestrial environments. μEVA has successfully recovered ancient endospores in cold biospheres (Greenland ice core, Antarctic Lake Vida, polar permafrost) and hyper-arid biospheres (Atacama Desert) on Earth as templates for determining life longevity and the search of extinct or extant life on Mars and other icy celestial bodies. Result authenticity has been validated by a comprehensive suite of experiments encompassing culture-based and culture-independent techniques such as epifluorescence microscopy, flow cytometry, fluorometry, bioluminescence and 16s rRNA analysis. In conclusion, μEVA is a sensitive analytical tool that opens a new realm in microbiology to provide insights into air sampling, sterility assessment and exobiology.

Table of contents

ACKNOWLEDGMENT iii
ABSTRACT vi
TABLE OF CONTENTS viii
LIST OF FIGURES xv
LIST OF TABLES xviii

CHAPTER 1: INTRODUCTION 1

1.1 INTRODUCTION 1
1.2 LIFE CYCLE OF AN SPORE-FORMING BACTERIA 5
1.3 DPA-TRIGGERED TERBIUM PHOTOLUMINESCENCE ASSAY 7
1.4 OUTLINE OF THESIS 10
1.5 REFERENCES 16

CHAPTER 2: REVIEW OF ENDOSPORE DETECTION TECHNOLOGY 21

2.1 ABSTRACT 21
2.2 INTRODUCTION 21
2.3 BIOMARKER METHODS 24
2.3.1 Calcium dipicolinate 25
2.3.2 Dipicolinic acid 27
2.3.3 DNA 31
2.4 OPTICAL PROPERTY AND STAINABILITY 34
2.4.1 Direct epifluorescent filtration technique 34
2.4.2 Coulter counter 35
2.4.3 Method of Schaeffer and Fulton 35
2.4.4 Phase contrast microscopy 36
2.4.5 Electron microscopy 38
2.4.6 Flow cytometry 38
2.5 METABOLISM 39
2.5.1 Impedance measurement 39
2.5.2 Microcalorimetry 40
2.5.3 ATP firefly luciferin-luciferase assay 40
2.6 BIOCHEMICAL TESTS 44
2.7 COLONY FORMATION 46
2.7.1 Culturing (plate count and most probable number) 47
2.7.2 Turbidity measurement 47

2.8 Spore coat 48
2.8.1 Immunoassay + Flow cytometry *49*
2.8.2 Immunofluorescence resonance energy transfer *49*
2.9 Spore detection instruments 50
2.10 Conclusion 54
2.11 References 55

CHAPTER 3: AN AUTOMATED FRONT-END MONITOR FOR ANTHRAX SURVEILLANCE SYSTEMS BASED ON THE RAPID DETECTION OF AIRBORNE ENDOSPORES 61

3.1 Abstract 61
3.2 Introduction 62
3.3 Materials and Methods 64
3.3.1 Chemicals *64*
3.3.2 Biological samples *65*
3.3.3 Anthrax Smoke Detector *65*
3.3.4 Spectrometry *66*
3.3.5 Simulated anthrax attack *67*
3.4 Results 68
3.4.1 Spectrometer time-gated performance *69*
3.4.2 Quantification of DPA and spores in water *69*
3.4.3 ASD response to simulated anthrax attack *70*
3.5 Discussion 71
3.6 Conclusion 73
3.7 References 74

CHAPTER 4: AIRBORNE ENDOSPORE BIOBURDEN AS AN INDICATOR OF SPACECRAFT CLEANLINESS 82

4.1 Abstract 82
4.2 Introduction 82
4.3 Methods and Procedure 85
4.3.1 Chemicals *85*
4.3.2 Microbiological samples *85*
4.3.3Microbial Event Monitor *86*
4.3.4 Air Sample Collection *87*
4.3.5 Determination of total biomass *88*

4.3.6 Correlating airborne and total biomass in a laboratory controlled environment *90*
4.3.7 Correlating airborne and total biomass in indoor and outdoor environemnts *91*
4.3.8 Comparison of biofilm-forming environmental isolate with lab-strain B. subtilis *92*
4.3.9 Data Analysis *93*
4.4 RESULTS 94
4.4.1 Comparison test of 3 different air samplers *94*
4.4.2 Aerosolized biofilm endospore testing in the laboratory *94*
4.4.3 Correlation of airborne and surface endospores in a closed laboratory environment *95*
4.4.4 Correlation of AEB and total biomass in indoor environments *96*
4.4.5 Correlation of AEB and total biomass in outdoor environments *97*
4.4.6 Comparison of biofilm-forming environmental-strain B. subtilis and lab-strain B. subtilis endospores *98*
4.5 DISCUSSION 98
4.6 CONCLUSION 102
4.7 REFERENCES 103

CHAPTER 5: RAPID STERILIZATION ASSESSMENT BY MONITORING INACTIVATION OF GERMINABLE *BACILLUS* ENDOSPORES 114

5.1 ABSTRACT 114
5.2 INTRODUCTION 114
5.3 METHODS 117
5.3.1 Chemicals *117*
5.3.2 Preparation of endospore stock suspension *117*
5.3.3 Sample Preparation for μEVA experiments *118*
5.3.4 The μEVA instrument *119*
5.3.5 Endospore germination and germinable endospore assignment *119*
5.3.6 Phase contrast microscopy for measuring total endospore concentration *120*
5.3.7 Inactivation experiments *120*
5.3.8 Statistical analysis *121*
5.3.9 Spectroscopy *122*
5.4 RESULTS 123
5.4.1 Monitoring single endospore germination dynamics *123*
5.4.2 Sensitivity, dynamic range, and false positive rate *124*
5.4.3 Monitoring thermal and UV sterilization of Bacillus atrophaeus endospores *125*
5.5 DISCUSSION 126
5.6 REFERENCES 129

CHAPTER 6: TIME-GATED LUMINESCENCE MICROSCOPY OF SURFACE BACTERIAL SPORES AS A RAPID BIOBURDEN ASSESSMENT OF SPACECRAFT HARDWARE AND ASSEMBLY ENVIRONMENTS 140

6.1 Abstract 140
6.2 Introduction 141
6.3 Methods 143
6.3.1 Chemicals 143
6.3.2 Preparation of endospore stock suspension 144
6.3.3 Coupon cleaning and inoculation 144
6.3.4 Swab-rinse method 145
6.3.5 NASA Standard Assay 147
6.3.6 Sample preparation for μEVA experiments 147
6.3.7 The μEVA instrument 148
6.3.8 Endospore germination and assignment 149
6.3.9 Viability ratio 150
6.3.10 Surface sampling and NASA standard assay 150
6.3.11 Vaporized hydrogen peroxide inactivation 151
6.3.12 Oxygen plasma inactivation study 152
6.3.13 Clean room sampling 152
6.3.14 Statistical analysis 152
6.4 Results 153
6.4.1 Surface sampling of pure spore suspension on metal coupons 154
6.4.2 Surface sampling of endospores in a spacecraft assembly cleanroom 155
6.4.3 Monitoring of endospore inactivation to vaporized hydrogen peroxide 155
6.4.4 Monitoring of endospore inactivation to oxygen plasma 156
6.5 Discussion and Conclusion 156
6.6 References 160

CHAPTER 7: METHOD DEVELOPMENT FOR ASTROBIOLOGIAL EXPLORATION 168

7.1 Abstract 168
7.2 Sporulation of psychrophilic endospores 168
7.2.1 Introduction 169
7.2.2 Methods 171
7.2.3 Results 177
7.2.4 Discussion 180

7.2.5 Conclusion *183*
7.3 MICRO- AND MACRO-GERMINATION KINETICS 183
7.3.1 Introduction *184*
7.3.2 Methods *187*
7.3.3 Results *195*
7.3.4 Conclusion *198*
7.4 METHODS TO INCREASE CULTURABILITY 199
7.4.1 Introduction *199*
7.4.2 Methods *201*
7.4.3 Results *204*
7.4.4 Discussion *206*
7.5 REFERENCES 208
CHAPTER 8: ENDOSPORES IN COLD BIOSPHERE 222
8.1 ABSTRACT 222
8.2 INTRODUCTION 223
8.3 MATERIALS AND METHODS 230
8.3.1 Materials *230*
8.3.2 Validation of ice core decontamination protocol *231*
8.3.3 GISP2 ice core handling *231*
8.3.4 Permafrost handling *234*
8.3.5 Ice core analysis using spectroEVA *235*
8.3.6 Ice core analysis using μEVA *237*
8.3.7 Ice core cultivation *239*
8.3.8 Lake Vida Cultivation *241*
8.3.9 Permafrost cultivation *242*
8.3.10 Permafrost metabolic study *243*
8.3.11 Fluorescence microscopy *245*
8.3.12 Phase contrast microscopy *247*
8.3.13 Method of Schaeffer and Fulton *248*
8.3.14 Flow cytometry *249*
8.4 RESULTS 250
8.4.1 Validation of ice core decontamination protocol *251*
8.4.2 Ice core SpectroEVA *251*
8.4.3 Ice core μEVA *255*
8.4.4 Ice core microscopy and flow cytometry *256*
8.4.5 Ice core cultivation *257*

8.4.6 Lake Vida analysis *258*
8.4.7 Permafrost analysis *260*
8.5 DISCUSSION 264
8.5.1 Comparison of spectroEVA and μEVA at 295-m depth *266*
8.5.2 Viability assessment at 295-m depth *266*
8.5.3 Towards endospore longevity experiments *268*
8.5.4 Our results in the context of literature reports *276*
8.5.5 Insights from Lake Vida analysis *277*
8.5.6 Insights from permafrost analysis *278*
8.6. CONCLUSION 280
8.7 REFERENCES 282

CHAPTER 9: ENDOSPORES IN HYPER-ARID BIOSPHERE 309

9.1 ABSTRACT 309
9.2 INTRODUCTION 310
9.3 METHODS 315
9.3.1 Materials *315*
9.3.2 Soil sampling *315*
9.3.3 Air sampling *316*
9.3.4 Resistance experiment *317*
9.3.5 Water augmentation experiment *317*
9.3.6 Measure of soil water activity, pH, E_H, eC and temperature in field *318*
9.3.7 Anion exchange chromatography *319*
9.3.8 Total organic carbon (TOC) measurement *319*
9.3.9 Phospholipid fatty acid (PLFA) analysis *319*
9.3.10 Radioactive carbon dating *319*
9.3.11 Cell extraction from soils *320*
9.3.12 Cultivation *321*
9.3.13 μEVA *324*
9.3.14 SpectroEVA *325*
9.3.15 Extraction of DPA *327*
9.3.16 ATP measurement *328*
9.3.17 Microscopic enumeration *329*
9.3.18 Ecology study and strain identification *330*
9.3.19 Sporulation *331*
9.3.20 Spore size measurement *332*
9.3.21 Hydrophobicity *332*

9.3.22 Germination *333*
9.3.23 UV inactivation *334*
9.4 Results & Discussion 335
9.4.1 Spatial and temporal heterogeneity in Site A and Site E *336*
9.4.2 Water augmentation *340*
9.4.3 Air sampling *342*
9.4.4 Depth profile *343*
9.4.5 Determination of DPA by terbium dipicolinate fluorescence assay *345*
9.4.6 Other interesting sampling locations *345*
9.4.7 Ecological Study *347*
9.4.8 Germination model *348*
9.4.9 Germinability and culturability between lab strains and environmental strains *350*
9.4.10 Role of DPA on spore resistance *352*
9.4.11 Inheritance of properties in spores *353*
9.5 Conclusion 354
9.6 References 358

CHAPTER 10: CONCLUSION 389

10.1 Development of Automated Bacillus Spore Viability Instrumentation for Sterilization Validation, Biodefense and Astrobiology 390
10.1.1 Statement of problem *391*
10.1.2 Background and relevancy to previous work *393*
10.1.3 General methodology and procedures to be followed *395*
10.1.4 Proposed work *396*
10.1.5 Expected results *402*
10.1.6 Significance and application *402*
10.2 Development of a Rapid Endospore Detector 405
10.2.1 Statement of problem *406*
10.2.2 Background *407*
10.2.3 General methodology *410*
10.2.4 Expected results *418*
10.2.5 Conclusion *421*
10.3 References 422

List of figures

Figure 1.1 Images of endospores *18*
Figure 1.2 Life cycle of an endospore-forming bacterium *19*
Figure 1.3 Photochemistry of Tb-DPA luminescence assay *20*
Figure 2.1 Energy transition of the metal-to-ligand charge transfer between DPA and Fe^{2+} *59*
Figure 2.2 Comparison of Anthrax Smoke Detector and PCR detection system *60*
Figure 3.1 Energy transfer and Stokes shift of Tb-DPA luminescence assay *76*
Figure 3.2 Instrument prototype of the Anthrax Smoke Detector (ASD) *77*
Figure 3.3 Filter set transmittance spectra of the ASD time-gated spectrometer *78*
Figure 3.4 Dose response of the ASD spectrometer to pure DPA *79*
Figure 3.5 Comparison of the ASD spectrometer performance on pure DPA and heat-treated endospores *80*
Figure 3.6 ASD measurement of a simulated anthrax attack *81*
Figure 4.1 Operating principles of different air samplers *105*
Figure 4.2 Bioefficiency comparison of different air samplers *106*
Figure 4.3 Correlation of airborne and surface endospores in a laboratory-controlled closed system *107*
Figure 4.4 Correlation of airborne and surface endospores in everyday environments *108*
Figure 4.5 Air sampling measurement as a timecourse of resident activity tested in the Marshall Space Flight Center *109*
Figure 4.6 Air sampling in the Atacama Desert, Chile *110*
Figure 4.7 Phase contrast micrograph of the sporulating culture of a biofilm-forming spore-former isolated from Mojave Desert, CA *111*
Figure 4.8 A 2-compartmental model describing the dynamics between airborne and total biomass in a closed system *112*
Figure 5.1 Instrument prototype and principle of µEVA *131*
Figure 5.2 Germination timecourses monitored by refractility loss and DPA release *133*
Figure 5.3 Comparison of the detection of low concentration of endospores (< 50 cfu mL^{-1}) using µEVA and a culture-based method *134*
Figure 5.4 Monitoring of the culturability and germinability loss of during heat inactivation and UV irradiation experiments *135*
Figure 5.5 Single endospore germination of lab-strain and environmental endospores *136*
Figure 5.6 Excitation spectrum of pure DPA and germinating spores measured at front face configuration on an agarose substrate *137*

Figure 5.7 Comparison of μEVA and TSA plating at high endospore concentration regimes *138*
Figure 5.8 Comparison of spectroEVA and μEVA *139*
Figure 6.1 Spectral overlap of Tb-DPA luminescence spectra with the experimnetal filter set in the ASD spectrometer *162*
Figure 6.2 Flowchart illustration of the NASA standard assay procedure *163*
Figure 6.3 Recovery of endospores from coupons surface *164*
Figure 7.1 Phase contrast images of psychrophilic endospore-forming bacteria *212*
Figure 7.2 Recovery of endospores from coupon surface *213*
Figure 7.3 Determination of optimal heat-shock temperature for screening mesophilic and psychrophilic endospores from a mixed endospore population *214*
Figure 7.4 Thermal inactivation curves of typical mesophilic and psychrophilic endospores *215*
Figure 7.5 Single endospore germination of B. subtilis fitted to a model based on a rectangular pulse approximation *216*
Figure 7.6 Characterization of the microgermination model parameters of lab-strain and environmental-strain endospores *217*
Figure 7.7 Effectiveness of a stochastic model in modeling macrogermination kinetics *218*
Figure 7.8 Effect of germinant incubation in the enhancement of endospore culturability *219*
Figure 8.1 Validation of ice core decontamination protocol using a fabricated ice core *287*
Figure 8.2 Ice core decontamination and handling procedure *288*
Figure 8.3 Permafrost decontamination procedure *289*
Figure 8.4 SpectroEVA results on ice cores (age = 295 yr) *290*
Figure 8.5 SpectroEVA results on ice cores (age = 20,000 yr) *291*
Figure 8.6 μEVA image and endospore germination timecourse in an ice core sample (age = 295 yr) *292*
Figure 8.7 Microscopy and flow cytometry analyses on ice cores *293*
Figure 8.8 SpectroEVA results on Lake Vida brine water *294*
Figure 8.9 Phase contrast micrograph of an aerobic subculture of Lake Vida sample – presence of two endospores in one mother cell *295*
Figure 8.10 Size distribution of endospores observed in Lake Vida *296*
Figure 8.11 Germination timecourse and μEVA time-lapse images of endospores found in permafrost *297*
Figure 8.12 Epifluorescence microscopy images of microorganisms found in permafrost *298*
Figure 8.13 Use of tetrazolium chloride to detect metabolic activities in a permafrost sample *299*
Figure 8.14 Monitoring of ATP and DPA levels of a permafrost sample over 7 days upon exposure to nutrients *300*

Figure 8.15 Viability Venn diagram *301*
Figure 8.16 Viability plots of 12 ice cores along a depth transect (from 295 yr to 110,000 yr) *302*
Figure 9.1 Comparison of microbial abundance of sites A & E based on heterotrophic cell counts in the Atacama Desert *372*
Figure 9.2 Measurement of in situ microbial response to water augmentation in the Atacama Desert *373*
Figure 9.3 Measurement of microbial response to water augmentation under simulated laboratory conditions *374*
Figure 9.4 Weather monitoring and air sampling in the Atacama Desert *375*
Figure 9.5 Culture-based, μEVA, TOC and PLFA analyses on 6 samples along a depth transect in a soil pit in the Atacama Desert *376*
Figure 9.6 Determination of germination-capable endospores in the Atacama Desert by μEVA *377*
Figure 9.7 Qualitative determination of DPA from Atacama soil samples using spectroEVA *378*
Figure 9.8 Comparison of spread plating and μEVA results across 30 different heat shocked Atacama Desert soil samples *379*
Figure 9.9 Hydrophobicity of lab-strain and environmental-strain endospores *384*
Figure 9.10 Kinetics of L-alanine-induced germination on lab-strain and environmental-strain endospores isolated from the Atacama Desert *385*
Figure 9.11 DPA density vs. spore volume across thermophilic, mesophilic and psychrophilic lab strains and environmental strains *386*
Figure 9.12 UV and heat inactivation plots of endospore isolated from the Atacama Desert *387*
Figure 9.13 Correlation of DPA density to thermal resistance and UV resistance across thermophilic, mesophilic and psychrophilic lab strains and environmental strains *388*
Figure 10.1 Photochemistry of Tb-DPA assay and μEVA instrumentation *425*
Figure 10.2 Prototype design of a portable μEVA instrument *426*
Figure 10.3 Germination timecourse of single B. atrophaeus endospores monitored by DPA release and refractility change *427*
Figure 10.4 Design of a high throughout biological indicator module *428*
Figure 10.5 96-well filtration unit *429*
Figure 10.6 Prototype design of a microfluidic chip encompassing different microbial detection assays *430*
Figure 10.7 Microfluidic implementation of the ATP luciferin-luciferase assay *431*

List of tables

Table 3.1 Bioefficiency comparison between different air samplers *113*
Table 6.1 μEVA and NASA standard assay sampling results in a class 100 clean room facility..... *167*
Table 7.1 Properties of laboratory-strain and environmental-strain psychrophilic endospores..... *220*
Table 7.2 Germination parameters of laboratory-strain and environmental-strain psychrophilic endospores..... *221*
Table 8.1 Summary of permafrost microbiological analysis data *304*
Table 8.2 Summary of GISP2 ice core, Lake Vida and permafrost analysis data *305*
Table 8.3 Summary of the viability ratios of GISP2, Lake Vida and permafrost samples *307*
Table 9.1 Physical measurements of the samples collected in the 2007 Atacama Desert expedition *364*
Table 9.2 Microbiological results on the Atacama Desert samples..... *368*
Table 9.3 Species list of endospores used in the ecology study *380*
Table 9.4 DPA content, resistance and germination properties of different endospores *382*

CHAPTER 1: INTRODUCTION

1.1 Introduction

Bacterial spore (i.e., endospore), discovered in 1876 by Cohn[1], Koch[2,3] and Tyndall[4] independently, is one of the hardiest dormant life forms on earth[5] formed during the resting stage in the life cycle of spore-forming genera such as *Bacillus*, *Clostridium, Sporosarcina* and others (Figure 1.1). They are formed within vegetative cells during sporulation, which is frequently triggered in response to adverse environmental changes. Spores are renowned for their resistance against deleterious agents and stresses, such as freezing, boiling, pressure, desiccation and attack by a wide variety of toxic molecules[6,7]. Spore DNA is protected from the environment by a surrounding spore coat comprised of calcium ions, dipicolinic acid and protein layers[8-10]. DPA (dipicolinic acid, 2,6-pyridinedicarboxylic acid) is a unique chemical found only in bacterial spores and can be released from the core into the surrounding by inducing germination (e.g., with L-alanine[11,12]) or physical lysing (e.g., autoclaving, microwaving[13]). With no detectable metabolism, bacterial spores can remain viable for many years[14]. Some controversial reports claim that spores entombed in a bee trapped in amber 25-40 million years ago have been revived[14], and an even more spectacular claim details the recovery of spores from 250-million-year-old halite

crystals[15]. The extreme resistance of bacterial spores has even been exploited to check the performance of autoclaves[16,17]. Once favorable conditions return, spores undergo germination and outgrowth to become vegetative cells that cause contaminations, food spoilage, diseases, etc. Owing to their high resistance to physical extremes, spores are ubiquitous and can be recovered from almost all extreme environments on Earth.

In this thesis, I will focus on the study of *Bacillus*, which is a genus of rod-shaped and Gram-positive bacteria under the Firmicutes division, with C + G values ranging from 32% - 62%. A majority of the *Bacillus* species are strict aerobes or facultative anaerobes producing endospores in the presence of oxygen. Several species, e.g., *B. infernus* and *B. arseniciselenatis*, are found to be strictly anaerobic[18,19]. A recent taxonomic reclassification has broken *Bacillus* into *Geobacillus*, *Paenibacillus*, *Lactobacillus*, etc. Most of the species are mesophilic with some psychrophiles and thermophiles. *Bacillus* species can be divided into three groups based on morphology of the sporangia.

Group I encompasses ellipsoidal or cylindrical endospores situated centrally to terminally in the progenitor mother cell with non-swollen sporangia. It contains most of the human pathogenic species including *B. anthracis*, the causative agent of anthrax, and *B. cereus*, causing food poisoning with symptoms similar to

staphylococcal food poisoning. A lot of benign soilborne endospores such as *B. subtilis* and *B. pumilis* are also found in this group. Group II is composed of ellipsoidal endospores situated centrally to terminally in a swollen sporangium. This group is mainly characterized by insect pathogens such as *B. larvae* and *B. lentimorbus* causing American foulbrood in honeybees and milky disease in Japanese beetle, respectively. Group III consists of spherical endospores situated sub-terminally to terminally in sporangia. Some of the psychrophilic *Bacillus* species are found in this group, notably *B. psychrophiles* and *B. longisporus*.

Spores are interesting subjects to study from both a scientific and application perspective. They are the ideal model for dormancy, resistance and survivability in the nature. They account for a large majority of the microbial flora on Earth and take up unique roles in homeland security, sterilization validation, and astrobiology.

Detection of pathogenic endospores has been an increasingly important issue in the safety and security of each country. Most of the *Bacillus* species are harmless soil-borne microorganisms. The most virulent species is *Bacillus anthracis*. Upon contact with animals, it can cause either cutaneous anthrax, inhalational anthrax or gastro-intestinal anthrax. Inhalational anthrax draws the most attention because of convenient airborne spore delivery and high lethal rate. The lethal dose at which 50% of an untreated exposed population would die (LD_{50}) from inhalational anthrax is

believed to be between 2,000 and 55,000 spores, with a nominal value of 8,000 to 10,000 spores. Accidental release of anthrax from a military compound in Chkalovsky, Russia in 1979 has led to the death of at least 70 people[20]. *B. anthracis* is undoubtedly the notorious bacteria causing national upheavals during the anthrax attack. In 2001 *B. anthracis* endospores have been weaponized in US postal offices to cause 22 inhalational anthrax cases, of which 5 people died. Spores entering lungs are carried by macrophages to the mediastinal lymph where they germinate, outgrow and produce lethal toxins. The incubation time (the time from the bioweapon exposure to the onset of the first symptom and disease) is 2 to 3 days for anthrax. Real-time detection of bioweapon release grants time and resources for emergency management to mitigate possible consequences, such as by appropriate medical care, limiting the spread of infection and timely decontamination.

Bacillus species are of great interests in sterilization control. *B. cereus* and *B. sphericus* survive and pasteurization and are the cause of milk coagulates. *B. thuringiensis* are natural insecticides. Residual endospores on spacecraft hardware surfaces after disinfection post potential jeopardy to the data collected from other planets. Understanding properties of endospores is important in preventing food spoilage and aids in NASA's objective in planetary protection.

Endospores are highly resilient dormant structures that can return to vegetative cells when favorable conditions are restored after exposure to radiation or temperature. Study of the viable number in endospores entombed in polar ices, suspended in frozen lakes and embedded in permafrost provides clues for determining long-term viability.

1.2 Life cycle of a spore-forming bacteria

Endospores can lay dormant for long periods and remain viable, even while exposed to harsh environmental conditions. When more favorable conditions are signaled by the presence of water, nutrients, and germinants, endospores may break dormancy and germinate to become metabolically active and multiply. Figure 1.2 outlines the life cycle of an endospore-forming bacterium. As an endospore proceeds through germination toward cell division, there are various stages, including spore activation, stage I germination (during which DPA is released and water rehydrates the spore), stage II germination (during which cortex hydrolysis occurs and metabolism begins), and finally outgrowth (during which cell division occurs)[21]. Each of these stages in the life cycle of endospore-forming organisms can be observed with the experimental techniques described below. Certainly outgrowth, manifested as visible colonies on growth media, is the most direct measurement of endospore viability. However, colony formation requires approximately 20 cycles of replication over several days of

incubation before the colony becomes visible, and is therefore not amenable for rapid endospore viability analysis. In contrast, observation of water influx with phase contrast microscopy, DPA release with Tb-DPA luminescence assays, and ATP production with the luciferin-luciferase bioluminescence assays provide rapid measures of endospore viability, since these events occur much earlier in the germination to outgrowth pathway.

The life cycle of endospore-forming bacteria comprises 3 different processes: vegetative growth, sporulation and germination. Vegetative growth occurs when nutrients are available and is characterized by cells growing logarithmically by symmetric fission. When nutrients become limiting, these bacteria might initiate the sporulation process. However, sporulation is not the only developmental option for the vegetative cell that can also follow diverse routes, expressing genes needed for general adaptation to adverse conditions, or genes needed to scavenge alternative nutrients and to increase competitiveness against other species that are using the same scarce energy resources. In such conditions various proteases and degradative enzymes (amylases, xylanases, cellulases, etc.), alternate chemotaxis pathways, different antibiotics and transport functions are expressed and/or activated. Some cells become competent for uptake of exogenous DNA, which is introduced into the

recipient's chromosome and may confer selective advantages to future generations living under adverse conditions.

1.3 DPA-triggered terbium photoluminescence assay

DPA-triggered terbium photoluminescence assay forms the basis of spore detection in my research. Tb^{3+} is a lanthanide ion, which is characterized by sharp and narrow emission bands, as well as a millisecond-long excited state lifetime (Figure 1.3). The native luminescence of Tb^{3+} is very weak attributed to its low oscillatory strength ($\approx 10^{-6}$) of the excitation bands[22]. The binding of a chelate, such as DPA, to Tb^{3+}, when excited with UV light, can transfer energy to the emissive state of Tb^{3+}, leading to great emission intensity enhancement (> 20,000 times)[23]. The original Tb^{3+} excitation spectrum (λ_{ex} = 270 nm) will be changed to a characteristic dual-peak spectrum (λ_{ex} = 273, 279 nm) upon complexation with DPA.

The valence 4*f* electrons of Tb^{3+} are rarely involved in bonding because they are shielded by the outer core 5*s* and 5*p* electrons. When Tb^{3+} absorbs a photon or is otherwise supplied with a sufficient quantum of energy, it reaches an electronically excited state. The low ligand-field splitting of the Tb^{3+} *f* electrons results in poor nonradiative electronic transitions generally. The only significant nonradiative deactivation of the emissive state of Tb^{3+} is through the O-H vibrations of coordinated

water molecules. This also explains why the lesser number of water molecules coordinated the higher the lifetime Tb^{3+} or terbium chelate can attain. Energy lose *via* radiative transition, with the emission of a photon as the electron transfer back into its lower energy orbital, is known as fluorescence. These *f-f* transitions are, nevertheless, Laporte forbidden because there is no change in parity. This results in Tb^{3+} absorption and emission spectra being consisting of sharp and narrow bands, low molar absorption coefficients in the near-UV and visible ranges (ε typically between 0.01 and 3 $M^{-1} cm^{-1}$), as well as a millisecond-long luminescence lifetime. Therefore, Tb^{3+} exhibits a very weak emission upon direct near-UV excitation.

Absorption of photons, optimally in the UV range, promotes DPA from ground state to a vibrationally excited singlet state. This excited singlet can lose its excess energy by both radiative and nonradiative decay. Upon complexation with DPA, the photophysical properties of Tb^{3+} are slightly perturbed owing to the well-shielded 4*f* electrons. Sensitized luminescence can be observed due to energy transfer from the lowest-lying DPA triplet excited state to the emissive $^5D_4$ state of Tb^{3+}. DPA acts as a light harvesting antenna to receive UV excitation and then transfers the energy to Tb^{3+}. Because the energy gap between the Tb^{3+} ground state and emissive states is very large (20,500 cm^{-1}), the luminescence enhancement is very significant according to the energy gap law.

DPA is thermodynamically and kinetically stable, thereby avoiding high energy oscillator in the first coordination sphere. It also has a matched electronic transition levels with Tb^{3+}, in which an efficient intersystem crossing is possible due to $\Delta E(^1\pi\,\pi^* - {}^3\pi\,\pi^*) \approx 5000\ cm^{-1}$, demonstrating a large conjugated π electron system. In additional to this, the energy difference, $\Delta E(^3\pi\,\pi^* - {}^5D_J) \approx 2500 - 3500\ cm^{-1}$, is well above the $^5D_4$ state of Tb^{3+} so that back transfer onto DPA triplet state is not possible.

Another favorable feature of Tb^{3+} is its retention in atomic properties upon ligand binding due to its well-shielded 4*f* electrons. Only minimal changes are observed in the emission spectra of Tb^{3+}. Therefore, sensitized luminescence turn-on can readily be observed by an up shift in the fluorescence spectra. Besides, excitation spectrum of the sensitized terbium luminescence will mimic the excitation spectrum of DPA energy donor moieties. This provides a basis for the distinctive identification of the ligand responsible for the sensitization. In the case of DPA, a characteristic split in the excitation spectrum is observed.

Background and autofluorescence signals are usually rapidly decaying processes with lifetimes on the timescale of 1 – 100 nanoseconds[24]. Terbium dipicolinate has a lifetime in the range of milliseconds[25,26]. Therefore, when excited by UV, the emitted Tb-DPA intensity can be observed without interference from autofluorescence and scattering light, resulting in a substantial increase in detection

sensitivity. Delayed luminescence intensity can thus be measured with a pulsed UV excitation, xenon flashlamp or laser, with minimal background interference.

1.4 Outline of thesis

Brooks *et al.* defined indicators as "measures, variables, or indices that represent or mimic either the structure or function of ecological processes and systems across a disturbance gradient[27]." In this thesis work, I evaluate the effectiveness of bacterial endospore as a biological indicator to characterize, track and predict changes in indoor air quality, spacecraft bioburden level, and extreme ecosystems on Earth. Specifically, this goal is achieved *via*: (1) development of new spectroscopy and microscopy methods to detect aerobic endospores; (2) application of culture-based and culture-independent methods to study endospores under various habitats. **Chapter 2** is a literature review of endospore detection methods, with a general introduction to culture-based and culture-independent techniques. I have emphasized on detection tools that are relevant to subsequent chapters. The rest of this thesis can be divided into 3 modules, namely, air sampling, sterilization validation and astrobiology.

The first module is devoted to the detection of airborne endospores. A good biological indicator has to be able to indicate impending changes and provide continuous assessment over a system. **Chapter 3** presents the implementation of an

autonomous air sampler, known as the Anthrax Smoke Detector (ASD), to quantify airborne endospores. The ASD is intended to serve as a cost-effective front-end monitor for anthrax surveillance systems. The principle of operation is based on measuring airborne endospore concentrations, where a sharp concentration increase signals an anthrax attack. The combination of time-gated spectroscopy and the unique photoproperties of terbium dipicolinate results in a sensitive and low detection limit. The ASD-technology can also be extended to the development of a miniature air sampling system to monitor indoor airborne endospore level in a closed system such as spacecrafts and life-support space stations as an indicator of the general hygiene level. Microbiological monitoring in confined spacecraft and space station environments during long-duration manned missions is instrumental to guaranteeing the health, safety and productivity of astronauts and crew members. **Chapter 4** tests the hypothesis that airborne endospore bioburden is an effective indicator of total biomass in a closed system. A correlation characterized by a two-compartmental model has been formulated from a laboratory controlled enclosure to everyday life examples such as offices and laboratories. Future work will follow to miniaturize the current prototype for a terminal integration with the life-support system.

The second module applies to the validation of sterilization. We focus on developing rapid and sensitive methods to detect endospores as surrogates for the

measurement of total biomass on a surface in the context of planetary protection. A microscopy version of the Tb-DPA luminescence assay, known as the microscopic endospore viability assay (acronym: μEVA) has been introduced in **Chapter 5,** fully validated with cultivation and phase contrast microscopy on enumerating pure endospore suspension and monitoring the thermal and UV inactivation of endospores. We have demonstrated a single endospore resolution with a linear measurement at low inocula. The application of μEVA on assessing endospores on surfaces is illustrated in **Chapter 6**, with an emphasis on the bioburden evaluation according to planetary protection regulations. Side-by-side comparison tests have been conducted using μEVA and the culture-based NASA standard assays in monitoring the surface hygiene level based on endospore concentration on coupons made of spacecraft materials and the Class 100 clean room in the Spacecraft Assembly Facility at JPL. This method is expected to be deployed as a new bioburden assessment standard in NASA for ensuring the cleanliness of spacecraft and associated facilities.

Chapters 7 through 9 cover the endospores analysis on environmental samples in extreme environments. Essentially all the methods delineated in previous chapters are developed again and tailored made for specific environmental samples. The goal is to use endospores as the indicator microbe in the study of different ecological systems to shed light on astrobiology questions. **Chapter 7** describes a wide variety

of experiments involving method development, instrument building and model formulation to prepare for the study of endospores under different extreme environments on Earth as models for the eventual exobiological search of life in other planets. So far, most of the assays are developed based on model laboratory endospore strains, such as *B. atrophaeus* and *B. subtilis*. Instruments are developed and modified to adapt to field analysis in desert and ice environments. New protocols and calibration curves are obtained with various endospore viability assays in working with environmental samples. Robustness of the assay has been improved by extending the analysis from mesophilic to thermophilic and psychrophilic endospores. Novel sporulation protocols have been developed to prepare pure and clean psychrophilic endospores for preliminary experiments towards detection of endospores in the ice biospheres. Microgermination and macrogermination models are formulated to give us insights into more complex environmental endospores based on simple and controlled model strains.

Chapter 8 describes the application of a combination of culture-based and culture-independent assays on endospores in extreme cold biospheres on Earth, including GISP2 (Green Ice Sheet Project 2) ice cores, Antarctic underground frozen brine Lake Vida, and polar permafrost. The decontamination, sample handling and analyses for each of these samples are depicted in detail in this chapter. Apart from

the Tb-DPA luminescence assays, many of other methods such as metabolic dyes, bioluminescence and flow cytometry are explored to determine the viability of resident microbes. 4 different viability ratios have been obtained independently based on different measurables in terms of culturability, germinability and total microscopy counts to characterize the microbial abundance and viability in each of these cold habitats. In particular, a transect of 12 depths extending from 295 to 110,000 years old have been analyzed to shed light on the longevity of the most resistant life form, i.e. endospores, in the best storage repository on Earth.

Chapter 9 examines another terrestrial model to Mars – a hyper-arid environment totally devoid of water. The Atacama Desert in Chile serves as the model system because it is the driest desert on Earth. Previous studies have reported a near-sterile state in the soils. My research group has been on a sampling expedition to the Atacama Desert for 10 days in September 2007 to carry out a series of *in situ* and sample return analyses with the goal to study the microbial diversity, abundance and the response of the effect of water on the native microbes. New culture-independent methods, such as phospholipid fatty acid and total organic carbon analyses were performed on the desert soils along with Tb-DPA based assays. Significant differences in culturability and germinability were obtained along a depth profile in a soil pit corresponding to ages approximately equal to 25,000 and 35,000 years ago

based on radioactive carbon dating. A spike in microbial response was also observed when sterile water was added into otherwise-sterile desert soils. Endospore isolates obtained from the Atacama Desert were compared with laboratory strains and other environmental isolates as an effort to investigate the long-debated ecological role of endospores in a particular environment. In particular, we assess the feasibility of using the abundance and viability of endospore as proxies to study the ecosystem in Atacama.

Chapter 10 concludes the thesis by by proposing two future projects built on the developed assays and tools. One of the projects aims to build a miniaturized μEVA instrument for portable field deployment. As science evolves into a high-throughput technology for the study of bacteria, new demands are continually being placed upon analysis time and turnaround efficiency in quantitative methods. Chief among these are increased detection sensitivity, portability, broad dynamic range and compatibility with other methods and portability into spacecraft mission. In this future work section, some of the current μEVA limitations, such as serial processing, bulkiness and manual operation, are interfaced with automated microfluidic chip, robotic high-throughput processing and a miniaturized design. The goal of the other project is to incorporate several synergistic and complementary microbial detection

assays onto a microfluidic chip. It is expected that both deliverables will be integrated into the life-detection system for future space explorations in due course.

1.5 References

1. Cohn, F. Untersuchungen uber Bacterien. IV. Beitrage zur Biologie der Bacillen. *Beitr. Biol. Pflanz.* **2**, 249-276 (1876).
2. Koch, R. Untersuchungen uber Bakterien V. Die Atiologie der Milzbrandkrankheit, begrundet auf die Entwicklungsgeschichte des *Bacillus anthracis. Beitr. Biol. Pflanz.* **2**, 277-310 (1876).
3. Koch, R. Untersuchungen uber Bakterien VI. Verfahren zur Untersuchung, zum Conservieren und Photographieren. *Beitr. Biol. Pflanz.* **2**, 399-434 (1877).
4. Tyndall, J. Further researches on the department and vital persitence of putrefactive and infective organisms froma a physical point of view. *Phil. Trans. Royal Soc.* **167**, 149-206 (1877).
5. Roberts, T.A., Hitchins, A. D. Resistance of spores. *The Bacterial Spore ed. Gould, G. W. and Hurst, A*, 611-670 (1969).
6. Aronson, A.I. and Fitz-James, P. Structure and morphogenesis of the bacterial spore coat. *Bacteriological Reviews* **40**, 360-402 (1976).
7. Driks, A. and Setlow, P., *Prokaryotic Development*. (American Society of Microbiology, Washington, D.C., 2000).
8. Church, B.D. and Halvorson, H. Dependence of the heat resistance of bacterial endospores on their dipicolinic acid content. *Nature* **183**, 124-125 (1959).
9. Byrne, A.F., Burton, T.H., and Koch, R.B. Relation of dipicolinic acid content of anaerobic bacterial endospores to their heat resistance. *Journal of Bacteriology* **80**, 139-140 (1960).
10. Berg, P.E. and Grecz, N. Relationship of dipicolinic acid content in spores of *Bacillus cereus* to ultraviolet and gamma radiation resistance. *Journal of Bacteriology* **103**, 517-519 (1970).
11. Foster, S.J. and Johnstone, K. Pulling the trigger: The mechanism of bacterial spore germination. *Molecular Microbiology* **4**, 137-141 (1990).
12. Johnstone, K. The trigger mechanism of spore germination. *Journal of Applied Bacteriology* **76**, 17S-24S (1994).
13. Vaid, A. and Bishop, A.H. The destruction by microwave radiation of bacterial endospores and amplification of the released DNA. *Journal of Applied Microbiology* **85**, 115-122 (1998).
14. Nicholson, W.L., Munakata, N., Horneck, G., Melosh, H.J., and Setlow, P. Resistance of Bacillus endospores to extreme terrestrial and extraterrestrial environments. *Microbiology and Molecular Biology Reviews* **64**, 548-572 (2000).

15. Cano, R.J. and Borucki, M.K. Revival and identification of bacterial spores in 25-million-year-old to 40-million-year-old Dominican amber. *Science* **268**, 1060-1064 (1995).
16. Vreeland, R.H., Rosenzweig, W.D., and Powers, D.W. Isolation of a 250 million-year-old halotolerant bacterium from a primary salt crystal. *Nature* **407**, 897-900 (2000).
17. Dart, R.K., *Microbiology for the Analytical Chemist*. (The Royal Society of Chemistry, Cambridge, UK, 1996).
18. Switzer Blum, J., Burns Bindi, A., Buzzelli, J., Stolz, J.F., and Oremland, R.S. *Bacillus arsenicoselenatis*, sp. nov., and *Bacillus selenitireducens*, sp. nov.: two haloalkaliphiles from Mono Lake, California that respire oxyanions of selenium and arsenic. *Archives of Microbiology* **171**, 19-30 (1998).
19. Boone, D.R. *et al*. *Bacillus infernus* sp. nov., an Fe (III)-and Mn (IV)-reducing anaerobe from the deep terrestrial subsurface. *International Journal of Systematic and Evolutionary Microbiology* **45**, 441-448 (1995).
20. Meselson, M. *et al*, (1994), Vol. 266, pp. 1202-1208.
21. Setlow, P. Spore germination. *Current Opinion in Microbiology* **6**, 550-556 (2003).
22. Richardson, F.S. Terbium(III) and europium(III) ions as luminescent probes and stains for biomolecular systems. *Chemical Reviews* **82**, 541-552 (1982).
23. Hindle, A.A., Hall, E. A. H. Dipicolinic acid (DPA) assay revisited and appraised for spore detection. *Analyst* **124**, 1599-1604 (1999).
24. Lakowicz, J.R., *Principles of Fluorescence Spectroscopy*. (Plenum, New York, 1983).
25. Jones, G. and Vullev, V.I. Medium effects on the photophysical properties of terbium(III) complexes with pyridine-2,6-dicarboxylate (supporting information). *Journal of Physical Chemistry A* **106**, 8213-8222 (2002).
26. Jones, G. and Vullev, V.I. Medium effects on the stability of terbium(III) complexes with pyridine-2,6-dicarboxylate. *Journal of Physical Chemistry A* **106**, 8213-8222 (2002).
27. Brooks, R.P., O'Connell, T.J., Wardrop, D.H., and Jackson, L.E. Towards a regional index of biological integrity: the example of forested riparian ecosystems. *Environmental Monitoring and Assessment* **51**, 131-143 (1998).

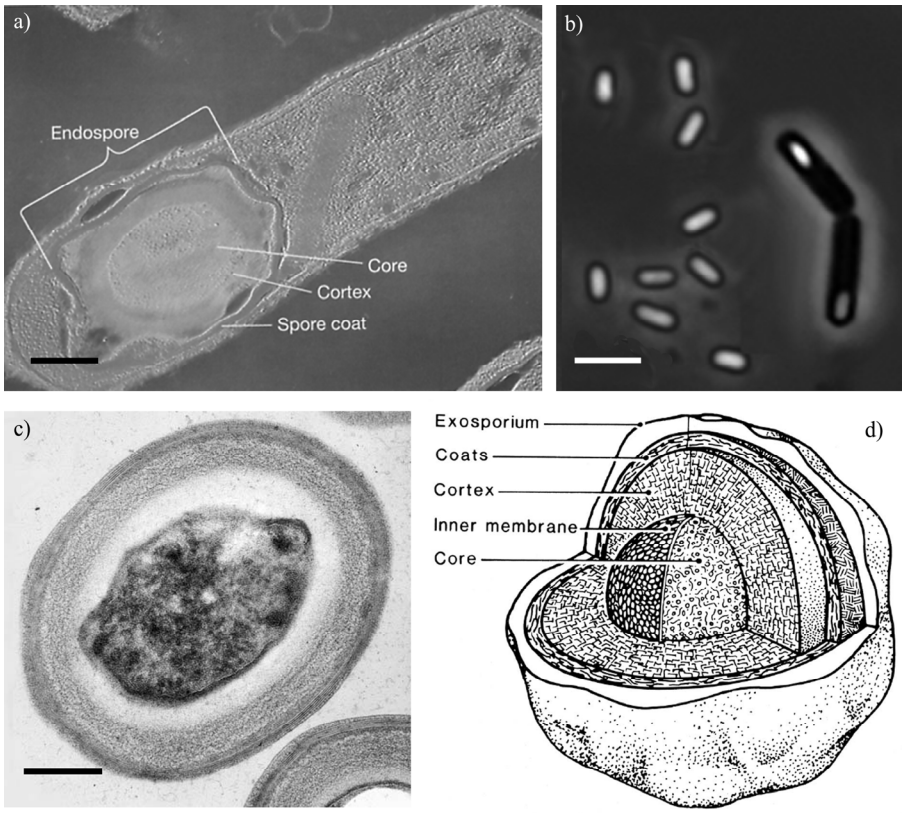

Figure 1.1 | (a) Transmission electron micrograph of a bacterial spore embedded within a *Clostridium perfringens* vegetative cell. Scale bar = 0.3 µm. **(b)** Bacterial spores appear phase-bright observed under a phase contrast microscope and are readily distinguished from the phase-dark rod-shaped vegetative mother cell. Scale bar = 2 µm. **(c)** Cross section of a TEM of an endospore of *Geobacillus stearothermophilus*. Scale bar = 0.2 µm. **(d)** Schematic representation of the internal structure of a typical bacterial spore, reproduced from Foster and Johnstone (1990).

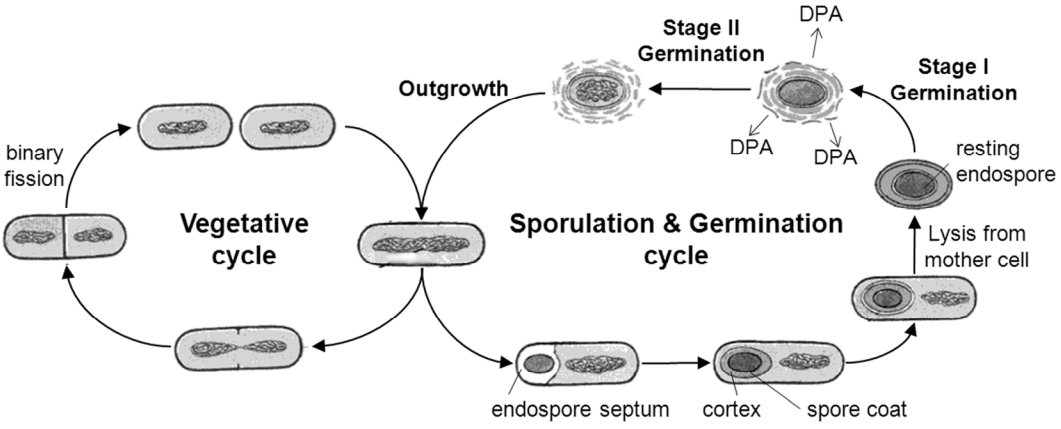

Figure 1.2 | Life cycle of an endospore-forming bacterium.

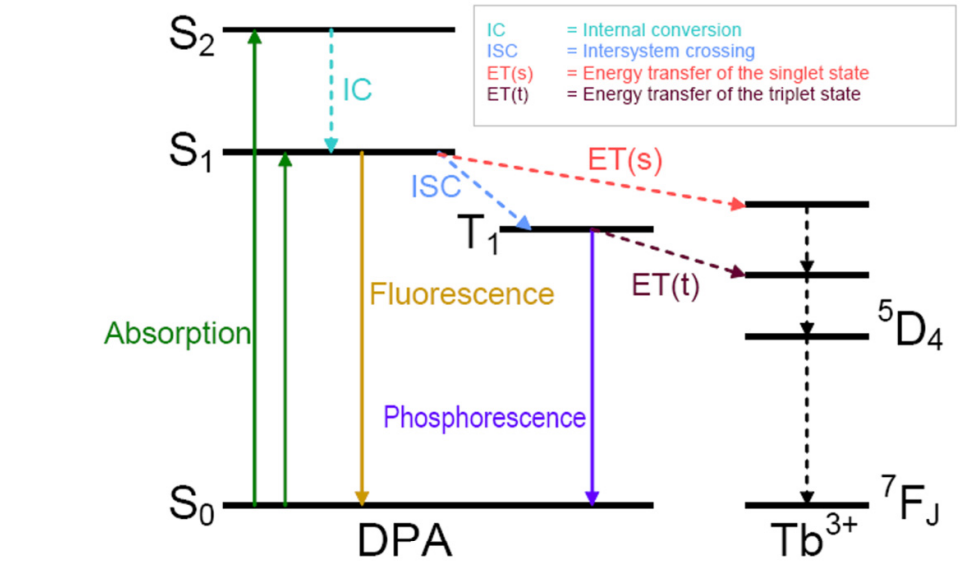

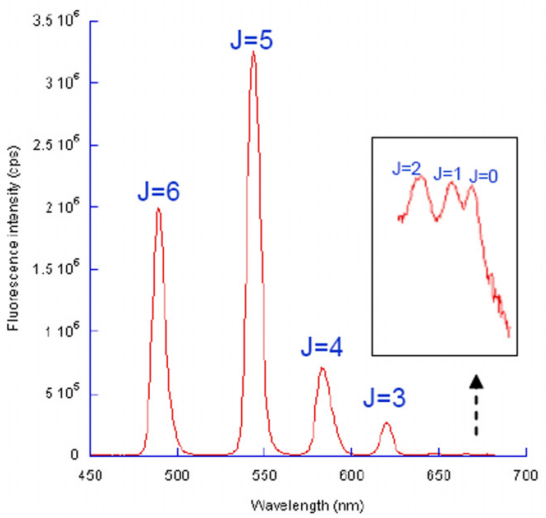

J	wavelength (nm)	Property
6	480 – 505	Hypersensitive
5	535 – 555	Strongest optical activity
4	580 – 600	Hypersensitive
3	615 – 625	Strong optical activity
2	640 – 655	Weak; hypersensitive
1	660 – 670	Weak
0	675 – 680	Weak

Figure 1.3 | Jablonski diagram showing the energy transfer process from DPA to Tb^{3+}. UV excitation harvested by DPA is transferred to Tb *via* radiative decay processes. The subsequent energy transitions from $^5D_4$ to ^7F_J correspond to each characteristic emissive band in the Tb-DPA emission spectrum. Transition from $^5D_4$ to ^7F_J is the most intense and contributes to the visible green luminescence.

CHAPTER 2: REVIEW OF ENDOSPORE DETECTION TECHNOLOGY

2.1 Abstract

Rapid monitoring of bacterial endospores is of key importance in addressing homeland security and astrobiology questions. Apart from the traditional culture-based techniques, unique constituents and distinctive physiological processes associated with endospores were targets for assessing their number and viability. A lot of new biomarker-based chemical, spectroscopic and molecular biological assays have been developed to exploit dipicolinic acid, sporulation gene and the germination process as proxy for enumerating endospores and assigning their viability. This review describes the history and recent advances of endospore methods, as well as the applicability and efficacy of these assays under different contexts. Each of the methods tested in this study has its advantages, and integration of two or more of these techniques provides complementary information to increase the degree of confidence.

2.2 Introduction

What defines microbiology is that everything is in micrometer scale. Microorganisms are not visible to naked eyes unless they form colonies or are observed under a microscope. Microorganisms are everywhere but determination of the number of diversity of viable microbes from an environmental sample is by no means easy. The detection scheme generally falls into two big categories. One is to amplify the bacteria or any chemical marker inherent in the bacteria, e.g., agar-based techniques, turbidity and PCR. The other is to use sensitive instruments such as microscope and flow cytometer to provide

resolution for examination of individual bacterium. Pre-treatment usually entails staining or tagging with antibodies and indicator molecules. Culturing is the classical gold standard to determine the cell number and biomass, but is susceptible to underestimation because of the presence of viable-but-not-culturable microbes. Microscopy is feasible method for microbial enumeration but suffers from obscurity when handling highly complex environmental samples. Alternative methods that detect cellular components such as DNA and RNA have been an important tool to identify a much wider variety of microbes with high sensitivity and accuracy despite its high cost and labor intensive operation.

Detection of viable endospores presents an even greater challenge due to the impermeable spore coat, extreme resistance to lysis, and undetectable metabolic activities. Many current diagnostic techniques fail on the detection of endospores. The impermeable spore coat prevents endospores from staining and therefore invalidates most of the microscopy and flow cytometry techniques. Extreme resistance to lysis makes already genetic materials inaccessible by conventional DNA extraction protocols. In addition, endospores are packaged with a minimal amount of genetic materials, which poses extra difficulties for molecular biology methods. The absence of measurable metabolic rates exhibited by endospores helps them escape from respiration and microcalorimetry assays. Last but not least, separating and identifying the endospore subpopulation from a microbial community is an added challenge due to their dormancy, which nullifies the credibility of many other techniques, e.g., plate counts, ELISA, cell sorting, optical/electron microscopy, which require cell outgrowth to produce sufficient quantities for detection.

Fortunately, some of the unique cell components in endospores, such as dipicolinic acid (DPA, diaminopimelic acid (DAP)[1] and sporulation genes, present as signature biomarkers for various chemical assays. Recent advances on methodologies such as Tb-DPA assays, micro-mass spectrometry, microelectromechanical systems, microfluidics and optoelectronics offers novel technological possibilities for rapid, automated and portable endospore detection with high sensitivity. Germination is a process whereby endospores transition from a dormant state into a metabolically active reproducing bacterial cell. Some methods take advantage of this fact by examining the physiological changes in a sample upon introduction of endospore-specific dormancy-breaking signals.

The intentional release of *Bacillus anthracis* spores *via* mail in 2001 has led to 22 cases of life-threatening anthrax infections. The potential catastrophe caused by bioweapon disseminated by bacterial spores (hereinafter referred to as "spores") underscores the need for rapid and sensitive spore detection assays. The call for long-term Mars missions by President Bush in 2004 is likely to tighten the stringency on microbial monitoring in a closed-loop life support system and interplanetary spacecraft bioburden reduction. Rapid spore detection technology will increase the confidence in life detection data for Mars return missions and reduce the probability of contaminating the Martian surface. The best spore detection instrument should be able to detect and identify spores rapidly in complex matrix. The instrument should be portable, sensitive, robust and amenable to a wide applicability with a minimum of false positives. The advent of new fluorimetric and molecular biological methods, there has been a revival of interest in spore research in recent years.

Currently, there is a new wave of research endeavor employing a comprehensive suite of traditional and new methods to assess the viability of bacterial spores. Previous review articles review microbial detection technologies with respect to specific detection methods. The integration of endospore detection techniques, however, obscures the differentiation among different approaches. Researchers often use a suite of different analysis techniques to study spore behavior and properties. For instance, spores stained by DNA-intercalating dyes can be assayed and observed by fluorimetric, cytometric and microscopic methods. Therefore, instead of outlining each individual technique one by one, emphasis will be put on the detection of physical constituent, morphology and physiological processes associated with a single endospore. This review chapter summarizes important advances in the detection of endospores organized in a way following distinct biomarkers and physiological processes in the life cycle of a spore-forming bacterium, from sporulation, activation, germination, to outgrowth and vegetative phase. This placement is to highlight the contrast between culture-based and culture-independent techniques.

2.3 Biomarker methods

Sporulation is a unicellular differentiation involving drastic morphological changes associated with active biosynthesis and degradation. While the sporulation process has been covered in Chapter 1, I will shed light on the unique chemical composition and morphology of endospores as a means for detection. The detection methods outlined in this section are direct observation of endospores morphology chemical assays on specific biomarkers.

2.3.1 Calcium dipicolinate

The chemical composition and morphology of endospores differ from their progenitor vegetative cells in many ways, highlighted by unique substances such as DPA and 1000-fold concentration of calcium depot.

2.3.1.1 Intrinsic fluorescence

DPA and calcium always exist in a ratio of 1:1 in the spore protoplast with DPA constituting 5% – 15% and calcium 1% – 3% of the dry weight, but Ca-DPA is otherwise rare in nature[2-4]. Spores can be identified *via* the intrinsic fluorescence of Ca-DPA[5]. This method does not rely heavily upon growth or metabolism of the organisms, but measure intrinsic properties of the spores.

Alimova *et al.* have noted a change in fluorescence of *Bacillus subtilis* spores over a period of 7 days with respect to the non-sporeforming bacteria *Staphylococcus aureus*[6]. They hypothesize this is due to the emergence of the DPA fluorescence peak (λ_{ex} = 345 nm, λ_{em} = 410 nm) over the usual tryptophan. They also identified another fluorescing species found only in spores, which was deduced to be a type of siderophore.

Clearly *et al.* have developed a method and prototype device for the detection of spores on surfaces[7]. It uses multiple intrinsic fluorescence markers, including Ca-DPA, and has a sensitivity of about 100 cells cm^{-2} on glass surface. Upon UV irradiation at 254 nm, Ca-DPA emits a characteristic spectrum at 406 nm[8]. Intrinsic fluorescence enables non-intrusive determination of the analyte, which is a very desirable property in environmental microbiology because one can detect the microbial content without disturbing the microenvironment in which microbes reside. It also has a short detection

time and a large dynamic range contingent on the intensity of the excitation source. Major drawbacks, however, include discrimination from the background fluorescence and specificity. Ca-DPA can be extracted from spores *via* lysis or induction of germination.

2.3.1.2 Surface-enhanced Raman spectroscopy

Ca-DPA can also be detected using surface-enhanced Raman spectroscopy on stable silver films over nanosphere (AgFON) substrates where which the intensity of the Raman vibration transitions of DPA is enhanced by several orders of magnitude. An UV excitation enhances the bands due to the aromatic DPA molecule. The strongest peak of Ca-DPA at 1020 cm^{-1} is used to correlate the surface-enhanced Raman intensity and spore concentration. A limit of detection (LOD) of about 2.6×10^3 spores with a data acquisition period of 1 minute and a laser power of 50 mW was obtained. In another publication, a portable surface-enhanced Raman spectroscopy device has yielded a spectrum from 10^4 spores in 5 seconds, the first report result that utilizes a compact vibrational spectrometer for the detection of *Bacillus* spores. The LOD is highly contingent on the binding affinity of the silver surface and DPA. This method, however, requires highly skilled personnel and the materials are relatively expensive and short-lived because the silver nanosphere substrate has a limited shelf life.

2.3.1.3 Anti-Stokes Raman spectroscopy

Femtosecond adaptive spectroscopic techniques for coherent anti-Stokes Raman spectroscopy (FAST CARS) can specifically target at DPA and the divalent cation

chelated with DPA. This method increases the resonant Roman signal strength of DPA by maximizing the ground-state quantum coherence via matching laser pulses in the femtosecond range[9]. Therefore, the coherence between two vibrational states of a molecule is prepared with one set of laser pulse, and then probed with a higher frequency in a coherent Raman configuration, making this assay orders of magnitude more sensitive than incoherent Raman spectroscopy.

2.3.2 Dipicolinic acid

2.3.2.1 DPA extraction

DPA can be extracted by an acidified ethyl acetate phase separation method. A suspension of endospores is boiled in 20 mL 3 N H_2S0_4 for 15 minutes to release bound DPA. An aliquot of about 3 mL of the suspension is transferred to a 125 mL separatory funnel, with 15 volumes of ethyl ether added, and the whole flask is shaken for efficient extraction. The partition coefficient between ether and water was found to be 0.46. The ether phase containing the DPA is aliquoted out and the ethyl phase is allowed to evaporate under room temperature. A small volume of water is added to the residue to obtain a relatively pure concentrated DPA extract from endospores for further analysis. On the other hand, high temperature, high pressure and physical rupture with glass beads can also extract DPA from endospores.

2.3.2.2 DPA release via germination

DPA is released during the early stage of germination from endospores. Both chemical and physical induction of germination has indicated the release of DPA. For instance,

amino acids such as L-alanine, nucleosides such as inosine and cationic surfactant, dodecylamine, are all effective germinants for germination. While quantifying endospores as colony-forming units (CFU) after heat shock treatment requires days of incubation, the process of endospore germination can be initiated and observed on the timescale of minutes by the addition of germinants such as L-alanine, L-asparagine, or glucose[10-14]. The ability to germinate is a strong indicator of viability, and inactivation of germinability can readily be correlated with inactivation of culturability.

2.3.2.3 UV absorption spectroscopy, gas chromatography and mass spectrometry

After extraction, the aqueous DPA extract can be further eluted, separated on a chromatogram and consequently measured at 270 nm. DPA possesses a characteristic UV spectrum. The fingerprint pattern of fragment DPA ions can be detected by mass spectrometry.

2.3.2.4 Ferric colorimetric assay

A rapid and quantitative colorimetric assay for DPA in bulk solution was first proposed by Janssen *et al.* in 1958[15]. This assay has been employed as an endospore detection metric in a number of literature, but not much follow-up work was done in the assay improvement or optimization over the years[16,17]. Following a DPA extraction protocol from endospores, it is based on a color change from pale green to reddish brown upon the interaction of Fe^{2+} with DPA due to a new transition in the UV/visible region. A linear relationship has been shown between the optical density at 440 nm and endospore concentration. This assay has not been used for a long because of the relatively high limit

of detection (around 1.8 mM) and the ferric dipicolinate complex is unstable unless with the addition of a reducing agent such as ascorbic acid.

Metal-to-ligand charge transfer (MLCT) is a type of electronic transition responsible for the intense color of many transition metal complexes. Divalent ferrous ion is electron-rich and has a low oxidation state; DPA is a good π-acceptor ligand with low-lying π^* orbitals, which collectively favor an electron transition from the *d* orbitals of Fe^{2+} to the empty π^* orbitals of DPA (Figure 2.1). Charge transfer transitions are both spin allowed and Laporte allowed, and therefore they are often thousand times much intense than *d-d* transitions bands. A transfer of charge from Fe^{2+} to the aromatic DPA resembles an internal redox reaction in which Fe^{2+} is oxidized to Fe^{3+}. The original light green Fe^{2+} will be changed to reddish brown upon charge redistribution with DPA, with a large molar extinction coefficient 1000 to 50000 dm^3 mol^{-1} cm^{-1}.

2.3.2.5 Spectroscopy of Tb-DPA luminescence

The DPA release during germination can be observed with a spectroscopic analysis of endospore viability based on Tb-DPA luminescence (i.e., spectroEVA). The Tb-DPA luminescence assay was further optimized in 1999 by Hindle and Hall[18] , who were able to obtain a detection limit of 2 nM DPA and 10^4 *Bacillus subtilis* spores mL^{-1} with the use of 1 M sodium acetate buffer (pH 5.6) with a concentration of 10 μM terbium chloride. The pH of 5.6 was found to be most desirable, allowing for the highest fluorescence intensity and longest fluorescence lifetime of the $Tb(DPA)^+$ complex, while still maintaining a balance between deprotonation of the DPA^{2-} species and solubility of the Tb^{3+} species. SpectroEVA is a spectroscopy-based endospore viability assay that

measures the germinable endospore concentrations in bulk suspension with Tb-DPA luminescence intensities[19] tabulated against a calibration curve using *B. atrophaeus* spores, which contain an average 10^8 DPA molecules per spore. The total endospore concentration may also be determined with spectroEVA by forcing DPA release by physical lysis of the total endospore population (e.g., with autoclaving), which enables the percentage of germinable endospores in a sample to be calculated. This was recently demonstrated and validated in comparison to phase contrast microscopy results, and successfully applied to environmental ice core samples from Greenland[20], which contained 295 ± 19 germinable spores mL^{-1} and 369 ± 36 total spores mL^{-1} (i.e., the percentage of germination-capable endospores is 79.9% ± 9.3%). Results from side-by-side comparison experiments using spectroEVA, phase contrast microscopy, and traditional heterotrophic plate counts on *B. atrophaeus* suspensions showed that of the total spore population, 49% ± 4% germinated as per spectroEVA, 54% ± 4% germinated as per phase-bright to phase-dark transition, and 28% ± 7% produced visible colonies. SpectroEVA was also applied to rapidly measure loss of spore germinability as a function of UV exposure to determine the lethal dosage, and correlated this to loss in culturability. These results show that spectroEVA can be used as a rapid alternative over standard culture-based methods for monitoring the efficacy of sterilization processes.

2.3.2.6 Time-gated microscopy of Tb-DPA luminescence

The DPA release during germination can be observed with a direct microscopic analysis of endospore viability based on Tb-DPA luminescence (i.e., microEVA or μEVA)[20]. Rather than requiring full outgrowth before enumeration, we probe for viability much

earlier—during stage I germination when DPA is released and water begins to enter the core. In μEVA experiments, individual germinable spores are counted in a microscope field of view after germinant addition. As the spores germinate, ~10^8 molecules of DPA are released into the immediate area surrounding the spore. DPA combines with Tb^{3+} in the matrix to form the Tb^{3+}-DPA luminescence halos under UV excitation, and are enumerated in a microscope field of view. The germinating spores manifest as bright spots in the field of view that grow in intensity over a period of three to five minutes. DPA release during germination resulted in bright luminescent spots due to Tb-DPA complex formation with the Tb^{3+} that was present in the surrounding agarose medium. *Bacillus* endospores are in standard use as biological indicators for evaluating the effectiveness of sterilization processes. μEVA has been applied to monitor inactivation to sterility of initial 5×10^6 CFU endospore populations in aqueous suspension as a function of thermal (95°C) and UV (254 nm, 22 μW cm^{-2}) dosage. μEVA and culturing yielded similar D-values for both inactivation methods; thermal inactivation D-values were 4.74 min and 4.80 min, respectively, while UV inactivation D-values were 30.52 minutes and 30.43 minutes, respectively.

2.3.3 DNA

Nucleic acids, the building blocks of DNA and RNA, are universally present in all living cells and may be used as a general indicator of microbial biomass[21]. A disadvantage is that viability cannot be determined.

2.3.3.1 Polymerase chain reaction

The polymerase chain reaction (PCR) has gained wide acceptance as an exponential nucleic acid amplification technique and is frequently used for research and clinical applications. Quantitative PCR methods are shown to be extremely sensitive, with detection limits of fewer than 10 cells mL^{-1}, and analysis times of approximately 3 h[22].

Using real-time PCR detection system, anthrax spores in environmental samples can be analyzed quantitatively with the standard curve obtained by comparing CT value and serial dilutions of genomic DNA and pure spores, as well as soil samples containing anthrax spores at the correlation coefficient of 0.99. TaqMan real-time PCR system shows up to 10^4 spores in a soil sample without prior cultivation steps, allowing identification of an anthrax attack within 3 h after arrival of the sample in the laboratory

Pathogenic *B. anthracis* carries two plasmids, pXO1 (174 kbp) with the toxin genes *pag*, *lef* and *cya* encoding the protective antigen, lethal factor, and edema factor protein, respectively, and pXO2 (95 kbp) with the encapsulation genes cap A, cap B, and cap C. These genes have been used as virulence markers to detect pathogenic *B. anthracis* strains

While the speed and sensitivity of nucleic acid analysis based on PCR have been significantly improved, the PCR technique requires that the bacteria and spores be disrupted to make the endogenous DNA available for amplification. Bacterial spores are particularly difficult to process, as their nucleic acid is encased in a very resistant shell. Spore lysis methods have included chemical, enzymatic, mechanical, and thermal treatments.

Lawrence Livermore National Laboratory scientists have also developed a four-chamber, battery powered, handheld instrument referred to as the Handheld Advanced Nucleic Acid Analyzer (HANAA)[23]. The HANAA is an instrument capable of rapid detection and identification of biowarfare and bioterrorism agents in the field using a TaqMan-based PCR assay. It is a highly automated device, able to automatically prepare samples, then simultaneously test up to four different samples for two different DNA sequences each, and report the results in about 30 min. The HANAA system could, in principle, detect as few as 10 individual bacteria including *B. anthracis*. The total time of spore disruption and detection using the minisonicator and the Advanced Nucleic Acid Analyzer (ANAA) was less than 15 min.

2.3.3.2 Fluorescence coupled with peptide nucleic acid probes

A fast and ultrasensitive method has been developed by Castro and Okinaka[24], and deals with the detection of spore-specific nucleic acids and sequences. Two fluorescent probes are used, each labeled with a different fluorescent tag specific to complimentary nucleic acid base sequences of bacterial or viral origin in a sample. The sequence can be either DNA or RNA, and can pertain to either a certain taxonomic group or a physiological function of the target organism. Highly specific hybridization of the combined fluorescent probes occurs in the presence of the target, leading to high sensitivity and low background for simultaneous detection of both signals. This method was able to detect *B. anthracis* in the presence of *B. globigii* with a low signal-to-noise ratio after 200 seconds, and without a need for PCR.

2.4 Optical property and Stainability

2.4.1 Direct epifluorescent filtration technique

The principle of the direct epifluorescent filtration technique (DEFT) is that viable microorganisms fluoresce (orange-red) when stained with acridine orange, whereas non-viable cells do not[25]. Thus, examination and counting of cells under a fluorescent microscope can provide a quantitative assessment of the number of viable cells present. In practice, the liquid to be tested is filtered through a membrane filter, which is then stained with acridine orange and examines microscopically[26].

The method has been used on microbiological quality control, for the rapid estimation of microbial counts in foods, beverages, poultry and for detecting organisms in urine and in intravenous fluids. Couto & Hogg, due to problems with acridine orange, used two fluorescers (a commercially available) – SYTO 9 and propidium iodide, as a rapid detection method for bacteria in wine[27]. Using both the traditional plating methods and the DEFT technique, inactivation's kinetics were shown to be similar – i.e. not method dependent. Decker, who compared several dye systems, also used SYTO 9 and propidium iodide to examine the state of viability of *Streptococcus sanguinis* and *Strepcococcus mutans*[28].

In another study, the fluorochrome (acridine orange or diamidino-2-phenylindole) is added to the filtered sample for a contact time of a few minutes and then filtered through a polycarbonate membrane. The membrane is rinsed with a volume of distilled equal to the original sample volume. The microorganisms are finally counted using epifluorescence microscopy. Under UV light, acridine orange stains deoxyribonucleic acid (DNA) green, and ribonucleic acid (RNA) is stained orange. Actively growing

bacteria can therefore be distinguished from inactive bacteria on the basis of their higher RNA contents, monitoring germination of single *Bacillus* endospores in soil using direct fluorescence microscopy acridine orange is used to stain the bacteria immobilized in the sandwiches direct microscopy of endospore germination in vitro environments and in complex soil microcosms.

2.4.2 Coulter counter

The Coulter counter manufactured by Coulter Electronics Inc. (Canada) has been widely used to count endospores. A suspension of cells is passed through a small orifice that has two electrodes suspended on either side. Resistance caused by the orifice is measured by passing current between the electrodes. The pulse generated by each cell is amplified and recorded electronically, giving a count of the number of cells flowing through the aperture. Cells can be counted in the medium in which they are growing. Cell concentrations must be kept low for accurate results since high cell densities limit the accuracy by coincidence counts when more than one cell occupies the counting orifice. This problem can be solved by diluting the cell suspension, taking care to avoid shrinkage of cells due to osmotic stress. Endospore appear as phase bright bodies.

2.4.3 Method of Schaeffer and Fulton

The Schaeffer and Fulton method in staining endospores involves an acid pre-treatment[29,30]. A smear of air dried sample was heat fixed on a microscope slide, covered with a piece of blotting paper soaked with malachite green, and then placed over a boiling water bath for 5 min. The overlying blotting paper is kept most by constant introduction

of malachite. The slide is then cooled down and washed with deionized water until no residual green stain is left. Placed in a staining jar with safranin for 2 min, the slide is rinsed until no residual red stain is left. The smear is examined using a 100× oil immersion objective. Endospores are green-stained oval/round bodies and vegetative cell will be stained red. This method is not quantitative due to unknown number of cells being washed out during the staining procedure. If successfully stained, green endospores are clearly apparent and compelling evidence for the presence of spores although, in practice, this method has proved unreliable.

2.4.4 Phase contrast microscopy

The easiest and quickest way to demonstrating endospores in a culture in by phase contrast microscopy using an oil-immersion objective with 60× or 100× magnification. In simple native preparations highly refractile spores are easily seen as bright bodies within or outside dark contrasted cells. Lipid globules or air bubbles which might be present may have a somewhat similar appearance but are easily distinguished with some experience. For better viewing (and for micro-photometry), it is sometimes useful to immobilize cells and to keep them in focus by using agar coated microscope slides[31]. This helps to better interpret shape and size of cells, sporangia and spores. This technique also avoids tumbling motions of the cell, which can often result in vertically positioned rod shaped cells which can then, then viewed “end-on,” resemble spores. Another interesting method is the “acid popping” of spores[32-34] where a fixed microscopic mount is viewed while a strong acid is passed through the preparation. On contact with the acid,

spores will rehydrate and lose their high refractility and turn immediately from bright to dark.

During the first stage of germination, water uptake and DPA release occurs concurrently[14,35,36]. The water uptake can be observed by phase contrast microscopy as the phase-bright endospores transition into phase-dark germinated spores. Endospores are highly refractile round or oval structures formed within bacterial cells. During germination spores change from bright to dark as viewed under a phase contrast microscope[37,38]. Loss of refractility is due to the influx of water, swelling of cell and excretion of dry matter from the germinating spore[39,40]. Phase contrast microscopy can be carried out on a normal microscope slide-cover slip setup or on solidified agar covered with a cover slip under an oil immersion objective. This technique has been applied to observe germination of both *Bacillus* and *Clostridium* spores[41-43].

The degree of spore refractility can be correlated to the course of germination, which follows a biphasic kinetics[44,45]. In the first phase, spores change into partial phase dark and lose part of the heat resistance. The proteinaceous coat becomes more porous, leading to the hydrolysis of water and removal of calcium dipicolinate from the spore core. The second phase marks the complete hydration of the spore core and degradation of the spore cortex, which render the spore phase dark. Duration of germination depends on a number of factors, such as species, inoculum size, germinants, temperature and the optics used for observation. The reported phase transition for individual bacterial spores ranges from 75 seconds to approximately an hour[46,47]. An inverse relationship has been reported between the spore inoculum size and germination time[48].

There are, however, some limitations inherent with this technique. For example, lipid inclusions may be mistakenly assigned as spores because they are phase bright and are about micron size. It is impossible to observe spores in environmental samples such as soils without a rigorous separation process. Nevertheless, phase transition observed under the microscope provides a strong evidence for spore germination. When used in conjunction with other spore detection assays, phase contrast microscopy proves to be a very useful validation test and provides total and germinable counts of spore suspensions[19].

2.4.5 Electron microscopy

The specialized technique involves the use of an electron microscope, the resolution of which made it superior to the light microscope for the estimation of bacterial size. The use of scanning electron microscopy for counting bacteria on membrane filters has been reported previously. However, the use of electron microscopic techniques as a low-cost rapid method for biomass estimation is unlikely to be realized due to the high cost of instrumentation, the high operator skill required as well as the difficulty in producing quantitative preparations.

2.4.6 Flow cytometry

Several reviews have appeared that discuss the principles of flow cytometry[49,50]. The method has been used to evaluate antibacterial and antoprotozoal activity. In a typical flow cytometry, individual particles pass through an illumination zone at the rate of several thousand cells per second; appropriate detectors measure the magnitude of a pulse

representing the extent of light scattered. By 'labeling' the cells with fluorescent molecules, e.g., an appropriate dye, that have high specificity to one particular cellular constituent, it is possible to measure the content of that constituent[51]. Flow cytometry can be used to detect viable and dead bacterial cells, and has been employed to assess the lethal effects of biguanides and other biocides on spores.

2.5 Metabolism

All living cells respire and produce metabolites, each possessing unique intrinsic fluorescence property. Although endospores elicit a non detectable level of metabolism, metabolites such as reduced pyridine nucleotides, oxidized flavoproteins and ATP can readily be detected during the later phase of germination and outgrowth. ATP can be detected using a firefly luciferin/luciferase bioluminescence system. Other metabolites can be detected based on their intrinsic fluorescence using microspectrofluorometry, epifluorescence techniques. Multi wavelength intrinsic fluorescence detection enables pattern recognition algorithms for microbial fingerprinting. Intrinsic fluorescence markers

2.5.1 Impedance measurement

When bacteria grow, they produce metabolites which alter the conductivity of the medium, a property first observed in 1898. With the use of modern electrical measuring equipment, this nineteenth-century observation has been put to use as a rapid impedance microbiology technique[52]. However, use of charged antimicrobials, such as silver ions or cationic surfactant biocides, can lead to interpretive problems.

2.5.2 Microcalorimetry

Microcalorimetry, as a rapid analytical method for biocide testing, is based upon the principle that bacteria and other microorganisms produce heat when they metabolize. Microcalorimeters can detect the small amount of heat produced[53]. Any surviving cells, following an inimical treatment, will, during subsequent incubation, metabolize and produce heat. Morgan *et al.* used microcalorimetry to examine the effect of antomicrobials on *Streptococcus mutans* and suggested that the data obtained by this technique gave a "better indication of antimicrobial efficacy than merely determining concentrations at which an antimicrobial agent is bacteriostatic or bactericidal"[54].

The overall metabolic capacity, as measured by the heat released by cells, the number of cells of a sample is dependent on the number of cells present and can be measured using a microcalorimeter such as the Thermal Activity Monitor. Spores, after induced to germinate, start actively metabolizing and produce heat which can be measured using microcalorimetry.

2.5.3 ATP firefly luciferin-luciferase assay

Adenosine 5'triphosphate (ATP) is the primary source of chemical energy and a ubiquitous energy currency in all living organisms. The use of a firefly (*Photuris pyralis*) enzyme to quantify ATP in biological systems was first proposed by McElroy and Strehler in the 1940s[55,56]. The detection is based on the conversion of chemical energy to light energy during the breakdown of ATP. Firefly luciferase catalyzes the ATP-dependent oxidative decarboxylation of luciferin in the presence of oxygen and

magnesium ions into AMP and light. One photon of light is produced per molecule of ATP hydrolyzed when ATP is the limiting component in the reaction[57]. Measurement of ATP is a direct indication of cellular metabolism and is often reckoned as a metric for viability[58,59].

First, nonmicrobial ATP is eliminated from the sample using a somatic cell releasing agent and a subsequent incubation in apyrase or ATPase. Bacterial cells are then disrupted using chemicals such as benzalkonium chloride. The ATP released is quantified using the luciferin-luciferase reaction. A differential filtration procedure is also reported to separate somatic from microbial cells[60]. Several different ATP reagents are available commercially and the protocol has been optimized over the years. For instance, a mutant luciferase resistant to benzalkonium chloride has been isolated to achieve maximum extraction of intracellular ATP from microbes and inactivation of the ATP-eliminating enzymes for removal of extracellular ATP[61]. Hattori *et al*. achieved a detection limit of 7.7 cfu mL^{-1} using vegetative cells of *B. subtilis*, while Promega Corporation reports a detection limit of 10 cfu mL^{-1} of vegetative cells of *B. cereus*.

Challenges are encountered in the detection of endospores using the luciferin/luciferase system. While a vegetative bacterium contains approximately 10^{-17} mole of ATP per cell[62], dormant spores of a number of *Bacillus* species have no detectable biosynthetic or metabolic activity and contain low levels of ATP[63-65]. Kodaka *et al*. reported that an endospore contains about 10^{-21} mole ATP per cell, four orders of magnitude lower than that of a vegetative bacterium[66]. In addition, ATP cannot be sufficiently extracted from endospores, unlike their vegetative counterparts, due to a nonporous and hardy proteinaceous spore coat[67-69]. Theoretically speaking, if the current

luminometers can detect approximately ten vegetative bacilli cells per milliliter, the limit of detection for endospores will be 10^5 endospores mL^{-1}.

There are several approaches for endospore detection using the firefly luciferase assay. One method is the screening for endospores by heat shock at 80°C for 15 minutes allowing only spores to survive, followed by incubation and detection of ATP in the subsequent outgrowth of vegetative cells. In this manner, bacterial outgrowth from endospores on test strips was measured after five hours of incubation to validate the sterilization efficiency of autoclaves[70]. This method is relatively faster than the traditional cultivation method, but can only provide semi-quantitative counts of the original endospore population.

Other approaches take advantage of the production of ATP from endospores during germination. Less than 1% of the adenine nucleotide pool in spores is ATP, but it accounts for 80% in vegetative cells. Most of the nucleotides in endospores are stored in the form of 3-phosphoglyceric acid[64]. Nevertheless, within the first minute of germination, the large depot of 3-phosphoglyceric acid is catabolized into ATP[71]. In addition, coat porosity increases after the onset of germination, which permits easy extraction of intracellular ATP[72]. Fujunami *et al.* measured a large increase in light intensity of *B. subtilis* spores after 30 minutes of incubation in nutrient broth supplemented with L-alanine in the presence of various white powders[73]. Rapid accumulation of ATP upon nutrient induced germination also held true for anaerobic *Clostridium* spores[74].

Pressured-induced germination of *B. subtilis* at 100 MPa resulted in a rapid production of ATP, but no ATP was formed during germination at 600 MPa[75], while

hydrogen peroxide-treated spores can germinate, but accumulate very little ATP. The mechanism of ATP accumulation during germination is still not very clear. Further study may shed light on the subject of endospore viability and the phenomenon of germinable-but-not-culturable.

Direct extraction of ATP from endospores is also another feasible method for detection. Venkateswaran used ATP as a biomarker of viable microorganisms in clean-room facilities. The use of benzalkonium chloride (Kikkoman International, Inc.) completely lyzed vegetative cells and endospores in surface swab samples to release ATP for detection. A low ATP-CFU ratio has been associated with endospores, ranging from 10^{-18} to 10^{-20} moles ATP per CFU[76].

Compared with other endospore detection techniques, ATP bioluminescence measurements offer many advantages, such as high sensitivity, large dynamic range, high specificity, and rapidity. The luciferase assay can easily be automated for high throughput processing. The instruments tend to be inexpensive, portable and can detect viable bacteria in relatively complex media, such as powder and milk. False positives are rare because the enzyme is highly specific for ATP, and ATP is lost rapidly upon cell death. Nevertheless, the assay suffers from drawbacks such as a low level of ATP in endospores and interference from extracellular and somatic ATP. Also the assay is not species-specific and some food samples have been shown to contain inhibitory substances that interfere with luciferase activity[77].

At present, the ATP assay is mainly used to detect and enumerate vegetative cells of pathogenic bacteria for food quality control and hygiene testing[78]. It has been used to detect as few as 10^4 cfu mL^{-1} of bacteria in milk in five to ten minutes[79], a bacterial

population of 10^5 cfu mL^{-1} in fruit juice[80] and 5×10^4 cfu g^{-1} in meat[81]. The application of the ATP assay on endospore detection in foodstuffs is still in its initial phase. Because endospores are the likely candidates for surviving pasteurization, steaming, and vacuum processes, the ATP assay could be expected to play a bigger role in the detection of pathogenic foodborne endospores in the future.

More recently, the ATP luciferase assay has shown promising results in detecting anthrax spores. The lysin *plyG*, isolated from a phage that infects *B. anthracis* was used to specifically target and lyse germinating *B. anthracis* spores causing a pronounced release of intracellular ATP. ATP could be detected within 60 minutes of the addition of germinants from as few as 100 spores using a phage sensitive *B. cereus* as a surrogate for *B. anthracis*[82]. The ATP assay was also used to detect airborne bacterial spores. A detection limit of 10^5 cfu mL^{-1} was reported using aerosolized *B. globigii* spores—a surrogate for *B. anthracis*[83]. In a nutshell, the luciferin-luciferase reaction could potentially be used for the detection of anthrax spores and validation of decontamination regimes after an anthrax attack.

2.6 Biochemical tests

Biochemical tests are also among traditional microbiological methods for spore identification and detection. Identification protocols have been developed for target microbes. For instance, the following table outlines a series of biochemical and cultivation tests to test the presence of *B. anthracis*. Based on the differential metabolic requirement and cultivation requirement, spores can be detected and identified manually or automatically.

Microbes interact with their environment; they metabolize nutrients in the media and excrete waste products. An alternative to enumeration is to directly measure, biochemically, the alterations in the microbial environment or microbial metabolism following an inimical process. Quastel & Whetham studies the action of antimicrobials on the dehydrogenases of *E. coil*[84]. The principle of triphenyltetrazolium chloride reduction by bacteria was utilized by Hurwitz & McCarthy in developing a rapid test for evaluating biocidal activity against *E. coli*. In essence, cells exposed to a biocide are removed by filtrate, excess biocide quenched and the filter transferred to a growth medium containing TTC[85]. During subsequent incubation at 37°C, formazan is extracted and color development measured spectrophotometrically. The method permits a 2-3 $\log_{10}$ reduction cycle to be followed and inactivation kinetics to be calculated. The incubation period takes about 4-5 h to provide a minimum detection level of 10^5 cfu mL^{-1}.

MicroLog has developed BioLog plates to identify microorganisms based on metabolism on 96 wells of various pre-dried carbon sources and nutrients. Positive growth will turn the tetrazolium violet redox dye purple. A fingerprint of color change across the 96 wells reflect the bacteria's metabolic needs on various substrates and susceptibility to antimicrobial agents. More than 8000 bacterial species can readily be identified, including many of the *Bacillus* genus. Custom-made substrates can also be prepared to identify specific species. Drawback of this method is that and long incubation time is often necessary anaerobic species may present practical problems in oxygen exclusion, and bacterial isolate has to be obtained a priori. A microbial identification system developed by BioMérieuxhas shown success in identifying *B. anthracis* spores.

Fatty acid profiles from pure culture of spores serves as another biochemical test for detection. Cellular fatty acids are first converted to fatty acid methyl esters, and subsequently separated and identified using a gas chromatography. *Bacillus* spores can be identified by this method[86].

Each of these cultivation and biochemical tests are inherently time consuming, depending on self amplification of the biological sample *via* growing and metabolism. With the introduction of automation and miniaturization, detection time and technician time are all greatly shortened.

2.7 Colony formation

Evaluation of spore count is based upon the ability of spores to grow in either a liquid broth media or an agar gelled media or on the surface of a membrane filter after heat-shock treatment. Viable count methods may be further divided into spread plate count, membrane filter method and the most probable number (MPN) method. In the plate count method, serial dilutions of the cell sample are spread onto agar plates which are subsequently incubated at an appropriate growth temperature. The number of colonies is counted and multiplied by the dilution factor to obtain viable count in terms of cfu mL^{-1} in the original sample. When counting anaerobic sporeformers it may be necessary to treat diluents to remove dissolved air prior to use. The main disadvantage of the plate count method is the long incubation period (typically 24-72 h and may be longer for environmental species) and the difficulty of aseptic processing in the field.

2.7.1 Culturing (plate count and most probable number)

First of all, the inoculum will be heat shocked at 80°C for 15 minutes to select for endospores. Enumeration of spore count is based upon the ability of spores to grow into a visible colony on agar plates or turn turbid in liquid culture media. Advantage of viable count is that it gives actual cell number and diversity of the sample under analysis. Nevertheless, this method is very labor and material intensive and requires long elapse time for completion. When analyzing environmental samples, the culturability may be as low as 0.1% or 0.01%, known as the viable but not culturable (VBNC) phenomenon. So, using cultivation-based methods tends to underestimate the total spore counts. Although automatic plating is made possible, such as Petrifoss, the entire process may still take 24 hours to weeks, or maybe months for the growth of extremophilic spores. Depending on the specific technique, membrane filter and most probable number methods, conventional cultivation yields a limit of detection of around 10 viable cells per milliliter.

Recently, a miniaturized and multiplexed micro-cultivation method, coupled with fluorescence microscopy, has been developed[87]. Micro-colony formation can be observed in as short as 2 hours. 336 mini-compartments are etched on an aluminum oxide filter at a density of 200/cm^2, resting on top of nutrient agar, supports individual cell to grow.

2.7.2 Turbidity measurement

Turbidity is another widely used method for the estimation of cells in suspension. The turbidity of a spore suspension can be determined using spectrophotometry by measuring the light lost from the beam by scattering and absorption. The relationship used is Beer's law but the term extinction coefficient is replaced by a constant called the turbidity

coefficient. A standard calibration curve of log Io/I against either the total count or the dry weight is used. Transferring cells from one medium to another or washing the cells can disturb the osmotic potential across the cell membrane. This may change the cell surface area/volume ratio and refractive index and hence the turbidity, without altering the cell count or total mass. The calibration curve applies only to a particular microorganism grown under a particular set of growth conditions. If any change in the growth conditions occurs a new curve must be prepared. In addition, cells grown in high carbohydrate or fat media frequently have a high turbidity. This method is, however, not compatible for determining number of spores in environmental samples.

2.8 Spore coat

Philips and Martin showed that it is possible to detect *Bacillus* spores with specificity using fluorescent-conjugated polyclonal antibodies directed towards the spore coat, based on the interaction between antibodies and bacterial spore cell surface antigens[88-90]. Limitations of the technique are due to the test being specific to the particular microorganism and serotype. In order to broaden the spectrum of the technique, antibodies which are complementary to a range of microorganisms and different serotypes need to be raised.

Cardosi *et al.* described a sensitive two-site, enzyme-linked immunoassay for *Clostridium perfringens* phospholipase C (atoxin). The approach incorporated an electrochemical detection step based on thin-layer hydrodynamic voltammetry coupled with fast liquid chromatography with electrochemical analysis (LCEC).

2.8.1 Immunoassay and Flow cytometry

Stopa was able to obtain a detection limit of approximately 10^3 colony-forming units cfu mL^{-1} for *B. anthracis* using flow cytometry in conjunction with a rapid immunoassay[91]. The advantages of using flow cytometry include: (1) combination of scatter signal and fluorescence intensity to enhance selectivity and distinguish between related strains, reducing false positives, and (2) limiting detection to a certain fluorescence intensity allows for further constraints to be placed on samples ordinarily labeled as positive, resulting in higher specificity. For instance, *B. anthracis* could be distinguished from *B. subtilis* var. *niger*, though *B. megaterium* and *B. thuringensis* were not resolvable.

2.8.2 Immunofluorescence resonance energy transfer

Bruno *et al.* reports new immunofluorescence resonance energy transfer (immuno-FRET) assays for the detection of *B. cereus* spores and *E. coli* vegetative cells. Both utilize dual labels – one fluorescent and one quencher – such that the fluorescence of the former is quenched by the latter when both are bound to the spore or cell. Limits of detection for both spores and cells were in the 10^5 spores/cells mL^{-1} range, with a detection time of less than 30 minutes.

Zahavy *et al.* have also adapted FRET to an immunofluorescence method to detect bacterial spores[92]. Coupling FRET to an immunoassay minimizes the potential for false positives, as two different reporter molecules are required to label the antigen surface. The system was tested with *B. anthracis* spores, and selectivity was improved by a factor of 10 with respect to *B. thuringiensis* subsp. *Istraelensis* and 100 with respect to

B. subtilis. It is mentioned that using multiple labeled polyclonal antibody molecules against different determinants of the spore may enhance selectivity further.

2.9 Spore detection instruments

Yung *et al.* have developed a fully automated anthrax smoke detector (ASD)[93-95]. The ASD is intended to serve as a cost-effective front-end monitor for anthrax surveillance systems. The principle of operation is based on measuring airborne endospore concentrations, where a sharp concentration increase signals an anthrax attack. The ASD features an air sampler, a thermal lysis unit, a syringe pump, a time-gated spectrometer, and endospore detection chemistry comprised of dipicolinic acid (DPA)-triggered terbium ion (Tb^{3+}) luminescence. Anthrax attacks were simulated using aerosolized *B. atrophaeus* spores in fumed silica, and corresponding Tb-DPA intensities were monitored as a function of time and correlated to the number of airborne endospores collected. A concentration dependence of 10^2-10^6 spores mg^{-1} of fumed silica yielded a dynamic range of 4 orders of magnitude and a limit of detection of 16 spores L^{-1} when 250 L of air were sampled. Simulated attacks were detected in less than 15 minutes. A comparison between ASD and PCR-based detectors performance has been summarized in Figure 2.2.

Eversole *et al.* have demonstrated a prototype single particle fluorescence analyzer (SPFA) to simultaneously monitor ambient concentrations of both biological and nonbiological aerosols[96]. The instrument pulls air through a nozzle at approx. 300 liters per minute and monitors particles between 1 and 10 μm in diameter *in situ* using laser-induced excitation and detection of two specific bands: UV (300–400 nm) and visible (400–600 nm). Discrimination between biological and nonbiological aerosols is effected

through comparison of these emission intensities to a calibrated reference. The latest outdoor field testing of the instrument resulted in a detection probability of 87% for the target aerosols ova albumin, MS-2 phage, *Erwinia herbicola* vegetative cells and *B. subtilis* spores, with airborne concentrations of 5 particles per liter. Further, the absolute quantitative detection efficiencies for individual biological aerosols all averaged over 70%, with the measurement response time proportional to the particle measurement rate.

Agranovski *et al.* have devised an instrument for real-time continuous monitoring of bioaerosols called the Ultraviolet Aerodynamic Particle Size Spectrometer (UVAPS)[97]. The instrument is capable of providing time-of-flight, light scattering and fluorescence measurements for particles ranging from 0.5 to 15 μm in diameter. Aerosolized spores (*Bacillus subtilis*), vegetative cells (*B. subtilis*, *Pseudomonas fluorescens*) and non-bacterial elements (NaCl, latex, peptone water, nutrient agar) were all used to test the selectivity, sensitivity, efficiency and limit of detection of the instrument. Results indicated that the UVAPS was able to detect bacterial spores with limited capability, and only the *B. subtilis* vegetative cells produced a strong fluorescent signal, with a limit of detection of approximately 10^7 particles m^{-3}. Further, strong false positives from nonbacterial elements were also observed. Particle counting efficiency depends on particle concentration, and has a "saturation" level of 10^6 particles m^{-3}.

Another instrument designed and tested by McBride *et al.*, called the fully autonomous pathogen detection system (APDS), is capable of continuous monitoring for bioaerosols[98]. The instrument is composed of an aerosol collector, a fluidics module for sample preparation and immunoassay detection using a flow cytometer. The immunoassay uses a sandwich format, where antigen-specific antibodies immobilized on

beads bind the analyte, which is then detected using secondary fluorescently labeled antibodies. This analysis requires 60 s to complete. The system was tested with release of *B. anthracis* and *Yersinia pestis*, both of which it was able to detect with no false positives. Plus, with a collection interval of 30 to 60 min and a capability of continuous unattended operation for 8 days, the system can be easily integrated into a central security network. The system will ultimately utilize an orthogonal detection approach including antibody-based (immunoassays) and nucleic acid-based (PCR) assays to reduce false positives.

An instrument developed by Cheng *et al.*, is used to aerosolize bacterial spores to improve fluorescence detection of aerosols[99]. As opposed to using only single-excitation wavelength approaches, the authors utilize multiple wavelengths of excitation and fluorescence detection. The system, including an aerosol generator, chamber, aerosol monitoring instrumentation and laser-induced fluorescence detection system, was able to obtain fluorescence measurements on *Escherichia coli*, *Staphylococcus aureus*, *Bacillus subtilis* var. *niger*, and *Bacillus thuringiensis*, but was not able to distinguish between them.

Brosseau *et al.*, utilize the autofluorescent chemicals naturally found in bacteria (spore and vegetative cells) and fungi, such as riboflavin, nicotinamide adenine dinucleotide phosphate (NADPH) and tryptophan, to detect biological aerosols[100]. Nebulized spores and bacterial cells of *Bacillus subtilis* subsp. *niger*, as well as various other bacteria and even fungal spores were evaluated using an Ultraviolet Aerodynamic Particle Sizer (UV-APS). It was found that fluorescence appears to be species-dependent, but identification of bioaerosols was made difficult due to high variability.

Scientists at Lawrence Livermore National Laboratory have also invented a stand-alone system for rapid, continuous monitoring of multiple airborne biological threat agents in the environment. This system, the autonomous pathogen detection system (APDS), acts as a biological "smoke alarm" and is targeted for domestic applications in which the public is at high risk of exposure to covert releases of bioagent (such as mass transit, office complexes, and convention centers), and as part of a monitoring network for urban areas and major gatherings.

The APDS is completely automated, offering aerosol sampling, in-line sample preparation fluidics, multiplex flow cytometer detection and identification assays, and orthogonal, flow-through PCR (nucleic acid) amplification and detection. For the flow-cytometry subsystem, small "capture" beads 5 μm in diameter are coated with antibodies specific to the target pathogens. The beads are color-coded according to which antibodies they hold. Once the pathogens attach to their respective antibodies, more antibodies (labeled with a fluorescent dye), are added to the mixture. A labeled antibody will stick to its respective pathogen, creating a sort of bead sandwich—antibody, pathogen, and labeled antibody. The beads flow one by one through a flow cytometer, which illuminates each bead in turn with a laser beam. Any bead with labeled antibodies will fluoresce. The system can then identify which agents are present, depending on the color of the capture bead.

Advantages include:(1) the ability to measure up to 100 different agents and controls in a single sample; (2) the flexibility and ease with which new bead-based assays can be developed and integrated into the system; (3) low false-positive and false-negative detection due to the presence of two orthogonal detection methods; (4) the ability to use

the same basic system components for multiple deployment architectures; (v) the relatively low cost per assay and minimal consumables.

2.10 Conclusion

Endospores have been the focus of intense research for decades and their detection technique can be summarized as a 3-pronged approach. Pasteurization is firstly used to prove the existence of and select for endospores from a sample. Direct recognition and demonstrate of endospore morphology and cellular components can be achieved, with delicate heat or acid pretreatment, using microscopic, fluorimetric and cytometric methods. Analyses of the physiological changes associated with a pasteurized microbial population as responses to dormancy-breaking and germinative signals are good metrics to assess endospore viability. In general, individual methods suffer from various disadvantages that include a lengthy analysis time; high cost of instrumentation; lack of sensitivity; and lack of amenability to the online monitoring and interfering characteristics of environmental samples. Despite the significant improvements that have been made, there is still no ideal biosensor for the detection of endospores. However, determination of DPA has promising results in recent years and can be a potential keynote endospore detection method in the future. True in other scientific fields, a combination of the aforementioned methods is usually entailed to increase our degree of confidence. In conclusion, this chapter reviews the detection technology of the spore-forming members of *Bacillus* and related genera, which are capable of producing a resting cell structure called endospores to survive extremes of time and environment.

2.11 References

1. Fahmy, F., Mayer, F., and Claus, D. Endospores of *Sporosarcina halophila*: characteristics and ultrastructure. *Archives of Microbiology* **140**, 338-342 (1985).
2. Powell, J.F. and Strange, R.E. Biochemical changes occurring during sporulation in *Bacillus* species. *Journal of Biochemistry* **63**, 661-668 (1956).
3. Murrell, W.G., in *The Bacterial Spore*, edited by G. W. Gould (Academic Press, New York, 1969), pp. 245-270.
4. Thompson, R.S. and Leadbetter, E.R. On the isolation of dipicolinic acid form endospores of *Sarcina ureae*. *Archives of Microbiology* **45**, 27-32 (1963).
5. Sarasanandarajah, S., Kunnil, J., Bronk, B.V., and Reinisch, L. Two-dimensional multiwavelength fluorescence spectra of dipicolinic acid and calcium dipicolinate. *Applied Optics* **44**, 1182-1187 (2005).
6. Alimova, A. *et al*. Native fluorescence and excitation spectroscopic changes in *Bacillus subtilis* and *Staphylococcus aureus* bacteria subjected to conditions of starvation. *Applied Optics* **42**, 4080-4087 (2003).
7. Cleary, F.C., Lloyd, C.R., and Powers, L., presented at the Molecular, Cellular and Tissue Engineering, 2002. Proceedings of the IEEE-EMBS Special Topic Conference on, 2002 (unpublished).
8. Nudelman, R., Bronk, B. V., Efrima, S. Fluorescence emission derived from dipicolinic acid, its sodium, and its calcium salts. *Applied Spectroscopy* **54**, 445-449 (2000).
9. Scully, M.O. *et al*. FAST CARS: Engineering a laser spectroscopic technique for rapid identification of bacterial spores. *Proceedings of the National Academy of Sciences of the United States of America* **99**, 10994-11001 (2002).
10. Hills, G.M. Chemical factors in the germination of spore-bearing aerobes - the effect of yeast extract on the germination of *Bacillus anthracis* and its replacement by adenosine. *Biochemical Journal* **45**, 353-362 (1949).
11. Hills, G.M. Chemical factors in the germination of spore-bearing aerobes - the effects of amino acids on the germination of *Bacillus anthracis*, with some observations on the relation of optical form to biological activity. *Biochemical Journal* **45**, 363-370 (1949).
12. Hills, G.M. Chemical factors in the germination of spore-bearing aerobes - observations on the influence of species, strain and conditions of growth. *Journal of General Microbiology* **4**, 38-47 (1950).
13. Setlow, P. Germination and outgrowth. *The Bacterial Spore, vol. II, G. W. Gould and A. Hurst (ed.)*, 211-254 (1983).
14. Gould, G.W. and Hurst, A., *The Bacterial Spore*. (Academic Press, New York, 1969).
15. Janssen, F.W., Lund, A.J., and Anderson, L.E. Colorimetric assay for dipicolinic acid in bacterial spores. *Science* **127**, 26-27 (1958).
16. Morimoto, I. and Tanaka, S. Spectrophotometric determination of iron with 2,6-pyridinedicarboxylic acid and 2,4,6-pyridinecarboxylic acid. *Analytical Chemistry* **35**, 141-144 (1963).
17. Rotman, Y. and Fields, M.L. Chemical composition and heat resistance of *Bacillus strearothermophilus* spores. *Journal of Food Science* **34**, 345 (1969).
18. Hindle, A.A., Hall, E. A. H. Dipicolinic acid (DPA) assay revisited and appraised for spore detection. *Analyst* **124**, 1599-1604 (1999).
19. Shafaat, H.S. and Ponce, A. Applications of a rapid endospore viability assay for monitoring UV inactivation and characterizing Arctic ice cores. *Applied and Environmental Microbiology* **72**, 6808-6814 (2006).
20. Yung, P.T., Shafaat, H.S., Connon, S.A., and Ponce, A. Quantification of viable endospores from a Greenland ice core. *FEMS Microbiology Ecology* **59**, 300-306 (2007).
21. Singh, A., Kuhad, R.C., Sahai, V., and Ghosh, P. Evaluation of biomass. *Advances in biochemical engineering/biotechnology*. **51**, 47-70 (1994).
22. Heid, C.A., Stevens, J., Livak, K.J., and Williams, P.M. Real time quantitative PCR. *Genome Research* **6**, 986 (1996).
23. Higgins, J.A. *et al*. A handheld real time thermal cycler for bacterial pathogen detection. *Biosensors & Bioelectronics* **18**, 1115-1123 (2003).
24. Castro, A. and Okinaka, R.T. Ultrasensitive, direct detection of a specific DNA sequence of *Bacillus anthracis* in solution. *Analyst* **125**, 9-11 (1999).
25. Pettipher, G.L. and Rodrigues, U.M. Rapid enumeration of bacteria in heat-treated milk and milk products using a membrane filtration-epifluorescent microscopy technique. *Journal of Applied Microbiology* **50**, 157-166 (1981).
26. Pettipher, G.L. Review: The direct epifluorescent filter technique. *International Journal of Food Science and Technology* **21**, 535-546 (1986).
27. Couto, J.A. and Hogg, T. Evaluation of a commercial fluorochromic system for the rapid detection and estimation of wine lactic acid bacteria by DEFT. *Letters in Applied Microbiology* **28**, 23-26 (1999).
28. Decker, E.M. The ability of direct fluorescence-based, two-colour assays to detect different physiological states of oral streptococci. *Letters in Applied Microbiology* **33**, 188-192 (2001).
29. Schaeffer, A.B. and Fulton, M.D. A simplified method of staining endospores. *Science* **77**, 194-194 (1933).
30. Bartholomew, J.W. and Mittwer, T. A simplified bacterial spore stain. *Biotechnic and Histochemistry* **25**, 153-156 (1950).

31. Claus, D. and Berkeley, R.C.W., in *Bergey's Manual of Systematic Bacteriology*, edited by P. H. A. Sneath, N. S. Mair, M. E. Sharpe et al. (The Williams & Wilkins Co., Baltimore, 1986), Vol. 2, pp. 1105-1139.
32. Warth, A.D. Liquid chromatographic determination of dipicolinic acid from bacterial spores. *Applied and Environmental Microbiology* **38**, 1029-1033 (1979).
33. Fitz-James, P.C., Robinow, C.F., and Bergold, G.H. Acid hydrolysis of the spores of *B. cereus*; a correlation of chemical and cytological findings. *Biochimica et Biophysica Acta* **14**, 346-355 (1954).
34. Robinow, C.F. Observations on the structure of *Bacillus* spores. *Journal of General Microbiology* **5**, 439-457 (1951).
35. Woese, C. and Morowitz, H.J. Kinetics of the release of dipicolinic acid from spores of *Bacillus subtilis*. *Journal of Bacteriology* **76**, 81-83 (1958).
36. Sacks, L.E. Chemical germination of native and cation-exchanged bacterial spores with trifluoperazine. *Applied and Environmental Microbiology* **56**, 1185-1187 (1990).
37. Powell, E. The appearance of bacterial spores under phase-contrast illumination. *Journal of Applied Bacteriology* **3**, 342-348 (1957).
38. Pulvertaft, R.J.V. and Haynes, J.A. Adenosine and spore germination: phase contrast studies. *Journal of General Microbiology* **5**, 657-663 (1951).
39. Lewis, J.C., Snell, N.S., and Burr, H.K. Water permeability of bacterial spores and the concept of a contratile cortex. *Science* **132**, 544-545 (1960).
40. Ross, K.F.A. and Billing, E. *Journal of General Microbiology* **13**, 119 (1957).
41. Rowley, D.B. and Feeherry, F. Conditions affecting germination of Clostridium botulinum 62A spores in a chemically defined medium. *Journal of Applied Bacteriology* **104**, 1151-1157 (1970).
42. Levinson, H.S. and Hyatt, M.T. Sequence of events during Bacillus megaterium spore germination. *Journal of Bacteriology* **91**, 1811-1818 (1966).
43. Hitchins, A.D., Kahn, A.J., and Slepecky, R.A. Interference contrast and phase contrast microscopy of sporulation and germination of Bacillus megaterium. *Journal of Bacteriology* **96**, 1811-1817 (1968).
44. Vary, J.C. and Halvorson, H.O. Kinetics of germination of *Bacillus* spores. *Journal of Bacteriology* **89**, 1340-1347 (1965).
45. Hashimoto, T., Frieben, W.R., and Conti, S.F. Microgermination of *Bacillus cereus* spores. *Journal of Bacteriology* **100**, 1385-1392 (1969).
46. Hashimoto, T., Frieben, W.R., and Conti, S.F. Germination of single bacterial spores. *Journal of Bacteriology* **98**, 1011-1020 (1969).
47. Leuschner, R.G.K. and Lillford, P.J. Effects of temperature and heat activation on germination of individual spores of Bacillus subtilis. *Letters in Applied Microbiology* **29**, 228-232 (1999).
48. Caipo, M., Duffy, S., Zhao, L., and D., S. *Bacillus megaterium* spore germination is influenced by inoculum size. *Journal of Applied Microbiology* **92**, 879-884 (2002).
49. Lloyd, D., *Flow Cytometry in Microbiology*. (Springer-Verlag, New York, 1993).
50. Davey, H.M. and Kell, D.B. Flow cytometry and cell sorting of heterogeneous microbial populations: the importance of single-cell analyses. *Microbiology and Molecular Biology Reviews* **60**, 641 (1996).
51. Shapiro, H.M., in *Flow Cytometry for Biotechnology*, edited by L. A. Sklar (Oxford University Press, 2005).
52. Silley, P. and Forsythe, S. Impedance microbiology - a rapid change for microbiologists. *Journal of Applied Microbiology* **80**, 233-243 (1996).
53. Beezer, A.E., *Biological Microcalorimetry*. (New York: Academic Press, London, 1980).
54. Morgan, T.D., Beezer, A.E., Mitchell, J.C., and Bunch, A.W. A microcalorimetric comparison of the anti-*Streptococcus mutans* efficacy of plant extracts and antimicrobial agents in oral hygiene formulations. *Journal of Applied Microbiology* **90**, 53-58 (2001).
55. McElroy, W.D. The energy source for bioluminescence in an isolated system. *PNAS* **33**, 342-345 (1947).
56. McElroy, W.D. Factors influencing the response of the bioluminescent reaction to ATP. *Archives of Biochemistry* **22**, 420 (1949).
57. Karl, D.D.M. Cellular nucleotide measurements and applications in microbial ecology. *Microbiological reviews* **44**, 739-796 (1980).
58. Chappelle, E.W. and Levin, G.V. Use of the firefly bioluminescence reaction for rapid detection and counting of bacteria. *Biochem. Med* **2**, 41-52 (1968).
59. Thore, A.A., Ansehn, S.S., Lundin, A.A., and Bergman, S.S. Detection of bacteriuria by luciferase assay of adenosine triphosphate. *Journal of clinical microbiology* **1**, 1-8 (1975).
60. Cross, J. Harnessing the firefly. *Food Manufacture* **67**, 25 (1992).
61. Hattori, N.N. *et al*. Enhanced microbial biomass assay using mutant luciferase resistant to benzalkonium chloride. *Analytical biochemistry* **319**, 287-295 (2003).
62. Philip, E.S. A review of bioluminescent ATP techniques in rapid microbiology. *Journal of Bioluminescence and Chemiluminescence* **4**, 375-380 (1989).
63. Church, B.D. and Halvorson, H. Intermediate metabolism of aerobic spores: I. Activation of glucose oxidation in spores of *Bacillus cereus* var *terminalis*. *Journal of Bacteriology* **73**, 470-476 (1957).

64. Setlow, P. and Kornberg, A. Biochemical studies of bacterial sporulation and germination. XXII. Energy metabolism in early stages of germination of *Bacillus megaterium* spores. *Journal of Biological Chemistry* **245**, 3637-3644 (1970).
65. Setlow, P. and Kornberg, A. Biochemical studies of bacterial sporulation and germination. XXIII. Nucleotide metabolism during spore germination. *Journal of Biological Chemistry* **245**, 3645-3652 (1970).
66. Kodaka, H., Fukuda, K., Mizuochi, S., and Horigome, K. Adenosine triphosphate content of microorganisms related with food spoilage. *Japanese Journal of Food Microbiology* **13**, 29-34 (1996).
67. Jenkinson, H.F., Kay, D., and Mandelstam, J. Temporal dissociation of late events in Bacillus subtilis sporulation from expression of genes that determine them. *J. Bacteriol.* **141**, 793-805 (1980).
68. Makino, S., Ito, N., Inoue, T., Miyata, S., and Moriyama, R. A spore-lytic enzyme released from Bacillus cereus spores during germination. *Microbiology* **140**, 1403-1410 (1994).
69. Henriques, A.O. and Moran, C.P. Structure and assembly of the bacterial endospore coat. *Methods: A Companion to Methods in Enzymology* **20**, 95-110 (2000).
70. Webster, J.J., Walker, B.G., Ford, S.R., and Leach, F.R. Determination of sterilization effectiveness by measuring bacterial growth in a biological indicator through firefly luciferase determination of ATP. *Journal of Bioluminescence and Chemiluminescence* **2**, 129-133 (1998).
71. Singh, R.P., Setlow, B., and Setlow, P. Levels of small molecules and enzymes in the mother cell compartment and the forespore of sporulating *Bacillus megaterium*. *Journal of Bacteriology* **130**, 1130-1138 (1977).
72. Santo, L.Y. and Doi, R.H. Ultrastructural analysis during germination and outgrowth of Bacillus subtilis spores. *Journal of Bacteriology* **120**, 475-481 (1974).
73. Fujinami, Y. *et al*. Sensitive detection of bacteria and spores using a portable bioluminescence ATP measurement assay system distinguishing from white powder materials *Journal of Health Science* **50**, 126-132 (2004).
74. Hausenbauer, J.M., Waites, W.M., and Setlow, P. Biochemical properties of *Clostridium bifermentans* spores. *Journal of Bacteriology* **129**, 1148-1150 (1977).
75. Wuytack, E.Y., Boven, S., and Michiels, C.W. Comparative study of pressure-induced germination of *Bacillus subtilis* spores at low and high pressures. *Applied and Environmental Microbiology* **64**, 3220-3224 (1998).
76. Venkateswaran, K., Hattori, N., La Duc, M.T., and Kern, R. ATP as a biomarker of viable microorganisms in clean-room facilities. *Journal of Microbiological Methods* **52**, 367-377 (2003).
77. Leach, F.R. and Webster, J.J. Commercially available firefly luciferase reagents. *Methods in Enzymology* **133**, 51-70 (1986).
78. Griffiths, M.W. The role of ATP bioluminescence in the food industry: New light on old problems. . *Food Technology* **50**, 64-66 (1996).
79. Griffiths, M.W. Applications of bioluminescence in the dairy industry. *Journal of Dairy Science* **76**, 3118-3125 (1993).
80. Ugarova, N.N., Brovko, Y.L., and Kutuzova, G.D. Bioluminescence and bioluminescent analysis: recent development in the field. *Biokhimiya* **58**, 1351-1372 (1993).
81. Basol, M.S. and Gogus, U. Methods of antibiotic applications related to microbiological quality of lamb by PCA and bioluminescence. *Journal of Food Science* **61**, 348-349 (1996).
82. Schuch, R., Nelson, D., and Fischetti, V.A. A bacteriolytic agent that detects and kills *Bacillus anthracis*. *Nature* **418**, 884-889 (2002).
83. Stopa, P.J., Tieman, D., Coon, P.A., Milton, M.M., and Paterno, D. Detection of biological aerosols by luminescence techniques. *Field Analytical Chemistry & Technology* **3**, 283-290 (1999).
84. Quastel, J.H. and Whetham, M.D. Dehydrogenations produced by resting Bacteria. I. *Biochem. J* **19**, 520 (1925).
85. Hurwitz, S.J. and McCarthy, T.J. 2, 3, 5-Triphenyltetrazolium chloride as a novel tool in germicide dynamics. *Journal of Pharmaceutical Sciences* **75**, 912-916 (1986).
86. Song, J.M., Culha, M., Kasili, P.M., Griffin, G.D., and Vo-Dinh, T. A compact CMOS biochip immunosensor towards the detection of a single bacteria. *Biosens Bioelectron* **20**, 2203-2209 (2005).
87. Jago, P.H. *et al*. An evaluation of the performance of ten commercial luminometers. *Journal of Bioluminescence and Chemiluminescence* **3**, 131-145 (1989).
88. Phillips, A.P. and Martin, K.L. Immunofluorescence analysis of *Bacillus* spores and vegetative cells by flow cytometry. *Cytometry* **4**, 123-131 (1983).
89. Phillips, A.P. and Martin, K.L. Dual-par arnet er scatter-flow immunofluorescence analysis of *Bacillus* spores. *Cytometry* **6**, 124-129 (1985).
90. Phillips, A.P. and Martin, K.L. Investigation of spore surface antigens in the genus *Bacillus* by the use of polyclonal antibodies in immunofluorescence tests. *Journal of Applied Microbiology* **64**, 47-55 (1988).
91. Stopa, P.J. The flow cytometry of Bacillus anthracis spores revisited. *Cytometry* **41**, 237-244 (2000).
92. Zahavy, E., Fisher, M., Bromberg, A., and Olshevsky, U. Detection of frequency resonance energy transfer pair on double-labeled microsphere and *Bacillus anthracis* spores by flow cytometry. *Applied and Environmental Microbiology* **69**, 2330-2339 (2003).
93. Lester, E.D. and Ponce, A. An anthrax "smoke" detector: Online monitoring of aerosolized bacterial spores. *IEEE Engineering in Medicine and Biology Magazine* **21**, 38-42 (2002).

94. Yung, P.T., Lester, E.D., Bearman, G., and Ponce, A. An automated front-end monitor for anthrax surveillance systems based on the rapid detection of airborne endospores. *Biotechnology and Bioengineering* **98**, 864-871 (2007).
95. Lester, E.D., Gregory, B., and Ponce, A. A second-generation anthrax "smoke detector". *IEEE Engineering in Medicine and Biology Magazine* **23**, 130-135 (2004).
96. Eversole, J.D. Continuous bioaerosol monitoring using UV excitation fluorescence: Outdoor test results. *Field Analytical Chemistry and Technology* **5**, 205-212 (2001).
97. Agranovski, V., Ristovski, Z., Hargreaves, M., Blackall, P. J., Morawska, L. Performance evaluation of the UVAPS: influence of physiological age of airborne bacteria and bacterial stress. *Journal of Aerosol Science* **34**, 1711-1727 (2003).
98. McBride, M.T. *et al*. Autonomous detection of aerosolized *Bacillus anthracis* and *Yersinia pestis*. *Analytical Chemistry* **75**, 5293-5299 (2003).
99. Cheng, Y.S. Detection of bioaerosols using multiwavelength UV fluorescence spectroscopy. *Aerosol Science and Technology* **30**, 186-201 (1999).
100. Brosseau, L.M. Differences in detected fluorescence among several bacterial species measured with a direct-reading particle sizer and fluorescence detector. *Aerosol Science and Technology* **32**, 545-558 (2000).

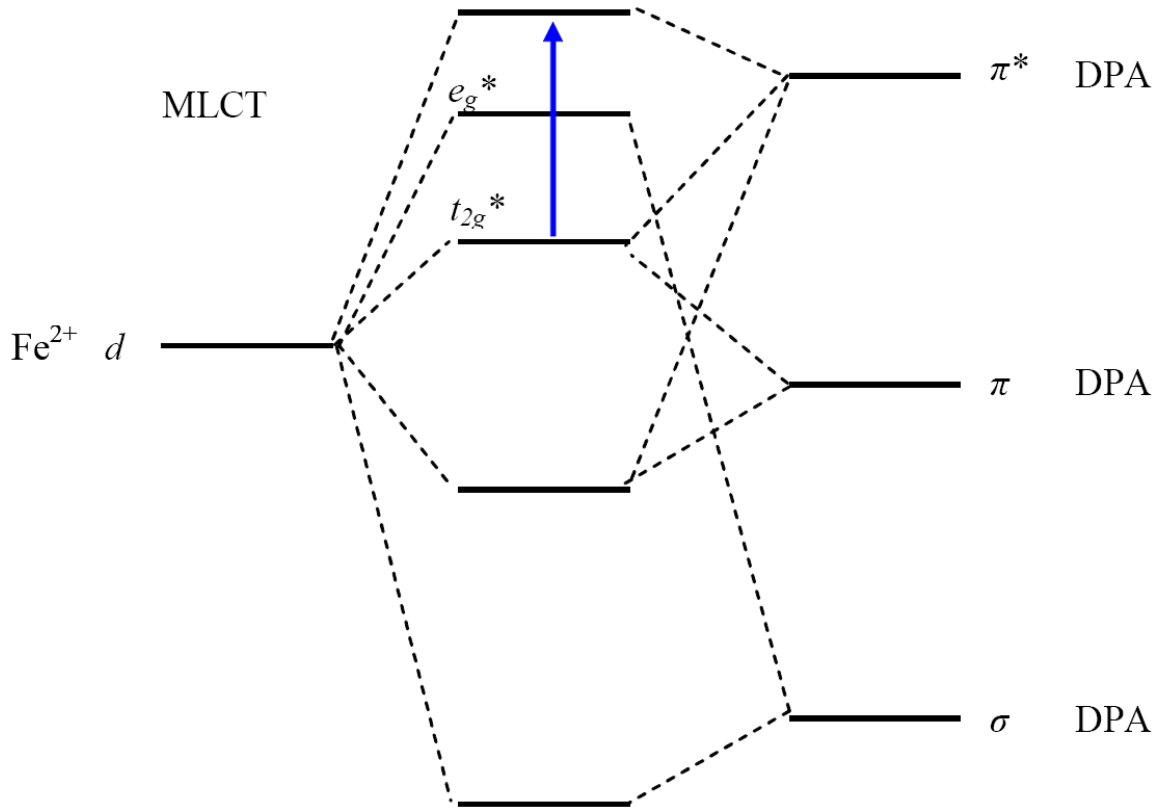

Figure 2.1 | Energy transition of the metal-to-ligand charge transfer (MLCT) between DPA and Fe^{2+}.

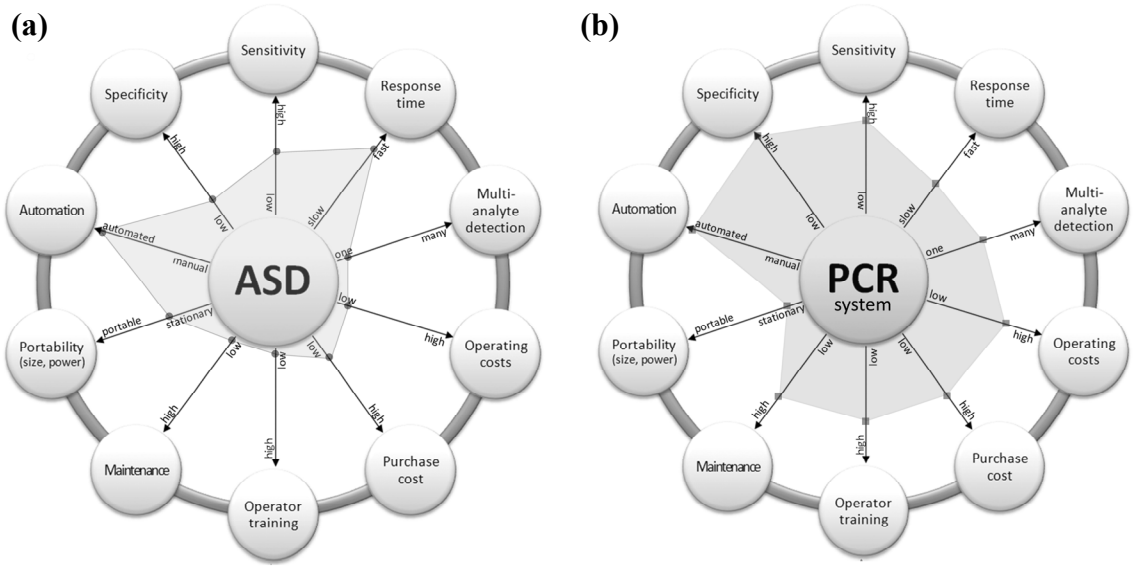

Figure 2.2 | Spider charts illustrating instrument characteristics for **(a)** anthrax smoke detector (ASD) and **(b)** example of a polymerase chain reaction (PCR) system, such as the Biohazard Detection System. These spider charts serve to qualitatively illustrate the relation and potential synergies of characteristics between different instruments. Quantitative comparison will require categories such as portability and specificity to be broken out into measurable subcategories. For example, portability could be quantified in terms of size, mass, and power consumption, and specificity can be quantified in terms of false positive rate and detection confidence. (*Adapted from Figure 7, page 15 in Chemical and Biological Sensor Standards Study by Carrano et al.*).

CHAPTER 3: AN AUTOMATED FRONT-END MONITOR FOR ANTHRAX SURVEILLANCE SYSTEMS BASED ON THE RAPID DETECTION OF AIRBORNE ENDOSPORES[†]

3.1 Abstract

A fully automated anthrax smoke detector (ASD) has been developed and tested. The ASD is intended to serve as a cost-effective front-end monitor for anthrax surveillance systems. The principle of operation is based on measuring airborne endospore concentrations, where a sharp concentration increase signals an anthrax attack. The ASD features an air sampler, a thermal lysis unit, a syringe pump, a time-gated spectrometer, and endospore detection chemistry comprised of dipicolinic acid (DPA)-triggered terbium ion (Tb^{3+}) luminescence. Anthrax attacks were simulated using aerosolized *Bacillus atrophaeus* spores in fumed silica, and corresponding Tb-DPA intensities were monitored as a function of time and correlated to the number of airborne endospores collected. A concentration dependence of 10^2-10^6 spores/mg of fumed silica yielded a dynamic range of 4 orders of magnitude and a limit of detection of 16 spores/L when 250 L of air were sampled. Simulated attacks were detected in less than 15 minutes.

[†] Reprinted with permission from Biotechnology and Bioengineering 2007, 98 (4), 864-871
Pun To Yung[1], Elizabeth D. Lester[1], Greg Bearman[2] & Adrian Ponce[1,2]
[1] California Institute of Technology, Pasadena, CA 91125
[2] Jet Propulsion Laboratory, Pasadena, CA 91101

3.2 Introduction

While the 2001 anthrax attack led to 22 cases of life-threatening infections, including 5 deaths[1], it also taught us that even massive exposures to *Bacillus anthracis* spores can be effectively treated with a simple antibiotic regimen[2]. However, for treatment to be effective it must be initiated soon after exposure. Anthrax progresses over 1-6 days with initial flu like symptoms and leads to high mortality rates within 36 hours after the onset of respiratory distress[3,4]. In the case of an attack, rapid "detect-to-treat" technologies are critical for identifying exposed victims for prompt treatment. Considering the health and economic impacts of an anthrax attack, the need for a rapid, cost effective, and automated anthrax surveillance system remains high but unfulfilled. This need is further amplified by the possibility of a scaled-up attack, where for example, it has been estimated that a 100 kg release of *B. anthracis* spores in Washington, D.C. would result in up to 3 million deaths [5].

In general, an anthrax surveillance system requires a method of bioaerosol sampling[6-9] coupled with an analysis method with high specificity and sensitivity for detecting *B. anthracis* spores. Rapid analysis methods based on nucleic acid or antigen detection are under intense investigation for this application, and have been reviewed in detail [10,11]. In one of the most promising examples, the U.S. Postal Service has employed an anthrax surveillance system, named the Biohazard Detection System, which is based on real-time PCR with fully automated microfluidic sample handling developed by Cepheid[12]. However, the cost of continuous operation due to reagent consumption and maintenance is exceedingly high given the number of postal facilities in need of monitoring[13]. In an effort to reduce the operation costs of an anthrax surveillance system

by approximately two orders of magnitude, we have developed and tested an automated anthrax smoke detector (ASD) that measures airborne bacterial spores using an air sampler coupled to a simple, robust, and inexpensive chemical test. The ASD is intended to serve as a front-end monitor for species-specific anthrax surveillance systems, where in the case of a bacterial spore event, the ASD triggers the expensive-to-operate validation technology to confirm the result.

The ASD employs a rapid chemical test for the detection of bacterial spores based on dipicolinic acid (DPA)-triggered terbium ion (Tb^{3+}) luminescence[14-18], which is closely related to a colorimetric assay first developed in 1958[19]. DPA is present in high concentrations (up to 1 molar, ~15% of dry weight) in the core of bacterial spores[20]. For all known life forms, DPA is unique to bacterial spores and can thus be used as an indicator molecule for the presence of bacterial spores[21]. Thermal lysis (i.e., rupture) of spores *via* dry heat or autoclaving efficiently releases DPA into the surrounding matrix[19,22], which enables DPA to bind to terbium ions with high affinity. Under UV excitation, the Tb-DPA complex formation triggers intense green luminescence[14-17,23] (Figure 3.1), signaling the presence of bacterial spores. Luminescence intensities can then be correlated to bacterial spore concentrations[24].

The ASD implementation of the terbium luminescence assay in conjunction with an aerosol capture device, thermal induced bacterial spore lysis, and a miniature time-gated spectrometer enables inexpensive and fully automated measurement of airborne bacterial spores every 15 minutes. While in operation, the ASD samples 16.7 L of air per minute and collects micron-sized particles, including airborne bacterial spores if present, onto a meshed quartz fiber tape. After collection, the sample is automatically processed with

the thermal lysis unit at ~250˚C to release DPA from any captured spores. Addition of the $TbCl_3$ reagent solution *via* syringe pump forms the luminescent Tb-DPA complex. Finally, the Tb-DPA luminescence intensity is measured under pulsed UV excitation using the time-gated spectrometer. A sharp increase in airborne bacterial spore concentration is a strong signature of an anthrax attack, because (1) bacterial spores, rather than the vegetative cells are capable of surviving in the atmosphere[25] and are thus excellent vehicles for *B. anthracis* dispersal, and (2) natural background concentrations are very low, varying between 0.01 and 1 spore/L [26].

Here we report the first fully automated application of the ASD [23,27] for monitoring aerosolized bacterial spore concentrations during a simulated anthrax attack with surrogate *B. atrophaeus* spore powders.

3.3 Materials and Methods

3.3.1 Chemicals

Pyridine-2,6-dicarboxylic acid (99%), terbium (III) chloride hexahydrate, 99.999%, fluorescein and fumed silica were purchased from Aldrich (St. Louis, MO) and were used as received. 1 M sodium acetate buffer was prepared and an equal concentration of acetic acid was added until pH 5.8 was obtained. Tb-DPA solutions were prepared in 3.5-ml disposable methacrylate cuvettes (Perfector Scientific, Atascadero, CA) for fluorimetric measurement. All solutions were freshly prepared and used within one week using 0.2-μm filter sterilized 18.2 MΩ-cm deionized water (Water Pro Plus, Labconco, Kansas City, MO).

3.3.2 Biological samples

An endospore suspension of *B. atrophaeus* ATCC 9372 was purchased from Raven Biological Laboratory, Inc. (Omaha, Nebraska). Stock suspension used in this study contained $3.1\times10^{10} \pm 4.5\times10^{9}$ spores/ml counted with a hemocytometer (Hausser Scientific, Horsham, PA) under phase contrast microscopy, as well as $1.4\times10^{10} \pm 8.9\times10^{8}$ CFU/ml counted by tryptic soy agar spread plating. Spores, maintained in 40% ethanol at 4°C before use, were purified from vegetative cells fragments and free DPA in the suspension by centrifuging at 13,200 rpm for 10 minutes, washing and resuspending in deionized water twice. Pure spore suspension was sterilized in an autoclave (Tuttnauer 2540E, Brinkmann Instruments, Inc., Westbury, NY) at 124°C for 15 minutes to release DPA. The suspension was cooled and acidified with 1 N hydrochloric acid to reach pH 1.0. Cell debris was removed *via* filtering through a 0.2-μm filter. The filtrate was subsequently neutralized with 1 N sodium hydroxide and represented the autoclaved spore sample.

3.3.3 Anthrax Smoke Detector

The ASD is operated in full automation with a software interface implemented in LabVIEW™ 7. Figure 3.2 shows a schematic of the ASD system, which consists of 5 components:

Spooling mechanism (Metone, Grants Pass, OR). A roll of quartz tape (Whatman, Florham Park, NJ) installed on the spool was advanced through five sample collection and processing stages in series. In the first position, air samples were collected onto a

spot on the filter tape. The tape was then advanced to the second position for thermal lysis of the collected spores. In the third position, a drop of $TbCl_3$ solution was added. Finally, in the fourth position, spore concentration was quantified using Tb-DPA luminescence assay with the time-gated spectrometer. When this sequence of monitoring is completed, used tape would be wound up in another roll to serve as a physical history of the sampling record that can be retrieved at a later point in time.

Air sampler (Metone, Grants Pass, OR). The impaction air sampler applied suction to draw air through the tape at a rate of 16.7 liters per minute. Duration of air sampling is adjustable to suit different purposes. Aerosol was collected onto a circular spot (~7 mm) on the tape.

Thermal spore lysis unit. A soldering iron with a 1-cm diameter cylindrical tip was motor-driven to press against the filter tape. The iron contact time with the sample on the tape was 10 seconds at 250°C (operated at 30W).

Reagent ($TbCl_3$) addition pump. A syringe pump (PSD/4, Hamilton, Reno, NV) supplied 20 µl of $TbCl_3$ through a delivery nozzle onto the sample spot.

Time-gated spectrometer. Samples impregnated on the tape were analyzed by the spectrometer, with details as follows:

3.3.4 Spectrometry

The spectrometer consists of a 24 W pulsed xenon flashlamp (FWHM ~5 µs and tailing out to ~50 µs), a photomultiplier tube (Hamamatsu R6353P, Bridgewater, NJ), 2 concave aluminum mirrors and 2 bandpass filters (Figure 3.3). Pulsed excitation light at 10Hz was focused on samples with a concave aluminum turning mirror and band-limited by an

interference filter (50% pass bandwidth 255–280 nm, 23% maximum transmittance). Luminescence from the sample traversed through a bandpass filter (50% pass bandwidth 538–553 nm, 70% maximum transmittance) and another concave aluminum mirror to enter the PMT. The filter set was chosen to overlap with the excitation and emission spectra of Tb-DPA (Figure 3.3). Time gating was achieved by a delayed detection of the sample luminescence after each flash, according to a chosen delay time. Throughout all measurements in this study, the PMT was operated at 950 V, photocathode aperture set to be 15 mm × 10 mm, delay and integration time was 100 μs and 2 ms, respectively. The entire assembly was shielded from ambient light using a black anodized aluminum enclosure. The spectrometer was custom constructed by Jobin Yvon, Edison NJ.

Cuvettes and tape matrix were measured at a distance of 15 mm from the spectrometer. Each cuvette had a final concentration of 10 μM $TbCl_3$ with DPA (125 nM to 30.5 pM) or autoclaved spores (4.4×10^5 to 1.0×10^2 spores mL^{-1}) in 1 M sodium acetate buffer at pH 5.8. 20 μL of the aqueous sample was pipetted onto quartz tape, forming a 7-mm spot, for luminescence measurement. Spectrometer reading was taken while the spot remained translucent (i.e., before the solvent evaporated).

3.3.5 Simulated anthrax attack

2.0×10^6 *B. atrophaeus* spores, as counted using a hemocytometer, were suspended in 100% methanol and then inoculated to 20 mg of fumed silica. The slurry was allowed to dry overnight under room temperature with constant shaking. The flocculent powder thus formed was used for spore aerosolization experiment. Aerosolization of bioaerosol was simulated by holding a spatula with 20 mg spore-spiked fumed silica near the air sampler

intake while the pump was on. The air sampler was operated for 1 minute to collect silica onto the quartz filter. Spectrometer reading was taken following thermal lysis and $TbCl_3$ addition. Samples were run in ascending order of concentration to minimize contamination.

3.4 Results

The ASD consists of (1) an air sampler using an air filtration tape made of quartz fiber mesh, (2) a thermal lysis unit that presses a hot element onto the tape to release DPA from captured spores, (3) $TbCl_3$ reagent addition pump, and (4) a time-gated spectrometer for measuring Tb-DPA luminescence intensity. In an effort to characterize ASD performance, the time-gated functionality of the spectrometer was evaluated against a challenging, highly fluorescent background. Then a series of concentration dependence experiments with pure DPA solutions and autoclaved spore suspensions were performed to determine limits of detection under ideal conditions (Figure 3.5). Next we integrated the spectrometer into the ASD system, and measured a calibration curve using known concentrations of *B. atrophaeus* spores doped into fumed silica (i.e., anthrax powder surrogate) that were manually added to the quartz fiber air filtration tape to determine dynamic range and limits of detection under operating conditions. Finally the ASD was activated in automatic mode to monitor airborne spore concentrations. At time zero, simulated anthrax powders, consisting of *B. atrophaeus* in fumed silica, were aerosolized and detected with the ASD (Figure 3.6).

3.4.1 Spectrometer time-gated performance

Short excitation pulses followed by delayed luminescence detection effectively rejects short-lived background fluorescence, which enables the ASD to successfully operate in realistic environments laden with varying concentrations of fluorescent interferents. In an effort to test the time-gated performance of the spectrometer (delay = 100 μs, integration = 2000 μs), the average (n = 5) emission intensities of solutions containing both 250 μM fluorescein (τ_{em} = 4 ns, λ_{ex} = 485 nm, λ_{em} = 530 nm) and 10 μM $TbCl_3$ (τ_{em} = 0.6 – 2.0 ms, λ_{ex} = 278 nm, λ_{em} = 543 nm) were analyzed as a function of DPA concentration = 10 nM to 100 μM) in gated and ungated modes. In the ungated mode, the fluorescein emission intensity masks the Tb-DPA emission, while in the gated mode the Tb-DPA emission follows Beer's law over 4 orders of DPA concentration, thus clearly demonstrating the near complete discrimination of fluorescein emission from that of Tb-DPA.

3.4.2 Quantification of DPA and spores in water

Performance of the time-gated spectrometer in response to pure DPA (Aldrich) and spores as a function of concentration in 10 μM $TbCl_3$ aqueous solution was assessed. Luminescence intensities were measured with a delay of 100 μs. The DPA standard curve was best fit to a linear power fit (R^2 = 0.998) over 3 orders of magnitude (Figure 3.6). Limit of detection (LOD) was calculated as 0.4 nm DPA, based on a 3-σ value corresponding to a confidence level of 90%[28]. The limit of quantitation (LOQ) was calculated as 1.2 nm DPA, based upon 10 times the noise level of the background. The

endospore standard curve was also best fit to a linear power fit ($R^2 = 0.998$) over 3 orders of magnitude yielding LOD and LOQ as 1.0×10^3 and 2.8×10^3 spores/ml, respectively (Figure 3.6).

For autoclaved spore suspensions in water, the concentration of DPA present in solution is proportional to spore concentration. The luminescence intensity of autoclaved spore samples was compared to the DPA standard curve (Figure 3.5), from which we obtained a spore-DPA ratio of 0.343 fmol DPA per *B. atrophaeus* spore that is in good agreement with the reported 0.365 fmol DPA per *B. subtilis* spore[17]. *B. atrophaeus*, formerly known as *B. subtilis* var. *niger* or *B. globigii*[29], is a strain of *B. subtilis*. Performance of the spectrometer with pure DPA solutions and autoclaved spore suspensions is comparable to that of a conventional bench-top fluorimeter.

3.4.3 ASD response to simulated anthrax attack

Figure 3.6 shows the spectrometer standard curve for spore-spiked fumed silica manually added to the ASD quartz filter tape. After thermal lysis and reagent addition, luminescence intensities are linearly correlated to the inoculated spore population in fumed silica ($R^2 = 0.999$). Based on this standard curve, the LOD and LOQ was calculated as 4.0×10^3 and 1.1×10^4 total spore population collected, respectively. Given that air is sampled at a rate of 16.7 L/min for 15 minutes, the theoretical LOD and LOD of the instrument is approximately 16 spores/L and 44 spores/L of air, respectively. Longer sampling times would yield correspondingly improved LOD and LOQ. Figure 3.6 shows the timecourse of an automated operation of the ASD. A simulated anthrax attack consisting of 2.0×10^6 *B. atrophaeus* spores in 20 mg fumed silica was initiated at

time t = 0. A real-time Tb-DPA luminescence intensity spike was noticed, corresponding to 1.3×10^6 total spores collected as determined by comparison to the standard curve (figure 3.5).

3.5 Discussion

The ASD is an integrated and automated air sampling, sample processing, and detection system for airborne bacterial spores, and is intended as an inexpensive front-end monitor for anthrax surveillance systems. The principle of operation is based on the fact that, in an attack, *Bacillus anthracis* is dispersed in bacterial spore form, since vegetative cells cannot survive the desiccation during aerosolization. Therefore, a large increase of airborne bacterial spore concentration is a strong signature of an anthrax attack. In the case of an ASD measurement of a bacterial spore event, confirmatory testing by the anthrax surveillance system (e.g., DNA analysis *via* real-time PCR) would be triggered to validate the ASD result. The combination of the ASD as a front-end monitor with an anthrax surveillance system would drastically cut operating costs (~100-fold) while maintaining low false positive rates of species-specific detection methods.

The ASD employs time-gated detection of long-lived terbium dipicolinate luminescence, which is a sensitive assay for the detection of trace amounts of endospores in real world environments, such as office buildings, subway stations, and post offices. Such environments are filled with a plethora of fluorescent compounds that can confound fluorescence-based assays. Time-gated detection, however, essentially eliminates background fluorescence by taking advantage of the fact that fluorescent compounds

have lifetimes in the nanosecond regime[30], whereas terbium complexes have lifetimes in the millisecond regime[31].

The false positive rate for the ASD is expected to be very low, because false positives due to fluorescent interferents is essentially eliminated with time-gated detection, and false positives due to natural bacterial spore concentration fluctuations (i.e., 0.01-1 bacterial spores per liter of air) are unlikely because they are below the limit of detection. Nonetheless, false positives due to concentrated non-*B. anthracis* spore samples remain possible (e.g., hoax using other species, or *B. thuringiensis* spores used in agriculture), but again these events would be rapidly identified during confirmatory testing by a given anthrax surveillance system.

False negatives due to masking of *B. anthracis* spores by confounding agents are expected to be lower for bacterial spore detection vs. species-specific detection, because DPA is required for spore survival[32,33] while antigen or DNA targets can be modified with molecular biology methods to the extent that detection is compromised but virulence is maintained. Since approximately 10^8 molecules of DPA are present in each bacterial spore, as compared to a few copies of DNA for example, no expensive sample amplification schemes are required which lowers the complexity of the instrument and corresponding costs.

The detection threshold (i.e., LOD) for DPA in aqueous solution when using the Tb-DPA luminescence assay can be limited by instrumentation, such as excitation source (e.g., Xe-flash lamp versus UV LED[34]) or type of detector (e.g., PMT versus CCD), but is ultimately governed by the binding constant between Tb^{3+} and DPA ($K_a = 10^{8.7}$)[35-37]. Indeed, below nanomolar concentration (i.e., ~10^3 spores/mL), the percentage of DPA

molecules bound to Tb^{3+} approaches nil. Since binding is required to trigger the luminescence turn-on, detection below those concentrations is not possible regardless of the excitation source or detection system. We have shown that DPA and spore concentration dependence experiments using a bench-top fluorimeter (Jobin-Yvon Fluorolog-3). The performance by both instruments is comparable, albeit the fluorimeter is equipped with a higher intensity xenon lamp source and double monchromators, suggesting that a simple xenon flashlamp in conjunction with a PMT suffices to obtain the binding constant constrained limit of detection.

The ability to detect 16 spores/L in 15 minutes with full automation and inexpensive operation costs qualifies the ASD as a rapid front-end monitor for anthrax surveillance systems. We contend that bacterial spore is the ideal detection target for a front-end anthrax monitor, because (1) it enables low operating costs, (2) it is going to be the vehicle for anthrax delivery, and (3) false positives due to natural fluctuations are expected to be very rare, and verifiable when coupled with species-specific detection technology. We envision that the ASD will serve as a front-end instrument for anthrax surveillance systems, capable of long-term, cost-effective, unattended monitoring of airborne bacterial spores.

3.6 Conclusion

In conclusion, we have demonstrated quantification of aerosolized bacterial spores with a response time of 15 minutes, a detection limit of 16 spores per liter of air, and a dynamic range of 4 orders of magnitude using a bioaerosol sampler, thermal spore lysis, and a

time-gated spectrometer, which promises tremendous reduction in operating costs for anthrax monitoring.

3.7 References

1. Jernigan, D.B. *et al*. Investigation of bioterrorism-related anthrax, United States, 2001: epidemiologic findings. *Emerging Infectious Diseases* **8**, 1019-1028 (2002).
2. Tahernia, A.C. Treatment of anthrax in children. *Archives of disease in childhood* **42**, 181-182 (1967).
3. Meselson, M. *et al*. The Sverdlovsk anthrax outbreak of 1979. *Science* **266**, 1202-1208 (1994).
4. Weyant, R., Ezzell, J., and Popovic, T. Basic laboratory protocols for the presumptive identification of Bacillus anthracis. *Center for Disease Control* (2001).
5. Office of Technology Assessment, U.C. Proliferation of Weapons of Mass Destruction. *Washington DC: US Government Printing Office*, 53-55. Publication OTA-ISC-559 (1993).
6. Cox, C.S. and Wathes, C.M., *Bioaerosols Handbook*. (Lewis Publishers, Inc., 1995).
7. Griffiths, W.D. and Decosemo, G.A.L. The assessment of bioaerosols: a critical review. *Journal of Aerosol Science* **25**, 1425-1458 (1994).
8. Griffiths, W.D., Stewart, I.W., Futter, S.J., Upton, S.L., and Mark, D. The development of sampling methods for the assessment of indoor bioaerosols. *Journal of Aerosol Science* **28**, 437-457 (1997).
9. Baron, P.A. and Willeke, K., *Aerosol measurement: principles, techniques, and applications*. (Wiley, New York, 2001).
10. Katie, A.E., Harriet, A.C., and Antje, J.B. Bacillus anthracis: toxicology, epidemiology and current rapid detection methods. *Analytical and Bioanalytical Chemistry* **384**, 73-84 (2006).
11. Levine, S.M., Tang, Y.-W., and Pei, Z. Recent advances in the rapid detection of Bacillus anthracis. *Reviews in Medical Microbiology* **16**, 125-133 (2005).
12. Ulrich, M.P. *et al*. Evaluation of the Cepheid GeneXpert® system for detecting Bacillus anthracis. *Journal of Applied Microbiology* **100**, 1011-1016 (2006).
13. Knight, J. US postal service puts anthrax detectors to the test. *Nature* **417**, 579-579 (2002).
14. Pellegrino, P.M., Fell, N.F., and Gillespie, J.B. Enhanced spore detection using dipicolinate extraction techniques. *Analytica Chimica Acta* **455**, 167-177 (2002).
15. Rosen, D.L. Bacterial endospore detection using photoluminescence from terbium dipicolinate. *Reviews in Analytical Chemistry* **18**, 1-21 (1999).
16. Sacks, L.E. Chemical germination of native and cation-exchanged bacterial spores with trifluoperazine. *Applied and Environmental Microbiology* **56**, 1185-1187 (1990).
17. Hindle, A.A. and Hall, E.A.H. Dipicolinic acid (DPA) assay revisited and appraised for spore detection. *Analyst* **124**, 1599-1604 (1999).
18. Rosen, D.L. Airborne bacterial endospores detected by use of an impinger containing aqueous terbium chloride. *Applied Optics* **45**, 3152-3157 (2006).
19. Janssen, F.W., Lund, A.J., and Anderson, L.E. Colorimetric assay for dipicolinic acid in bacterial spores. *Science* **127**, 26-27 (1958).
20. Gould, G. and Hurst, A., *The Bacterial Spore*. (Academic Press, New York, 1969).
21. Slepecky, R. and Foster, J.W. Alterations in metal content of spores of Bacillus megaterium and the effect on some spore properties. *Journal of Bacteriology* **78**, 117-123 (1959).

22. Rotman, Y., Fields, M. L. Release of dipicolinic acid from spores of Bacillus spearothermophilus NCA-1518. *Journal of Food Science* **34**, 343 (1969).
23. Lester, E.D. and Ponce, A. An anthrax "smoke" detector: Online monitoring of aerosolized bacterial spores. *IEEE Engineering in Medicine and Biology Magazine* **21**, 38-42 (2002).
24. Shafaat, H.S. and Ponce, A. Applications of a rapid endospore viability assay for monitoring UV inactivation and characterizing Arctic ice cores. *Applied and Environmental Microbiology* **72**, 6808-6814 (2006).
25. Nicholson, W.L., Munakata, N., Horneck, G., Melosh, H.J., and Setlow, P. Resistance of Bacillus endospores to extreme terrestrial and extraterrestrial environments. *Microbiology and Molecular Biology Reviews* **64**, 548-572 (2000).
26. Pastuszka, J.S., Kyaw Tha Paw, U., Lis, D.O., Wlazlo, A., and Ulfig, K. Bacterial and fungal aerosol in indoor environment in Upper Silesia, Poland. *Atmospheric Environment* **34**, 3833-3842 (2000).
27. Lester, E.D., Gregory, B., and Ponce, A. A second-generation anthrax "smoke detector". *IEEE Engineering in Medicine and Biology Magazine* **23**, 130-135 (2004).
28. Gilfrich, J.V. and Birks, L.S. Estimation of detection limits in x-ray fluorescence spectrometry. *Analytical Chemistry* **56**, 77-79 (1984).
29. Fritze, D. and Pukall, R. Reclassification of bioindicator strains Bacillus subtilis DSM 675 and Bacillus subtilis DSM 2277 as Bacillus atrophaeus. *International Journal of Systematic and Evolutionary Microbiology* **51**, 35-37 (2001).
30. Lakowicz, J.R., *Principles of Fluorescence Spectroscopy*. (Plenum, New York, 1983).
31. Jones, G. and Vullev, V.I. Medium effects on the photophysical properties of terbium(III) complexes with pyridine-2,6-dicarboxylate. *Photochemical & Photobiological Sciences* **1**, 925-933 (2002).
32. Church, B.D. and Halvorson, H. Dependence of the heat resistance of bacterial endospores on their dipicolinic acid content. *Nature* **183**, 124-125 (1959).
33. Paidhungat, M., Setlow, B., Driks, A., and Setlow, P. Characterization of spores of Bacillus subtilis which lack dipicolinic acid. *Journal of Bacteriology* **182**, 5505-5512 (2000).
34. Li, Q.Y. *et al*. Mid-ultraviolet light-emitting diode detects dipicolinic acid. *Applied Spectroscopy* **58**, 1360-1363 (2004).
35. Grenthe, I. Stability relationships among the rare earth dipicolinates. *Journal of the American Chemical Society* **83**, 360-364 (1961).
36. Cable, M.L., Kirby, J.P., Sorasaenee, K., Gray, H.B., and Ponce, A. Bacterial spore detection by [Tb3+ (macrocycle)(dipicolinate)] luminescence. *Journal of American Chemical Society***, accepted**.
37. Cable, M.L., Kirby, J.P., Sorasaenee, K., Gray, H.B., and Ponce, A. Bacterial spore detection by [Tb^{3+}(macrocycle)(dipicolinate)] luminescence. *Journal of American Chemocal Society* **129**, 1474-1475 (2007).

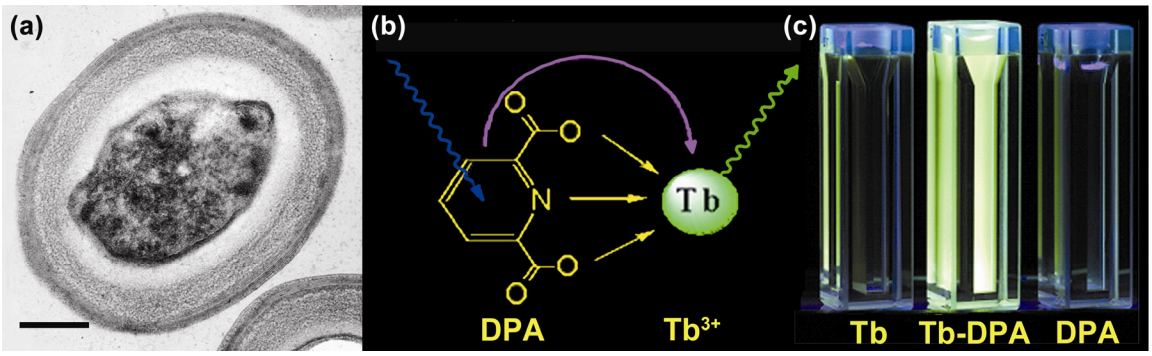

Figure 3.1 (a) Electron micrograph of an endospore of *Geobacillus stearothermophilus*. A large depot of DPA is deposited at the spore core, comprising ~15% of dry weight. *Courtesy of Stuart Pankratz.* **(b)** General spore detection mechanism based on DPA-triggered Tb-luminescence. DPA binds to Tb ions with a high binding constant. DPA has a high molar extinction coefficient and efficiently transfers energy to Tb ion, triggering an intense green luminescence with an enhancement of more than 20,000 times. **(c)** Demonstration of DPA-triggered Tb-luminescence in quartz cuvettes bottom illuminated by a mercury UV lamp.

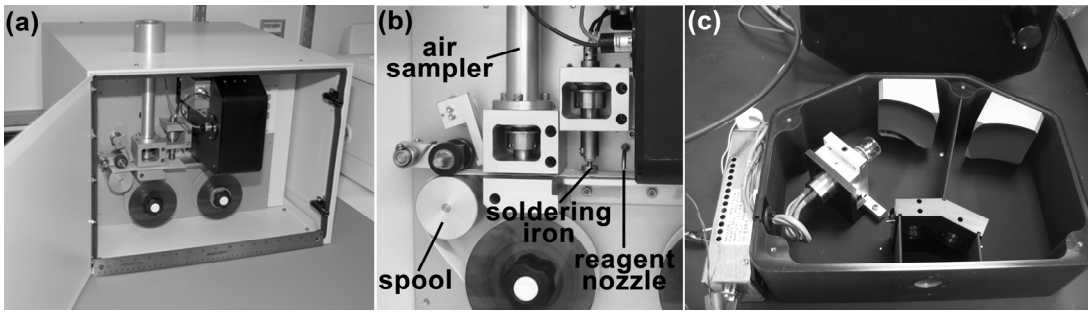

Figure 3.2 Anthrax Smoke Detector **(a)** Anthrax Smoke Detector (ASD) enclosed in an 18" cubic stainless steel case. Driven by a vacuum pump, the particulate matter 10 (PM10) inlet head collects airborne particles with diameters of <10 μm onto a quartz fiber tape. **(b)** Close-up view of the ASD highlighting the spooling mechanism for automatic tape advancement, thermal lysis unit, reagent addition nozzle, and time-gated spectrometer. **(c)** Optics of the time-gated spectrometer consisting of a xenon flashlamp (lower left corner), two aluminum concave mirrors, excitation and emission filters, and PMT (upper right corner, on the spectrometer case lid).

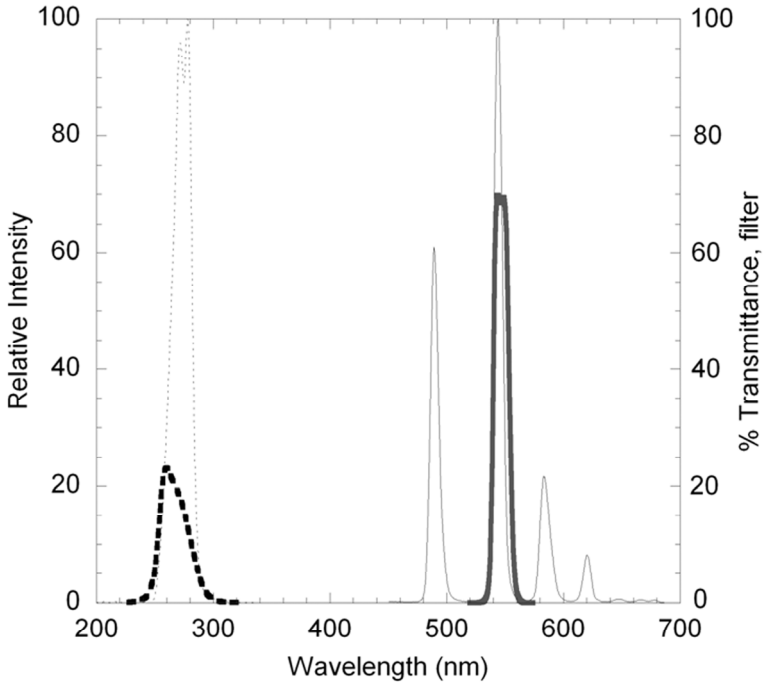

Figure 3.3 Spectral bandpass of emission and excitation filters compared to excitation and emission spectra of terbium dipicolinate. The excitation spectrum of terbium dipicolinate (λ_{em} = 544 nm, 100 μM $TbCl_3$ + 10 μM DPA in 1 M sodium acetate buffer at pH 5.8), and corresponding emission spectrum (λ_{em} = 278 nm) are shown in thin dashed and solid lines, respectively. The transmittance spectra of the excitation and emission interference filters are shown in thick dashed and solid lines, respectively.

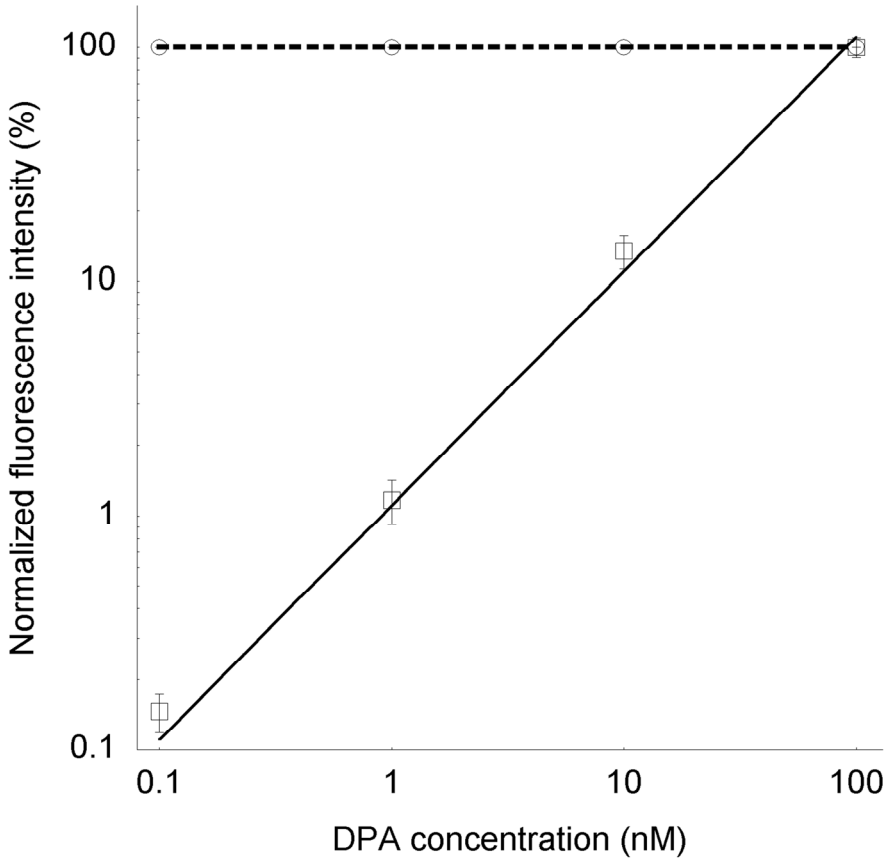

Figure 3.4 DPA concentration dependence of 250 μM fluorescein and 10 μM $TbCl_3$ with (solid line) and without (dashed line) time gating (λ_{ex} = 280 ± 5 nm, λ_{em} = 530 – 550 nm).

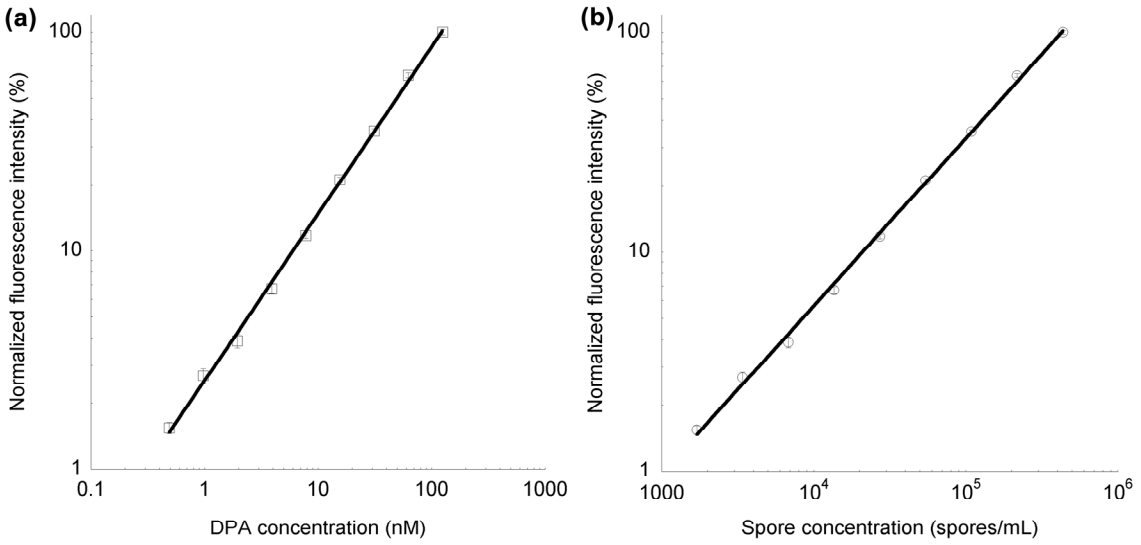

Figure 3.5 Time-gated detection (100 μs delay) of **(a)** DPA and **(b)** spores in 10 μM $TbCl_3$ buffered in 1 M sodium acetate at pH 5.8 (n=5). **(a)** Log-log plot of intensity with DPA concentration. The line represents a power fit, equivalent to a linear fit on a linear scale plot, of the standard curve (R^2 = 0.998). **(b)** Log-log plot of intensity with spore population. The line represents a power fit, equivalent to a linear fit on a linear scale plot, of the standard curve (R^2 = 0.998).

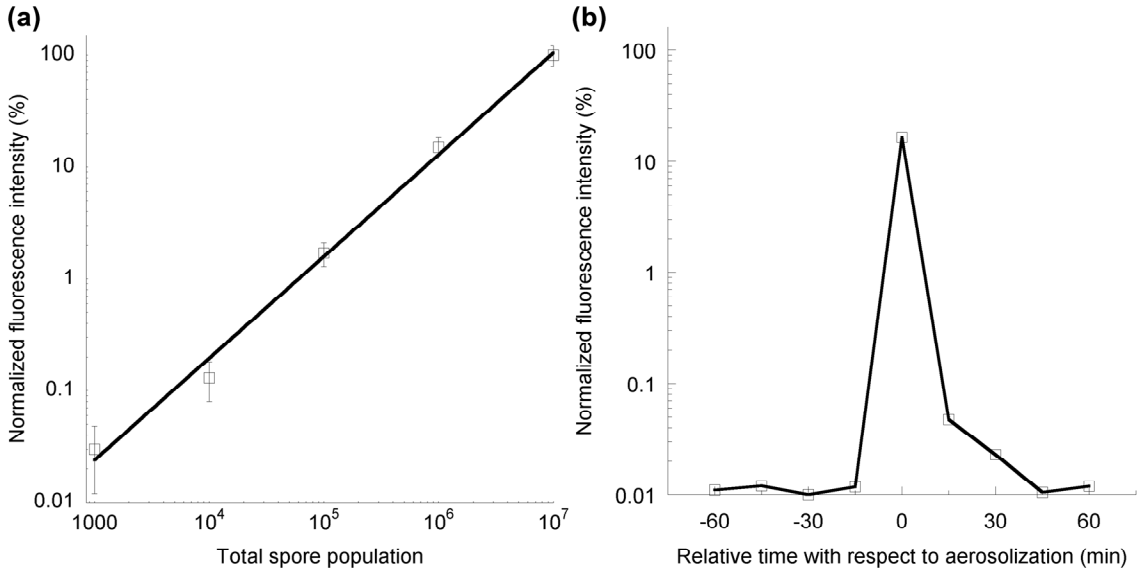

Figure 3.6 Simulated anthrax attack (n=5). **(a)** Standard curve of surrogate *B. atrophaeus* spores aerosolized in fumed silica measured with the ASD. **(b)** An anthrax attack was simulated at time 0 using fumed silica spiked with *B. atrophaeus*. Real-time intensity spike indicates a large increase in airborne spores, corresponding to a total of 1.3 x 10^6 spores being collected.

CHAPTER 4: AIRBORNE ENDOSPORE BIOBURDEN AS AN INDICATOR OF SPACECRAFT CLEANLINESS

4.1 Abstract

Microbiological monitoring in confined spacecraft and space station environments during long-duration manned missions is instrumental to guaranteeing the health, safety and productivity of astronauts and crew members. An autonomous air sampling detector provides early detection of a microbial event for timely decontamination and mitigation. The success of air sampling in a closed-loop habitat will be enhanced if the correlation underlying airborne endospore bioburden (AEB) and total biomass is better understood. In this study, we conduct controlled experiments and investigate the relationship between AEB and total biomass using a two-compartmental model in simulated closed environments. A combination of culture-dependent and culture-independent methods is used. AEB is found to correlate the total biomass in a controlled enclosure under laboratory condition. A positive, but less obvious, correlation was found between AEB and total biomass in daily closed environments. AEB can therefore be used as an indicator of spacecraft cleanliness and bioburden level that the flight crew can tolerate without compromising their health.

4.2 Introduction

Environmental monitoring in closed-loop life support systems has become one of NASA's top priorities since President Bush unveiled that Unites States Space Exploration

Policy in January 2004, which calls for long-term missions to moon and Mars. Microbial monitoring is essential to avoid crew health problems and biodegradation of spacecraft components[1]. A rapid change in microbial concentration indicates a breakdown of environmental control either by allowing conditions that foster microbial growth (e.g., rapid biofilm formation due to temperature, humidity, and nutrient availability) or by a breakdown of environmental control/treatment hardware[2]. These failure modes need to be detected as early as possible. A biosensor instrument is required to investigate the environmental conditions associated with living and working in a spacecraft and how do these measurables affect astronauts' health and well-being. The NASA Advanced Environmental Monitoring and Control Program (AEMC) document for technology development requirements[3] states that (i) "the frequency of microbial monitoring should be once in two days and must not put additional workload on the crew;" (ii) "instrument response time of approximately two hours after collection is a good goal for future technology development;" and (iii) "present methods take days. The long term goal may be set at monitoring the bioparticles on a continuous basis."

Maintaining health in a confined space system over extended periods of time is a challenging microbiological task[4,5]. A general tendency toward increased cell growth, biomass production, and growth rate has been observed with the length of spacecraft[6], accompanied with a significant increase in the airborne microbial counts during flight[7,8]. A decrease in T lymphocytes have been reported on the human immune system[9,10]. In addition there are reports indicating that space flight decreases certain gamma globulins (IgA, IgG) and β-2-glycoprotein fraction[11]. Such findings suggest that the stress of space flight may be accompanied by a transient impairment in functioning at the cellular and

hormonal immune system, which may result in an increased risk of infectious disease during flight[12]. In fact, some of the early missions reported a high incidence of infectious diseases, in some cases over 50%. The most common were gastroenteritis and respiratory, urinary tract, and skin infections. Since that time, comprehensive preflight examinations have decreased the incidence of infections.

NASA's planetary protection program currently uses bacterial spores as indicator species in their surface bioburden reduction analysis required prior to launch of interplanetary spacecraft. Bacterial spores are ideal indicator species to validate bioburden reduction on surfaces, because they are the most resistant life forms towards sterilization regimens and are frequently found on barren spacecraft hardware surfaces[13-15]. Thus, validation of bacterial spore reduction to a certain concentration threshold guarantees that other, less resistant microorganisms are reduced to lower concentrations. In particular, crew members are expected to be exposed continuously to bioaerosol for long periods of time in an enclosed life-support system. Pathogenic endospores are considered more contagious and dangerous than vegetative bacteria because endospores can survive and be transported through air in a dormant yet viable state, anthrax being the most typical example. A question arises here – can airborne endospore bioburden (AEB) be used as an indicator for total biomass in an enclosed system?

Towards these ends, the first prototype Microbial Event Monitor (MEM) has been developed as a rapid and automated airborne endospore monitoring system which consists of an air sampler, a spore lysis system, an endospore-specific fluorescent indicator, and a photon detector. In this study, we will fully characterize the correlation of AEB and total biomass in a laboratory controlled closed environment using novel air

sampler and endospore viability assays. The derived model will be extended to daily indoor environments such as laboratories and offices, and compared with previously results obtained in the Environmental Control and Life Support System (ECLSS) at Marshall Space Flight Center. The correlation has also been testified in the Atacama Desert, the most arid desert and closest Mars analog on Earth. *B. atrophaeus* has long been employed as the model endospores to study aerosolization and dispersal issues. We propose the use of an endospore-forming species, isolated from local Mojave Desert, which possesses delicate aerial colony projections for airborne dispersal of endospores as a new model organism for aerosolization studies.

4.3 Methods and Procedure

4.3.1 Chemicals

Terbium (III) chloride hexahydrate, 99.999%, L-alanine and other salts were purchased from Sigma (St. Louis, MO) and were used as received. Ultrapure^{TM} agarose (> 90%) was purchased from Invitrogen (Carlbad, CA). Tryptic soy agar (TSA), nutrient broth and agar were obtained from Becton, Dicksinon and Company, (Sparks, MD).

4.3.2 Microbiological samples

B. atrophaeus (ATCC 9372) spores were purchased from Raven Biological Laboratories. *B. subtilis*, an environmental isolate from Mojave Desert subsurface soil, vegetative cells were grown on TSA and inoculated onto a sporulation medium after reaching exponential growth phase. The sporulation medium contained 1.6% nutrient broth, 1.6% agar, 0.2%

KCl, 0.05% $MgSO_4$, 1 mM $Ca(NO_3)_2$, 100 μM $MnCl_2 \cdot 4H_2O$, 1 μM $FeSO_4$ and 0.1% glucose (pH 7.0). After incubation at 37°C for 1 week, cells were suspended into sterile deionized water. 95% of the cells have formed spores free of sporangia. Spores were harvested and separated from vegetative cells and debris by centrifugation at 6,300 g, washing 10 times and sonication (25 kHz) for 5 min. The spore suspension was incubated in lysozyme (0.2 mg mL^{-1}) and trypsin (0.1 mg mL^{-1}) at 30°C with constant stirring overnight to lyse and degrade vegetative cells. Spores were purified by 8 cycles of centrifugation (6,300 g) and washed with sterile deionized water until > 99.9% of the cells were fully refractile with no noticeable cellular debris. Spore suspensions were stored at 4°C in the dark before use. Total spore concentrations were determined using a Petroff-Hausser hemocytometer and CFU concentrations were determined using TSA spread plating in triplicate measurements.

4.3.3 Microbial Event Monitor

The MEM is composed of (1) an air sampler that captures airborne spores, (2) a spore lysis component to release the unique chemical marker (dipicolinic acid, DPA) from the spores, and (3) a photon detector that measures the DPA triggered terbium (Tb) luminescence intensity, where the intensity of the luminescence correlates to the concentration of bacterial spores in the sample. The MEM is based on previous work from the development of the Anthrax Smoke Detector (ASD) for bioterrorism countermeasures[16-18], which is based on the same general principles as those described above. The MEM, however, needs to be more sensitive than the ASD, because ambient background concentrations for microbial monitoring range from 0.1 - 1 spores per liter of

air[19], which is much lower than the large changes in spore concentration associated with an anthrax attack. Detailed instrumentation and operating principle of the ASD have been reported previously.

4.3.4 Air Sample Collection

Three air samplers were used in this study, abbreviated as the SAS, MEM and E-BAM (Figure 4.1). The SAS (Surface Air Systems) twin head duo 360 air sampler (Bioscience International, Rockville, MD) uses a standard impaction method to capture airborne particulate on the agar surface of a Petri dish. It is set to sample at a rate of 125 L min^{-1} in this study. The MEM stands for Microbial Event Monitor, which is an all-in-one sensor to measure the airborne endospore concentration as a first prototype to be incorporated in future spacecrafts. It consists of a PM_{10} air inlet that collects airborne particles with an aerodynamic dynamic less than or equal to 10 μm. The sampling rate is 16.7 L min^{-1} in this experiment. The E-BAM (Met One Instruments, Rowlett, Texas) consists of a PM_{10} air inlet and β-attenuation gauge. The radioactive beta source C_{14} is less than 75 microcurie and a half life of 5,730 years. A sampling rate of 16.7 L min^{-1} is used, which is approximately the inhalation rate for human aeroallergens and aeropathogens should collect the same size fraction and concentration as are inhaled and collected by the human respiratory system.

Bioefficiency of the air sampling unit of the 3 air samplers, MEM, SAS and E-BAM, were compared to see if the culturable results were reproducible. The three samplers were operated simultaneously, each sampling 5000 L of air for various amounts of time in an indoor environment. Both the MEM and E-BAM sampled 5 hours onto a

filter tape matrix. Microorganism collected on the filter would be extracted by a 5-min vortexing and 2-min sonication in PBS buffer supplemented with 50 mM sodium pyrophosphate and 0.1% Tween-80. The suspension would be heat treated in an 80°C water bath for 15 min to inactivate vegetative cells and select for endospores before plating on tryptic soy agar (TSA) in triplicate. The SAS collected samples directly onto TSA plates for 30 min in duplicate. From previous experiments, the plates were subsequently dry heated in an oven at 80°C for 120 min in order to kill all vegetative cells, thereby selecting for endospores. Petri dishes were incubated for 72 hours at 37°C. The colonies on each Petri dish were recorded in CFU (colony forming unit), and converted to CFU per liter of air (cfu L^{-1}) subsequently.

Different media may be used depending on the target microorganisms. For instance, R2A would be used to culture environmental microorganisms. Cycloheximide (50 μg mL^{-1}) would be supplemented to the agar to inhibit fungal growth. R2A would usually be incubated at room temperature. Rose bengal agar (RBA) would be used to select for fungal growth at room temperature. Endospores could be screened *via* heat shock of suspension would be carried out in an 80°C water bath for 15 *min* or of agar plates would be carried out in an 80°C dry oven for 120 min. Malt extract agar supplemented with rose bengal and fluid thioglycollate broth to test for the proportion of aerobic, microaerophilic and anaerobic bacteria in a sample.

4.3.5 Determination of total biomass

Surface swab samples were collected by following the NASA standard procedures for the microbial examination of space hardware[20]. The samples were collected using the swab-

rinse method. Autoclaved cotton swabs and water were used in surface sampling. The swabbed surface areas are not greater than 26 cm^2. The solutions of 5 mL were divided 2.5 mL each into heat shocked and non-heat shocked and cultured on R2A plates. Each room was swabbed twice, and each swab was re-suspended into water, vortexed, sonicated, and plated onto culture media. Heat shock and non-heat shock samples were used to compare the vegetative cells and spore formers. The plates were incubated at 37^oC for 3 days. The colonies on each Petri dish were recorded in CFU, and converted to CFU per square centimeter surface (cfu cm^{-2}) subsequently.

Phase-contrast and epi-fluorescence microscopy were applied to assess the total biomass as well. The slides were examined using a Nikon Eclipse microscope equipped with a cooled CCD camera. Acridine orange (0.04% w/v) was used to stain the bacteria. The later were placed on the surface of the staining solution for 2 min. Excess stain was removed by rinsing twice in sterile water for 2 min. The filters were then dried for 10 min before mounting on microscope slides. The microscope used was a Nikon Eclipse epifluorescence microscope equipped with a 100 W xenon lamp. For microscopy, a filter with an excitation wavelength of 450-490 nm was used. Cells were counted with a Nikon Eclipse microscope at 1000× magnification (lamp: xenon, Ex: 450-490, FT 510, LP 515). The filtration volume of 500 μL yielded 20-60 stained cells in the counting grid (125 × 125 nm). A minimum of 400 cells (10-20 fields of view) were enumerated. Images were analyzed using IP-Lab software.

To improve the quality of phase contrast images, the suspension to be tested was diluted approximately to a suitable concentration and several drops (20 μL) were placed individually on marked areas on two or three dried plates of the agarose medium. The

inoculated plates were covered with a glass coverslip. The preparation was examined by light-field phase-contrast illumination under a 60 × oil-immersion objective lens.

4.3.6 Correlating airborne and total biomass in a laboratory-controlled environment

The experiment was carried out inside an enclosed inflatable polyethylene chamber with built-in gloves (27 × 30 in AtmosBag, Sigma). It was a totally isolated environment with temperature ranging from 20.5 - 22.5°C. The interior was disinfected by wiping with full strength bleach (ultra-Chlorox, 6.25% sodium hypochlorite) and thorough rinsing with 0.2-μm filtered water 3 times. The AtmosBag was dried at 70°C in an oven before in AtmosBag was filled up with atmospheric gas with inlet connected to a 0.2-μm filter to a final operating volume of 12 L.

A known number of endospores were suspended in 100% ethanol and dispersed as aerosols by a Lovelace nebulizer (model 01-400) and a vibrating stream generator inside the AtmosBag. The nebulizer was operated at 15 psi. Endospores were allowed to settle down for 30 min after aerosolization. After all, the SAS air sampler was deployed to measure the airborne endospore concentration at a flow rate of 16.7 L min^{-1}. Surface total biomass was evaluated by μEVA, culturing, phase-contrast and epifluorescence microscopies. In addition, passive air sampling was evaluated by placing fallout plates inside the AtmosBag in triplicates, 3 facing upward and 3 mounted upside down.

In order to quantify the representative PM10 values inside the enclosure, active and passive air sampling were carried out at least 10 in away from the fan to avoid hot spots with high traffic volume. Placement of air sampler and Petri dishes is mapped using

conventional geostatistical methods such as construction of a variogram to model the correlation that exists as a function of distance between sampling spots[21,22].

4.3.7 Correlating airborne and total biomass in indoor and outdoor environemnts

The same air and surface total biomass sampling procedure as described above carried out in the following indoor environments: Jet Propulsion Laboratory (JPL) buildings 300-114, 302-336, 302-337, 302-332, 202-101. The 6 sampling sites include: new and old chemistry/microbiology labs, new and old offices, ductless fume hoods, and bio-hood. The air samples are collected using SAS air sampler, and the surface samples are collected using a deviation of NASA standard assay. Each sample is collected four times with one negative control. The error bars are standard error. The heat-shocked data are too low in counts to do any significant statistical analysis, while the non-heat shocked data have higher counts. The data presented will all be from the non-heat shock results.

A second experiment was conducted to validate the hypothesis, that bacterial spore concentration represents total microbial contamination, on which the microbial event monitor is based. Samples were taken of the microbial content of the air and surfaces in a spacecraft relevant environment (MSFC simulated cabin) including airborne bacterial spores. Sampling began one day prior to occupation, with chamber sealed for 24 hours to allow for equilibration. Sampling continued on days 1, 6, 9 and 14 of occupation. In addition, a one-day time course of sampling was conducted on day 6, at 5:00, 5:30, 6:00, 8:00, 10:00, 12:00, 14:00, 16:00, 18:00, 18:30 and 19:00 during normal operation of the facility. All sampling was conducted at the rear right section of the cabin.

Outdoor environments include Yungay in Atacama Desert, Chile (S 24° 04.941' W 069° 55.167', elevation 959 m). The E-BAM machine was not used in outside air sampling because of its bulkiness. The SAS sampler was positioned 1 foot above the ground and in a specific orientation such that the left sampling head always faced the windward side and the right sampling head always faced the leeward side. Outdoor air samples were collected at different times of day over a 5-day period. Minimal activity occurred during sample collection. Weather station was used to track the environmental physical changes. Fallout plates were prepared in the form of PDMS (polydimethylsiloxane) film inside Petri dishes and left exposed in the desert for 12 hours day or night. PDMS is a hydrophobic and highly adhesive silicone-based polymer used as a collection substrate for fallout bacteria. After collection, PDMS films were peeled and plated directly onto R2A plates with sterile tweezers.

4.3.8 Comparison of biofilm-forming environmental isolate with lab-strain *B. subtilis*

The environmental-strain *B. subtilis* formed dark brown fruiting bodies on full strength TSA incubated at 37°C in 3 day, whereas the lab-strain *B. subtilis* formed smooth milky colonies. Both laboratory and environmental strains were induced to germinate in a defined medium. Determination of size, hydrophobicity, wet density, DPA content and germination kinetics were reported earlier.

4.3.9 Data Analysis

The number of bacterial colony forming units (CFU) on each plate was adjusted for multiple impaction using a positive hole conversion table as needed. Data were converted to CFU per liter of air. The F test (two-way analysis of variance) was used to determine whether significant differences in the number of CFU per liter per sampling session existed among the sampling devices and sampling locations. The Student-Newman-Keuls (SNK) multiple comparison test was used to make pairwise comparisons to determine more specifically which sampling devices or locations differed from one another. The data analyses were performed using Matlab.

The plate count result in this experiment follows two different distributions depending on the mean count per plate. When mean count is < 10, it follows a Poisson distribution; otherwise, it is a normal distribution. In a Poisson distribution, 95% confidence interval can be obtained from a statistical table. In a normal distribution, 95% confidence interval is calculated using the well-defined mean and standard deviation.

The positive-hole correction method determines a statistical probability count of colony-forming units[23]. It represents a count of the jets that delivered the endospores to the agar plates and the conversion of the jet number to a particle count by using the "positive hole" conversion formula.

$$\mathrm{Pr} = \mathrm{N} \times \sum_{\mathrm{x}=0}^{\mathrm{r}+1} \left(\frac{1}{\mathrm{N}-\mathrm{x}}\right),$$

where *Pr* is the expected number of viable particulates to produce *r* positive holes and *N* is the total number of holes per stage. This formula is based on the principle that as the number of viable particles being impinged on a given plate increases, the probability of the next particle going into an unpenetrated hole decreases. Thus, when 9 of 10 of the

holes have each received 1 or more particles, the next particle has but 1 chance in 10 of going into an unpenetrated hole. Therefore, on average, 10 additional particles would be required to increase the number of positive holes by 1.

4.4 Results

4.4.1 Comparison test of 3 different air samplers

The mean concentrations of airborne culturable endospores for each sampler are listed in Table 4.1. The bioefficiency differences in among the three air samplers were not significant ($p = 0.384$). Statistically significant differences were noted at different indoor office sites ($p < 0.0001$). In Figure 4.2, the data for all airborne bacterial concentration and the 3 samplers are shown as box plots. The data were shown to be normally distributed using Jarque-Bera test. The 3 air samplers demonstrate similar bioefficiency and therefore in the subsequent study, SAS will be used because it has the smallest standard error (Table 4.1).

4.4.2 Aerosolized biofilm endospore testing in the laboratory

Bacterial endospores that were grown in surface biofilm on microbial growth media were demonstrated to undergo airborne transport as a result of mild air turbulence under ambient conditions. Cultures of bacterial endospores (*Bacillus subtilis* 3160) were grown on tryptic soy Agar (TSA) bacterial growth medium. Two weeks after the culture was initiated, to allow time for the formation of bacterial endospores on the surface of the biofilm, an SAS air sampler was used to measure the concentration of spores which could

easily be transported by moderate air flow over the surface of the biofilm. It was determined that greater that 200 bacterial endospores could be recovered from 1000L of air passed over the biofilm. This finding demonstrated that under laboratory conditions, surface microbial biofilm can release bacterial endospores that can be transported through the air, resulting in the airborne spread of potentially dangerous microorganisms from surfaces.

4.4.3 Correlation of airborne and surface endospores in a closed laboratory environment

A total of 10^5 cfu of *B. subtilis* endospores were dispersed and aerosolized using a nebulizer inside a 12 L AtmosBag with a surface area of 68.6 cm × 76.2 cm. A computer exhaust fan was installed the AtmosBag to emulate natural air turbulence. Air and surface sampling were carried out to assess the airborne and total surface biomass after 30, 120, 240 *min* and then on a daily basis after 4 days (Figure 4.3). Immediately after aerosolization, ~30% of the initial bacterial endospore inoculum were suspended in air and only 30% were deposited on surfaces. After 1 day of settlement, we have observed a ratio of airborne to surface endospores to be ~1:4, with 8% airborne and 33% on the surface. Passive air sampling was evaluated by placing fallout plates inside the AtmosBag in triplicates at various point of time for an hour, 3 facing upward and 3 mounted 10 cm upside down. The rate of passive endospore infall was measured to be 0.632 cfu/cm^2·hr and up-rise rate was measured to be 0.106 cfu/cm^2·hr.

4.4.4 Correlation of AEB and total biomass in indoor environments

In Figure 4.4, the bacterial counts represent the heterotrophic vegetative portion because the endospore population in most of the cases was extremely low. The data show a weak positive correlation between airborne and surface bacteria. We can see that most of the data points align diagonally, showing an airborne to surface bacteria ratio of around 10 to 100. Heavily used and lightly used laboratories demonstrated a significant difference in terms of airborne and surface bacteria ($p < 0.01$). Laboratories also exhibit a higher bacterial counts then offices ($p < 0.0001$). Inhabited and uninhabited offices do not show a statistically significant difference ($p = 0.1239$). The level I biohazard cabinet shows extremely low concentration as expected, because the purpose of a bio-hood is to keep the air inside free from contamination. The ductless fume hood does not have low concentrations because it is designed to keep harmful chemical vapor inside the hood filter and is not a sterile environment. The data from different locations form distinct clusters, especially the distinction between labs, offices and the biohazard cabinet. The ductless fume hood showed a greater variation because its function is to protect the operator by drawing ambient air inside the hood. In the lab where anaerobic endospores research was executed, there is corresponding increase in airborne and surface proportion of anaerobic bacteria from the fluid thioglycollate cultures.

Preliminary indoor sampling showed a week correlation between human activity and airborne/surface bacterial concentration. To further testify this hypothesis, we compared these with the results of sampling in the Environmental Control and Life Support System Module at Marshall Space Flight Center support the hypothesis that bacterial spore bioburden can represent the total microbial content of an environmental

system. Time-course data indicated an increase in total microbial counts during the time of occupation and a decrease after the cabin was not in use. Data obtained from three different types of bacterial growth media (R2A, RBA and TSA) did not show any significant trends related to the type of media used for either the one day time course (day 6) or the 15 day time course of sampling. RBA and R2A counts showed slight increases with a single peak in each at 14:00 on day 6. Sampling data demonstrated a significant difference in the total CFUs obtained from each of the methods used. Fallout plate data shows no immediate trend across the plate types but with a significant increase over time. Surface sampling done by RODAC plating collected data on the total CFU on a surface the approximate area of a 100mm diameter circle. Surface testing indicates a general increase in surface microbial content from an average of 3 cfu plate^{-1} to 19 cfu plate^{-1}. Spore content of the air samples was indicative of the total microbial bioburden (Figure 4.5).

4.4.5 Correlation of AEB and total biomass in outdoor environments

Figure 4.6 shows the microbiological sampling results with SAS in the Atacama Desert and corresponding weather conditions measured by a portable weather station. Diurnal variation in the number of culturable bacteria was observed, positively correlated with relative humidity and wind speed, and inversely correlated with the air temperature and UV irradiation. Fallout plates made of PDMS were used. No CFU was recovered during the 12 hours of daytime. 4 ± 2 CFU plate^{-1} were obtained during the 12 hours at night. The intense UV irradiation can be the cause for the inactivation of airborne bacteria during the day.

4.4.6 Comparison of biofilm-forming environmental-strain *B. subtilis* and lab-strain *B. subtilis* endospores

The ability to form fruiting bodies could be passed on over 3 generations with intermittent sporulation, germination and outgrowth. Cultures of bacterial endospores (*B. subtilis* 3160) were grown on TSA bacterial growth medium. Two weeks after the culture was initiated, to allow time for the formation of bacterial endospores on the surface of the biofilm, an SAS air sampler was used to measure the concentration of spores which could easily be transported by moderate air flow over the surface of the biofilm. It was determined that approximately 100 endospores could be recovered from 1000 L of air passed over the biofilm. A strain of *B. subtilis* that form biofilm and delicate aerial structure was isolated from Mojave Desert (Figure 4.7). Two weeks after colony formation on TSA, approximately 1000 endospores were recovered when 1000 L of air passed over the culture. This finding demonstrated that under laboratory conditions, surface microbial biofilm can release bacterial endospores that can be transported through the air, resulting in the airborne spread of potentially dangerous microorganisms from surfaces. No significant differences were observed in the unit DPA content and germination properties between these endospores.

4.5 Discussion

Maintaining human health in confinement presents a unique challenge, which is significantly exacerbated in space flight by the effects of microgravity, the duration of the mission, and the possible interaction with contaminants in the spacecraft[24]. To manage the risk, we have previously described the development of MEM as a real-time autonomous air monitor in a

spacecraft enclosed habitat, capable to detect as low as 100 endospores L^{-1} of air when 500 L of air were sampled in 15 min. Apart from technological development, one must fully understand the correlation between AEB level with the total biomass in an enclosed system with no outside ventilation in order to help promulgation of exposure limits and safety levels, as well as maximum allowable concentrations for airborne bacterial spores.

Suspended particulate matter of a diameter less than 10 μm (PM10) was used as a measure of air quality in this study. It was well establish that sustained exposure to elevated PM10 values was associated with a variety of health problems[25]. Regulatory limits for PM10 values have therefore been imposed[26,27]. In this study, we have employed the PM10 value, log transformed, as the variable of interest.

In this study, we have measured AEB and total biomass in a closed system under laboratory controlled conditions and everyday indoor environemnts. A quantitative correlation and mathematical model has been established under ideal conditions, such as volume, air flow, turbulence and the number of microbes. The principal components of each AEB and surface bacterial abundance is subjected to the analysis of variance (two-way ANOVA) followed by a pairwise multiple comparisons. Principal component analysis of the pairwise AEB and total biomass in indoor closed environments, such as laboratory, offices, laminar flow hoods, produced two factors that accounts for 49% (eigenvalue = 3.5) and 19% (eigenvalue = 1.5) of the total variance in the data set. Clustering of component scores indicates an apparent tendency to form separate cluster assignments under different environments. It is noticed the ratio of AEB and total biomass can be projected with high accuracy using our model system when minimal human activities are involved. As human activities and environmental factors play a bigger role in the system, a positive correlation can still be observed between AEB and

total biomass, but these systems are difficult to model due to increased complexities as shown in separate studies. A more comprehensive study on the effect of PM10 values due to temporal and spatial behaviors is expected in future studies.

We used a three-pronged approach to testify the hypothesis. First, we demonstrated a reproducible bioefficiency among three air samplers (SAS, MEM, E-BAM) to validate the use of SAS in subsequent studies because of its compactness and portability. Second, we performed air and surface sampling inside an AtmosBag under controlled conditions. A two-compartmental mathematical model has been developed to characterize the transport of airborne and surface endospores in this 12-L enclosure. The model was extended to analyze a number of indoor areas, including laminar flow hoods, laboratory and office spaces. Third, we studied the effect of human activities and environmental factors in the correlation of airborne and total biomass in a system.

We describe the system as a two compartment system such that there is exchange of materials between them. q_1 and q_2 are defined as state variables describing the number of airborne endospores and the number of endospores on the surface. Exchange occur by endospores transgressing some physical barrier, characterized by two rate constants, k_{12}, is the number of endospores transferred from air to surface per unit time and k_{21} represents the number of endospores aerosolized from surface into the air per unit time. The basic assumption for the compartmental model is that endospores are distributed homogenously in the entire system. The 2-compartment model structure is given as followed. The model dynamics with state variables can be described in Figure 4.8, where u_1 and u_2 in this system are delta function inputs. The two rate constants can be measured by fallout plates (n = 10). The number of airborne endospore depositing on surfaces was

20.1 ± 7.2 cfu h^{-1} and the number of endospores being aerosolized was 2.0 ± 1.4 cfu h^{-1}. Therefore, k_{12} and k_{21} were calculated to be 0.0193 cfu min^{-1} cm^{-2} and 0.4109 cfu min^{-1} cm^{-2}, respectively after unit conversion. Solving the system of differential equations, we have obtained plots very close to actual results under ideal situation. While this is a very simplistic model assuming well-controlled condition (especially air turbulence), it truly reflects the environment inside a spacecraft. We then showed qualitatively that the number of total endospores in a closed system was positively correlated with the degree of human activity in Marshall Space Flight Center. Moreover the time course in a spacecraft relevant environment (i.e., the MSFC simulated cabin) of airborne bacterial spores shows a trend that is highly correlated to the time course of the environment, human commensal, and fungal spore concentrations. This implies that a change in airborne bacterial spore concentration can be used to indicate a corresponding change in total microbial content in the cabin.

Air sampling has been carried out in the Atacama Desert to verify the model that we have developed. The results high depend on the environmental factor, such as wind, relative humidity and UV irradiation. PDMS was used as collection substrate for fallout plates. During the day, the air was devoid of culturable microorganisms and fallout plate also indicated zero counts. At night, counts were observed in both air sampling and fallout plates. This shows that there exists an exchange of airborne and surface microbes in the absence of UV irradiation. In addition, the wind speed was 5 times greater than that in the daytime, reaching a peak velocity of 25 km h^{-1}, which may be another reason for the presence of aerosolization and deposition of microbes *via* wind as an agent. In conclusion, in an outdoor environment, lots of other factors are dominating the airborne

bacterial concentration. In addition, surface bacteria are difficult to extract due to (1) extreme radiation and temperature of the surface, (2) complex soil matrix and (3) sources of contaminations from human and animal activities.

The MEM monitors the concentration of airborne bacterial spores in cabin air as an indicator for total microbial concentration. Spore-forming bacteria of the genus *Bacillus* are frequently among the most abundant genera in aerobic biofilms, and are likewise among the most abundant genera found in the air and on surfaces. As a biofilm grows, the population of the ever-present sporeforming bacteria and their endospores increase proportionally. In fact, recent reports demonstrate that spore-forming species in environmental biofilms form fruiting bodies, filled with bacterial spores that rise above the biofilm to facilitate their release into the air. Thus, the airborne bacterial spore concentration can be correlated to total microbial concentrations. In this experiment, we also examined the aerosolization properties of a biofilm-forming endospore-forming species isolated from the Mojave Desert. Although it has been reported that properties of endospores depend largely on the sporulation condition, this environmental species still retained its biofilm colony morphology after 3 generations. As expected, these biofilm-forming endospores were 5 times more susceptible to aerosolization than laboratory strain *B. atrophaeus* endospores that do not form biofilms. Nevertheless, the DPA content, hydrophobicity and germination characteristics of this environmental strain are all similar to *B. atrophaeus* endospores.

4.6 Conclusion

In conclusion, we have determined a quantitative relationship between airborne

endospores and total biomass in an enclosed environment. Airborne endospore bioburden has the potential to be used in monitoring surface bioburden to anticipate buildup on critical spacecraft hardware and expedite remediation. We propose the use the MEM as an autonomous biosensor to monitor ARB in spacecrafts and space stations coupled with a measurement of the two-way microbial transfer (deposition and aerosolization) by simple fallout plate methodology achieved by convenient and compact culturing assays such as the Petri-films. Work continues in instrument miniaturization and model optimization. Future applications of the MEM is space habitat or in planetary exploration will depend on NASA's needs, but eventual deployment of the MEM as one part of a fully automated environmental monitoring and control system is envisioned.

4.7 References

1. Rodgers, E.B., Seale, E.B., Boraas, M.E., and Sommer, C.V., in *19th Intersociety Conference on Environmental Systems* (Volume IV-Appendix G Task 7 Report Advanced Instrumentation: Technology Database Enhancement, San Diego, CA, 1989).
2. Branda, S.S., Gonzalez-Pastor, J.E., Ben-Yehuda, S., Losick, R., and Kolter, R. Fruiting body formation by *Bacillus subtilis*. *Proceedings of the National Academy of Sciences of the United States of America* **98**, 11621-11626 (2001).
3. Jan, D. AEMC Technology Development Requirements. (1998).
4. Nicogossian, A.E., Huntoon, C.L., and Pool, S.L., *Space Physiology and Medicine*. (Lea & Febiger, Philadelphia, PA, 1994).
5. Gardner, D.E., in *Toxicology of the Lung*, edited by D. E. Gardner, J. D. Crapo, and R. O. McClekkan (CRC Press, 1999).
6. Mennigmann, H.D. and Lange, M. Growth and differentiation of *Bacillus subtilis* under microgravitiy. *Naturwissenschaften* **73**, 415-417 (1986).
7. Pierson, D.L. Microbial contamination of spacecraft. *Gravitational and Space Biology Bulletin* **14**, 1-6 (2001).
8. Novikova, N. *et al*. Survey of environmental biocontamination on board the International Space Station. *Research in Microbiology* **157**, 5-12 (2006).
9. Taylor, G.R. Overview of spaceflight immunology studies. *J Leukoc Biol* **54**, 179-188 (1993).
10. Sonnenfeld, G. The immune system in space, including Earth-based benefits of space-based research. *Curr Pharm Biotechnol* **6**, 343-349 (2005).
11. Smith, S.M. Red blood cell and iron metabolism during space flight. *Nutrition* **18**, 864-866 (2002).

12. Konstantinova, I.V., Rykova, M.P., Lesnyak, A.T., and Antropova, E.A. Immune changes during long-duration missions. *Journal of Leukocyte Biology* **54**, 189 (1993).
13. Venkateswaran, K., Chung, S., Allton, J., and Kern, R. Evaluation of various cleaning methods to remove bacillus spores from spacecraft hardware materials. *Astrobiology* **4**, 377-390 (2004).
14. La Duc, M.T., Satomi, M., and Venkateswaran, K. *Bacillus odysseyi* sp. nov., a round-spore-forming bacillus isolated from the Mars Odyssey spacecraft. *International Journal of Systematic and Evolutionary Microbiology* **54**, 195-201 (2004).
15. Venkateswaran, K. *et al*. Molecular microbial diversity of a spacecraft assembly facility. *Systematic and Applied Microbiology* **24**, 311-320 (2001).
16. Lester, E.D. and Ponce, A. An anthrax "smoke" detector: Online monitoring of aerosolized bacterial spores. *IEEE Engineering in Medicine and Biology Magazine* **21**, 38-42 (2002).
17. Lester, E.D., Gregory, B., and Ponce, A. A second-generation anthrax "smoke detector". *IEEE Engineering in Medicine and Biology Magazine* **23**, 130-135 (2004).
18. Yung, P.T., Lester, E.D., Bearman, G., and Ponce, A. An automated front-end monitor for anthrax surveillance systems based on the rapid detection of airborne endospores. *Biotechnology and Bioengineering* **98**, 864-871 (2007).
19. Pastuszka, J.S., Paw, U.K.T., Lis, D.O., Wlazlo, A., and Ulfig, K. Bacterial and fungal aerosol in indoor environment in Upper Silesia, Poland. *Atmospheric Environment* **34**, 3833-3842 (2000).
20. Anonymous. NASA standard procedures for the microbiological examination of space hardware, NHB 5340.1D. *Jet Propulsion Laboratory Communication, National Aeronautics and Space Administration* (1980).
21. Lin, Y.P., in *Environmental Monitoring*, edited by G. B. Wiersma (CRC Press, Boca Raton, FL, 2004).
22. Cressie, N.A.C., *Statistics for Spatial Data*. (John Wiley, Hoboken, NJ, New York, 1993).
23. Macher, J.M. Positive-hole correction of multiple-jet impactors for collecting viable microorganisms. *American Industrial Hygiene Association journal* **50**, 561-568 (1989).
24. Taylor, G.R. Space microbiology. *Annual Reviews in Microbiology* **28**, 121-137 (1974).
25. Sun, L.I., Zidek, J.V., Le, N.D., and Ozkaynak, H. Interpolating Vancouver's daily ambient PM10 field. *Environmetrics* **11**, 651-663 (2000).
26. Cox, C.S. and Wathes, C.M., *Bioaerosols Handbook*. (Lewis Publishers, Inc., 1995).
27. Cox, L.H. Statistical issues in the study of air pollution involving airborne particulate matter. *Environmetrics* **11**, 611-626 (2000).

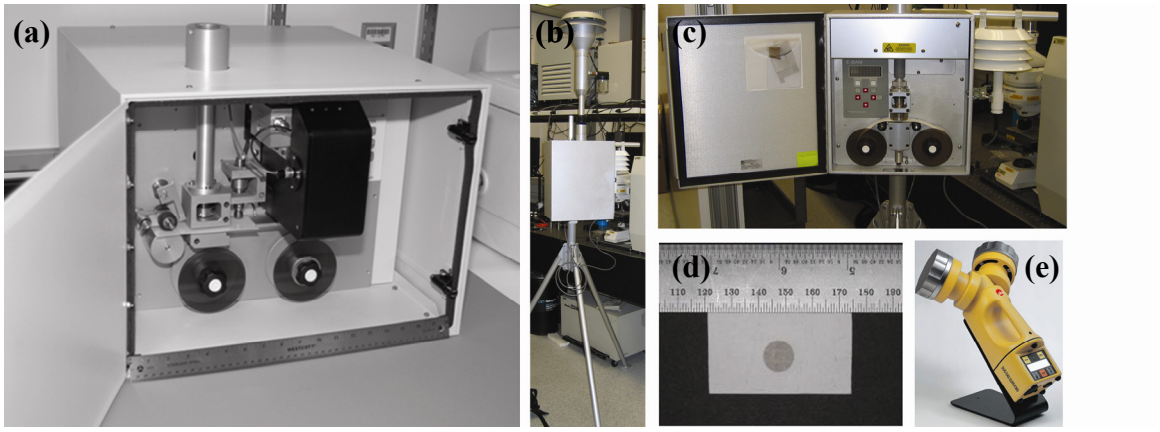

Figure 4.1 | **(a)** The Microbial Event Monitor (MEM) is a derivative product of the Anthrax Smoke Detector. **(b)** The E-BAM consists of a PM_{10} air inlet and β-attenuation gauge for air sampling. **(c)** Spooling mechanism for continuous air sampling of E-BAM. **(d)** Air samples of MEM and E-BAM are collected onto a 9-mm spot on filter tape. **(e)** The "duo sas-super 360" air sampler, abbreviated as SAS, consists of two independent aspirating heads for impaction air sampling

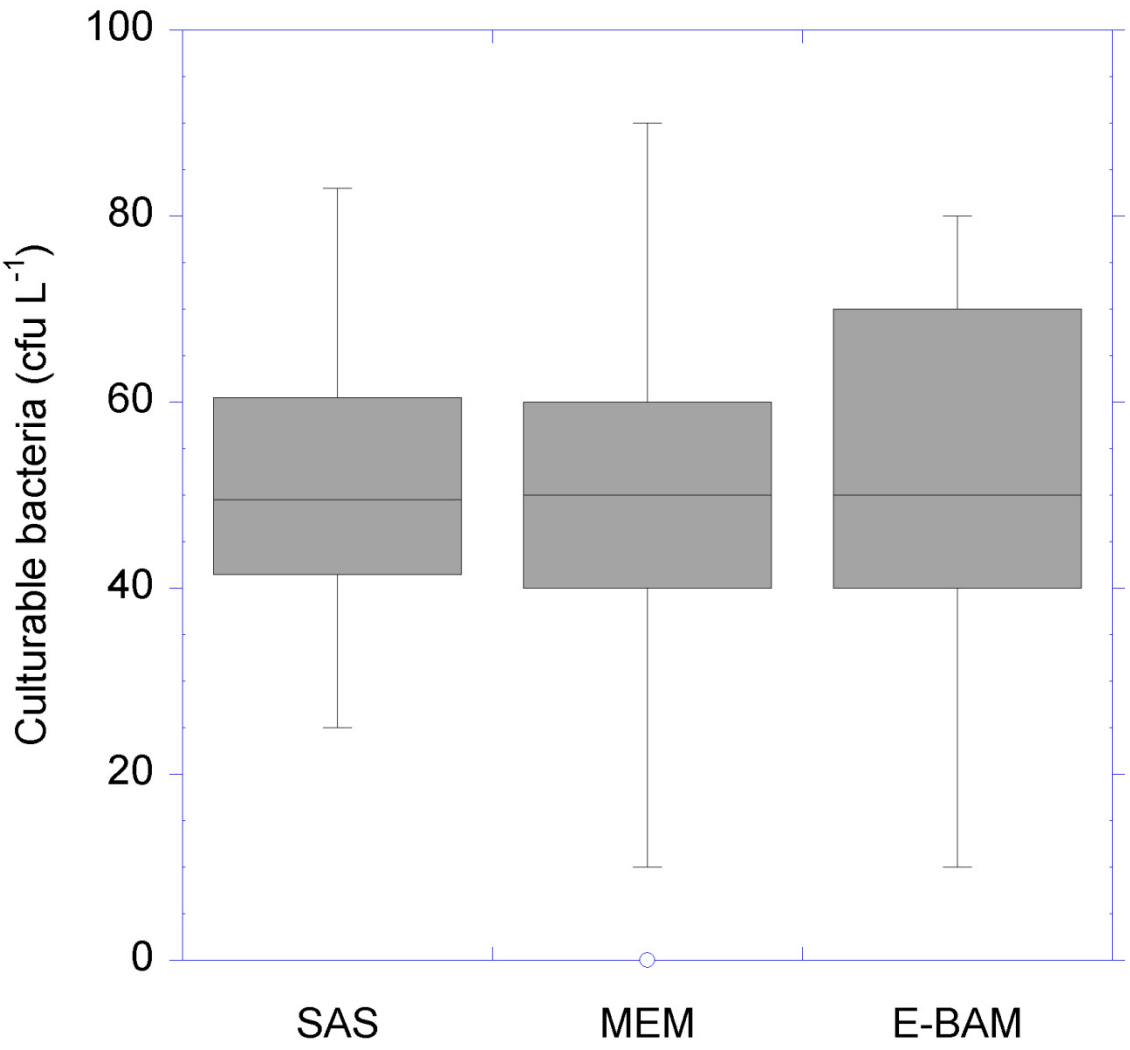

Figure 4.2 | Box plots of airborne culturable bacterial concentration isolated from 5000 L air samples of SAS, MEM, and E-BAM air samplers. The center horizontal line in each box is the median and the horizontal boundaries of the box above and below it are the 1st and 3rd quartiles. Therefore the height of the box, between these quartiles, represent the central 50% of the data. The position of the median, whether central or toward the upper or lower edge, is an indication of the symmetry of the distribution. The vertical lines are the whiskers and are a further measure of the amount of scatter of the data in each group. There are also outliers, represented with a circle in the MEM case. These are observations sufficiently detached form the rest of the data as to be regarded as discontinuous.

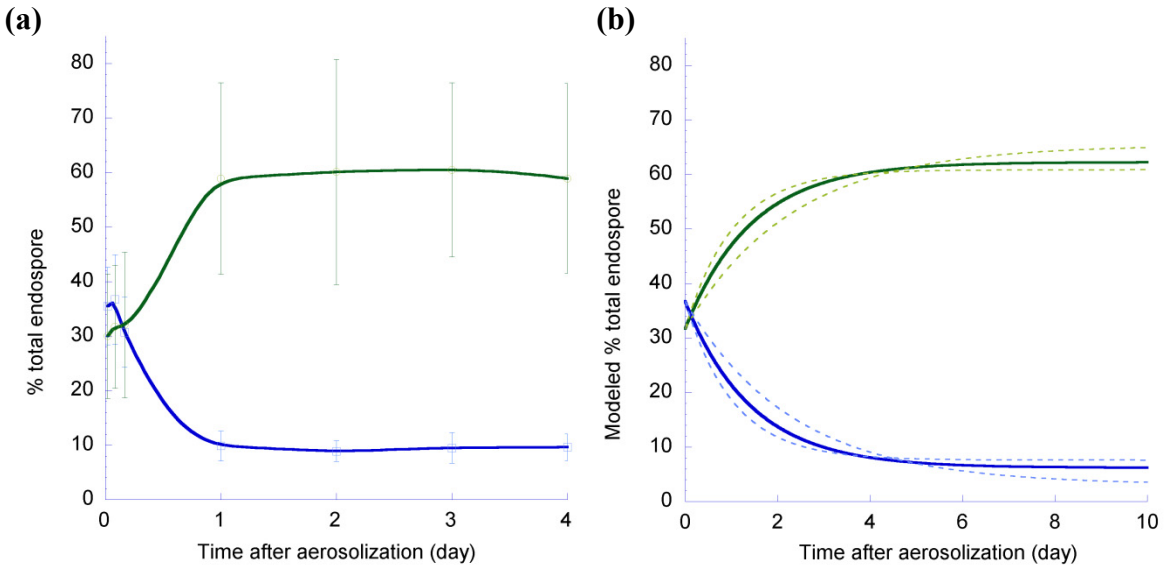

Figure 4.3 | **(a)** Monitoring of the airborne and surface endospore concentrations after an aerosolization event of 10^5 endospores. Inside a closed AtmosBag system. The green plot represents the surface endospores and blue plot represents the airborne endospores. **(b)** The close system kinetics can be modeled as a two-compartmental analysis and characterizd by a system of differential equations. It shows the modeled kinetics; dotted lines represent the 95% confidence interval generated by the model.

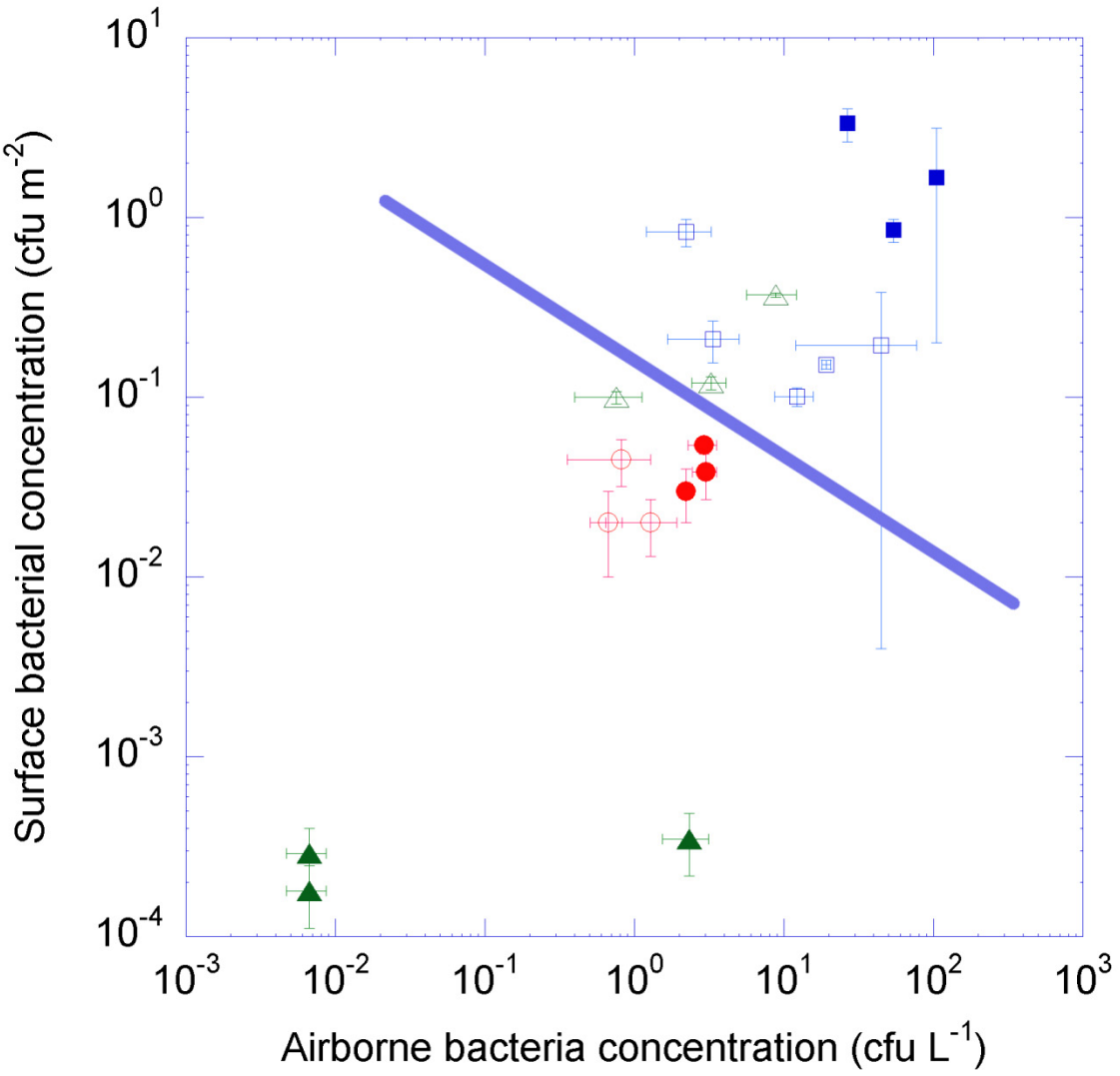

Figure 4.4 | Correlation of airborne and surface bacterial concentrations in indoor environments. The symbols are designated as: ■ laboratory operated for endospore research for many years; □ new laboratory that has also been operated for 2 months; ● Inhabited office; ○ uninhabited office; ▲ level I biohazard safety cabinet; Δ ductless fume hood.

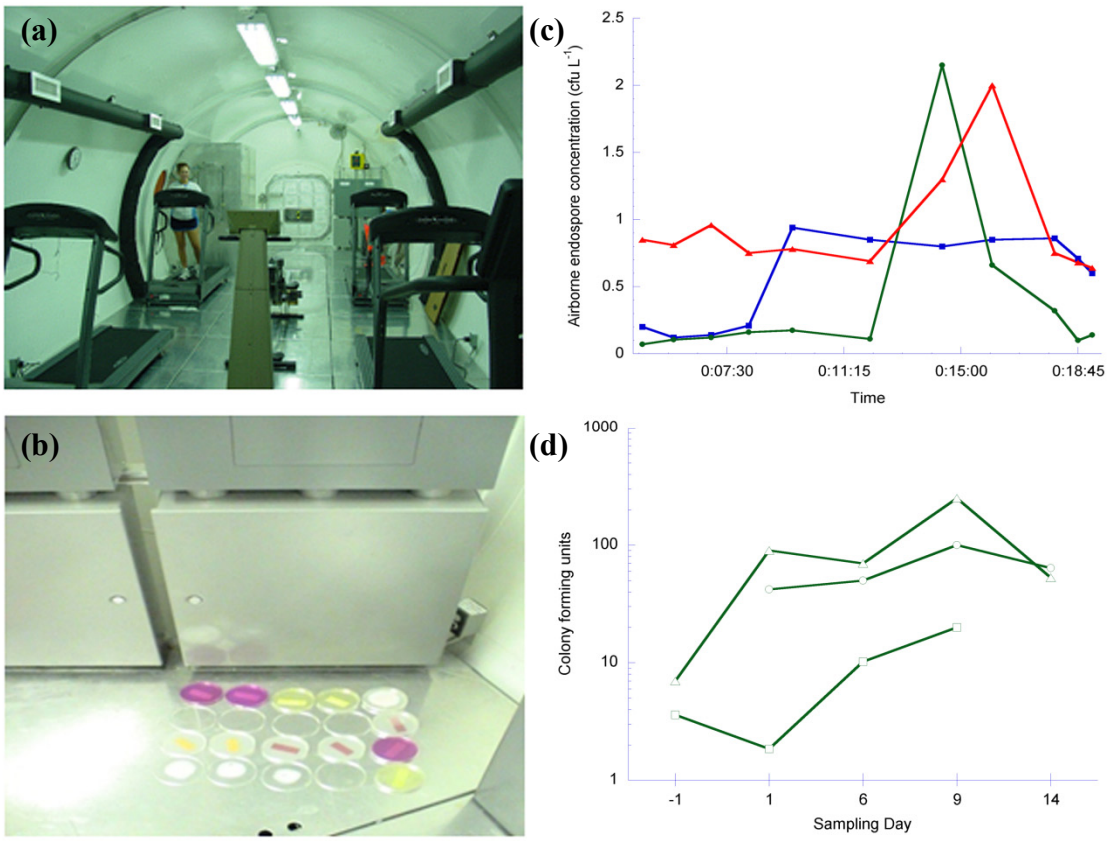

Figure 4.5 | **(a)** MSFC simulated spacecraft cabin and SAS air sampler used in cabin. **(b)** Fallout plates and time course of airborne microbial concentrations. **(c)** Plots represent 3 different media used with the SAS air samplers over the course of 14 hours on day 6. Blue plot represents TSA; green plot represents R2Ac and red plots represent RBA. **(d)** Plots represent the vegetative R2Ac plate counts: □ surface (cfu/25cm^2); ○ fallout (cfu/15min); Δ SAS air sampling (cfu/L).

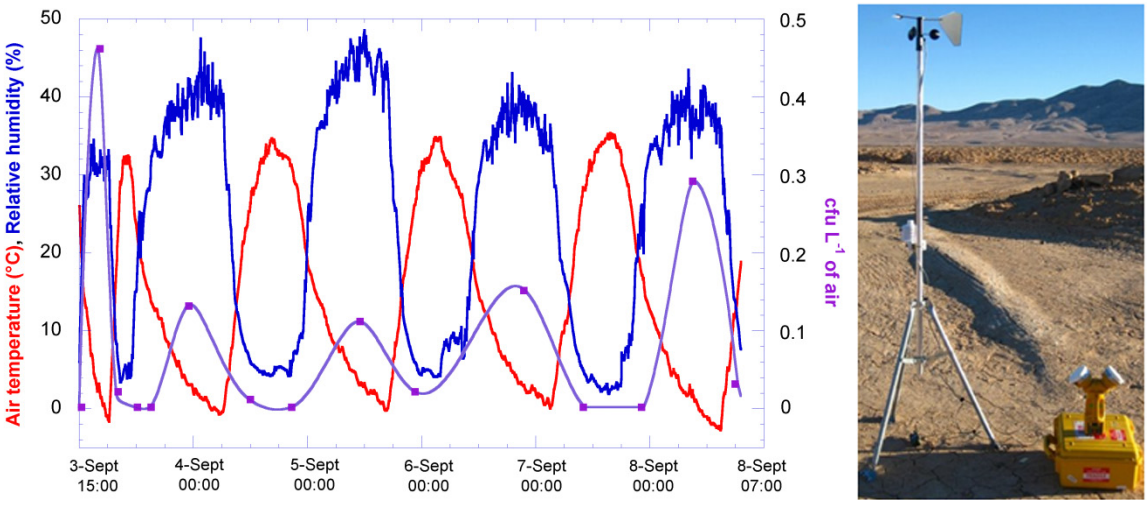

Figure 4.6 | Air sampling at the Atacama Desert.

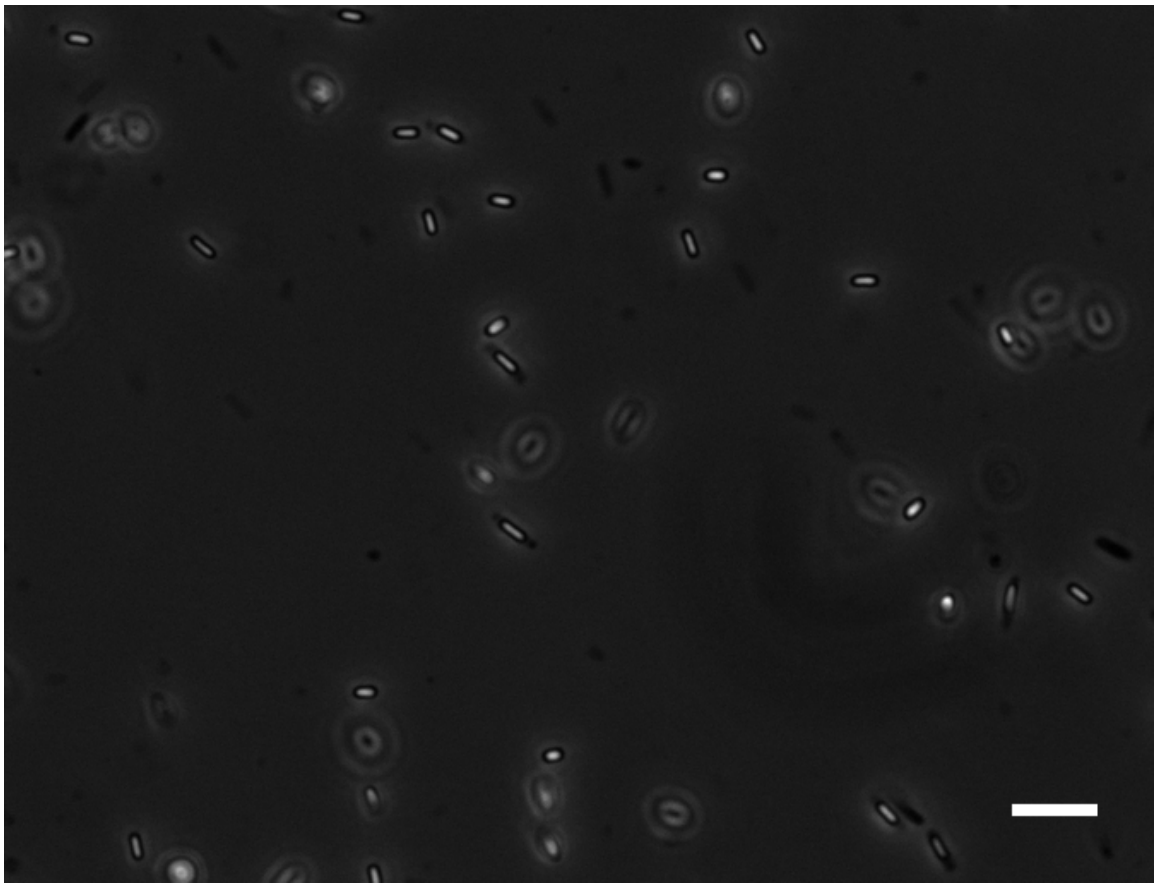

Figure 4.7 | Phase contrast micrograph of *B. subtilis* endospores, with distinct aerial structure isolated from Mojave Desert, in the course of sporulation. Scale bar, 5 μm.

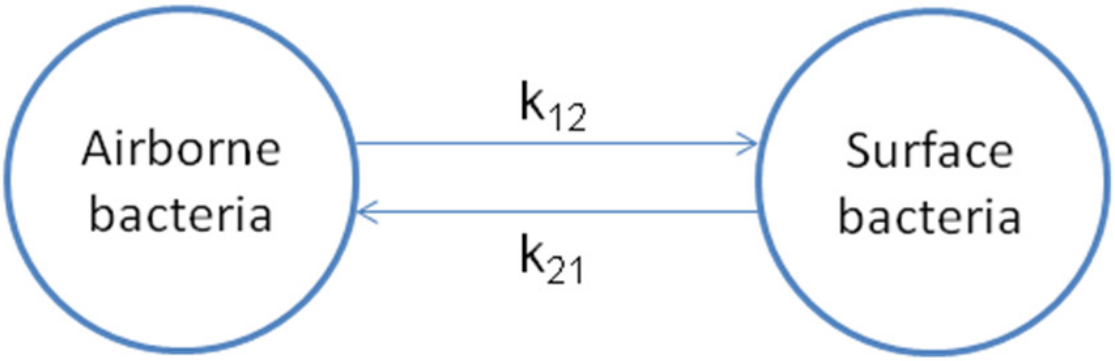

$$\frac{dq_1}{dt} = -k_{21}q_1 + k_{12}q_2 + u_1$$

$$\frac{dq_2}{dt} = k_{21}q_1 - k_{12}q_2 + u_2$$

Figure 4.8 | Two-compartmental mechanistic model of the correlation of airborne and surface endospores in a closed system.

	Mean cfu L^{-1} (standard error)					
Air Sampler	Site 1	Site 2	Site 3	Site 4	Site 5	All
SAS	54.58 (9.87)	45.25 (9.71)	46.00 (7.62)	70.25 (9.95)	40.83 (8.41)	51.38 (13.79)
MEM	53.33 (18.75)	52.50 (14.85)	47.50 (18.65)	55.83 (15.64)	32.5 (18.03)	48.33 (19.41)
E-BAM	56.67 (11.55)	48.33 (18.50)	49.17 (19.29)	65.00 (13.82)	27.5 (16.58)	48.33 (21.77)

Table 4.1 | Comparison of the bioefficiency of different air samplers.

CHAPTER 5: RAPID STERILIZATION ASSESSMENT BY MONITORING INACTIVATION OF GERMINABLE *BACILLUS* ENDOSPORES

5.1 Abstract

Bacillus endospores are in standard use as biological indicators for evaluating the effectiveness of sterilization processes. We describe a rapid endospore viability assay (EVA) capable of enumerating germinable endospores in 10-15 min. Germinating endospores release ~10^8 molecules of dipicolinic acid (DPA) when immobilized onto terbium ion (Tb^{3+})/L-alanine-doped agarose, which enables enumeration under UV excitation of resultant green luminescent spots with time-gated Tb-DPA luminescence microscopy (i.e., μEVA). The intensity timecourses of the luminescent spots were characteristic of the stage I germination dynamics. μEVA was applied to monitor inactivation of initial 5×10^6 CFU endospore populations to sterility as a function of thermal (95 °C) and UV (254 nm, 22 μW/cm^2) dosage in aqueous suspension. μEVA and culturing yielded nearly identical decimal reduction (D)-values for both inactivation methods, thus validating μEVA as a rapid alternative for monitoring sterilization processes.

5.2 Introduction

The era of modern microbiology began in the 1870s when the lifecycle of an endospore-forming pathogen, *Bacillus anthracis*, was elucidated using new methods for isolating pure cultures from single cell clones on solid growth media. Bacterial endospores are

dormant microbial structures that are highly resistant to chemical, physical, and radiation sterilization processes[1,2]. In fact, *Bacillus subtilis* endospores have survived for six years in space while exposed to high vacuum, temperature extremes, and intense solar and galactic radiation[3,4].

Since bacterial endospores are the last to remain viable during sterilization processes that readily kill vegetative bacteria, they are routinely employed as biological indicators (i.e., biodosimeters) to validate and monitor the effectiveness of sterilization methods, such as those employed in the medical device, pharmaceutical, health care, food preparation, and wastewater remediation industries[5]. Moreover, the rise of drug resistant pathogens (e.g., MRSA[6]), especially in hospitals, has further increased the importance of hygiene verification and validation of sterilization methods[7]. Even more ominous has been the usage of biological weapons such as the *B. anthracis* laden letters in 2001[8,9]. After the attack, biological indicators were deployed to evaluate the effectiveness of decontamination and restoration of postal facilities and the Senate building[10].

The effectiveness of sterilization processes are measured and reported in terms of sterility assurance levels (SALs), which are defined as the expected probability that a product remains contaminated with viable microorganisms after exposure to a validated sterilization process. A sterilization process that yields predictable SALs is considered to be validated. Confidence in achieving a required SAL is obtained by the use of biological indicators that present a considerably greater population and resistance challenge than the expected bioburden[11], and the most effective way to test the efficiency of a sterilization process is to place biological indicators within and on test products of interest.

Currently, endospore inactivation is quantified by measuring the log reduction in colony forming units (CFU). This method, however, requires several days of incubation, during which 20 cycles of cell replication ultimately yield visible colonies can then be enumerated. In contrast, endospore germination can be initiated and monitored on a timescale of minutes. Germination of *Bacillus* endospores can be triggered by simple biomolecules such as L-alanine, L-asparagine, or glucose[12,13], which causes the release of approximately 10^8 molecules of dipicolinic acid (DPA) from the core of the endospore during the first stage of germination. DPA exists in all bacterial endospores as 5%-15% of the cellular dry weight, and is a unique, defining constituent of endospores cellular dry weight[14,15].

Here we report details of a rapid endospore viability assay (EVA) in which *B. atrophaeus* endospores were immobilized on terbium ion (Tb^{3+})/L-alanine-doped agarose (Figure 5.1). The L-alanine serves to trigger germination, during which DPA is released from endospores. The Tb^{3+} subsequently binds DPA, resulting in green luminescent spots under UV excitation in a microscope field-of-view, which were enumerated as germinable endospores using time-gated Tb-DPA luminescence microscopy (i.e., μEVA). Here we validate μEVA against culturing as a method for rapid endospore viability assessment, and evaluate its application for monitoring endospore inactivation by thermal and UV sterilization regimens.

5.3 Methods

5.3.1 Chemicals

Terbium (III) chloride hexahydrate, 99.999%, L-alanine and other salts were purchased from Sigma (St. Louis, MO) and were used as received. Ultrapure™ agarose (>90%) was purchased from Invitrogen (Carlsbad, CA). Tryptic soy agar (TSA), nutrient broth and agar were obtained from Becton, Dicksinon and Company (Sparks, MD).

5.3.2 Preparation of endospore stock suspension

B. atrophaeus (ATCC 9372) endospores were purchased from Raven Biological Laboratories. *B. subtilis* (ATCC 27370) vegetative cells were grown on TSA and inoculated onto a sporulation medium after reaching exponential growth phase. The sporulation medium contained 1.6% nutrient broth, 1.6% agar, 0.2% KCl, 0.05% $MgSO_4$, 1 mM $Ca(NO_3)_2$, 100 μM $MnCl_2 \cdot 4H_2O$, 1 μM $FeSO_4$ and 0.1% glucose (pH 7.0)[16]. After incubation at 37 °C for 1 week, cells were suspended into sterile deionized water. With phase contrast microscopy, 95% of the cells formed endospores free of sporangia. Endospores were harvested and separated from vegetative cells and debris by centrifugation at 6,300 g, washing 10 times and sonication (25 kHz) for 5 min. The endospore suspension was incubated in lysozyme (0.2 mg/mL) and trypsin (0.1 mg/mL) at 30 °C with constant stirring overnight to lyse and degrade vegetative cells. Endospores were purified by 8 cycles of centrifugation (6,300 g) and washed with sterile deionized water until >99.9% of the cells were fully refractile with no noticeable cellular debris. Endospore suspensions were stored at 4 °C in the dark before use. Total endospore

concentrations were determined using a Petroff-Hausser hemocytometer and CFU concentrations were determined using TSA spread plating in triplicate measurements.

5.3.3 Sample Preparation for μEVA experiments

Endospore suspensions were filtered onto 0.2 μm polycarbonate membrane filters (Whatman, Florham Park, NJ) using filtration manifolds of different diameters depending on the desired concentration factor such that there were less than 300 endospores per microscopic field of view. To ensure that the endospore surface density was optimal for a given initial endospore concentration, suspensions of $>10^6$ sp mL^{-1} were filtered onto 25 mm diameter spots using glass filtration funnels, and suspensions of $<10^6$ sp mL^{-1} were filtered onto 1.5-mm^2 spots using a 96-well micro-sample filtration manifold (Schleicher & Schuell, Keene, NH). Endospores concentrated on the filter were transferred to a ~0.5 mm thick, 9 mm diameter slab of 1.5% agarose substrate containing 100 μM $TbCl_3$ and 20 mM L-alanine mounted in a silicone isolator (Molecular Probes, Eugene, OR) on a quartz microscope slide. After endospore transfer, the agarose surface was covered with a piece of 0.2-mm-thick polydimethylsiloxane (PDMS).

Polydimethylsiloxane (PDMS) was prepared by mixing the polymer base and curing agent (Sylgard, Dow Corning) in 10 to 1 ratio. After degassing, the mixture was cast over a 0.2-mm thick stainless steel mold and cured in an oven for 2 hours at 65 °C. Agarose, silicone isolator and PDMS were autoclaved at 121 °C for 15 min before use. A piece of PDMS was peeled off and attached on top of an endospore-laden agarose surface for sealing.

5.3.4 The μEVA instrument

The instrument consists of a time-gated camera (Photonics Research Systems, Salford, UK) mounted on a Nikon SMZ800 stereoscopic microscope (large working distance for xenon lamp), a xenon flashlamp (Perkin-Elmer, Waltham, MA) mounted at 45 degrees with respect to the sample, and a temperature controlled microscope slide holder (Thermal). The slide holder enabled endospores to germinate at 37 °C. The CCD camera has a resolution of 752 × 582 pixels at 14 bits with a chip size of 2/3 inch. The camera has 50% sensitivity between 430-730 nm, with peak sensitivity at 550 nm. It was Peltier-cooled to 40 °C below ambient temperature and was synchronized to the xenon lamp *via* TTL pulses (300 Hz with tail time up to 50 μs). A highpass filter (03FCG067, Melles Griot) centered at 500 nm was placed along the light path on the emission side before reaching the microscope objective. We collected time stacks of time-gated images by real-time streaming with a delay of 100 μs and exposure time of 5 s in each frame.

5.3.5 Endospore germination and germinable endospore assignment

Endospore germination on agarose surface followed the reported micro-germination dynamics[17]. DPA released from single *B. atrophaeus* and *B. subtilis* endospores manifested as individual bright spots in 15 minutes under time-gated microscopy due to local formation of Tb-DPA. We performed image analysis in Matlab to obtain background-subtracted stack of time-gated images. Assignment of germinable endospores was made based on intensity and size. Adaptive thresholding was applied to segment pixels that were 3 times brighter than the background with a characteristic rising intensity. Each bright spot must exhibit a continuous rising intensity over the course of

germination in order to register an endospore count. This criterion eliminated false positives by not counting sporadic bright spots and long-lived luminescent interference. The 8-connected adjacent pixels were analyzed to screen for endospore clumps. The number of endospores present was calculated by dividing the squared sum of neighboring pixel brightness by the mean brightness of an individual endospore determined empirically. This was done in a recursive way until all of the pixels were counted and marked. Germinable endospore units would be reported as too numerous to count if they exceeded 300 in a field of view. Further dilution would be carried out in those cases.

5.3.6 Phase contrast microscopy for measuring total endospore concentration

Total number of endospores was determined by direct enumeration using a hemocytometer counting chamber under phase contrast microscopy. At high concentrations (i.e., $>10^6$ sp mL^{-1}), populations were calculated based on average of 10 random microscopic fields of view. At low concentrations (i.e., $<10^6$ sp mL^{-1}), an air-dried smear of known volume of endospore suspension was imaged. The entire area of the smear would be counted due to low numbers and uneven spatial distribution. Motorized stage and automatic counting algorithm expedited the capturing and analysis of more than 100 images per sample.

5.3.7 Inactivation experiments

Heat resistance and UV resistance were measured by germinability (DPA release) and culturability (colony formation on TSA) of water-suspended endospores. In the heat

inactivation experiment, 2 mL of *B. atrophaeus* endospores in sealed glass vials were heat treated in a water bath at 95 °C. Vials were removed and placed in ice at different time intervals for μEVA and CFU enumeration. Lethality of the process includes only the holding period at 95 °C. In the UV inactivation experiment, 2-mL aliquot of *B. atrophaeus* endospores contained in a 6 cm diameter glass Petri dish was exposed to 254 nm UV from a mercury lamp (UVP, Upland, CA), coupled with a 0.7 neutral density filter. Uniform UV exposure was achieved by agitating the Petri dish on an orbital shaker (60 rpm). The area of aliquot spread on the dish, and therefore the amount of energy delivered in joules was determined to be 22.9 $\mu W/cm^2$. After varying lengths of irradiation, endospore suspensions were transferred into vials under ice for subsequent μEVA and CFU enumeration.

5.3.8 Statistical analysis

In this study, bacterial counts could be categorized into 2 regimes of distribution. High count regimes were defined as containing >10 counts per field of view for μEVA, and >10 counts per growth plate for culturing experiments, which followed Gaussian distribution. A square root transformation was performed on some of the data to homogenize the variance and normalize the negative skewness. Normality was tested using the Shapiro-Wilk test by looking at skewness and kurtosis of the distribution. Parametric analyses such as Student t-test was used to determine the confidence interval and F-test was used to examine differences between the sample variances. Low count regimes were defined as containing <10 counts per field of view for μEVA, and <10 counts per growth plate for culturing experiments followed Poisson distribution. Non-

parametric analyses, such as Wilcoxon test, were used to determine the confidence interval, and Kruskal-Wallis test was used for variance analysis. We reported the 95% confidence interval based on 1.96 standard deviation of the normally distributed datasets. Data falling within 5% and 95% percentile ranking constituted the reported 95% confidence interval for the Poisson distributed datasets.

5.3.9 Spectroscopy

Spectroscopy was performed on endospore suspensions prepared to a final volume of 3 mL and contained 100 mM L-alanine and 10 μM $TbCl_3$, unbuffered, at pH 6.2 in disposable methacrylate cuvettes (Perfector Scientific). All solutions were freshly prepared using 0.2-μm filter sterilized 18.2 MΩ-cm deionized water and used within one week. Tb-DPA luminescence excitation spectrum (λ_{ex}= 250–360 nm, λ_{em} = 544 nm) and emission spectrum (λ_{ex} = 278 nm, λ_{em} = 515–580 nm) were recorded at room temperature with a Fluorolog 3 fluorimeter (Jobin Yvon) with double monochromators. Emission intensities were quantified by integrating the area under the 544-nm peak with baseline subtraction, and translated into endospore concentration by comparing to a calibration curve determined. Endospore suspension in cuvettes was measured at a right-angled configuration. Endospores immobilized on agarose were measured in front face. A 500-nm highpass filter (Omega Filters) was placed at the entrance of the emission monochromator to prevent second-order diffraction.

5.4 Results

We validated μEVA for analysis of germinable endospores in water suspension using a three-pronged approach. First, we confirmed the assignment that μEVA luminescent spots are germinable endospores by comparing single endospore germination dynamics observed with phase contrast microscopy and μEVA. Second, we evaluated μEVA sensitivity, dynamic range, and false positive rate in comparison to standard TSA culturing. Third, we applied μEVA versus TSA culturing to monitor thermal and UV inactivation of *B. atrophaeus.*

5.4.1 Monitoring single endospore germination dynamics

A comparison of phase contrast microscopy and μEVA time-lapse images are shown in Figure 5.2. After a brief microlag period, DPA release, followed by water influx, takes place during the first stage of germination[12,18]. DPA release was observed with μEVA *via* DPA complexation with the Tb^{3+}-doped into the agarose matrix. The water uptake can be observed with phase contrast microscopy as phase bright endospores transition into phase dark germinated endospores. The timecourse data clearly show the coincidence of DPA release and water uptake going to completion in approximately 15 min, which is consistent with stage I germination[17]. The microlag time reported by μEVA and phase contrast microscopy was 3 and 8 min, respectively, which is also consistent with the sequence of germination[13]. In addition, time-lapse excitation spectra observed during germination show characteristic Tb-DPA excitation spectra (λ_{max} = 271 and 279 nm, Figure 5.6) confirming the release of DPA under μEVA conditions. In combination, these data establish that μEVA observables are germinating endospores.

5.4.2 Sensitivity, dynamic range, and false positive rate

To further validate μEVA, we performed parallel germination and culturing experiments over seven orders of magnitude in endospore concentration. Figure 5.3 shows the germinable endospore concentrations measured with μEVA, and culturable endospore concentrations measured with TSA plate counting plotted against total endospore concentrations as determined with phase contrast microscopy in the trace concentration regime of 0 - 52 spores mL^{-1}. Sterile samples did not yield false positive counts, which enabled us to achieve the ultimate sensitivity of one germinable endospore per μEVA field of view. Of the total endospore concentrations, μEVA revealed that 56.7% ± 4.4% were germinable endospores and TSA culturing determined that 38.4% ± 3.5% were culturable endospores. The ratio of germinable/culturable was 1.48, which is consistent with the fact that a subset of the total endospore population is germinable-but-not-culturable. Similar to plate counting, where dilution factors are applied until the concentration yields 30-300 cfu $plate^{-1}$, μEVA requires concentrations that are less than 200 germinable endospores per field of view. Figure 5.7 shows μEVA versus TSA plate counting results after application of appropriate dilution factors to samples in the 10^1 - 10^6 endospores mL^{-1} concentration range.

5.4.3 Monitoring thermal and UV sterilization of *Bacillus atrophaeus* endospores

The inactivation of *B. atrophaeus* endospores using thermal treatment at 95 °C and UV irradiation at 254 nm with a power of 22.9 $\mu W/cm^2$ was monitored from an initial

inoculum of 10^7 phase bright spores/mL to sterility with μEVA and TSA plate counting (Figure 5.4). The endospore inactivation followed a first-order decay[19] reaction preceded by a shoulder and followed by a tail. The log endospore survivor curve can be simulated by a model described by Geeraerd *et al.* (2000) using a system of differential equations[20],

$$\frac{dN}{dt} = -k_{max} \cdot N\left(\frac{1}{1 + C_c}\right),$$

$$\frac{dC_c}{dt} = -k_{max} \cdot C_c,$$

where N denotes the endospore population, k_{max} is the maximum inactivation rate, and C_c is the number of hypothetical critical components inside endospores that induce a shoulder behavior associated with the inactivation regimen. The decimal reduction value (D-value) is defined as the time in minutes at a particular constant temperature or UV irradiation power to reduce the viable population by a factor of 10 in the log-linear regime[21]. Heat inactivation D-values were found to be 4.74 and 4.80 min, using μEVA and TSA plate counting, respectively. UV inactivation D-values were calculated to be 30.52 and 30.43 min, using μEVA and TSA plating, respectively. The similarity in μEVA and TSA plate counting D-values and inactivation timecourses demonstrated that μEVA is a rapid alternative to monitor endospore inactivation. For a given inactivation dosage, the germinable endospore population remaining was always greater than culturable population (Figure 5.3) making germinable endospores a more conservative biological indicator, consequently yielding increased confidence for achieving a desired SAL.

5.5 Discussion

Since Koch identified endospore-forming pathogens from diseased animals in 1876, endospores became the gold standard for sterilization validation. The definition for viability had originally been synonymous with culturability[22] until the discovery that viable-but-not(yet)-culturable (VBNC) populations comprise more than 99% of environmental microorganisms[23]. For laboratory strains, including biological indicator species, colony formation is certainly the most direct measurement for viability. This, however, requires approximately 20 cycles of replication over several days of incubation before colonies become visible, and is therefore not amenable for either rapid or automated endospore viability assessment.

Rapid endospore viability assessment is achieved by measurement of early observables in the germination-replication pathway. In particular, DPA release with subsequent water uptake can be observed during stage I germination, which occurs within minutes of germinant addition. A shorter microlag time was observed using μEVA because DPA release takes place earlier than water influx. In our investigation, we have demonstrated that individual germinable endospores can be enumerated on a timescale of 10 min *via* Tb-DPA luminescence with μEVA. We validated μEVA for monitoring sterilization processes with reproducible correlation to heterotrophic plate counts. The thermal and UV inactivation experiments monitored by μEVA and heterotrophic plate counts show that germination is an excellent indicator of viability, and that inactivation of germinability and culturability are correlated as evidenced by the reproducible inactivation curves and corresponding D-values.

In μEVA experiments, individual germinable endospores are counted in a microscope field-of-view after germinant addition. As endospores germinate, ~10^8 DPA molecules are released into the immediate area surrounding the endospore. DPA then combines with Tb^{3+} in the agarose matrix to form the Tb-DPA luminescence halos under UV excitation[24]. The germinating endospores manifest as bright spots that grow in intensity over a period of 3-5 min., and are enumerated in a microscope field of view. The characteristic germination timecourse allows unambiguous assignments of germinating endospores. The duration of germination depends on a number of factors, such as species, inoculum size, germinants, and temperature. The reported phase transition for individual bacterial endospores ranges from 75 seconds to approximately an hour[17]. This is manifested in the observed μEVA time course overlays for different species with germination times ranging from 7 to 22 min (Figure 5.5).

Previously, we reported on a related method where germinating endospores were enumerated in bulk suspension by luminescence spectroscopy (i.e., SpectroEVA), where Tb-DPA luminescence intensities were tabulated against a *B. atrophaeus* endospore calibration curve[25]. Results obtained by a comparison of μEVA and spectroEVA showed that the two methods are in good agreement (Figure 5.8). The μEVA approach is superior to spectroEVA because μEVA is capable of enumerating single endospores while the limit of detection of spectroEVA is 1,000 spores mL^{-1}. This advantage is gained because in μEVA experiments the mM DPA halos surrounding single germinated endospores are readily imaged with high contrast, whereas germination of single endospores in bulk suspension (~1 mL) gives rise to mere fM DPA concentrations, which are far below LOD for spectroEVA.

The unique photophysical and chemical characteristics of the Tb-DPA luminescence[26] endospore viability assay make μEVA a powerful instrument tool for endospore viability assessment and validation of sterilization. With μEVA, we take advantage of the long luminescent lifetime (τ = 0.5 to ~2 ms) of Tb-DPA[27], enabling the use of time gating to effectively remove background fluorescence (i.e., interferent fluorophores with nanosecond lifetimes). Time gating eliminates potential false positive causing features and renders the image background dark. Elimination of this background enables a striking increase in image contrast and detection sensitivity even for the most challenging environmental extracts (Figure 5.5, blue data), including near sterile Atacama Desert[28,29], Chile soil extracts, Greenland ice cores[30], and Arctic permafrost, and Antarctic lakes (Lake Vida).

μEVA is not only much more rapid than culture dependent methods (10-15 min vs. 2-3 days), but the simple chemistry, instrumentation, and image analyses are all amenable for automation. Automated viability assessment of endospores will have the potential to find application in many areas where microbial inactivation needs to be monitored and assured, including health care, food, and pharmaceutical industries. Specific examples for applications include, automated performance testing for autoclaves, milk powder production lines, wastewater treatment facilities, and validation of bioagent inactivation after a biological attack. In the case of an anthrax attack, rapid viability assessment technology will aid field personnel to rapidly determine the viability of anthrax endospores before and after countermeasures. In the case of biological attacks with other agents (e.g., *Y. pestis*, *F. tularensis*, *Brucella*, and *Burkholderia* species,

Variola and Foot and Mouth Disease (FMD) viruses), *Bacillus* endospores can be used as a biological indicator for monitoring decontamination efficiency.

5.6 References

1. Nicholson, W.L., Munakata, N., Horneck, G., Melosh, H.J., and Setlow, P. Resistance of *Bacillus* endospores to extreme terrestrial and extraterrestrial environments. *Microbiology and Molecular Biology Reviews* **64**, 548-572 (2000).
2. Setlow, P., in *Bacterial Stress Response*, edited by G. Storz, Hengge-Aronis, R. (ASM Press, Washington, D.C., 2000), pp. 217-230.
3. Horneck, G., Bucker, H., and Reitz, G. Long-term survival of bacterial spores in space. *Advances in space research: the official journal of the Committee on Space Research (COSPAR)* **14**, 41-45 (1994).
4. Nicholson, W.L. Using thermal inactivation kinetics to calculate the probability of extreme spore longevity: Implications for paleomicrobiology and lithopanspermia. *Origins of Life and Evolution of the Biosphere* **33**, 621-631 (2003).
5. Rutala, W.A. and Weber, D.J. Disinfection of endoscopes: review of new chemical sterilants used for high-level disinfection. *Infection control and hospital epidemiology* **20**, 69-76 (1999).
6. Boyce, J.M. *et al*. Meticillin-resistant *Staphylococcus aureus. The Lancet Infectious Diseases* **5**, 653-663 (2005).
7. Dancer, S.J. Importance of the environment in meticillin-resistant *Staphylococcus aureus* acquisition: the case for hospital cleaning. *The Lancet Infectious Diseases* **8**, 101-113 (2008).
8. Higgins, J.A. *et al*. A field investigation of Bacillus anthracis contamination of US Department of Agriculture and other Washington, DC, buildings during the anthrax attack of October 2001. *Applied and Environmental Microbiology* **69**, 593-599 (2003).
9. Small, D., Klusarwitz, B., and Muller, P. Evaluation of Bacillus anthracis contamination inside the Brentwood Mail Processing and Distribution Center, District of Columbia. *Morbidity and Mortality Weekly Reports* **50**, 5 (2001).
10. Sharp, R.J. and Roberts, A.G. Anthrax: the challenges for decontamination *Journal of Chemical Technology & Biotechnology* **81**, 1612-1625 (2006).
11. Pflug, I.J. and Evans, K.D. Carrying out biological qualification, the control operation of moist-heat (steam sterilization) processes for producing sterile pharmaceuticals and medical devices. *PDA journal of pharmaceutical science and technology* **54**, 117-135 (2000).
12. Gould, G.W. and Hurst, A., *The Bacterial Spore*. (Academic Press, New York, 1969).
13. Setlow, P. Spore germination. *Current Opinion in Microbiology* **6**, 550-556 (2003).
14. Powell, J.F. Isolation of dipicolinic acid (pyridine-2-6-dicarboxylic acid) from spores of *Bacillus megaterium. Biochemical Journal* **54**, 210-211 (1953).
15. Halvorson, H.O. and Howitt, C., in *Spores*, edited by H. O. Halvorson (Burgess Publishing Company, Minneapolis, 1961), Vol. II, pp. 149-165.
16. Nicholson, W. and Setlow, P., in *Molecular biology methods for Bacillus*, edited by SM Cutting (John Wiley and Sons, Sussex, England, 1990), pp. 391-450.
17. Hashimoto, T., Frieben, W.R., and Conti, S.F. Microgermination of *Bacillus cereus* spores. *Journal of Bacteriology* **100**, 1385-1392 (1969).
18. Sacks, L.E. Chemical germination of native and cation-exchanged bacterial spores with trifluoperazine. *Applied and Environmental Microbiology* **56**, 1185-1187 (1990).

19. Chick, H. An investigation of the laws of disinfection. *Journal of Hygiene* **8**, 92-158 (1908).
20. Geeraerd, A.H., Herremans, C.H., and Van Impe, J.F. Structural model requirements to describe microbial inactivation during a mild heat treatment. *International Journal of Food Microbiology* **59**, 185-209 (2000).
21. Bigelow, W.D. The logarithmic nature of thermal death time curves. *Journal of Infectious Disease* **29**, 528-536 (1921).
22. Kell, D.B., Kaprelyants, A.S., Weichart, D.H., Harwood, C.R., and Barer, M.R. Viability and activity in readily culturable bacteria: a review and discussion of the practical issues. *Antonie van Leeuwenhoek* **73**, 169-187 (1998).
23. Barer, M.R. and Harwood, C.R. Bacterial viability and culturability. *Advances in Microbial Physiology* **65**, 2776-2780 (1999).
24. Grenthe, I. Stability relationships among the rare earth dipicolinates. *Journal of the American Chemical Society* **83**, 360-364 (1961).
25. Shafaat, H.S. and Ponce, A. Applications of a rapid endospore viability assay for monitoring UV inactivation and characterizing arctic ice cores. *Applied and Environmental Microbiology* **72**, 6808-6814 (2006).
26. Cable, M.L., Kirby, J.P., Sorasaenee, K., Gray, H.B., and Ponce, A. Bacterial spore detection by [Tb^{3+}(macrocycle)(dipicolinate)] luminescence. *Journal of the American Chemical Society* **129**, 1474-1475 (2007).
27. Jones, G. and Vullev, V.I. Medium effects on the photophysical properties of terbium(III) complexes with pyridine-2,6-dicarboxylate (supporting information). *Journal of Physical Chemistry A* **106**, 8213-8222 (2002).
28. Navarro-Gonzalez, R. *et al*. Mars-like soils in the Atacama Desert, Chile, and the dry limit of microbial life. *Science* **302**, 1018-1021 (2003).
29. Connon, S.A., Lester, E.D., Shafaat, H.S., Obenhuber, D.C., and Ponce, A. Bacterial diversity in hyperarid Atacama Desert soils. *Journal of Geophysical Research-Biogeosciences* **112** (2007).
30. Yung, P.T., Shafaat, H.S., Connon, S.A., and Ponce, A. Quantification of viable endospores from a Greenland ice core. *FEMS Microbiology Ecology* **59**, 300-306 (2007).

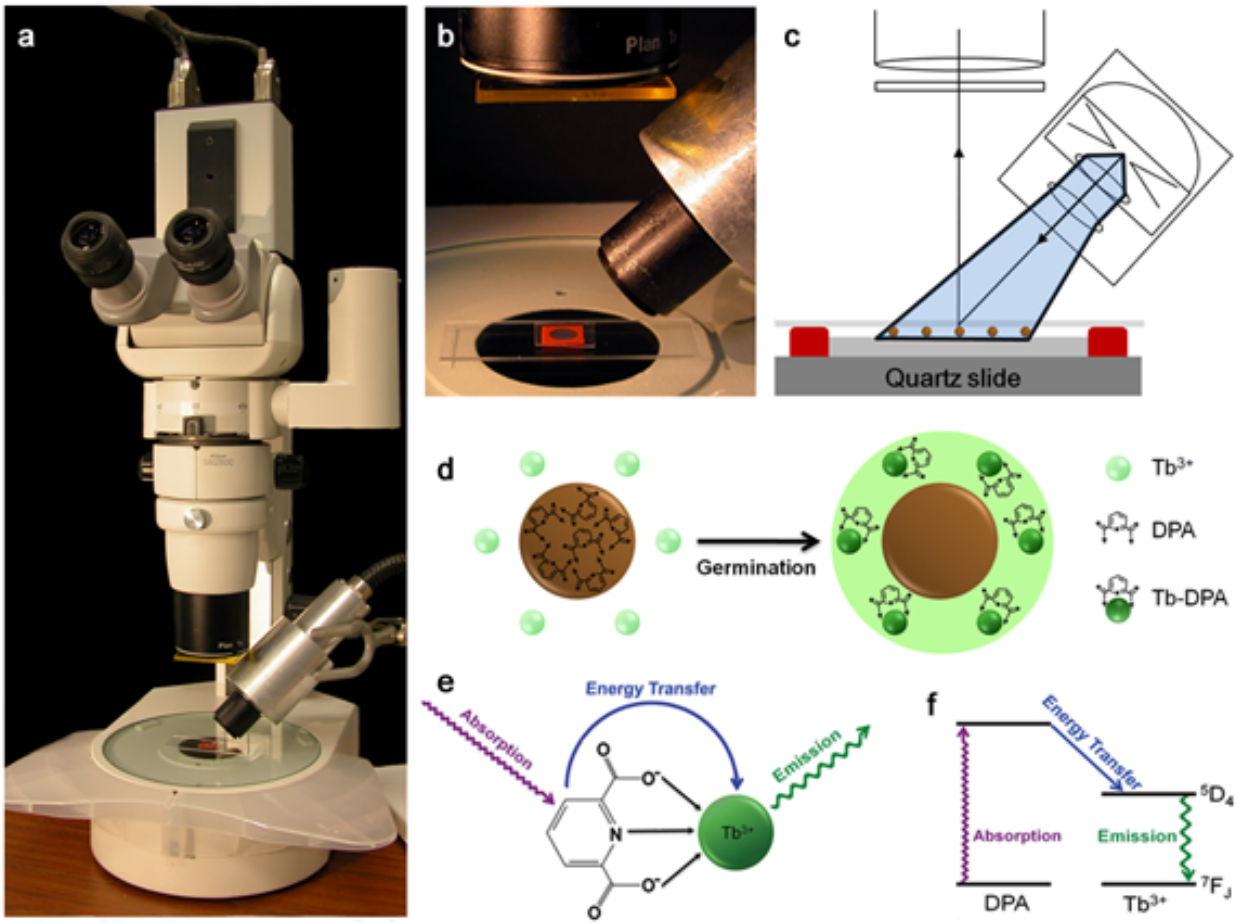

Figure 5.1 | **(a)** Configuration of the μEVA instrument used in this investigation, consisting of a stereomicroscope mounted with a time-gated camera and a xenon flash lamp for UV excitation. **(b)** Sample well on quartz microscope slide containing Tb^{3+}/L-alanine doped agarose. **(c)** Schematic representation of the sample slide, consisting of a quartz slide on which Tb^{3+}/L-alanine doped agarose is confined by red rubber gasket well. Endospores (brown circles) are inoculated onto agarose substrate and subsequently covered with a thin layer of PDMS. **(d)** Inoculated endospores germinate due to L-alanine, causing the release of ~10^8 molecules of DPA and subsequent formation of highly luminescent Tb-DPA complexes that appear as discrete bright spots in the microscope field of view. **(e)** Absorption-energy transfer-emission photophysics of the

Tb-DPA luminescence assay. DPA acts as a light harvester that transfers excitation energy to luminescent terbium ion. **(f)** Energy (Jablonski) diagram of the Tb-DPA photophysics.

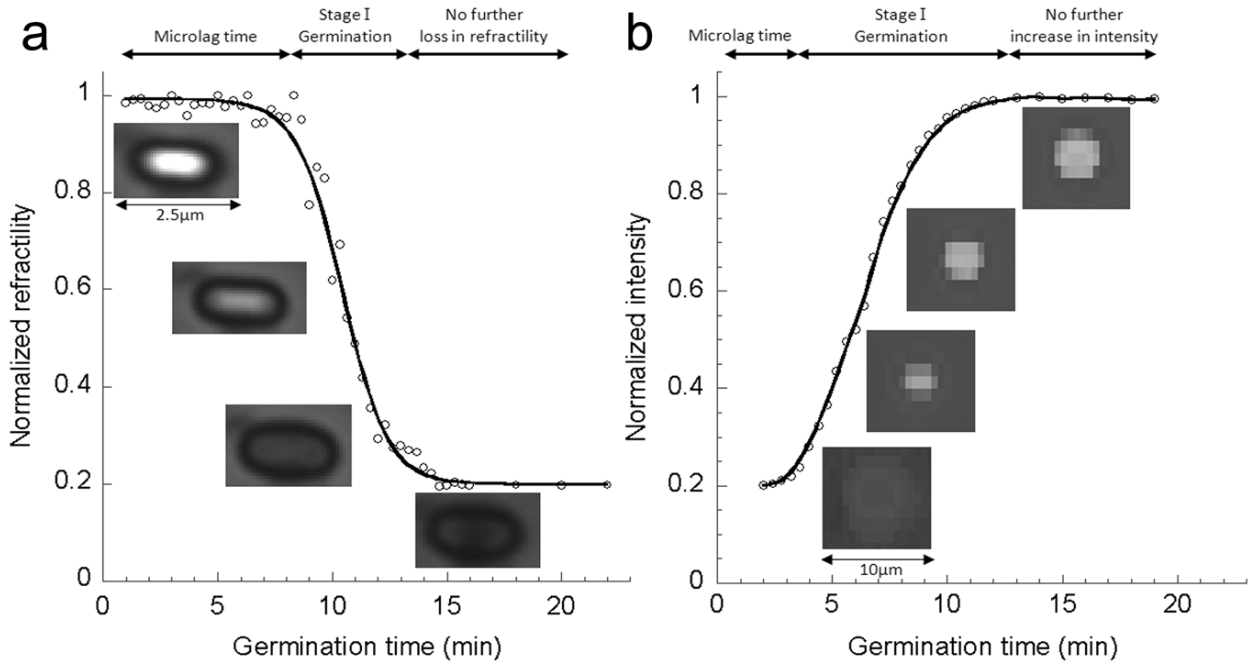

Figure 5.2 | Germination time courses of single *B. atrophaeus* spores at 22 °C monitored by **(a)** phase transition from bright to dark as observed under phase contrast microscopy, and **(b)** Tb-DPA luminescence using µEVA.

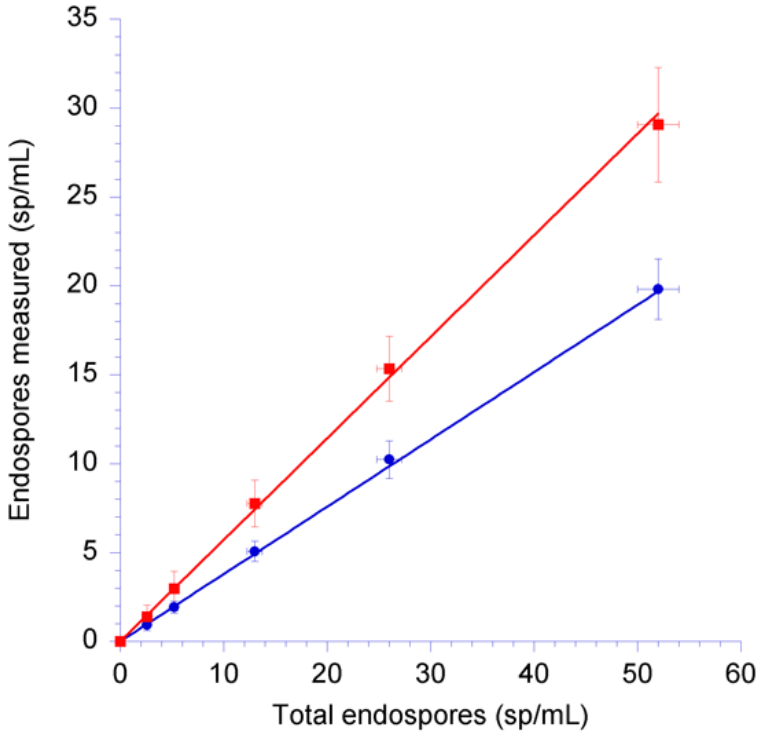

Figure 5.3 | Endospore concentration dependence showing a comparison of µEVA (red data) and heterotrophic plate (blue data) measurements as a function of total endospore concentration as determined by phase contrast microscopy.

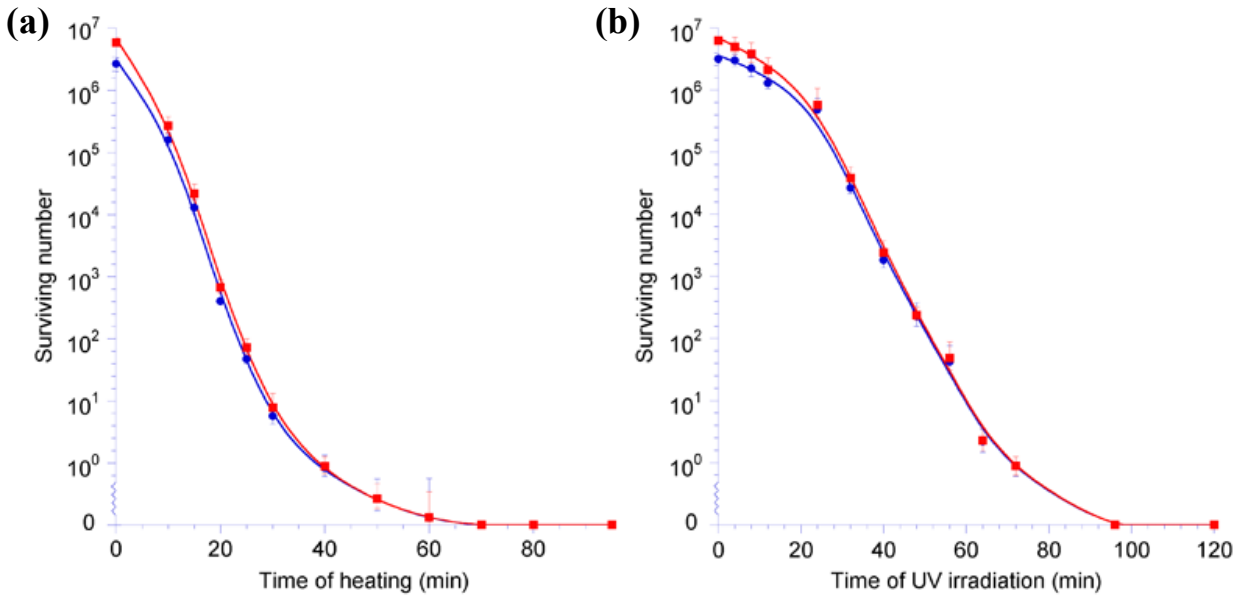

Figure 5.4 | Inactivation of *B. atrophaeus* spores showing µEVA (red) and heterotrophic plate (blue) counts as a function of inactivation dose for **(a)** heat inactivation at 95 °C and **(b)** UV inactivation with a mercury lamp irradiating samples at 254 nm with a power of 22.9 µW/cm^2. The inactivation data were fit to a semi-empirical model reported by Geeraerd *et al.* (2000).

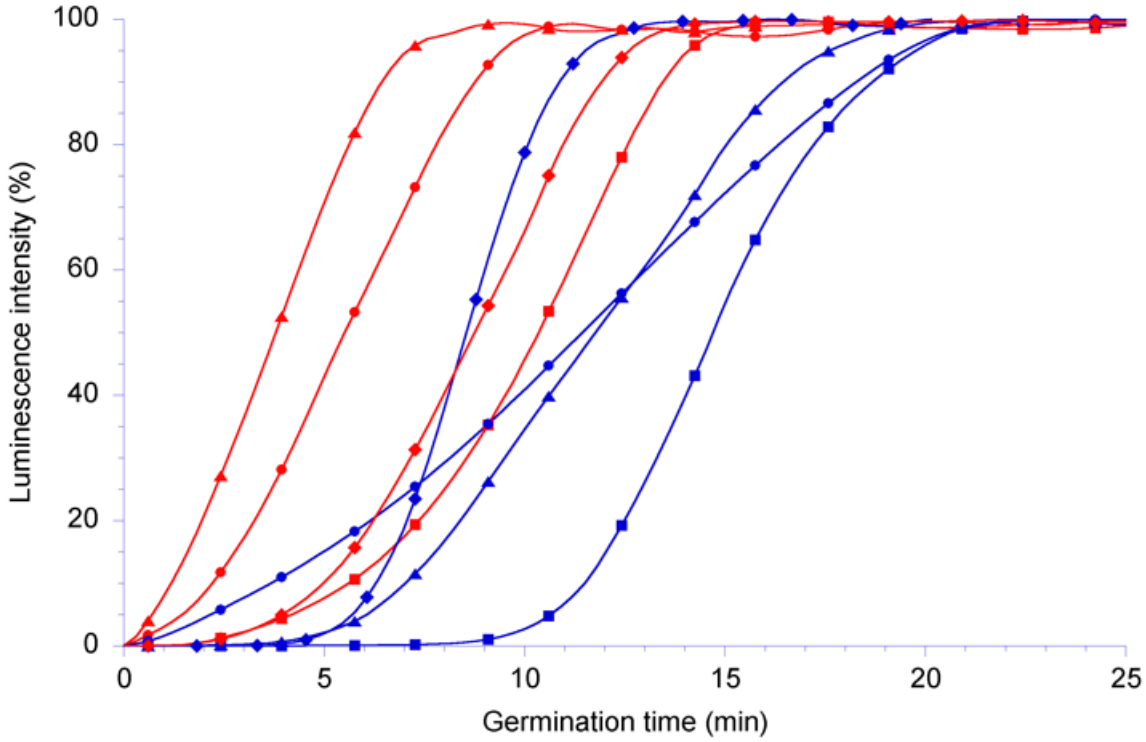

Figure 5.5 | Germination time course plots of pure laboratory strain endospores (red) and environmental samples (blue) measured by μEVA. Each of the above curves represents an average of 10 endospore germination timecourses. Symbol and color assignment: *B. atrophaeus* (red circle); *B.* cereus (red square); *B. subtilis* (red diamond); *G. stearothermophilus* (red triangle); Atacama Desert, Chile extract (blue circle); Lake Vida, Antarctica extract (blue square); Greenland ice core (GISP2) extract (blue diamond); Alaska permafrost extract (blue triangle).

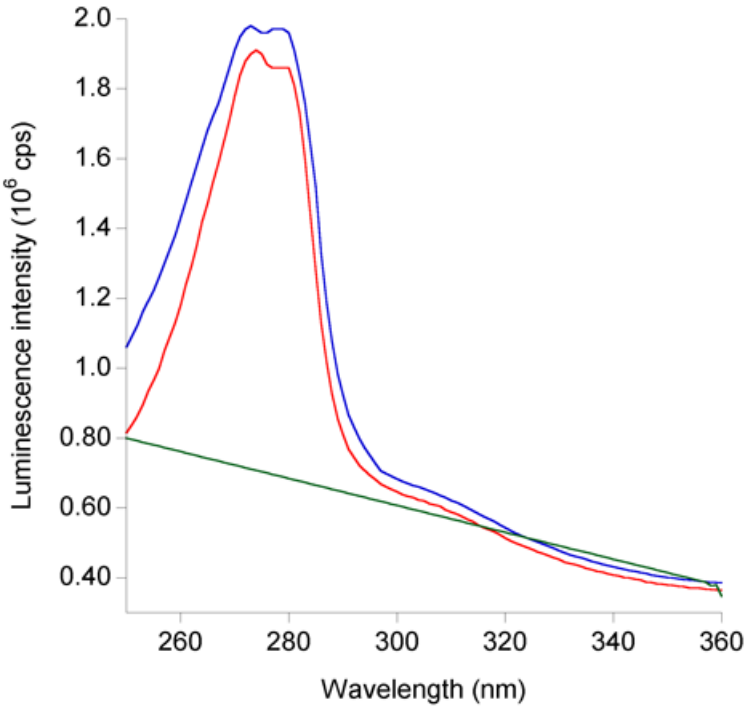

Figure 5.6 | Excitation spectrum (λ_{em} = 545 nm) of the agarose substrate of μEVA when 10^8 *B. atrophaeus* endospores were inoculated, taken with a Fluorolog-3 fluorimeter at a front-face configuration. The dual excitation peaks (λ_{ex} = 271, 279 nm) indicated the presence of Tb-DPA released from germinating spores. Blue plot represents the spectrum of pure DPA inoculated on agarose; red plot represents germinating endospores on agarose and the green plot shows the agarose substrate.

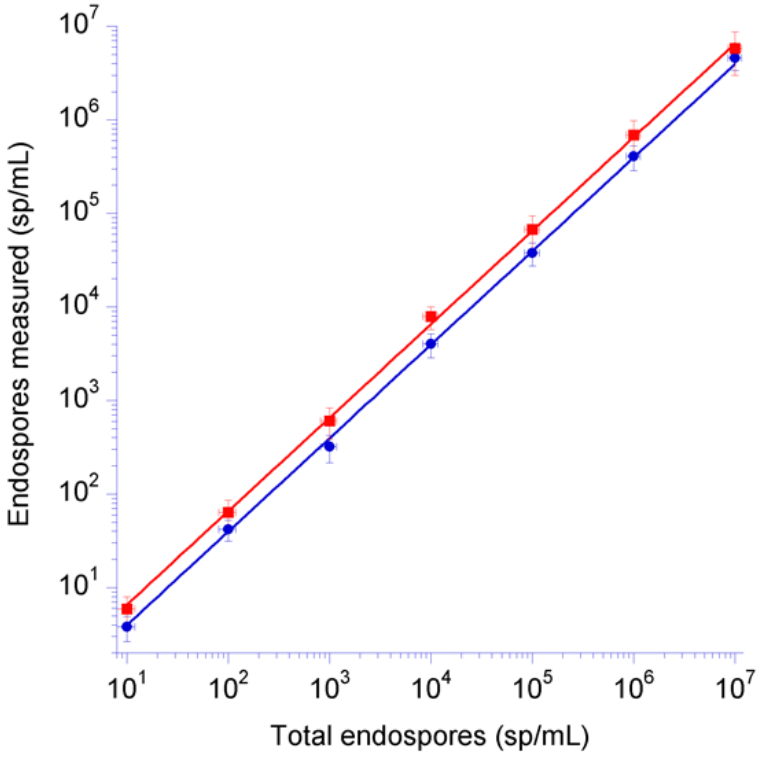

Figure 5.7 | Comparison of µEVA and spread plating on TSA by enumerating pure spore suspension of *B. subtilis* over 6 orders of magnitude. Red plot was obtained using µEVA and blue plot shows the colony forming units (CFU) measured using TSA spread plating.

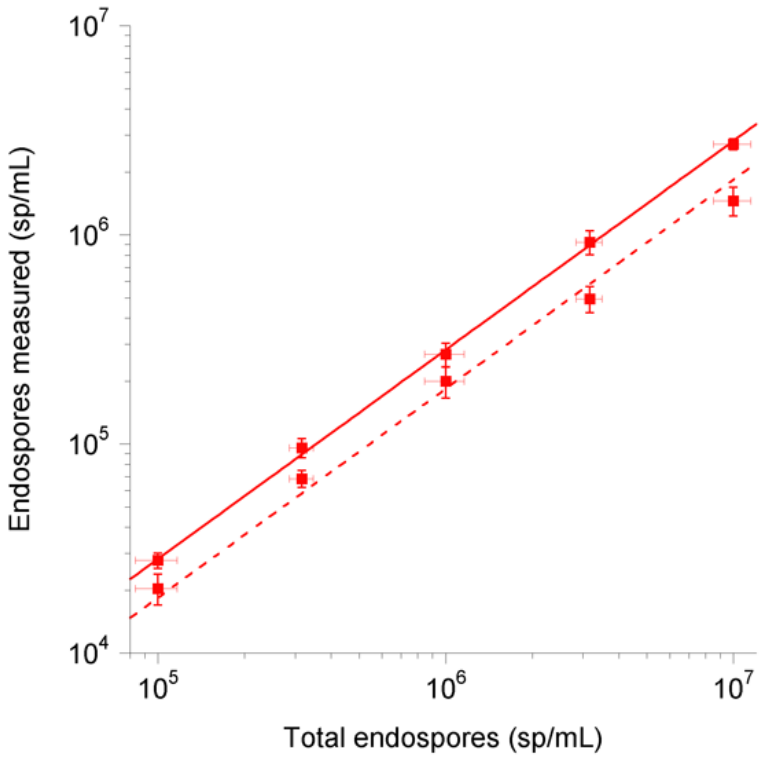

Figure 5.8 | Comparison of µEVA and SpectroEVA performance. Both red plots represent the germinable endospore population, solid line is obtained using µEVA and broken line is obtained using spectroEVA.

`

CHAPTER 6: TIME-GATED LUMINESCENCE MICROSCOPY OF SURFACE BACTERIAL SPORES AS A RAPID BIOBURDEN ASSESSMENT OF SPACECRAFT HARDWARE AND ASSEMBLY ENVIRONMENTS

6.1 Abstract

To prevent forward contamination to other celestial bodies, stringent requirements have to be imposed during the assembly, test, and launch operations (ALTO) processes of future explorations that involve invasive acquisition techniques and sample return missions. A luminescence time-gated microscopy technique (known as microscopic endospore viability assay or μEVA) has been developed to assess bioburden level as a function of germinable bacterial spore concentration on spacecraft-like surfaces and spacecraft assembly clean rooms in compliance with planetary protection guidelines. This method is based on direct counting of individual bacterial spore under a time-gated microscope, where the contrast is generated by a highly luminescent complex that forms between dipicolinic acid released from bacterial spores during germination and terbium ions in the substrate. Terbium dipicolinate acts as intrinsic probe for each germinating spore due to its high luminescence and long lifetime. In this study, we compared the surface sampling efficacy between μEVA and a culture-based NASA standard assay on bacterial spore recovery from surrogate spacecraft surfaces and clean room facilities. On a stainless steel metal surface, 25%-30% of germinable *B. atrophaeus* spores were recovered using μEVA and 10%-15% of cultivable endospores were recovered using NASA standard assay. The spore counts recovered from spacecraft assembly clean rooms were highly correlated. μEVA and culturing yielded similar D-values for the inactivation

of bacterial spores on metal surfaces; vaporized hydrogen peroxide inactivation D-values were 12.68 min and 13.39 min, respectively, while oxygen plasma inactivation D-values were 14.03 min and 16.86 min, respectively.

6.2 Introduction

Bacterial spores are dormant structures formed during the resting stage in the life cycle of genera such as *Bacillus* and *Clostridium*. They are formed within vegetative cells during sporulation, which is frequently triggered in response to adverse changes in the environment. The DNA of a spore is protected from the environment by a surrounding spore coat comprised of calcium ions, DPA and protein layers. With no detectable metabolism, bacterial spores can persist in environmental extremes, such as freezing[1], boiling[2], pressure[3,4] and desiccation[5]. Once favorable conditions return, spores undergo germination and outgrowth to become vegetative cells that can actively multiply to cause contaminations, food spoilage, diseases, etc.

Bacillus endospores are of crucial importance in astrobiology. Owing to their high resilience, endospores are candidates to survive in space and even interplanetary travel[6-9], giving rise to the theory of *Panspermia* by Arrhenius in 1903[10,11]. It hypothesized that microscopic forms of life, such as endospores, were dispersed in space by the radiation pressure from the sun, thereby seeding life from one planet to another. Spore survival in the space environment has been extensively studied[12]. The theory of *Panspermia* was verified with a modification by the introduction of *rock ejecta* that serves as vehicles for spore space travel[13]. Therefore, presence of endospores on spacecrafts can potentially

cause false positives during exobiological life detection missions and both forward and backward contaminations.

Planetary protection is the regulations imposed on robotic space missions to prevent biological contamination of future exploration sites and, in sample return missions, to protect the Earth from extraterrestrial contaminants. Viable microbes are of prime concern for spacecraft cleanliness. Currently, bioburden level on spacecrafts during ALDO processes is represented by the concentration of surface bacterial spores present and is routinely assessed by a culture-based NASA standard assay, ensuring that the bioload of spacecrafts are below a threshold level prior to launch. The NASA Procedures and Guidelines document NPG 8020.12b[14] describes planetary protection provisions for robotic extraterrestrial missions. Among the required provisions for category III-V missions is a terminal microbiological assay that determines spacecraft bioburden levels prior to launch. For example, Class IVa planetary missions, comprising landers and probes without life-detection experiments, must meet a bioburden limit of 3×10^5 spores/vehicle (and less than 300 spores m^{-2}). Missions with life-detection experiments must undergo additional procedures to ensure that the total bioload does not exceed 30 spores[15].

However, the NASA standard assay (NHB 5340.1B) method takes over three days, a time frame that is not always in concert with the rigid schedule of spacecraft assembly. μEVA can be used to expedite the detection and enumeration procedure. μEVA is a lifetime-gated microscopy technique to count individual spores in a microscope field of view, where the contrast is generated by the formation of long-lived and brightly luminescent terbium dipicolinate complex. DPA (dipicolinic acid, 2,6-

pyridinedicarboxylic acid) was uniquely found in large quantities in bacterial spores[16] and can serve as a signature proxy for spore presence[17]. DPA release is visualized as a spreading halo originated from each spore during germination, where which approximately 100 million molecules of DPA bind with Tb^{3+} ions doped in the surrounding matrix, manifesting itself as a bright spot in the field of view that grow in intensity over a timescale of minutes. Time-lapse pictures elicit focal points of concentrated DPA with characteristic temporal luminescence increase, where which each is scored an endospore count. μEVA can be coupled to a swab-rinse or wipe-rinse technique to sample endospores on a surface.

In this study, we describe validation tests between the μEVA and the NASA standard assay in enumerating bacterial spores in from metal coupon surfaces, clean room environments, and during vaporized hydrogen peroxide and oxygen plasma inactivations in terms of accuracy, precision, limit of detection, linearity and robustness.

6.3 Methods

6.3.1 Chemicals

Terbium (III) chloride hexahydrate, 99.999%, L-alanine and other salts were purchased from Sigma (St. Louis, MO) and were used as received. Ultrapure agarose (>90%) was purchased from Invitrogen (Carlbad, CA). Tryptic soy agar (TSA), nutrient broth and agar were obtained from Becton, Dicksinon and Company, (Sparks, MD).

6.3.2 Preparation of endospore stock suspension

B. atrophaeus ATCC 9372 endospores were purchased from Raven Biological Laboratories. *B. subtilis* ATCC 27370 vegetative cells were grown on TSA and inoculated onto a sporulation medium after reaching exponential growth phase. The medium contained 1.6% nutrient broth, 1.6% agar, 0.2% KCl, 0.05% $MgSO_4$, 1 mM $Ca(NO_3)_2$, 100 μM $MnCl_2 \cdot 4H_2O$, 1 μM $FeSO_4$ and 0.1% glucose (pH 7.0). After incubation at 37°C for 1 week, cells were scraped and suspended into sterile deionized water. 95% of the cells have formed spores free of sporangia. Spores were harvested and separated from vegetative cells and debris by centrifugation at 6,300 g, washing 10 times and sonication (25 kHz) for 5 minutes. The spore suspension was incubated in lysozyme (0.2 mg/mL) and trypsin (0.1 mg/mL) at 30°C with constant stirring overnight to lyze and degrade vegetative cells. Spores were finally purified by 8 cycles of centrifugation (6,300 g) and washed with sterile deionized water until > 99.9% of the cells were fully refractile with no noticeable cellular debris. Spore suspensions were stored at 4°C in the dark before use. Total spore concentrations were determined using a Petroff Hausser hemocytometer and CFU concentrations were determined using TSA spread plating in triplicate measurements.

6.3.3 Coupon cleaning and inoculation

Stainless steel sheets (40” × 80” or 100 cm × 200 cm) were procured and cut into 2” × 2” coupons in the machine shop at California Institute of Technology (Caltech). Coupons

were cleaned and inoculated as described in the methods section. Cotton applicators (Puritan, Guilford, ME) of length 15 cm were used to swab the coupon surfaces.

Coupons were rinsed with both 18.2 MΩ-cm deionized water and acetone to remove surface impurities and stains. They were then cleaned with clean room grade polyester wipes (BD Consumer Healthcare, Franklin Lakes, NY) saturated with 70% isopropyl alcohol. Each coupon was autoclaved at 121°C for 15 minutes inside a glass Petri dish. The sterile coupons were inoculated with endospores of *B. atrophaeus* and *B. subtilis*. 500 µL of spore suspension was added aseptically evenly onto the coupons using a multichannel pipettor, with final inoculum sizes of 0, 0.4, 1, 4, 12, 38, 119 and 376 CFU/coupon, respectively. Care was taken to spread the suspension evenly over the surface but not to drip over the edge. Coupons were air dried at room temperature inside a biohazard cabinet inside Petri dishes without controlling the humidity overnight.

6.3.4 Swab-rinse method

The procedures for sampling the coupons and processing the spores were similar to those described in NASA handbook 5340.1D (NHB 5340.1D)[18]. Sterile cotton applicators were used to sample the coupons (1 applicator per coupon). A single applicator was moistened in sterile water (Nanopure, 18 MΩ-cm) and the coupon was swabbed 3 times with the same cotton applicator. The coupon was rotated 90° after the first swab sampling, and 45° after the second swab sampling. The swab head was placed into 20 ml of sterile water and mixed by vortexing for 5 to 10 seconds. A total of 5 coupons were swabbed for each inoculum size. The applicator head in water was sonicated for 2 min at 25 kHz to recover spores.

A 10 ml aliquot was removed and subjected to a heat shock (15 min at 80 ± 2°C). The remaining 10 ml was not subjected to the heat shock. A 5 ml aliquot of the heat-shock sample and a 5 ml aliquot of the non-heat shock sample were removed for use in μEVA. The remaining 5 ml of the heat shock sample and the remaining 5 ml of the non heat shock sample were used in the pour plate method of the NASA standard assay. Positive and negative controls were run for each set of coupons as necessary.

After the coupons were swabbed (or not swabbed as in the positive control), they were aseptically transferred to sterile 600 ml beakers. 40 ml of sterile water was added to the coupons. The coupons were sonicated for 2 min at 25 kHz to recover any spores that were remaining on the surface. A 10 ml aliquot was removed and subjected to a heat shock (15 min at 80 ± 2°C). A separate 10 ml aliquot was not subjected to the heat shock. A 5 ml aliquot of the heat shock sample and a 5 ml aliquot of the non heat shock sample were removed for use in the lifetime gated imaging assay. The remaining 5 ml of the heat shock sample and the remaining 5 ml of the non heat shock sample were used in the pour plate method of the NASA standard assay.

The samples were: (1) heat shock swab; (2) no heat shock swab; (3) heat shock coupon; (4) no heat shock coupon. The positive control consisted of: (1) heat shock coupon; (2) no heat shock coupon. Negative controls included: (1) TSA media controls (media only in the Petri dish); (2) swab water control (water that the swab was dipped into before it was used to swab the coupon); (3) dilution water control (water that was used to make the dilutions before the recovered spores were diluted and plated). Figure 6.2 outlines the experimental procedure in a flowchart.

6.3.5 NASA Standard Assay

The following procedure was used to perform the pour plate method of the NASA standard assay (NHB 5340.1D)[18]. In the NASA standard assay of flight hardware for Planetary Protection implementation, it is usually not necessary to make dilutions of the samples before plating. However, some inoculum sizes in this experiment required that serial dilutions be made so that the number of colonies in a Petri dish was countable.

The samples were stored at 4°C for about an hour after heat shock and before dilutions were made. Serial 10-fold dilutions were made for each sample. For the dilutions, 4.5 ml of water was used as the diluent. A 0.5 mL sample was removed and added to the diluent to produce a 10-fold serial dilution. The dilution range was 10^0 (undiluted) to a 10^{-5} dilution. The pour plate method was used. 2 mL aliquots of the diluted samples were placed into 2 Petri dishes (4 ml total). Approximately 25 mL of sterile, molten TSA was added to each plate and gently swirled. A mediaclave (Integra Biosciences, Chur, Switzerland) was used to dispense the sterile media. The plates were allowed to harden and were incubated at 32°C for 3 days. The colonies on the plates were counted after incubation

6.3.6 Sample preparation for μEVA experiments

Spore suspensions were filtered onto 0.2 μm polycarbonate membrane filters (Whatman, Florham Park, NJ) using filtration manifolds of different diameters depending on the desired concentration factor such that there were less than 300 spores per microscopic

field of view. To ensure that the spore surface density was optimal for a given initial spore suspension concentration, suspensions of $>10^6$ sp mL^{-1} were filtered onto 25-mm-diameter spots using glass filtration funnels, and suspensions of $<10^6$ sp mL^{-1} were filtered onto 1.5-mm^2 spots using a 96-well micro-sample filtration manifold (Schleicher & Schuell, Keene, NH). Spores concentrated on the filter were rubbed and transferred to a ~0.5 mm thick, 9 mm diameter slab of 1.5% agarose substrate containing 100 μM $TbCl_3$ and 20 mM L-alanine mounted in a silicone isolator (Molecular Probes, Eugene, OR) on a quartz microscope slide. After spore transfer, the agarose surface was covered with a piece of 0.2-mm-thick polydimethylsiloxane (PDMS). Figure 6.2 illustrates the final sample configuration.

Polydimethylsiloxane (PDMS) was prepared by mixing the polymer base and curing agent (Sylgard, Dow Corning) in 10 to 1 ratio. After degassing, the mixture was casted over a 0.2-mm thick stainless steel mold and cured in an oven for 2 hours at 65°C. Agarose, silicone isolator and PDMS were autoclaved at 121°C for 15 min before use. A piece of PDMS was peeled off and attached on top of a spore-laden agarose surface aseptically for sealing.

6.3.7 The μEVA instrument

The instrument consists of a time-gated camera (Photonics Research Systems, Salford, UK) mounted on a Nikon SMZ800 stereoscopic microscope (large working distance for xenon lamp), a xenon flashlamp (Perkin-Elmer, Waltham, MA) mounted at 45 degrees with respect to the sample, and a temperature controlled microscope slide holder (Thermal). The slide holder enabled spores to germinate at 37°C. The CCD camera has a

resolution of 752 x 582 pixels at 14 bits with a chip size of 2/3 inch. The camera has 50% sensitivity between 430-730 nm, with peak sensitivity at 550 nm. It was cooled to 40°C below ambient temperature and was synchronized to the xenon lamp *via* TTL pulses (300 Hz with tail time up to 50 μs). A highpass filter (03FCG067, Melles Griot) centered at 500 nm was placed along the light path on the emission side before reaching the microscope objective. We collected time stacks of time-gated images by real-time streaming with a delay of 100 μs and exposure time of 5 s in each frame (see Chapter 3).

6.3.8 Endospore germination and assignment

Spore germination on agarose surface followed the reported micro-germination kinetics[19-21]. DPA released from single *B. atrophaeus* and *B. subtilis* spores manifested as individual bright spots in 15 minutes under time-gated microscopy due to local formation of Tb-DPA on the L-alanine doped agarose germination substrate. We performed image analysis in Matlab to obtain background-subtracted stack of time-gated images. Assignment of endospores was made based on intensity and size. Adaptive thresholding was applied to segment pixels that were 3 times brighter than the background with a characteristic rising intensity. Each bright spot must exhibit a continuous rising intensity over the course of germination in order to register a spore count. This criterion minimized false positives by eliminating sporadic bright spots and long-lived luminescent interference. The 8-connected adjacent pixels were analyzed to screen for spore clumps. The number of spores present was calculated by dividing the squared sum of neighboring pixel brightness by the mean brightness of an individual spore determined empirically. This was done in a recursive way until all of the pixels were counted and marked.

Germinable spore units would be reported as too numerous to count if they exceeded 300 in a field of view. Further dilution would be carried out in this case.

6.3.9 Viability ratio

Viability ratio of spores was determined by dividing the population of germinable spores by total spores. Spores capable of releasing DPA during germination were considered viable. Total spore counts were either performed using a hemocytometer if the initial spore concentration was above 10^6 spores mL^{-1}. Low spore concentrations were counted using a phase contrast microscope. A smear of 10 μL or more of spores was prepared on a cover slip. After mounted on a microscope slide, the area of smear would be calculated under low magnification. About 100 images would be taken using a motorized microscope stage and automatic counting algorithm under a 60x phase contrast objective due to uneven spatial distribution. The number of total spores present in low concentration samples would be determined by calculating the area conversion factor. Viability ratio of spores was determined by dividing the number of germinable spore counts by the total number of spore counts.

6.3.10 Surface sampling and NASA standard assay

To validate this novel *Bacillus* endospore viability assay, side-by-side comparison experiments were performed on recovering *B. subtilis* pure endospores laden on metal coupons using μEVA and the NASA standard assay. The procedures for sampling the coupons and processing the spores were similar to those described in NASA handbook

5340.1D (NHB 5340.1D). A cotton applicator was moistened and the coupon was swabbed 3 times with the same cotton applicator. We rotated the coupon 90° after the first swab sampling, and 45° after the second swab sampling. The swab head was placed into 10 ml of sterile water and mixed by vortexing for 5 seconds. We sonicated the applicator head in water for 2 min at 25 kHz to enhance spore recovery. The aliquot was subjected to a heat shock for 15 min at 80 ± 2°C. 5 ml aliquot was cultivated in TSA using pour plating and colonies were counted after 72 hours of incubation at 37°C (n = 60). The remaining 5 ml was analyzed using our microscopy approach (n = 56).

6.3.11 Vaporized hydrogen peroxide inactivation

Vaporized hydrogen peroxide resistance was measured by germinability (DPA release) and culturability (colony formation on TSA) of spores laden on metal coupons. *G. stearothermophilus* ATCC 7953 endospores (Log 2967, mean population = 1.8×10^6 cfu coupon^{-1}) were used. In a preliminary test, 0.5 mL of hydrogen peroxide was vaporized at 45°C for 3 minutes in a chamber at Jet Propulsion Laboratory. 10^7 *B. atrophaeus* spores coupon^{-1} and 1.8×10^6 *G. stearothermophilus* TCC 7953 spores coupon^{-1} were placed inside sterilization pouches and subjected to vaporized H_2O_2 inactivation. *B. atrophaeus* and *G. stearothermophilus* endospores were incubated and germinated at 37°C and 55°C, respectively. In the concentration dependence experiment, *G. stearothermophilus* endospores strips with different durations of vaporized H_2O_2 inactivation treatment (0, 15, 30, 45, 60 min) were obtained from Steris Corporation using a LaCalhene two-glove isolator connected to a VHP1000ED system.

6.3.12 Oxygen plasma inactivation study

B. atrophaeus and *B. subtilis* endospores were inoculated onto a 2 mm × 2 mm piece of PDMS placed on a glass microscope slide. During plasma inactivation, the sample slide was placed within a glass vacuum chamber with oxygen and the plasma gas along with various inert buffer gases in the air. Once evacuated, process gases were slowly returned to the chamber in small quantities at approximately 200-600 millitorr. During this time, a current was charged for approximately one minute and discharged into a copper solenoid encircling the chamber. RF and electric fields generated at the center of the solenoid by the current running through the coil excited oxygen electrons at low pressures within the chamber therefore heating the gas into plasma which radiated visibly in violet. The degree of inactivation was measured by μEVA and direct plating on TSA.

6.3.13 Clean room sampling

Surface samples were collected in the Spacecraft Assembly Facility building at Jet Propulsion Laboratory, Pasadena. Proper gowns, gloves and protective gear were worn while sampling in the clean and. Samples were collected using the swab-rinse technique on the floor, metal plates, grooves on the ground as well as the Mars Science Laboratory hardware surface.

6.3.14 Statistical analysis

In this study, bacterial counts could be categorized into 2 regimes of distribution. High concentrations (>10 counts) followed Gaussian distribution. A square-root transformation

was performed on some of the dataset to homogenize the variance and normalize the negative skewness. Normality was tested using the Shapiro-Wilk test by looking at skewness and kurtosis of the distribution. Parametric analyses such as Student t-test was used to determine the confidence interval and F-test was used to examine differences between the sample variances. Low concentrations (<10 counts) followed Poisson distribution. Non-parametric analyses such as Wilcoxon test was used to determine the confidence interval, and Kruskal-Wallis test was used for variance analysis. We reported the 95% confidence interval based on 1.96 SD on the normally distributed datasets. Data fallen within 5% and 95% percentile ranking constituted the reported 95% confidence interval for the Poisson distributed datasets.

6.4 Results

The fundamental objective of this investigation was to compare the surface sampling efficacy between μEVA and the NASA standard assay in an effort to evaluate bioburden reduction on spacecraft surfaces. A side-by-side comparison of the two methods was carried out on determining the number of endospores inoculated on stainless steel coupons, on a concentration of 1000 spores/coupon down to sterility. Once a correlation had been established, the two assays were applied to evaluate the background endospore level in a spacecraft assembly clean room. Finally, the two methods were employed to assess the bioburden reduction effect by vaporized hydrogen peroxide and oxygen plasma, two new low-temperature techniques that might potentially be adopted by NASA for future sterilization endeavor on heat-liable spacecraft hardware.

6.4.1 Surface sampling of pure spore suspension on metal coupons

When sampling stainless steel coupons inoculated with *B. subtilis* 168 endospores ranging from 1 to 1000, μEVA recovered 21.2% ± 3.7% (n = 56) and the NASA standard assay recovered 6.8% ± 0.6% (n = 60) of the total population. Coefficients of determination of the linear plots are 0.9919 for μEVA and 0.9906 for NASA standard assay. False positive were not observed using sterile coupons. It has to be taken into consideration that the germinable population was found to be higher than the culturable population in the bacterial spore batch in this experiment. Of this population, 55.6% of the endospores were germinable and only 37.4% were culturable. So, if the recovery rate was calculated to be the number of measured endospores capable of germination divided by the total number of germinable endospores and measured cfu normalized by the total cfu. Then the adjusted recovery rate would be 38.1% ± 2.6% (n=56) for μEVA and the 18.2% ± 0.4% for NASA standard assay. The difference between the mean of the two assays were statistically significant in both cases. There was no difference between repeatability of the two assays at 90% confidence interval using the F-test.

The distribution of the number of recovered units was expressed in the form of a histogram in Figure 6.3. At low inoculum, the distribution of recovered units is Poisson distributed. The Poisson distribution approximated closely to a normal distribution when the inoculum size reached 100 spores coupon^{-1}. From 1 spore/coupon to 31.6 spores/coupon, the number of germinable units vs. culturable units showed correlation of 2.07 ± 0.20. At higher inoculum from 100 to 1000 spores/coupon, germinable to culturable counts elicited a 1:1 ratio at 1.04 ± 0.15.

6.4.2 Surface sampling of endospores in a spacecraft assembly clean room

Results of the 4 different sampling places were tabulated in Table 6.1. The distributions showed a general departure from Poisson distribution. The microbial population tended to have an aggregated or clustered type of distribution, rather than being spread around at random, leading to large proportion of empty samples but accompanied by a peak of clumping. Relatively large standard deviations were therefore observed. Most of the recovered microbes were heat-shock survivors as revealed by the insignificant differences between the heat shock and non-heat shock results in NASA standard assays ($p = 0.4060$). The difference between the results reported by both methods was not statistically significant ($p = 0.1532$). Associated with dust and lint, the visibly turbid groove sample extracts were found to contain more bacteria.

6.4.3 Monitoring of endospore inactivation to vaporized hydrogen peroxide

In the preliminary test carried out at the vaporized hydrogen peroxide facility at JPL. Under the specified condition, *B. atrophaeus* spores were all rendered dead less than 3 minutes of exposure. No germinable or culturable counts were obtained. In the case of *G. stearothermophilus*, μEVA recovered 1.71% ± 0.89% of the total germinable endospores and the NASA standard assay recovered 0.69% ± 0.41% of the total cfu after vaporized H_2O_2 inactivation. A systematic inactivation study of *G. stearothermophilus* as a function of vaporized hydrogen peroxide treatment time was conducted with courtesy from Steris Corporation. Figure 6.5a illustrates the inactivation data fitted to a log-linear plot. The coefficients of determination values were 0.9918 and 0.9901 for μEVA and NASA standard assay, respectively. The results obtained by both methods were highly correlated

(r = 0.9998). D-values were calculated as 12.68 ± 0.67 min and 13.39 ± 0.77 min using μEVA and NASA standard assay, respectively.

6.4.4 Monitoring of endospore inactivation to oxygen plasma

Figure 6.5b shows the microbial survivor curve followed first-order exponential inactivation kinetics from 0 to 30 min with good fitting to linear plots (R^2 = 0.9852 for μEVA and R^2 = 0.9884 for NASA standard assay). A sudden drop in germinability and culturability took place after 30 min. The two methods were highly correlated (r = 0.9997). The log-linear regime yielded D-values of 14.03 ± 1.56 min and 16.86 ± 3.96 min using μEVA and NASA standard assay, respectively.

6.5 Discussion and Conclusion

One of the fundamental tenets of microbiology is the use of cultivation in the enumeration of bacteria. The cultivation-based NASA standard assay has been the only method in validating the compliance of spacecraft bioburden reduction to planetary protection requirements at NASA. There are several limitations for the NASA standard assay. First, this process requires 3 days to complete. Thus, when plate counting is employed as the terminal microbiological assay, the spacecraft must be protected from recontamination. Second, a large number of bacterial spores can aggregate on individual particulates giving rise to a single CFU, and is thus a large underestimation of the bioburden. Third, colony-counting methods only account for cultivable spore-forming species, which constitute less than 1% in soil samples; a significant component of

spacecraft contamination is known to come from soil. Bypassing the lengthy outgrowth and colony-forming phases, μEVA proves to be a rapid and efficient assay combines time-gating and lanthanide luminescence photochemistry to detect germinable *Bacillus* endospores on surfaces. The unique photophysical and chemical characteristics of Tb-DPA make μEVA a powerful analytical tool for bioburden assessment in exobiological explorations.

Dry heat is currently used for the terminal decontamination process for spacecrafts. We have compared the inactivation kinetics of *Bacillus* endospores using μEVA and heterotrophic plate counts. In view of the increasing number of heat-liable electronics, there is an urging need to develop low-temperature sterilization regimen for spacecraft decontamination. Vaporized hydrogen peroxide and oxygen plasma are two potential candidates as both methods operate at relatively low temperature, around 45°C, and produce non toxic by-products towards the end of the sterilization process. We have compared the inactivation profile using μEVA and NASA standard assay on *Bacillus* endospores impregnated on metal strips. A high degree of correlation exists between the loss of germinability and culturability with respect to these two inactivation regimens.

The probability of obtaining a sterile spacecraft is enhanced significantly if the level of microbial contamination is relatively low prior to the terminal heat treatment. Therefore, spacecraft hardware is assembled inside class 100 clean rooms where microbial contamination can be minimized. Poisson and Gaussian distributions are observed in the pure endospore suspension recovery from coupon experiment, but not from the class 100 clean room sampling. A much greater degree of heterogeneity has been observed in the latter case, characterized by aggregation and patchiness. Some kind

of territorialism may favor the presence of microbial hot spots in the clean room. Variation may also be attributed by the larger variety of heat-shock survivors as revealed by the plate count results. At least 3 distinct colony morphologies and different germination kinetics have been observed in the clean room samples.

A quantitative relationship has been established between the two assays. μEVA and NASA standard assay are found to correlate in a 2:1 ratio at low inoculum regime and 1:1 at high inoculum regime. One plausible reason is that one of the intermediate extraction processes selects preferentially for germinable-but-not culturable endospore. It may give rise to the observed discrepancy, which becomes proportionately apparent at low concentrations. In general, more germinable endospores are recovered than culturable ones which may suggest that (1) germinable endospores endure heat shock, swabbing, sonication and vortexing processes better; (2) endospores lose their ability to form colonies during the sampling and extraction procedures. Endospores residing in a clean room environment are reported to be more resistant[22,23]. The first point is further substantiated by our clean room sampling results in which most of the germinable heat-shock survivors can form colonies.

The culturable endospore recovery rate, albeit low, is consistent with similar studies reported in the literature[24-26]. While the swab-rinse technique is not the most effective way to collect and extract microbes in suspension, it is adopted by the NASA standard assay and is thus used throughout this study. Both methods report a relatively high standard deviation. Angelotti *et al.* proposed that high variance in recovery was not inherent in the sampling, but was attributed by the intermediate extraction process[27]. So, we have proposed the use of PDMS roller in the collection and analysis of surface

endospores in future studies. The adhesive PDMS can readily collect endospores on a surface and can subsequently be pressed against a germination substrate for direct time-gated imaging, obviating steps such as resuspension, vortexing and sonication. Since μEVA is an endospore-specific method, there is no need to carry out an additional heat shock process to remove vegetative bacteria. As indicated in our data, the difference between heat shock and non heat shock μEVA data is statistically insignificant ($p = 0.8064$). This newly proposed PDMS sampling methodology is expected to facilitate the efficiency, precision and speed in the enumeration of surface endospores.

For a given population of endospores, a subset will germinate, and a subset of that population capable of germination will form colonies. The actual viable endospore population will fall between the populations capable of outgrowth and germination. The culture-based NASA standard assay will underestimate the viable endospore bioburden, due to viable-but-non-culturable (VBNC) populations; on the other hand, μEVA will overestimate the viable endospore bioburden since not every germinable endospore eventually develops into a visible colony. Therefore, μEVA and NASA standard assay are complementary methods in evaluating the upper and lower limits of bioburden level in planetary protection endeavors. In conclusion, we demonstrated that a basic microscope setup with time-gating image system is an effective tool for endospore detection, and the use of a solid substrate to induce *Bacillus* endospore germination and detect subsequent release of DPA, thus opening up new avenues for exploring the rich biology of endospores. We envision the μEVA as a general fluorescence lifetime imaging technique will contribute to the construction of a complete and high-throughput detection

system for endospores, providing insights into sterilization validation, astrobiology and planetary protection.

6.6 References

1. Roberts, T.A., Hitchins, A. D. Resistance of spores. *The Bacterial Spore ed. Gould, G. W. and Hurst, A*, 611-670 (1969).
2. Fox, K. and Eder, B.D. Comparison of survivor curves of *Bacillus subtilis* spores subjected to wet and dry heat. *Journal of Food Science* **34**, 518-521 (1969).
3. Jannasch, H.W., Wirsen, C.O., Molyneaux, S.J., and Langworthy, T.A. Comparative physiological studies on hyperthermophilic archaea isolated from deep-sea hot vents with emphasis on Pyrococcus strain GB-D. *Applied and Environmental Microbiology* **58**, 3472-3481 (1992).
4. Wuytack, E.Y., Boven, S., and Michiels, C.W. Comparative study of pressure-induced germination of *Bacillus subtilis* spores at low and high pressures. *Applied and Environmental Microbiology* **64**, 3220-3224 (1998).
5. Koike, J. *et al*. Survivor rates of some terrestrial microorganisms under simulated space conditions. *Advances in Space Research* **12**, 271-274 (1992).
6. Mileikowsky, C. *et al*. Natural transfer of viable microbes in space 1. From Mars to Earth and Earth to Mars. *Icarus* **145**, 391-427 (2000).
7. Nicholson, W.L., Munakata, N., Horneck, G., Melosh, H.J., and Setlow, P. Resistance of *Bacillus* endospores to extreme terrestrial and extraterrestrial environments. *Microbiology and Molecular Biology Reviews* **64**, 548-572 (2000).
8. Nicholson, W.L., Schuerger, A.C., and Setlow, P. The solar UV environment and bacterial spore UV resistance: considerations for Earth-to-Mars transport by natural processes and human spaceflight. *Mutation Research-Fundamental and Molecular Mechanisms of Mutagenesis* **571**, 249-264 (2005).
9. Fajardo-Cavazos, P., Link, L., Melosh, H.J., and Nicholson, W.L. *Bacillus subtilis* spores on artificial meteorites survive hypervelocity atmospheric entry: Implications for lithopanspermia. *Astrobiology* **5**, 726-736 (2005).
10. Arrhenius, S., *Worlds in the Making: The Evolution of the Universe*. (1908).
11. Burchell, M.J. Panspermia today. *International Journal of Astrobiology* **3**, 73-80 (2004).
12. Nicholson, W.L. Using thermal inactivation kinetics to calculate the probability of extreme spore longevity: Implications for paleomicrobiology and lithopanspermia. *Origins of Life and Evolution of the Biosphere* **33**, 621-631 (2003).
13. Gladman, B.J., Burns, J.A., Duncan, M., Lee, P., and Levison, H.F. The exchange of *impact ejecta* between terrestrial planets. *Science* **271**, 1387 (1996).
14. Office of Space Science, N.A.a.S.A., *Planetary Protection Provisions for Robotic Extraterrestrial Missions*. (Washington, D.C., 1999).
15. Board, S.S. and Council, N.R., *Preventing the Forward Contamination of Europa*. (National Academy Press, Washington, D.C., 2000).
16. Powell, J.F. Isolation of dipicolinic acid (pyridine-2-6-dicarboxylic acid) from spores of Bacillus megatherium. *Biochemical Journal* **54**, 210-211 (1953).
17. Murrell, W.G., in *The Bacterial Spore*, edited by G. W. Gould (Academic Press, New York, 1969), pp. 245-270.

18. Anonymous. NASA standard procedures for the microbiological examination of space hardware, NHB 5340.1D. *Jet Propulsion Laboratory Communication, National Aeronautics and Space Administration* (1980).
19. Hashimoto, T., Frieben, W.R., and Conti, S.F. Microgermination of *Bacillus cereus* spores. *Journal of Bacteriology* **100**, 1385-1392 (1969).
20. Hashimoto, T., Frieben, W.R., and Conti, S.F. Germination of single bacterial spores. *Journal of Bacteriology* **98**, 1011-1020 (1969).
21. Woese, C. and Morowitz, H.J. Kinetics of the release of dipicolinic acid from spores of *Bacillus subtilis*. *Journal of Bacteriology* **76**, 81-83 (1958).
22. Venkateswaran, K. *et al*. *Bacillus nealsonii* sp. nov., isolated from a spacecraft-assembly facility, whose spores are gamma-radiation resistant. *International Journal of Systematic and Evolutionary Microbiology* **53**, 165-172 (2003).
23. Link, L., Sawyer, J., Venkateswaran, K., and Nicholson, W. Extreme spore UV resistance of *Bacillus pumilus* isolates obtained from an ultraclean spacecraft assembly facility. *Microbial Ecology* **47**, 159-163 (2003).
24. Rose, L., Jensen, B., Peterson, A., Banerjee, S.N., and Arduino, M.J. Swab materials and *Bacillus anthracis* spore recovery from nonporous surfaces. *Emerging Infectious Diseases* **10**, 1023-1029 (2004).
25. Hodges, L.R., Rose, L.J., Peterson, A., Noble-Wang, J., and Arduino, M.J. Evaluation of a macrofoam swab protocol for the recovery of *Bacillus anthracis* spores from a steel surface. *Applied and Environmental Microbiology* **72**, 4429-4430 (2006).
26. Brown, G.S. *et al*. Evaluation of a wipe surface sample method for collection of *Bacillus* spores from nonporous surfaces. *Applied and Environmental Microbiology* **73**, 706-710 (2007).
27. Angelotti, R., Wilson, J.L., Litsky, W., and Walter, W.G. Comparative evaluation of the cotton swab and Rodac methods for the recovery of *Bacillus subtilis* spore contamination from stainless steel surfaces. *Health Laboratory Science* **1**, 289-296 (1964).

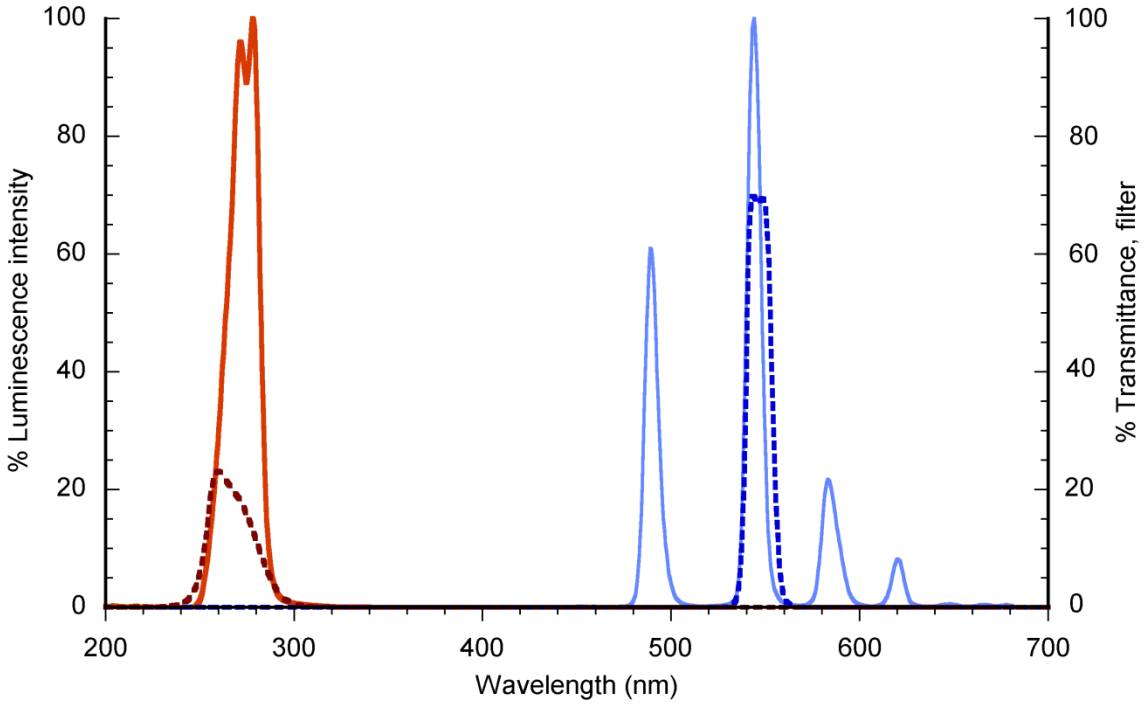

Figure 6.1 | Spectral overlap of different spectra. Excitation spectrum of terbium dipicolinate (10 μM $TbCl_3$ + 62.5 nM DPA in 1 M sodium acetate buffer at pH 5.8) at 544 nm emission wavelength is shown in solid red line. Excitation spectrum of the same terbium dipicolinate solution at 278 nm excitation wavelength is shown in solid blue line. The xenon flashlamp emission spectrum (red dashed line) is shown overlapping with Tb-DPA excitation band in the mid-UV 250 - 300 nm range. The xenon flashlamp provides a broadband emission wavelength from UV to IR, with peak intensity at 460 nm. Transmittance spectrum of the emission UV-blocking high-pass filter (blue dashed line) shows that it can effectively prevent most of the UV excitation from entering the camera. In addition to this, a delay of 100-μs discriminates the long-lived Tb-DPA signal from the short-lived xenon excitation. Green luminescence exhibited by Tb-DPA can thus be imaged by the lifetime-gated CCD camera.

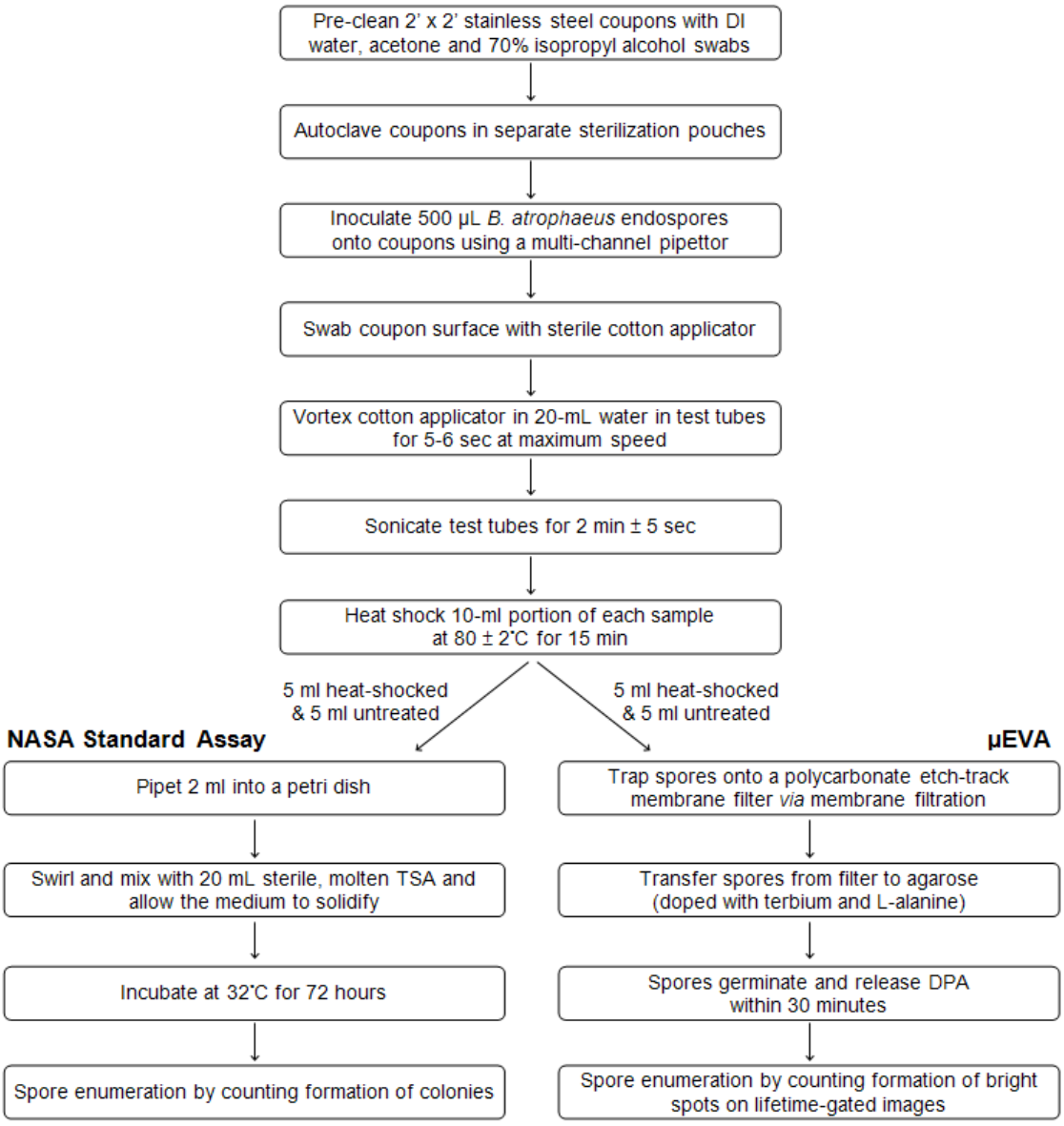

Figure 6.2 | Flowchart of the experimental procedure. Pre-cleaning, inoculation and swab-rinse technique were common for both assays. Heat shock selected for bacterial spores over vegetative cells. Extractions were split into halves and subjected to both assays for parallel comparison. The cultivation-based NASA standard assay used TSA pour plating to assess cultivable spore population in terms of CFU in 3 days. µEVA enumerates endospores in less than 30 minutes in terms of germinable units by inducing release of DPA *via* germination.

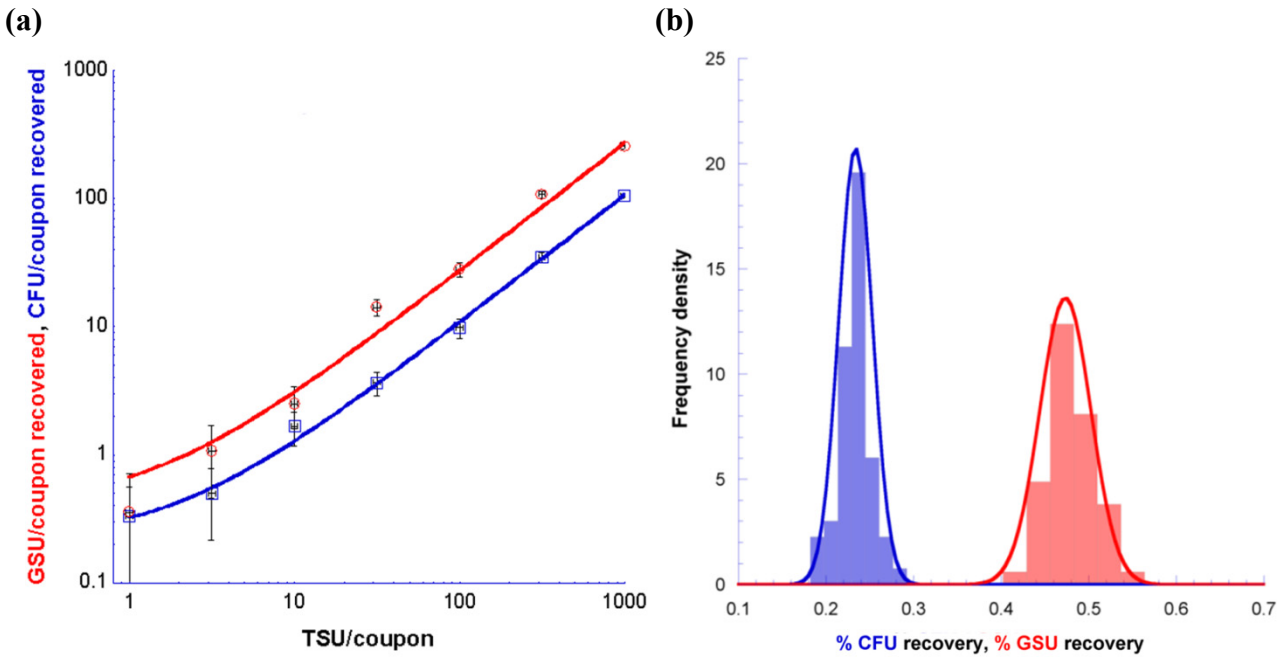

Figure 6.3 | (a) Recovery of endospores on stainless steel coupon surface using µEVA and NASA standard assay. µEVA measures the number of endospores capable of germination and NASA standard assay measures the number of endospores capable of forming colonies. **(b)** Histogram depiction of 1000 endospores/coupon. Both methods show a Gaussian distribution with normally distributed data.

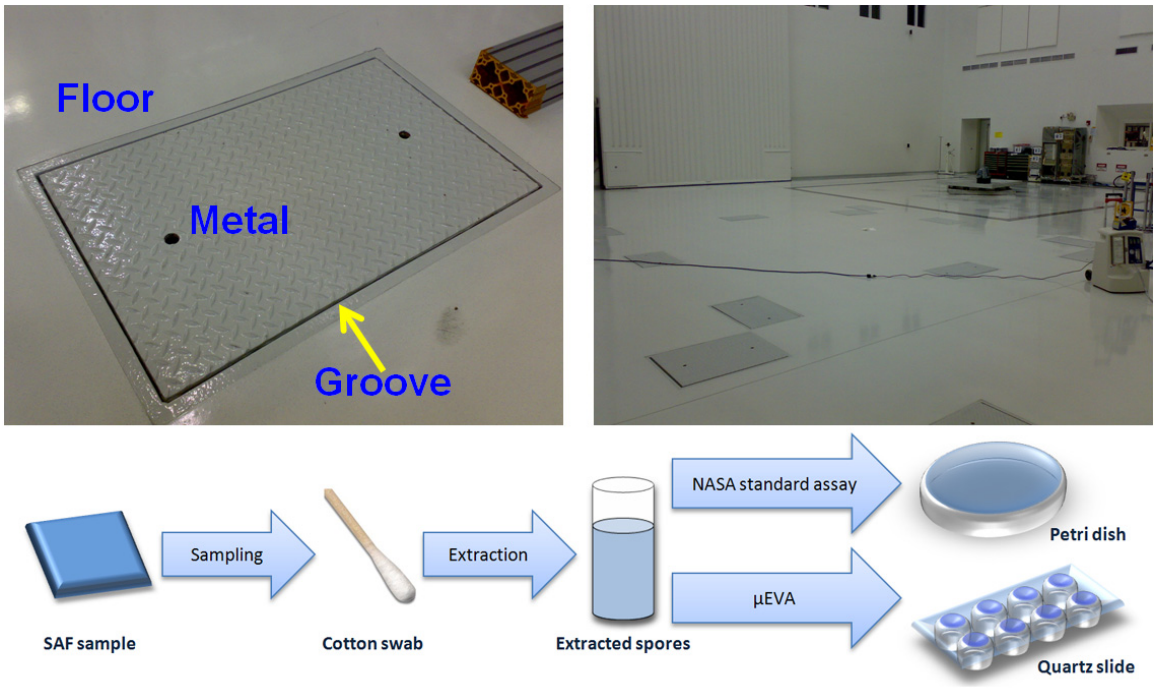

Figure 6.4 | Sample collection sites of the clean room inside the Spacecraft Assembly Facility (SAF) building at Jet Propulsion Laboratory.

(a) **(b)**

	NASA standard assay, cfu cm^{-2}		µEVA, germinable endospore cm^{-2}	
	Non-heat shock	Heat shock	Non-heat shock	Heat shock
Floor	0.29 (0.53)	0 (0)	0 (0)	0 (0)
Metal plate	1.33 (1.15)	1.22 (1.11)	1.33 (1.15)	1.33 (1.15)
Groove	2.60 (1.61)	2.60 (1.61)	3.75 (1.94)	3.00 (1.73)
MSL surface	1.40 (1.18)	0.80 (0.89)	0 (0)	0 (0)

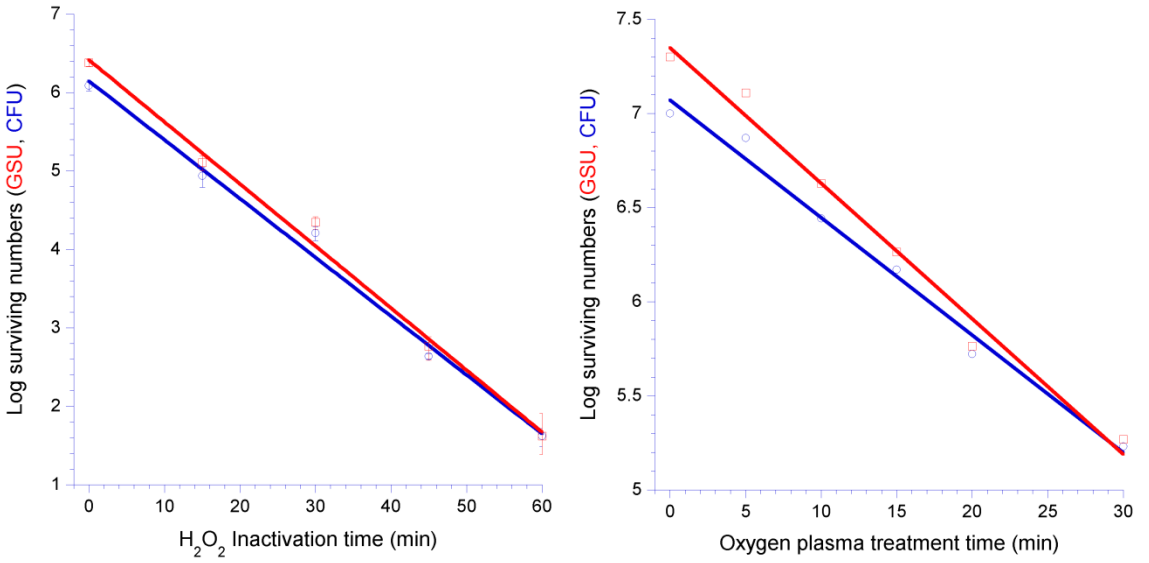

Figure 6.5 | (a) Survivor curve of *G. stearothermophilus* endospores when subjected to vaporized hydrogen peroxide inactivation is fitted with a log-linear plot, measured by µEVA (red) and NASA standard assay (blue). **(b)** Survivor curve of *B. atrophaeus* endospores to oxygen plasma measured by µEVA (red) and NASA standard assay (blue). The plot shows a log-linear regime and a sudden viability drop after 30 min.

Table 6.1 | (a) Survivor curve of *G. stearothermophilus* endospores when subjected to vaporized hydrogen peroxide inactivation is fitted with a log-linear plot, measured by μEVA (red) and NASA standard assay (blue). **(b)** Survivor curve of *B. atrophaeus* endospores to oxygen plasma measured by μEVA (red) and NASA standard assay (blue). The plot shows a log-linear regime and a sudden viability drop after 30 min.

CHAPTER 7: METHOD DEVELOPMENT FOR ASTROBIOLOGIAL EXPLORATION

7.1 Abstract

This chapter describes a wide variety of experiments involving method development, instrument building and model formulation to path way for the study of endospores under extreme environments on Earth as models for the astrobiological search of life in other planets. This chapter consists of 3 separate modules (1) development of a sporulation protocol for psychrophilic endospores; (2) mathematical modeling of the microgermination and macrogermination kinetics of *Bacillus* endospores; (3) methodology to increase culturable counts from endospores isolated from an environment.

7.2 Sporulation of psychrophilic endospores

Studying of psychrophilic bacterial spores in cyrospheres such as ice cores and permafrost has shed light on the understanding of how microorganisms can survive at subfreezing temperatures on Earth and possibly on Mars and other cold planetary bodies. This chapter describes the isolation of psychrophilic *Bacillus* species from soils in Jet Propulsion Laboratory and Lake Vida in Antarctica, as well as a comparison between environmental psychrophilic strains with laboratory cultured psychrophilic endospores in terms of endospore properties, heat resistance and germination kinetics. Novel sporulation techniques have been developed to produce synchronized and homogeneous psychrophilic *Bacillus* endospores. Psychrophilic endospores are more demanding than

their mesophilic counterparts in terms of sporulation requirement. Aeration and germination inhibitor, such as D-alanine, were added to the nutrient exhaustion sporulation medium in order to obtain large, pure and homogeneous spore batches for germination and resistance studies.

7.2.1 Introduction

Endospores under psychrophilic conditions are of great significance because 3-quarter of the earth's surface are covered with cold oceans and large land masses are maintained at low temperatures, which finds relevancy with lots of different icy celestial bodies. Study of endospores as the most resistant and long-lived survivor in various extreme cold biospheres, such as ice cores, polar lakes and alpine permafrost, hints to the exobiological search for life. When encountering nutritional deficiency, rod-shaped Gram-positive bacteria of the genera *Bacillus* and *Clostridium* differentiate to produce heat- and solvent-resistant endospores. Endospores have also been detected from these cold environments[1-4]. In the past several decades, mesophilic endospores such as *Bacillus subtilis*, *B. megaterium* and *B. anthracis* have been thoroughly studied due to their easy handling and fast growth rate. Yet endospore psychrophily has received little attention since Larkin and Stokes have reported on spore formation and germination at 0°C by aerobic spore-formers from soil, mud and water in 1966[5,6]. Cold-adapted microbes can broadly be categorized into two groupings, psychrophiles and psychrotolerants. Psychrophiles are defined to be microorganisms that have a growth temperature range from 22°C to 0°C or lower, with an optimum growth at about 15°C. On the other hand, psychrotolerants generally do not grow at zero but do at 3-5°C, and have optimum and maximum growth

temperatures above 20°C[7,8]. For simplicity, in what follows, the term psychrophile is used to cover both groups, unless there are specific and relevant differences. In this study, we revisit and study sporulation, germination, and resistance properties of psychrophilic endospores using an array of new microbiological techniques.

Work with Earth ice has raised the importance to develop proper protocols and method at low temperatures. Nevertheless, most of our understanding on sporulation, germination and resistance of endospores rest on the most-studied *B. subtilis* and its close mesophilic relatives. In order to study cold biosphere properly, we need to understand more about cold-tolerant endospore-forming bacteria. Towards this goal, the first step is to produce clean psychrophilic endospores in a synchronized and homogeneous way. Psychrophilic pores are routinely produced on fortified agar or in rich liquid media in previous studies, which results in heterogeneous batches. It has also been well established that bacterial spore properties are affected by the conditions during sporulation. Metal and lipid contents in particular are affected greatly by the preparatory method. Therefore, a novel sporulation protocol for psychrophilic spores have been developed that is of great importance for obtaining reproducible and homogeneous endospore batches for a thorough characterization of germination and other properties.

Considerable differences have been shown to exist between laboratory strain and environmental mesophilic endospores, including *B. subtilis* and *B. atrophaeus*, which are typically used as model strains in all types of spore work. Prolonged cultivation of bacteria in laboratory conditions can cause changes in gene expression patterns and loss of key properties for survival in the natural environment[9-11]. It is of prime importance to know the variability of key spore properties such as germination and heat resistance in

the natural psychrophilic population. Knowing the boundary conditions for heat tolerance in the environment can help determine an optimal heat shock temperature for screening endospores from vegetative cells. Gould *et al.* have investigated the germination behavior of crude spores isolated directly from soil and reported that a significant proportion of the spores did not respond to any germinative compound[12]. Response to various germinants is crucial to the application of endospore viability assays.

7.2.2 Methods

7.2.2.1 Bacterial strains and growth conditions

Bacillus longisporus (DSM 477) and *Bacillus psychrodurans* (DSM 11713) were obtained from the German Collection of Microorganisms and Cell Cultures. All solutions and agar media were pre-chilled to 4°C and held at this temperature on a cold tray during the whole inoculation procedure. Both of them were growth in nutrient broth incubated at 20°C in a shaking bath at 120 rev min^{-1}.

Environmental strains were isolated from JPL soils and Lake Vida from Antarctica using the single cell technique[13]. JPL subsurface soil samples were collected aseptically in sterile jars and Lake Vida brine sample was received as a gift. Soil and mud samples were diluted 1:10 in sterile 0.1% peptone and heated at 80°C for 15 min to inactivate vegetative cells. Lake Vida samples were heated without prior dilution. A 100-µl amount of the soil extract was inoculated onto tryptic soy agar (TSA) (Difco, Sparks, MD). 5-mL of the brine sample was inoculated into 25 ml of a medium consisting of 12.5 g of NaCl, 2 g of K_2HPO_4, 1.25 g of KH_2PO_4, 0.5 g of $MgSO_4 \cdot 7H_2O$, 0.125 g of $CaCl_2 \cdot 2H_2O$, 0.05 g of $MnSO_4 \cdot H_2O$, 2.5 g KNO_3 and 2.5 g of yeast extract in 1 liter of water.

0.2-µm filter sterilized Wolfe's mineral (0.5%) and vitamin (0.5%) solutions (ATCC) were added aseptically to the sterile medium at 60°C. The basal medium was made of the 1/5 of the autoclaved lake sample.

The samples were incubated for 2 to 4 weeks at 7°C. The cells harvested on agar plates and the broth were diluted accordingly and streaked on respective solid medium and incubated at 7°C for 2 weeks. Isolated colonies were restreaked several times to insure purity and were transferred to slants of agar for long-term storage. The strain identities were confirmed by analyzing the first 500 base pairs of the 16S ribosomal DNA gene.

7.2.2.2 Sporulation and endospore purification

Mesophilic endospores were prepared by using 2×SG sporulation agar because it is reported to give high spore densities[14]. All ingredients were obtained from Sigma unless otherwise noted. The medium consisted of: 16.0 g nutrient broth (Difco), 2.0 g KCl, 0.5 g $MgSO_4$ and 17.0 g agar in 1 litre of water. The medium pH was adjusted to 7, then autoclaved and cooled. The following components were added after cooling: 1.0 mL 1 M $Ca(NO_3)_2$, 1.0 mL 0.1 M $MnCl_2 \cdot 4H_2O$, 1.0 mL 1 mM $FeSO_4$ and 2.0 ml 0.5% glucose (w/v). 200 µL of fresh *Bacillus* vegetative cells in tryptic soy broth in exponential phase were added and spread over the agar surface. The plates were incubated at 30°C for 1 week. Spores were harvested using cotton applicators and suspended in sterile water. This mixture of spores and cells was centrifuged at 1300 g for 20 min, washed with sterile water 3 times. Lysozyme (50 µg mL^{-1}) was added in the presence of buffer (¼ volume TrisCl, 0.05 M, pH 7.2), and incubated with constant stirring at 37°C overnight.

Lysozyme was removed by centrifuging 8 times (at 1,300 g) and washing with sterile deionized water. The resultant spore suspension was stored at 4°C.

B. longisporus and *B. psychrodurans* and spore-forming isolates from JPL soil and Lake Vida were all sporulated using the same way except that the sporulation media for Lake Vida was supplemented with sea water broth[15] to mimic the natural environments. The sporulation media was composed of nutrient broth (Difco) with 0.5% yeast extract, 0.1% glucose, 0.7 mM $CaCl_2 \cdot 2H_2O$, 1mM $MgCl_2 \cdot 6H_2O$ and 50 mM $MnCl_2 \cdot 4H_2O$, supplemented with 1 mM methyl anthranilate and 1 mM D-alanine[16], at final pH of 7.0. Media for Lake Vida was further fortified with 1.5 g Bacto Peptone, 0.01 g $FePO_4 \cdot H_2O$, 750 ml sea water and 250 ml distilled water, adjusted to pH 7.0. Actively growing culture, consisting of vegetative cells and endospores, was heat treated at 65°C for 15 minutes and transferred to fresh medium several times[17] and finally inoculated into sporulation media augmented with an airlift system. The sporulation media was added to a 250-mL vacuum filtration flask fitted with a fritted glass gas silicone dispersion tube, two outlets, and a magnetic stir bar. The tube was connected to a fish tank pump through a 0.2-μm membrane filter. Sterile air was bubbled through the medium at a constant rate with an aspirator. The degree of sporulation was determined by direct microscopic counts. After incubation of 2 weeks at room temperature, 70% of the biological particles present were free "phase-bright" endospores.

After two washing steps and following resuspension in PBS, samples were heat shocked at 65°C and sonicated for 5 min to damage vegetative cells. The suspension was then incubated in lysozyme (50 mg mL^{-1}) at 37°C overnight to lyse the vegetative cells. The lysozome-treated suspension was put on top of an sodium bromide density gradient

and centrifuged at 5000 g (4°C) for 45 min. This gradient allowed the formation of successive stages of NaBr density with the addition of density beads: 1.5, 1.4, 1.3, 1.2, 1.1 and 1.0 g mL^{-1}.[18] The endospores formed a solid pellet with a light crème color at 1.33 g mL^{-1} density level, where debris and vegetative cells were found at the 1.1 and 1.2 g mL^{-1} levels, respectively, as thin, loosely packed, dark brownish upper layers. The isolated endospores were washed 10 times in 1 mL sterile water to get rid of any remaining lysozyme. More than 99% of the samples were composed of free 'phase-bright' endospores. The suspension was either kept at 4°C with the addition of 50 mM D-alanine to avoid germination or freeze-dried and stored as lyophilized powder at -20°C under the dark. The usual mesophilic endospore storage condition in deionized water at 4°C was not sufficient because psychrophilic endospores manage to germinate at a considerable rate at this temperature.

7.2.2.3 Growth characteristics of strains

Optimal and maximal growth temperatures of the endospores were determined at 4, 7, 15, 20, 30 and 37°C in TSB inoculated in 96-well microtiter plates. Growth was measured by monitoring optical density at 660 nm with a spectrophotometer (NanoDrop) after 2, 7 and 14 days of incubation and turbidity increases of >0.1 OD unit were scores as positive.

7.2.2.4 Characterization procedure

Concentration of bacterial endospores was determined by turbidity measurement and phase-contrast microscopy under a 60× oil immersion objective (Nikon Eclipse 80i, AG Heinze Co., Lake Forest, CA). Size and shape of endospores were determined from

malachite green staining. The Schaeffer-Fulton modification of Wirtz's spore stain was used[19]. DPA was measured with a fluorescent assay modified from Shafaat and Ponce[20]. Endospore suspension were autoclaved (134°C for 45 min), a treatment known to release all DPA[21], and pelleted at maximum speed for 10 minutes. The supernatant was assayed for DPA in a final volume of 800 µL containing 100 µL of supernatant and 700µL sodium acetate buffer (20 mM at pH 5.6) with freshly added $TbCl_3$ at a final concentration of 100 µM. Excitation spectra (λ_{ex} = 250 to 360 nm; λ_{em} = 544 nm) and emission spectra (λ_{ex} = 270 nm; λ_{em} = 515 to 580 nm) were measured with a Fluorolog-3 fluorimeter (Jobin Yvon, NJ) consisting of a 450-W xenon lamp for excitation, two double-monochromators set with 3 nm bandpass filter, and a Pelletier-cooled photomultiplier tube. A 500 nm cutoff filter (Omega Filters, Brattleboro, VT) was placed at the entrance of the emission monochromator. Standard curves of 0-100 µM DPA demonstrated straight lines (R^2> 0.99) with this method. Endospores were induced to germinate by a combination of L-alanine, inosine and sodium bicarbonate quantified by the described fluorimetric analysis and OD_{660} measurement.

The heat resistance of microbes was determined by subjecting a 100-µL mixture of 10^7 endospores and 10^7 vegetative cells in PCR tubes to controlled thermal cycles using a PCR machine. The bacterial suspension was kept at 4°C before and after the heat treatment. The temperature was ramped up quickly with 1 minute to the following temperatures: 50, 60, 70, 75, 80, 85, 90, and 95°C. A replicate of 8 tubes were used for each heat inactivation temperature. Heat treated bacterial suspension were pipetted into 96-well microtiter plates and incubated at the approximate temperature with mild agitation until visible turbidity was observed.

Spore surface hydrophobicity was measured according to the method described by Rosenberg *et al.*[22] Spores were suspended in water, and after measurement of the absorbance at 660 nm using a Nanodrop (A_{before}, values at 0.4-0.5), 20 µL of n-hexadecane (Sigma Aldrich) was added to 100 µL of spore suspension in a centrifuge tube. This mixture was vortexed for 1 min, after which the phases were allowed to separate for 15 min. Then, the absorbance of the aqueous phase was determined again (A_{after}), and the % transfer to the n-hexadecane was deduced by calculating $100 - (A_{after}/A_{before}) \times 100$.

The wet density of the whole endospore was measured with a Percoll gradient according to the method described by *Tisa et al.*[23] Spores were concentrated in 0.15 M NaCl, added to 90% (v/v) Percoll (Amersham Pharmacia Biotech) solution with 0.15 M NaCl, and subsequently centrifuged for 40 min at 10,000 g. While spore wet density was derived by comparison of the positions of the spores with those of density marker beads (Amersham Pharmacia Biotech) in the self-established gradient.

The spore core density was determined with Nycodenz density gradients[24] according to Lindsay *et al.*[25] as follows: spores were permeabilized with a decoating solution containing 0.1 M DTT, 0.1 M NaCl and 0.5% SDS according to Vary (1973)[26]. Permeabilized spores were equilibrated in 30% Nycodenz (1.159 g mL^{-1}). Semi-continuous gradients were made by letting discontinuous gradients diffuse overnight at 5°C. After centrifugation for 45 min at 3700 rpm, the spores formed a band at a certain position. The refractive index, which was linearly correlated with the density, from samples taken just above and below the band was measured with a spectrophotometer, and the average yielded the spore core density. Core water content was calculated

according to Lindsay *et al.*[25].

7.2.3 Results

Two psychrophilic isolates of *Bacillus* were successfully isolated and sporulated from JPL soil; 4 were isolated and produced as clean endospore suspensions from Lake Vida lake brine water. They grew well at 4°C, optimally at 20°C, and failed to grow at temperatures higher than 30°C. Their minimal and maximal growth temperatures were lower than those for mesophilic species of *Bacillus* by 10°C. Both sporulation and germination were observed to occur at lower temperatures than their mesophilic counterparts. The Lake Vida grew optimally in media supplemented with sea water broth.

One of the Lake Vida isolates contained two endospores in a single mother cell. Sporulation was observed *via* the typical seven steps[27]. DPA can be detected and the degree of heat and UV resistance were comparable to other psychrophilic endospores. Micro-cycle sporulation and germination events were observed in the sporulation medium, resulting in a heterogeneous mixture of vegetative, sporulating and sporulated cells. Endospores were observed to transition from phase bright to phase dark constantly in the sporulation medium. To remedy this situation, 1 mM methyl anthranilate and 1 mM D-alanine were added into the sporulation medium to inhibit the action of L-alanine-α-ketoglutarate aminotransferase[28], thereby preventing endospores from going through the germination pathway. A more synchronous and higher percentage of sporulation rate (~70%) could be obtained afterwards. Aerated sporulation broth fortified with yeast extract, glucose, and D-alanine was found to be the best sporulation medium for psychrophilic endospore-forming bacteria. With further cleaning and purification, final

pure psychrotolerant endospore suspensions of >95% were produced. Table 7.1 summarizes the morphological and physiological characterization of the spore samples. Figure 7.1 shows the phase contrast micrograph of some of the isolates.

The optimal germinant for mesophilic endospores was 50 mM L-alanine, whereas the optimal germinant for psychrophilic endospores was 50 mM L-alanine and 1 mM inosine. The optimal combination of germinants was studied on the psychrophilic endospores. The germination rate of environmental psychrophilic endospores was very low. Upon heat activation at 50°C and pre-incubation at 50 mM calcium dipicolinate, a ten-told increase in germination rate was observed among environmental psychrophilic endospores at 22°C. Figure 7.2 shows a comparison between the optimal germination temperature between mesophilic and psychrophilic endospores when induced by 50 mM L-alanine and 50 mM L-alanine plus 1 mM inosine. Mesophilic endospores germinated fastest and optimally at 37°C and psychrophilic endospores generally germinated best between 15°C and 22°C. Germination still proceeded at a slow but measurable rate at 4°C. However, the lowest possible germination for mesophilic endospores was 12°C.

The inhibitory effect of sodium bicarbonate on endospore germination was concentration dependent. The higher concentration of sodium bicarbonate, the slower the rate of germination. For instance, 1 mM sodium bicarbonate reduced L-alanine germination rate of *B. atrophaeus* and *B. longisporus* endospores by 42% and 46%, respectively. The effect of sodium bicarbonate on mesophilic and psychrophilic endospores was statistically insignificant ($p < 0.001$). The effect of the cationic surfactant, dodecylamine, in inducing endospore germination was also studied. 1 mM dodecylamine was used as the germinant without any buffer[29,30]. The highest rate of germination rate of

mesophilic endospores was 65°C and of psychrophilic endospores was 45°C.

Psychrophilic endospores were found to have a higher concentration of DPA per unit volume of endospores than mesophilic endospores. The endospore size of psychrophilic also tended to be smaller than that of mesophilic endospores. Vegetative cells and endospores were subjected to heat shock treatment at various temperatures. Optimal heat shock temperature was chosen at the temperature at which most of the vegetative cells were inactivated while most of the spore population remained. 60°C – 70°C was the range of optimal heat shock temperature for psychrophilic spores (Figures 7.3, 7.4). The UV resistance of psychrophilic endospores is statistically higher than that of mesophilic endospores as manifested by their high pigmented colonies.

Slope of the middle section of the inactivation curves, which yielded a reproducible D-value of 1 minute at 85°C, in line with previous reports. Spore surface hydrophobicity is caused by the presence of an exosporium[31] and plays a key role in adherence of the spores to surfaces[32], for example of food or food processing equipment. The obtained endospores were highly hydrophobic since over 95% of the endospores transferred from water to the n-hexadecane phase in the BATH assay[22]. In contrast, of *B. cereus* vegetative cells and spores from *B. subtilis*, which lack an exosporium, over 98% remained in the aqueous phase.

When determining the DPA content using spectroEVA, the spectrum tended to overshadow the characteristic dual peak of Tb-DPA because of the very background fluorescence and autofluorescence upon deep UV excitation. A phosphorimeter was used to performing time gating using the fluorimeter. Promising initial study has revealed a much better resolved spectrum.

7.2.4 Discussion

In this study, we have isolated a combination of psychrophilic and psychrotolerant endospore-forming bacteria from permanently low temperature environments, such as the Antarctic Lake Vida, from cold desert, such as the Atacama Desert in Chile, and in soil and fresh water in California. Although psychrophilic endospores are more likely to be isolated from the cold biosphere, they can often be found everywhere because of their ubiquity[33]. Endospores are exemplified by their extreme resistance, and the ability of psychrophilic endospore-forming bacteria to thrive at low temperatures harbors a wider range of survival characteristics (e.g., ability to withstand cold shock, desiccation, pH, salinity, cold shock.) Study of psychrophilic endospores is often hampered by the difficulty in obtaining pure spore suspension because of the extra challenge encountered during the sporulation process. In *Bacillus* the degree of synchrony during sporulation is usually relatively high among mesophilic species. Sporulation can occur in suitable media, 6 to 8 hours after development has started at the end of exponential growth[34,35]. The entire sporulation process takes 3–5 days to complete. Their psychrophilic counterparts, however, take approximately 2 weeks. Some sporulate faster and some sporulate slower. During this extended period, some of the endospores undergo germination and subsequently microcycle sporogenesis when germinating spores commit and reenter the sporulation cycle in the presence of utilizable nutrients[36]. Germination and microcycle sporulation are prevalent during sporulation of psychrophilic endospores as indicated by recurrent phase bright and phase dark transition due to the prolonged

sporulation period, adding to the heterogeneity of the spore batch. A clean and pure endospore sample is therefore difficult to obtain.

We have improvised several techniques in an effort to obtain high and synchronous sporulation in psychrophilic endospores. First, the bacterial culture is sequentially transferred several times with intervening pasteurization at 65°C, a temperature lower than the conventional 80°C, to obtain an initial endospore inoculum with synchronized growth rate and other properties[17]. Second, the growth and sporulation rates are increased by actively aerating the nutrient-exhaustion medium[37-39]. A high aeration rate enables aerobic *Bacillus* to utilize the intracellular reserve of poly-β-hydroxybutyric acid (PHB), whose depletion is critical to sporulation[40]. Third, germination inhibitors such as methyl anthranilate and D-alanine are added to the sporulation medium to prevent mature endospores from shut off the germination, vegetative and microcycle sporogenesis pathways. Methyl anthranilate inhibits the action of L-alanine-α-ketoglutarateaminotransferase and D-alanine acts as an allosteric competitor to prevent germinants from binding receptors on spore coat[28]. These three techniques collectively help obtaining a homogeneous suspension of endospores with a high and synchronized rate in less than two weeks.

The endospores of psychrophilic bacteria are typically 20% - 50% smaller in size than mesophilic endospores observed under phase contrast microscopy. The DPA content found in all these spores is similar which means that there is a higher density of DPA, i.e., DPA content per unit volume, in the protoplast of psychrophilic endospores. These psychrophilic spores are in generally less heat resistant but more UV resistant than mesophilic endospore, albeit these differences cannot solely be justified by DPA content.

Heat tolerance may be more related to the habitats where these spores reside, as well as core water and the DNA-binding small acid soluble proteins. UV resistance may be related to the pigment of the colonies – the colonies formed by psychrophilic endospores are usually brightly colored. It is well known that spore properties are affected by the sporulation conditions. Recent studies describing the effect of sporulation conditions on spore properties involve modulation of sporulation temperature[41-45] or compare spores produced from different media[46,47]. It will be interesting to assess the relationship of DPA density to spore resistance properties systematically using mutant strains in the future.

50 mM L-alanine and 1 mM inosine is found to be the best germinant for psychrophiles. A negative correlation is observed between inosine and the rate of germination. Inosine concentrations higher than 1 mM would inhibit germination. The germination kinetics of psychrophilic endospores is highly conserved with those of mesophilic endospores. For instance, sodium bicarbonate and D-alanine inhibit L-alanine induced germination in a similar way. Germination ceases with an equimolar of D- and L-alanine. Germination proceeds ten times slower with the presence of high concentrations of sodium bicarbonate. Germination is also observed to be temperature dependent in psychrophilic endospores. Psychrophilic endospores are capable of germinating at 4°C. The highest rate and largest fraction of germination are observed at 22°C. In contrast, mesophilic endospores do not germinate lower than room temperature and their optimal germination is at 37°C. In general, psychrophilic spore germination takes twice as much of time to reach maximum germination. This study provides useful information for germination-based endospore detection methods.

7.2.5 Conclusion

Study of psychrophiles is essential to the understanding of early lives on Earth. Endospores have widely been examined in ancient Earth ice and permafrost due to their longevity as analogues to study cold biospheres in other celestial bodies. The ability of these endospores to thrive and subsequently remain dormant at low temperature seems to have been acquired during evolutionary time. And in view of the glaciations periods suggested by the Snowball hypothesis, study of psychrophilic endospores can provide great insights in the testing of theories and development of methods to search for extraterrestrial life in other polar systems.

7.3 Micro- and macro-germination kinetics

Germination events of individual and a population of *Bacillus* endospores were monitored using phase-contrast microscopy, terbium-dipicolinic acid luminescence assay, fluorescence staining, flow cytometry and ATP luciferin-luciferase assay. In particular, we have adopted and developed mathematical models to describe microgermination and macrogermination kinetics by monitoring DPA release from endospores induced by L-alanine. The microgermination model is a differential equation approach to describe single endospore germination based on a 3-compartmental analysis. This model quantitatively describes the germination events of 4 laboratory and 4 environmental strain endospores. The microgermination model has been extrapolated into the macrogermination model based on a stochastic assumption of the heterogeneous population of individual endospores. Inconsistent results are obtained between micro- and macro-germination characteristics. The endospore inoculum size and time-to-germination

was found to vary in a logarithmic fashion. Plausible reasons are quorum sensing, feedback or feed-forward mechanisms during germination. In this study, we report the use of a combination of methods to study different properties of endospore, such as stainability, loss of heat resistance, drop in refractility, release of DPA, during the course of germination and re-affirm the sequence of physiological processes taking place during germination.

7.3.1 Introduction

When starved of nutrients *Bacillus*, *Clostridium* and cells from other genera initiate a series of genetic, biochemical and structural events that result in the formation of metabolically dormant endospores. They can remain dormant for extended periods and, partly because of their tough spore coat, have a significant resistance to extreme environmental factors including heat, radiation and toxic chemicals. Germination is the process whereby an endospore changes from a dormant state to reenter the vegetative mode of replication upon detection of favorable conditions.

The process of germination is a time-ordered sequence in which spores lose their characteristic resistance to heat, desiccation, pressure, vacuum, ultraviolet and ionizing radiations, antibiotics and other chemicals, extremes of pH and an increased permeability to a number of different molecules. Once a germinant binds to receptors in the inner membrane of spore, hydration of the cortex is accompanied with rapid degradation including a release of calcium dipicolinate and different chemicals from the spore core. Cortex hydrolysis and germ cell wall expansion follows with subsequent resumption of metabolism and macromolecular synthesis. Any of these observables can be used to track

and signify the germination timecourse of endospores. Hashimoto *et al.* has shown that single spore germination timecourse has two distinct phases based on spore refractility and optical density[48]. Partial dehydration occurs and DPA is released into the medium in the first rapid phase. Hydration of the spore core happens in the second phase. The first phase was reported to take 75 ± 15 sec and 3 - 4.5 minutes; second phase lasted ~2 min and ~7 min for *B. cereus* and *B. megaterium*, respectively.

It is known that endospore germination will be affected by a number of factors, including sporulation condition, germinant concentration, temperature and ionic strength of the medium[49-51]. So, in this experiment, all the laboratory grown strains are sporulated using the same protocol. All endospores were activated at 50°C for 30 minutes prior to exposure to a millimolar concentration of L-alanine, with the only difference in temperature between mesophilic and thermophilic endospore-forming bacteria. Dipicolinic acid (DPA) is a unique molecule in endospores. The terbium photoluminescence assay has been used to quantify endospore concentration based on the fluorimetric measurement of DPA concentration in a germinating endospore suspension. We have employed this method to examine the germination kinetics of endospores in a population large than 1000 sp mL^{-1} due to the assay limit of detection. On the other hand, single endospore germination kinetics was measured by refractility change under phase-contrast microscopy and a time-gated microscopic version of the Tb-DPA luminescence assay (i.e., μEVA). Single endospores are observed to transition from phase bright to phase dark using a phase contrast microscope; from null to formation of a bright spot under μEVA. In specific, μEVA measures intensity enhancement of the long-lived terbium dipicolinate complex as a function of DPA release from spores.

In addition to these, ATP synthesis, stainability and heat resistance were also measured to serve as index for germination to augment these fluorimetric and microscopic results. Dormant endospores are not stainable by fluorescent dyes because of the permeation barrier imposed by the spore coat and outer edge of the cortex unless specially treated by acids or heat. Germinating spores are, however, readily stainable by fluorescent markers and DNA-intercalating dyes due to activation of lytic enzymes and an increase in permeability of the endospore membranes, both of which are events in the process of endospore germination. Heat resistance is related to structural integrity of the spore coats and loss of heat resistance is observed almost concurrently with the onset of germination. Dormant spores have little if any detectable endogenous metabolism[52] and contain extremely low levels of ATP and reduced pyridine nucleotides. However, the low energy forms of ATP (e.g., ADP and AMP) and other compounds essential for metabolism and macromolecular synthesis are present in spores at levels similar to those in growing cells. Production of high energy compounds in the early minutes of spore germination is driven, in large part, *via* metabolism of energy reserved stored in the dormant spore. These compounds produced *via* metabolism of endogenous reserves then support considerable RNA and protein synthesis. However, continued rapid production of high energy compounds after the first 10-15 min of germination of these spores requires exogenous metabolites. Another major endogenous energy reserve of dormant spores is the amino acid generated *via* protein degradation early in spore germination. Approximately 15%-20% of the total proteins are degraded to free amino acids in the first 20 minutes of germination, which in turn is subsequently metabolized through oxidative reactions.

The early timecourse of germination of endospores, whether individual or in a population, has been reported to be sigmoidal using lots of the aforementioned methods. There is one account proposing a biphasic germination kinetic, which cannot be reproduced. A large variety of germination models, mechanistic or empirical, single endospore or a population, deterministic or stochastic, have been proposed in the literature. The logistic model is insufficient because it only describes the values of a particular set of experimental data, bearing little direct relation to the biological structure or the general physical laws. Mechanistic models, both deterministic and stochastic, have been proposed to account for germination kinetics based on some biological and physical understanding of the system. Although significant progress has been made in understanding the biochemical and genetic bases of the spore germination process, inconsistencies still exist and it is still unclear about the integration of individual endospore germination collectively into germination of an endospore population. For instance, Mohd *et al.* have reported germination of *Bacillus anthracis* spores into vegetative cells in 3 hours using atomic force microscopy and transmission electron microscopy[53]. Hashimoto *et al.* used time-lapse phase contrast microscopy to characterize germination on the timescale of minutes[48,54]. In this study, we have adopted a reported deterministic and a reported stochastic model, in conjunction with the new DPA detection methodologies, to study both micro- and macro-germination, as well as establish a link between the two germination models.

7.3.2 Methods

Germination was performed without heat activation, and initiated by the addition of 100 mM L-alanine and different concentrations of inosine (0, 0.01, 0.05 and 0.1 mM). Samples were incubated at 37°C and aliquots were taken at different time intervals and centrifuged at 5000 g for 5 min. The pellet was suspended in phosphate buffered saline (PBS) to a concentration of 10^6 to 5×10^6 spores mL^{-1}. The time course of germination in endospores was monitored by observing the change in absorbance of a sample at 600 nm in a spectrometer and change in DPA content at 278 nm in a fluorimeter. and then analyzed by spectroEVA as described before.

Deterministic Model

This model was originally developed for describing macrogermination based on drop in optical density of an endospore suspension[55]. Here, we modify this model to describe both micro- and macrogermination kinetics based on the increase of DPA release as a proxy for germination.

Germination is a time-ordered sequence of four distinct phases, consists of activation, commitment, stage I and stage II. In the activation phase, various pre-treatments, often consisting of exposure to elevated temperatures, results in an increase in both the rate and extent of germination. In the second phase, the spore is irreversibly committed to complete the germination process, and it will do so even on subsequent removal of the germinant. The spore next enters the phase called initiation of germination. During this phase, one observes the characteristic manifestation of the germination process, such as loss of heat resistance, release of spore materials, uptake of stains, loss

of refractility and loss of absorbance in spore suspensions. These events have been shown to occur in a time-ordered sequence[14,56-58]. This is a phase of degradative processes, culminating in drastic morphological changes. The final phase, called outgrowth, is a period of synthesis of new materials, the outcome of which is a vegetative cell.

The overall features of the experimental DPA release vs. time curves are reasonably well described by the phenomenological function $x_p(t)$, given by:

$$x_p(t) = x_0,\ t < t_0,$$

$$x_p(t) = x_\infty + K_1 e^{-\lambda_1(t-t_0)} - K_2 e^{-\lambda_2(t-t_0)},\ t \geq t_0.$$

Subject to the experimentally determined boundary conditions:

$$x_p(t_0) = x_0;\quad \left.\frac{dx_p(t)}{dt}\right|_{t=t_0} = 0,$$

where K_1, K_2, λ_1 and λ_2 are curve-fitting parameters, x_0 and x_∞ are the initial and final values of the DPA luminescence, and t_0 is the lag time. The condition on $x_p(t)$ leads to

$$x_\infty - x_0 = K_1 - K_2.$$

While the condition on the slope requires that

$$\lambda_1 K_1 = \lambda_2 K_2.$$

The rate at which spores enter state C is determined by the transition probabilities λ_A and λ_B, with λ_A being identified with the triggering event. The time rate of change in the number of spores in each of these states are given by

$$\frac{dA(t)}{dt} = -\lambda_A A(t),$$

$$\frac{dB(t)}{dt} = -\lambda_B B(t) + \lambda_A A(t).$$

And by the principle of conservation, we have

$$A(t) + B(t) + C(t) = A_0,$$

where A_0 is the concentration of spores which eventually germinate. The solution of the above system of simultaneous differential equations is

$$A(t) = A_0 e^{-\lambda_A t},$$

$$B(t) = \frac{\lambda_A}{\lambda_B - \lambda_A} A_0 \left[e^{-\lambda_A t} - e^{-\lambda_B t}\right],$$

$$C(t) = A_0 \frac{A_0}{\lambda_B - \lambda_A} \left[\lambda_A e^{-\lambda_B t} - \lambda_B e^{-\lambda_A t}\right].$$

The above description of germination is independent of any of the characteristic properties employed to follow the time course of this process. ε(t) is the contribution of a single spore to this index. In this model, ε maintains its initial value, ε_0, until the spore enters C, whereupon its time dependence can be described by the expression,

$$\varepsilon(t) = \varepsilon_0 + (\varepsilon_\infty - \varepsilon_0) \int_0^t \alpha(\tau) d\tau,$$

subject to the normalization condition

$$\int_0^\infty \alpha(\tau) d\tau = 1.$$

The observed index can then be expressed at any time t as

$$x(t) = \varepsilon_0 (N_0 - A_0) + \varepsilon_0 [A(t) + B(t)] + \int_0^t \frac{dC(t')}{dt'}\Big|_{t'=\tau} \varepsilon(t-\tau) d\tau,$$

where N_0 is the total spore concentration, $\varepsilon_0(N_0 - A_0)$ is the contribution of the non-germinable spores, $\varepsilon_0 A(t)$ and $\varepsilon_0 B(t)$ are due to spores in states A and B, respectively, and the integral expression is the contribution of spores have entered state C up to the time t. Note that $dC(t')/dt'\big|_{t'=\tau} d\tau$ is the number of spores which entered state C between τ and τ+dτ and each one of these spores contributes ε(t-τ) at time t. The last term in the previous equation can be integrated by parts.

$$x(t) = x_0 + (\varepsilon_\infty - \varepsilon_0) \int_0^t C(t-\tau) \alpha(\tau) d\tau,$$

where $x_0 = \varepsilon_0 N_o$. Thus x(t) is essentially the convolution of C(t) and α(t).

$$x(t) = x_0 + A_0(\varepsilon_\infty - \varepsilon_0)[F(t,0)] + \frac{\lambda_A}{\lambda_B - \lambda_A} e^{-\lambda_B t} F(t,\lambda_B) - \frac{\lambda_B}{\lambda_B - \lambda_A} e^{-\lambda_A t} F(t,\lambda_A),$$

where

$$F(t,\lambda) = \int_0^t e^{\lambda\tau}\alpha(\tau)d\tau.$$

To evaluate the asymptotic value of x(t), we note that

$$\lim_{t\to\infty} e^{-\lambda\tau} F(t,\lambda) = 0.$$

The above integral equation for x(t) can be transformed into a corresponding differential equation. Making use of the fact that

$$\frac{\partial F(t,\lambda)}{\partial t} = e^{\lambda\tau}\alpha(\tau).$$

In the successive differentiation of the equation, one obtains

$$F(t,0) = \frac{1}{A_0(\varepsilon_\infty - \varepsilon_0)\lambda_A\lambda_B}\left[\frac{d^2y(t)}{dt^2} + (\lambda_A + \lambda_B)\frac{dy(t)}{dt} + \lambda_A\lambda_B(y(t) - y_0)\right].$$

Subject to the boundary conditions

$$y(0) = y_0 = \varepsilon_0 N_0,$$

$$\left.\frac{dy(t)}{dt}\right|_{t=0} = 0.$$

By combining the previous equations, we can derive differential expressions for the functions ε(t) and α(t), which describe the manifestations of germination in the single spore case:

$$\epsilon(t) = \epsilon_0 + \frac{1}{A_0\lambda_A\lambda_B}\left[\frac{d^2y(t)}{dt^2} + (\lambda_A + \lambda_B)\frac{dy(t)}{dt} + \lambda_A\lambda_B(y(t) - y_0)\right],$$

and

$$\alpha(t) = \frac{1}{A_0(\varepsilon_\infty - \varepsilon_0)\lambda_A\lambda_B}\left[\frac{d^3y(t)}{dt^3} + (\lambda_A + \lambda_B)\frac{d^2y(t)}{dt^2} + \lambda_A\lambda_B\frac{dy(t)}{dt}\right].$$

The presence of a lag time occurs between the time at which a spore enters state C and the time that its change in ε begins. Since the observable manifestations of germination

occur in a time-ordered sequence, it is reasonable to conclude that each index has its characteristic lag time.

The function α(t) determines the rate of evolution of a manifestation of germination. The form of α(t) can be obtained directly by making measurements on a single spore. Alternatively, it can be deduced from measurements on a sample of spores using

$$x(t) = x_0 + A_0(\varepsilon_\infty - \varepsilon_0)[F(t,0)] + \frac{\lambda_A}{\lambda_B - \lambda_A} e^{-\lambda_B t} F(t,\lambda_B) - \frac{\lambda_B}{\lambda_B - \lambda_A} e^{-\lambda_A t} F(t,\lambda_A).$$

One starts with a convenient approximate form for α(t). The experimental results are then analyzed for best fit with the resulting expression to yield first estimates of the transitional probability parameters λ_A and λ_B. These estimates of the transition probabilities, together with the experimental values of y(t) and its derivatives can then be substituted into equation

$$\alpha(t) = \frac{1}{A_0(\varepsilon_\infty - \varepsilon_0)\lambda_A\lambda_B}\left[\frac{d^3y(t)}{dt^3} + (\lambda_A + \lambda_B)\frac{d^2y(t)}{dt^2} + \lambda_A\lambda_B\frac{dy(t)}{dt}\right],$$

to produce a new form for α(t). The new form of α(t) provides the starting point for the next iteration. The above procedure is repeated until the input and output functions agree within some prescribed tolerance limits. Since the experimental data are necessarily in discrete form, it is convenient in doing these iterations to recast equations in finite difference form.

In this model, α(t) is assumed to be a rectangular pulse subject to the normalization condition, we have

$$\alpha_a(t) = \begin{cases} 0, & t < t_0 \text{ and } t > t_0 + a \\ 1/a, & t_0 \le t \le t_0 + a \end{cases}$$

where a is the duration of the change in ε, and t_0 is the lag time. Substituting into

$$\varepsilon(t) = \varepsilon_0 + (\varepsilon_\infty - \varepsilon_0)\int_0^t \alpha(\tau)d\tau,$$

we get

$$\varepsilon_a(t) = \begin{cases} \varepsilon_0 & , t < t_0 \\ \varepsilon_0 + 1/a(\varepsilon_\infty - \varepsilon_0)(t - t_0) & , t_0 \le t \le t_0+a \\ \varepsilon_\infty & , t > t_0+a \end{cases}$$

We thus have

$x_a(t) = x_0$, $t < t_0$

$$x_a(t) = x_0 + A_0(\varepsilon_\infty - \varepsilon_0)\left[\frac{(t-t_0)}{a} + \frac{\lambda_A}{\lambda_B-\lambda_A}\frac{1-e^{-\lambda_B(t-t_0)}}{a\lambda_B} - \frac{\lambda_B}{\lambda_B-\lambda_A}\left(\frac{1-e^{-\lambda_A(t-t_0)}}{a\lambda_A}\right)\right],\ t_0 \le t \le t_0+a$$

$$x_a(t) = x_\infty + A_0(\varepsilon_\infty - \varepsilon_0)\left[\frac{\lambda_A}{\lambda_B-\lambda_A}\frac{e^{a\lambda_B}-1}{a\lambda_B}e^{-\lambda_B(t-t_0)} - \frac{\lambda_B}{\lambda_B-\lambda_A}\frac{e^{a\lambda_A}-1}{a\lambda_A}e^{-\lambda_A(t-t_0)}\right],\ t > t_0+a$$

Stochastic model

The stochastic model has been developed because of the unpredictable nature of spore germination. This model was originally developed by LeBlanc & Lefebvre to describe macrogermination based on a discrete and continuous random distribution of microgermination kinetics and microlag time of single endospores[59]. It assessed the average contribution of one spore to the DPA release mechanisms of a population of endospores. The microlag distribution was found to be skew-symmetric, and to extend over most of the sample germination time. Microgermination times were similarly distributed, but covered only one-tenth of the same timescale. These findings led to the conclusion that macrogermination curves were principally determined by the microlag distribution, and only incidentally influenced by the microgermination distribution.

In the model, the DPA level at any time t of a randomly selected endospore can be represented by

$$X_t = \varepsilon_{T_1}(t - T_0),$$

where T_0 and T_1 are non negative and independent random variables.

$E(X_t)$ is the mean DPA luminescence level of a single endospore at time t. We first determine the probability of the possible values of X_t for a fixed microgermination time. These probabilities are expressed in terms of $f_0(\tau_0)$, the density function of the variable T_0, and its distribution function F_0 is defined by

$$F_0(u) = \int_{-\infty}^{u} f_0(\tau_0)\, d\tau_0.$$

The final model is of the form

$$E(X_t) = \varepsilon_i + \int_0^{\infty} \int_{t-t_1-\tau_1}^{t-t_0} F_0(u)\, \varepsilon'_{T_1}(t-u) f_1(\tau_1) du d\tau_1.$$

Using this probabilistic approach, it is possible to show that the observed sigmoid-shaped absorbance cs. Time curve of a sample of germinating bacterial spores can be generated from the simple observation that the individual spore germination times are distributed over a range of values.

7.3.3 Results

Each of these observables reports comparable but slightly different kinetics, presumably due to underlying differences in the detection method and also the fact that each of the physiological changes is associated with a different interval and time scale of germination. When an endospore is committed to germinate, it follows a microlag period and a microgermination period *en route* to the outgrowth phase. Microlag period has been defined in the 1950s as the period at which a committed endospore remain its refractility. This term could be confusing when DPA release was used as the metric for the monitoring of germination timecourse. An endospore could have started releasing Ca-DPA without any apparent refractility change during the early minutes of germination. Phase transition has been correlated with a combination of events, including DPA and metal ion exudation, degradation of spore coat, influx of water, and swelling of endospores. When it starts to change from phase bright to phase dark, the period is termed microgermination during which DPA and metal ions are exuded from the endospores and water enters to rehydrate the core, leading to subsequent or arguably concurrent loss of heat resistance and increased stainability, followed by synthesis of macromolecules and production of ATP. A shorter microlag time was observed in the case of DPA release, which is consistent with the postulated time-ordered sequence of germination - Ca-DPA release precedes the water rehydration. Heat resistance and increased stainability were both shown to correlate to refractility more than DPA release, albeit the difference was not statistically significant ($p < 0.001$) due to the relatively long process of heat resistance and stainability assessment compared to the short time scale of germination. ATP can be detected during the late stage of germination II when a high

inoculum of spores was used. This ATP should be the reserve stored inside endospores and were utilized and could thus be assayed by luciferin. When a growth medium, such as tryptic soy broth, was provided, a continued rise in ATP could be observed in conjunction with the outgrowth phase where new molecules were being synthesized.

Although the initiation of spore germination may not require macromolecular synthesis or metabolic energy, generation of ATP as well as macromolecular synthesis begin within minutes or even seconds of the initiation process. Furthermore, these latter events often begin well before completion of some of the degradative reactions accompanying initiation. As a consequence, it is difficult to separate the periods of germination and outgrowth by measuring parameters such as the kinetics of macromolecular biosynthetic or degradative reactions.

Germination was carried out in bulk solution with 50 mM L-alanine in pH-controlled buffer at a total number of endospores of 10^3, 10^4, 10^5, 10^6, and 10^7. Another challenge was observed in the difference in the time-to-germination. The higher the concentration of spores, the longer the suspension takes to plateau in DPA concentration (defined to be within 95% of the final DPA concentration measured at the end of a 24-hour cycle). The reason for this correlation is still unclear. Inoculum size dependency of germination has been observed in our laboratory strains. This could be due to the stochastic nature of microgermination, quorum sensing among *Bacillus* spores or a feedback or feed-forward mechanism in the germination process. Microgermination kinetics has been studied and well characterized by monitoring the absorbance property of endospores during the course of germination. Several models have been proposed in the past, either through theory or empirical mathematical modeling. Endospores transition

from phase bright to phase dark during germination, accompanied with a drop in refractility and absorbance. Hashimoto et al. have measured the germination timecourse of a single endospore, known as microgermination. Microgermination is characterized by a microlag period in which endospores have been exposed to germinants and no physiological changes can yet be detected. Microlag is followed by a sigmoidal timecourse of germination, measured by either heat resistance, stainability, DPA release or refractility loss (Figure 7.5). A logistic model was first proposed to characterize such a microgermination system. Table 7.2 and Figure 7.6 demonstrate the microgermination model of 4 lab-strain and 4 environmental-strain endospores.

Endospore germination by itself is a stochastic process due to the heterogeneity of an endospore population. When endospores germinate, they release a large depot of chemicals. Among these, calcium dipicolinate and alanine have been postulated to play a role in affecting the germination kinetics. Ca-DPA is a very germinant and induces endospores to germinate *via* a mechanism different then nutrient induction. As more spores germinate in a population, more Ca-DPA is released to facilitate the rate of germination. On the other hand, alanine could be both a germinant and an inhibitor to endospores. As spores germinate, alpha-keto transalantrase will convert L-alanine into D-alanine, which is an allosteric inhibitor to germination. Quorum sensing may also a reason affecting macrogermination but not much study have been done on this respect so far.

Macrogermination will be characterized using spectroEVA and modeled using a stochastic model, which involves mixed continuous and discrete probabilities of different stages of germination. Macroscopically, endospores from a pure culture generally exhibit

a high degree of synchrony. And the microlag distribution is found to be skew-symmetric and to extend over most of the sample germination time. Microgermination time germination is skew distributed, but covers only about a tenth of the same time scale. Therefore, macroscopic germination is principally influenced by the microlag distribution, and only incidentally influenced by the microgermination distribution. The distribution shows that individual spores in a sample are highly heterogeneous and there exists some super-dormant spores that are very insensitive to germination induction. Figure 7.7 shows a stochastic model derived from microgermination kinetics. The microlag and microgermination distributions (both skew symmetric) were fitted into the stochastic model, which yielded a discrepancy from the actual data.

In μEVA, we are selecting the fraction of a low inoculum of endospores that respond fast to germinants. At high inocula, endospores are more easily affected by the skew-symmetric distribution of microlag times, leading to a much longer germination time. Whether endospore requires minutes to germinate or 24 hours to germinate is still a debate.

7.3.4 Conclusion

In this study, we apply and modify the previous models based on different observables during the germination process, notably the release of DPA from endospores. The model makes a clear distinction between the intrinsic aspects of the germination process and the observable changes consequent to germination. The intrinsic process consists of two successive random transitions between three spore states: triggerable, triggered and germinated. The observable changes begin with the spore's entry into the germinated

state. Each observable change, or manifestation, has a characteristic lag time, t_0, and a characteristic rate of evolution controlled by a function.

7.4 Methods to increase culturability

7.4.1 Introduction

A central problem in the study of endospores in extreme environments is the lack of reliable cultivation methods. Extreme environments are generally difficult to replicate in the laboratory and more difficult to maintain in order to culture native extremophiles. Only a tiny fraction of the organisms observed in environmental samples can be cultured in the laboratory. The ability to revive these dormant lives *in vitro* as well as the viable-but-not-culturable state is currently the biggest stumbling block in microbiology. Although new genetic and fluorescence microscopy techniques have been developed to complement culture-based techniques, cultivation still remains the most important and fundamental method to assess endospore viability. Endospores are susceptible to be neglected using these new techniques because they are usually non stainable and exceptionally difficult to be lysed for DNA analysis due to their tough cell wall. The recently developed endospore viability assays (EVA) are effective approaches to directly assess the viable endospore population in an environmental sample. Improvement in endospore culturing techniques will increase the fidelity of the EVA results. Extracting, culturing and identifying these native soilborne endospores also provide insight into understanding *in situ* endospore dormancy and the relation of their spatial or temporal distribution with respect to past geological events as analogous models for exobiological life exploration.

Endospores were independently discovered by Cohn (1876)[60], Koch (1876)[61,62], and Tyndall (1877)[63] as resting forms of life formed intracellularly in some genera such as *Bacillus* and *Clostridium*. They demonstrate exceptional dormancy, resistance and longevity conferred by their special chemical composition and ultrastructure. The genus *Bacillus* is considered heterogeneous compared with other bacterial genera. This is apparent from the variety of carbohydrate metabolism and from the DNA base pair composition (33-60 mol% G+C). Bacteria such as *B. subtilis* or *B. licheniformis* are robust, grow readily in most media, and can be easily isolated. Nevertheless, certain *Bacillus* species are very difficult to culture. First of all, they tend to exist in very low numbers in soils. They grow very slowly and sometimes in translucent colonies, which will readily be overshadowed and swarmed by migrating motile colonies of other fast-growing sporeforming species. Therefore, proper enrichment and isolation techniques are crucial in recovering these rare sporeforming bacteria.

Enrichment is generally viewed as increasing the proportional numbers of a particular type of organism in a sample by providing a selective environment for the growth of the desired organism. Both physical and nutritional constraints can be used. Enrichment seems to be a prerequisite for the isolation of hydrocarbon-utilizing *Bacillus* since the great majority of species do not grow or grow only weakly on these substrates[64]. Other carbon sources that have been used to isolate specific *Bacillus* types include agar, chitin and various other polysaccharides. Nitrogen nutrition has also been exploited for the enrichment of unusual bacilli. Urea-decomposing bacilli are common in soil.

There is a big reservoir of *Bacillus* species in the soil and various strains have been isolated from the extremes of desert and Antarctica. Generally, soils of low organic

content have a restricted flora dominated by *B. subtilis*, *B. licheniformis* and *B. cereus*; however, with increasing fertility, a wider range of species is encountered. It is advisable to sample exotic environments when searching for bacteria with particular characteristics, such as thermo- or pH tolerance, the frequency with which new species of *Bacillus* are isolated from normal soils suggests that many more taxa remain to be discovered given the correct enrichment and isolation condition.

Because of the aforementioned reasons, here we propose methodologies to improve the general culturability of endospores in terms of both number and variety from the soil habitat. Calcium dipicolinate (Ca-DPA) will be as a germinant during pre-incubation, combination of induced germination and heat shock temperature to select for slow-growing spore-forming species, optimization of heat shock treatment temperature for spore-forming species sampled from different temperature extremes, and the use of a high-throughput microtiter well technique to improve culturability of rare sporeforming species.

7.4.2 Methods

7.4.2.1 Chemicals and media

The following chemicals, dipicolinic acid, picolinic acid and L-alanine were purchased from Sigma (St. Louis, MO) and were used as received. Sodium hydroxide, calcium hydroxide and calcium chloride were purchased from Baker. Calcium dipicolinate was prepared by neutralizing calcium hydrogen and dipicolinate acid. Sodium dipicolinate Tryptic soy agar (TSA) was used for most the spread plate counting.

7.4.2.2 Preparation of spore suspensions

Spores of *Bacillus atrophaeus* (ATCC 9372) spores were purchased from Raven Biological Laboratories. Spores of *B. subtilis* (ATCC 27370) and *B. licheniformis* were prepared as described previously. Spores of psychrotrophic *B. longisporus* and thermophilic *Geobacillus stearothermophilus* were prepared as described before. The spore batches were stored at 4°C for less than 6 months. Unless indicated otherwise, a spore suspension in water, was heat activated at 50°C for 1 hour, centrifuged at maximum speed and resuspended in water with 0.01% Tween-80 to prevent clumping before use.

7.4.2.3 Preparation of soil samples

Soil samples were collected from JPL temperate soil, Mojave Desert arid soil, Atacama Desert hyper-arid soil and cold permafrost. Microorganisms Soil extraction method used was previously reported. The soil extracts were subjected to a heat treatment of different temperatures for 15 minutes to screen for spore.

7.4.2.4 Germination

To 2 mL of spore suspension, 0.6 ml of 0.4 M $CaCl_2$ solution was added. Germination was initiated by the addition of 1 mL of 0.2 M DPA at 20°C. The final volume was 5 ml. Germination was followed either by microscopic examination of stained spores in a phase contrast microscope or by measuring the decrease in optical density at 625 nm. In most cases, the germinant effect was assessed by spread plating onto TSA and incubated at the optimal growth temperature.

7.4.2.5 Delayed germination

Environmental samples were exposed to L-alanine and Ca-DPA for 2 hours of germination, followed by heat shock for 15 minutes. The samples were examined by phase contrast microscopy to examine for the degree of phase bright to phase dark transition as well as the residual phase bright bodies remaining.

7.4.2.6 24-well Bacillus spore enrichment

A 24-well microtiter plate method was developed to provide specific isolation medium for maximum recovery of endospore-forming bacteria. The following media were all minimal growth media. The 24 media consisted of (1) neutralized acid fertile soil extract agar; (2) neutralized acid desert soil extract agar; (3) neutralized acid rhizosphere soil extract agar; (4) 1/10 R2A adjusted to pH 3.0; (5) 1/10 R2A adjusted to pH 11.0; (6) yeast extraction with biotin; (7) 10% NaCl; (8) lysozyme; (9) nalidixic acid; (10) NH_4SO_4 and 5% urea; (11) novobiocin (25 μg mL^{-1}); (12) *Sporolactobacillus* isolation medium; (13) *Sporosarcina halophila* isolation medium and (14) *Sporosarci naureae* isolation medium. Each of the respective chemical was added as the sole carbon and nitrogen source in a minimal medium, namely (15) trimethylamine, (16) benzoate, (17) nitrate, (18) citrate, (19) propionate, (20) arginine, (21) allantoin, (22) succinate, (23) urea and (24) control. Once growth was observed, colonies were restreaked onto a more nutrient-rich media for isolation.

S. halophila isolation medium consisted of 5.0 g of peptone, 3.0 g of meat extract, 30.0 g of NaCl, 5.0 g of $MgCl_2$, 15.0 g of agar in 1 L of water, with pH adjusted to 7.5. The soil suspension was treated with ethanol, 50% (v/v) for 1 hour to kill vegetative bacterial cells. After 3 days of incubation at 3°C, mainly pigmented (yellow, orange, or pink) colonies of various sizes of *Bacillus* species will have developed. *S. ureae* isolation medium consisted of 30.0 g of L-asparagine $\cdot H_2O$, 3.4 g of KCl, 0.25 g of K_2HPO_4, 0.2 g of $(NH)_2SO_4$, 0.05 g of $MgSO_4 \cdot 7H_2O$, 2.5 mg of $FeSO_4 \cdot 7H_2O$, 0.25 mg of $MnCl_2 \cdot 4H_2O$, 1 mg of biotin, 5 mg of L-cysteine in 1 L of water, adjusted to pH 8.7 with1 M NaOH and supplemented with NaCl to a final concentration of 50 mM Na^+. *Sporolactobacillus* isolation medium consisted of 10.0 g of glucose, 10.0 g of polypeptone, 10.0 of yeast extract, 0.027 g of sodium citrate, 0.5 g of KH_2PO_4, 0.5 g of K_2HPO_4, 0.3 g of $MgSO_4 \cdot 7H_2O$, 0.01 g of NaCl, 10 mg of $MnSO_4 \cdot 5H_2O$, 1.0 mg of $CuSO_4 \cdot 5H_2O$, 1.0 mg of $CoC_2 \cdot 6H_2O$, 1.0 mg of $FeSO_4 \cdot 7H_2O$, 100 mL soil extract and 900 distilled water. Soil extract was prepared by autoclaving 100 g of soil mixed with 200 mL distilled water for 20 min at 130°C. The mixture was centrifuged to obtain a clear supernatant.

Plate counts were determined by spread plating on TSA preceded by heat shock followed and germinant incubation. Total spore concentrations were determined using a Petroff-Hausser hemocytometer and CFU concentrations were determined using TSA spread plating in triplicate measurements.

7.4.3 Results

Figure 7.8 shows that endospores only responded to calcium dipicolinate and L-alanine as germination potentiator to increase the final colony forming units by more than 2 times.

This method works for the cultivation of both laboratory and environmental endospores with varying degrees of improvement. For instance, the percent germination of *B. subtilis* 168 increased almost null to 40% when pretreated with germination incubation. No significant difference was observed in the case of *B. cereus* endospores.

Differences in germination rate can be exploited to provide additional selection. Spores of many of the common species such as *B. subtilis* and *B. cereus* germinate rapidly in simple media but spores of the less vigorous species do not. By incubating a heat-treated sample in a suitable medium for several hours and repeating the heat treatment, B. subtilis and similar organisms can be destroyed and spores of *B. macerans*, *B. polymyxa*, and other (rarer species) often remain. The use of selective agents to inhibit germination offers a powerful approach to the isolation of novel *Bacillus* strains. Experiments will be carried out this week.

The kinetics of L-alanine-induced and CaDPA-induced germination differs significantly. An 8 to 10 min lag and a slower germination rate are typical for CaDPA-induced germination. In L-alanine-induced germination, the lag period is only 1 to 2 min, followed by a germination rate about five times faster than obtained with CaDPA. The effect of prior heat-shock treatment on the rate of germination also depends on the germination agent employed. L-alanine-induced[65,66] and L-cysteine induced germination are heat-shock dependent. On the other hand, the rate of germination induced by CaDPA is unaffected by heat shock[67-69].

7.4.4 Discussion

It is an axiom in microbial ecology that since no single medium is able to support the growth of (even the known) spore-forming bacteria, there is, accordingly, no such thing as a total (viable) plate count. Thus, the development of selective media increases our insight into the populations of spore-forming bacteria present in a particular habitat. Useful selective media may be used on increased comprehension of the possession novel metabolic traits. Physical traits can also be used as for selection of sporangial subgroup II *Bacillus* species by pasteurization at 100°C rather than at 80°C, and with *B. xerothermodurans* by longer treatment at higher holding temperatures[70] .

Dormancy is the key to endospore's resistance to many agents, including heat, radiation, chemicals, and their survival over long period of time. Some endospores do not respond to germinants unless pretreated with some activating agents, such as sublethal heat, pressure, and chemicals. Since germination is upstream to outgrowth, multiplication and colony formation, enhancing the germinability is analogous to increasing the culturable counts. Germination can be triggered by physiological agents with nutrients including amino acids, purine nucleosides and sugars and these interact in a species and stereospecific manner with one of the number of receptors located in the spore's inner membrane[71-73].

A wide geographical distribution of spore-forming bacteria reflects their diverse nutritional requirements[74-76]. They can thrive in the soil habitat, from the cold permafrost to dry desert soils pushing forward the boundary conditions of survival. No single organism is known to possess the spectrum of life styles encompassed by the sporeformers. However, some of the organisms regarded as "more common" in terms of

distribution are those which grow relatively rapidly on complex laboratory media at near-neutral pH containing mixtures of sugars, nitrogenous materials, vitamins, etc. If soil preparations are plated and incubated, under both anaerobic and aerobic conditions, there is every reason to expect that the bacteria represented by organisms such as *B. fastidosus*, *B. pasteurii*, *S. ureae*, *D. nigrificans* or *C. acidiurici* will not grow and hence will not be regarded as present. This study aims to recover these hard-to-culture bacteria.

One explanation for the lag period during CaDPA-induced germination is that this period is required for enzymatic reactions involved in the breaking of dormancy. Such reactions maybe part of an activation stage common to many dormant systems, and are characterized by increased metabolic activity and decreased dependence on exogenous germinating stimulants. Conventional method involves a heat shock treatment of 80°C for 15 minutes or soaking in ethanol (50%) for 30 minutes to screen for soil-borne endospores. These prior treatments are essential because both endospores and vegetative form the same colonies on growth media. We investigated the optimal heat shock temperature with regard to soils samples collected from different temperature origins.

The samples were subsequently subjected to a sublethal heat treatment at 50°C, known as heat activation, and then plated onto heterotrophic medium. The first to note the direct activating effect of heat on spores were Curran and Evan[77], who noticed an increase in the colony count of milk after heat treatment. “A mild heating of the spores of mesophilic aerobes has been shown to hasten their subsequent germination“. They also found that this sublethal heating influences the number of spores which will subsequently germinate and form colonies.

7.5 References

1. Abyzov, S.S. *et al*, in *Space Life Sciences: Search for Signatures of Life, and Space Flight Environmental Effects on the Nervous System* (2004), Vol. 33, pp. 1222-1230.
2. Abyzov, S.S. *et al*. Antarctic ice sheet as an object for solving some methodological problems of exobiology. *Advances in Space Research* **23**, 371-376 (1999).
3. Christner, B.C., Mosley-Thompson, E., Thompson, L.G., and Reeve, J.N. Bacterial recovery from ancient glacial ice. *Environmental Microbiology* **5**, 433-436 (2003).
4. Castello, J.D. *et al*. Detection of tomato mosaic tobamovirus RNA in ancient glacial ice. *Polar Biology* **22**, 207-212 (1999).
5. Larkin, J.M. and Stokes, J.L. Taxonomy of psychrophilic strains of *Bacillus*. *Journal of Bacteriology* **94**, 889-895 (1967).
6. Larkin, J.M. and Stokes, J.L. Isolation of psychrophilic species of *Bacillus*. *Journal of Bacteriology* **91**, 1667 (1966).
7. Morita, R.Y. Psychrophilic bacteria. *Bacteriological Reviews* **39**, 144-167 (1975).
8. Russell, N.J., in *Extremophiles* (Eolss Publishers, Oxford, UK., 2003).
9. Branda, S.S., Gonzalez-Pastor, J.E., Ben-Yehuda, S., Losick, R., and Kolter, R. Fruiting body formation by *Bacillus subtilis*. *Proceedings of the National Academy of Sciences of the United States of America* **98**, 11621-11626 (2001).
10. Cooper, A., Drummond, A.J., and Willerslev, E. Ancient DNA: Would the real neandertal please stand up? *Current Biology* **14**, R431-R433 (2004).
11. Fux, C.A., Costerton, J.W., Stewart, P.S., and Stoodley, P. Survival strategies of infectious biofilms. *Trends in Microbiology* **13**, 34-40 (2005).
12. Gould, G.W. and Hurst, A., *The Bacterial Spore*. (Academic Press, New York, 1969).
13. Rotman, Y., Fields, M. L. Structure of spores of rough and smooth variants of Bacillus stearothermophilus with special reference to their heat resistance. *Journal of Food Science* **31**, 437 (1966).
14. Nicholson, W. and Setlow, P., in *Molecular Biology Methods for Bacillus*, edited by S. M. Cutting (John Wiley and Sons, Sussex, England, 1990), pp. 391-450.
15. Zobell, C.E. Action of microorganisms on hydrocarbons. *Bacteriological Reviews* **10**, 1 (1946).
16. Church, B.D., Halvorson, H., and Halvorson, H.O. Studies on spore germination: Its independence from alanine racemase activity. *Journal of Bacteriology* **68**, 393-399 (1954).
17. Buono, F., Testa, R., and Lundgren, D.G. Physiology of growth and sporulation in *Bacillus cereus* I. Effect of glutamic and other amino acids. *Journal of Bacteriology* **91**, 2291 (1966).
18. Nicholson, W.L. and Law, J.F. Method for purification of bacterial endospores from soils: UV resistance of natural Sonoran desert soil populations of Bacillus spp. with reference to B-subtilis strain 168. *Journal of Microbiological Methods* **35**, 13-21 (1999).
19. Schaeffer, A.B. and Fulton, M.D. A simplified method of staining endospores. *Science* **77**, 194-194 (1933).
20. Shafaat, H.S. and Ponce, A. Applications of a rapid endospore viability assay for monitoring UV inactivation and characterizing Arctic ice cores. *Applied and Environmental Microbiology* **72**, 6808-6814 (2006).
21. Janssen, F.W., Lund, A.J., and Anderson, L.E. Colorimetric assay for dipicolinic acid in bacterial spores. *Science* **127**, 26-27 (1958).

22. Rosenberg, M., Gutnick, D., and Rosenberg, E. Adherence of bacteria to hydrocarbons: A simple method for measuring cell-surface hydrophobicity. *FEMS Microbiology Letters* **9**, 29-33 (1980).
23. Tisa, L.S., Koshikawa, T., and Gerhardt, P. Wet and dry bacterial spore densities determined by buoyant sedimentation. *Applied and Environmental Microbiology* **43**, 1307 (1982).
24. Rickwood, D., Ford, T., and Graham, J. Nycodenz: A new nonionic iodinated gradient medium. *Analytical Biochemistry* **123**, 23-31 (1982).
25. Lindsay, J.A. and Murrell, W.G. Changes in density of DNA after interaction with dipicolinic acid and its possible role in spore heat resistance. *Current Microbiology* **12**, 329-333 (1985).
26. Vary, J.C. Germination of Bacillus megaterium spores after various extraction procedures. *Journal of Bacteriology* **116**, 797-802 (1973).
27. Fitz-James, P. and Young, E., in *The Bacterial Spore*, edited by G. W. Gould and A. Hurst (Academic Press, London, England, 1969), Vol. 1, pp. 39-72.
28. Cooney, P.H., Whiteman, P.F., and Freese, E. Media dependence of commitment in *Bacillus subtilis*. *Journal of Bacteriology* **129**, 901 (1977).
29. Foerster, H.F. and Foster, J.W. Endotrophic calcium strontium and barium spores of *Bacillus megaterium* and *Bacillus cereus*. *Journal of Bacteriology* **91**, 1333-1345 (1966).
30. Setlow, B., Cowan, A.E., and Setlow, P. Germination of spores of *Bacillus subtilis* with dodecylamine. *Journal of Applied Microbiology* **95**, 637-648 (2003).
31. Koshikawa, T. *et al*. Surface hydrophobicity of spores of *Bacillus* spp. *Journal of General Microbiology* **135**, 2717-2722 (1989).
32. Wiencek, K.M., Klapes, N.A., and Foegeding, P.M. Hydrophobicity of *Bacillus* and *Clostridium* spores. *Applied and Environmental Microbiology* **56**, 2600-2605 (1990).
33. Wynn-Williams, D.D., in *The Ecology of Cyanobacteria* (Kluwer Academic Press, Dordrecht, The Netherlands, 2000), pp. 341-346.
34. Grelet, N. Growth limitation and sporulation. *Journal of Applied Bacteriology* **20**, 315 (1957).
35. Schaeffer, P. Sporulation and the production of antibiotics, exoenzymes, and exotonins. *Bacteriological Reviews* **33**, 48-71 (1969).
36. Vinter, V. and Slepecky, R.A. Direct transition of outgrowing bacterial spores to new sporangia without intermediate cell division. *Journal of Bacteriology* **90**, 803-807 (1965).
37. Bernlohr, R.W. and Leitzmann, C., in *The Bacterial Spore*, edited by G. W. Gould and A. Hurst (Academic Press, London, England, 1969), Vol. 1, pp. 183-213.
38. Halvorson, H., in *The Bacteria: A Treatise on Structure and Function* (Academic Press, 1985).
39. Roth, N.G., Lively, D.H., and Hodge, H.M. Influence of oxygen uptake and age of culture on sporulation of *Bacillus anthracis* and *Bacillus globigii*. *Journal of Bacteriology* **69**, 455 (1955).
40. Slepecky, R.A. and Law, J.H. Synthesis and degradation of poly-β-hydroxybutyric acid in connection with sporulation of *Bacillus megaterium*. *Journal of Bacteriology* **82**, 37-42 (1961).
41. Atrih, A. and Foster, S.J. Analysis of the role of bacterial endospore cortex structure in resistance properties and demonstration of its conservation amongst species. *Journal of Applied Microbiology* **91**, 364-372 (2001).
42. Raso, J., Palop, A., Pagan, R., and Condon, S. Inactivation of *Bacillus subtilis* spores by combining ultrasonic waves under pressure and mild heat treatment. *Journal of Applied Microbiology* **85**, 849-854 (1998).

43. Raso, J., Pagan, R., Condon, S., and Sala, F.J. Influence of temperature and pressure on the lethality of ultrasound. *Applied and Environmental Microbiology* **64**, 465-471 (1998).
44. González, I., López, M., Martineez, S., Bernardo, A., and González, J. Thermal inactivation of *Bacillus cereus* spores formed at different temperatures. *International Journal of Food Microbiology* **51**, 81-84 (1999).
45. Melly, E. *et al*. Analysis of the properties of spores *of Bacillus subtilis* prepared at different temperatures. *Journal of Applied Microbiology* **92**, 1105-1115 (2002).
46. Cazemier, A.E., Wagenaars, S.F.M., and ter Steeg, P.F. Effect of sporulation and recovery medium on the heat resistance and amount of injury of spores from spoilage bacilli. *Journal of Applied Microbiology* **90**, 761-770 (2001).
47. Mazas, M., Gonzalez, I., Lopez, M., Gonzalez, J., and Sarmiento, R.M. Effects of sporulation media and strain on thermal resistance of *Bacillus cereus* spores. *International Journal of Food Science and Technology* **30**, 71-78 (1995).
48. Hashimoto, T., Frieben, W.R., and Conti, S.F. Germination of single bacterial spores. *Journal of Bacteriology* **98**, 1011-1020 (1969).
49. Moir, A. How do spores germinate? *Journal of Appliec Microbiology* **101**, 526-530 (2006).
50. Caipo, M., Duffy, S., Zhao, L., and D., S. *Bacillus megaterium* spore germination is influenced by inoculum size. *Journal of Applied Microbiology* **92**, 879-884 (2002).
51. Kell, D.B., Kaprelyants, A.S., Weichart, D.H., Harwood, C.R., and Barer, M.R. Viability and activity in readily culturable bacteria - a review and discussion of the practical issues. *Antonie van Leeuwenhoek* **73**, 169-187 (1998).
52. Church, B.D. and Halvorson, H. Intermediate metabolism of aerobic spores: I. Activation of glucose oxidation in spores of *Bacillus cereus* var *terminalis*. *Journal of Bacteriology* **73**, 470-476 (1957).
53. Mohd, S.Z. *et al*. Imaging and analysis of *Bacillus anthracis* spore germination. *Microscopy Research and Technique* **66**, 307-311 (2005).
54. Hashimoto, T., Frieben, W.R., and Conti, S.F. Microgermination of *Bacillus cereus* spores. *Journal of Bacteriology* **100**, 1385-1392 (1969).
55. Lefebvre, G.M. and Leblanc, R. The kinetics of change in bacterial spore germination. *Physiological Models in Microbiology*, 45-51 (1988).
56. Levinson, H.S. and Hyatt, M.T. Sequence of events during *Bacillus megaterium* spore germination. *Journal of Bacteriology* **91**, 1811 (1966).
57. Dring, G.J. and Gould, G.W. Sequence of events during rapid germination of spores of *Bacillus cereus*. *Journal of General Microbiology* **65**, 101-104 (1971).
58. Setlow, P. Spore germination. *Current Opinion in Microbiology* **6**, 550-556 (2003).
59. Leblanc, R. and Lefebvre, G.M. A stochastic model of bacterial spore germination. *Bulletin of Mathematical Biology* **46**, 447-460 (1984).
60. Cohn, F. Untersuchungen uber Bacterien. IV. Beitrage zur Biologie der Bacillen. *Beitr. Biol. Pflanz.* **2**, 249-276 (1876).
61. Koch, R. Untersuchungen uber Bakterien V. Die Atiologie der Milzbrandkrankheit, begrundet auf die Entwicklungsgeschichte des *Bacillus anthracis*. *Beitr. Biol. Pflanz.* **2**, 277-310 (1876).
62. Koch, R. Untersuchungen uber Bakterien VI. Verfahren zur Untersuchung, zum Conservieren und Photographieren. *Beitr. Biol. Pflanz.* **2**, 399-434 (1877).
63. Tyndall, J. Further researches on the department and vital persitence of putrefactive and infective organisms froma a physical point of view. *Phil. Trans. Roual SOc.* **167**, 149-206 (1877).
64. Priest, F.G., in *Bacillus*, edited by Colin R. Harwood (Springer, 1989).

65. O'Connor, R.J. and Halvorson, H.O. L-alanine dehydrogenase: A mechanism controlling the specicity of amino acid acid-induced germination of *Bacillus cereus* spores. *Journal of Bacteriology* **82**, 706 (1961).
66. Swank, R.W. and Walker, H.W. Characteristics of alanine-induced germination of PA 3679 NCA spores. *Journal of Food Science* **37**, 324-327 (1972).
67. Keynan, A., Murrell, W.G., and Halvorso, H.O. Dipicolinic acid content, heat-activation and concept of dormancy In bacterial endospore. *Nature* **192**, 1211-1212 (1961).
68. Keynan, A. and Halvorson, H.O. Calcium dipicolinic acid-induced germination of Bacillus cereus spores. *Journal of Bacteriology* **83**, 100-105 (1962).
69. Keynan, A., Evenchik, Z., Gould, G.W., and Hurst, A. The Bacterial Spore. *Vol* **2**, 1?8 (1983).
70. Bond, W.W., Favero, M.S., Petersen, N.J., and Marshall, J.H. Dry-heat inactivation kinetics of naturally occurring spore populations. *Applied Microbiology* **20**, 573-578 (1970).
71. Password, F. and View, I.S.I. How do spores germinate? *Journal of Applied Microbiology* **101**, 526-530 (2006).
72. Paidhungat, M. *et al*. Mechanisms of induction of germination of *Bacillus subtilis* spores by high pressure. *Applied and Environmental Microbiology* **68**, 3172-3175 (2002).
73. Hudson, K.D. *et al*. Localization of GerAA and GerAC germination proteins in the *Bacillus subtilis* spore. *Journal of Bacteriology* **183**, 4317 (2001).
74. Slepecky, R.A. and Leadbetter, E.R., in *Regulation of Bacterial Differentiation*, edited by P. Piggot (ASM Press, Washington, D.C., 1994), pp. 195-206.
75. Slepecky, R.A. and Leadbetter, E.R. On the prevalence and roles of spore-forming bacteria and their spores in nature. (1983).
76. Nicholson, W.L. Roles of *Bacillus* endospores in the environment. *Cellular and Molecular Life Science* **59**, 410-416 (2002).
77. Curran, H.R. and Evans, F.R. Heat activation inducing germination in the spores of thermotolerant and thermophilic aerobic bacteria *Journal of Bacteriology* **49**, 335-346 (1945).

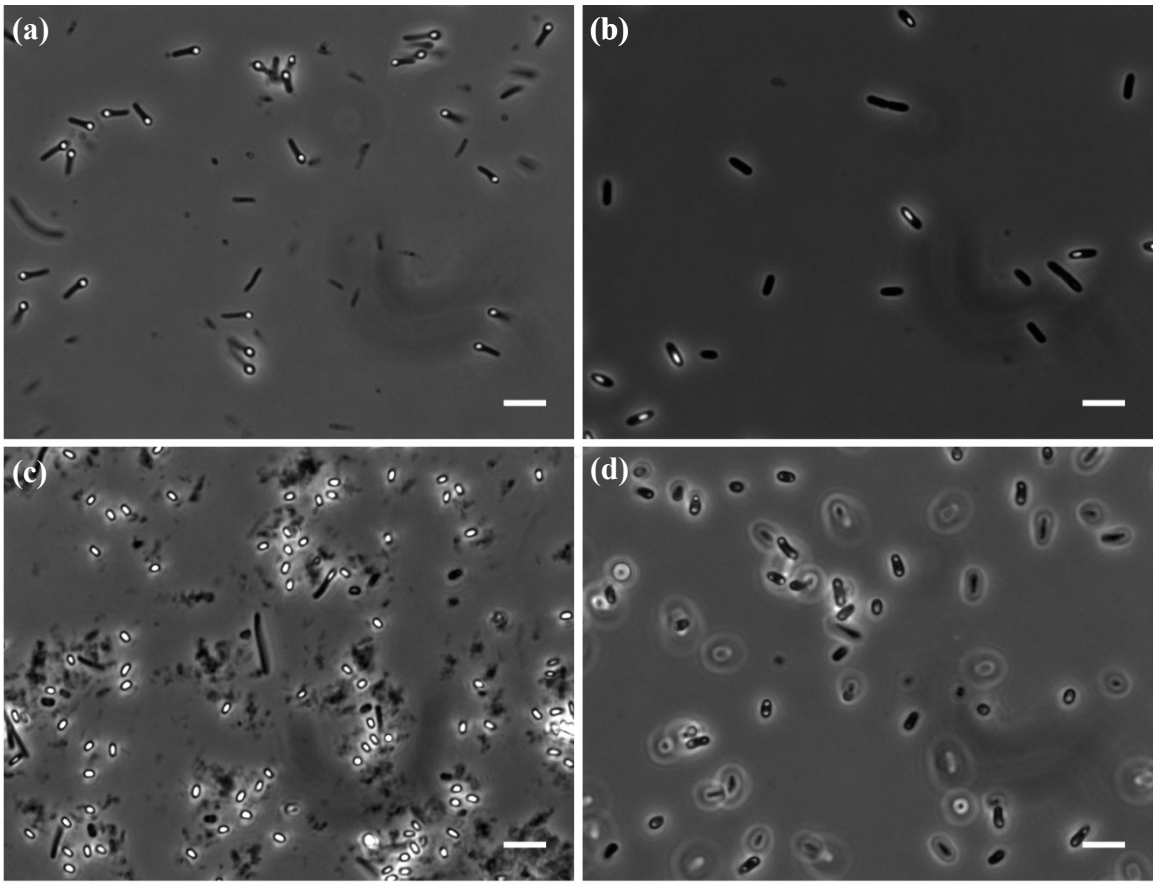

Figure 7.1 | Phase contrast micrographs of psychrophilic endospores. Scale bar, 5 μm. **(a)** lab-strain *B. psychrotolerance*; **(b)** lab-strain *B. longisporus*; **(c)** JPL soil isolate; **(d)** Lake Via isolate. Notice each mother cell contains two endospores.

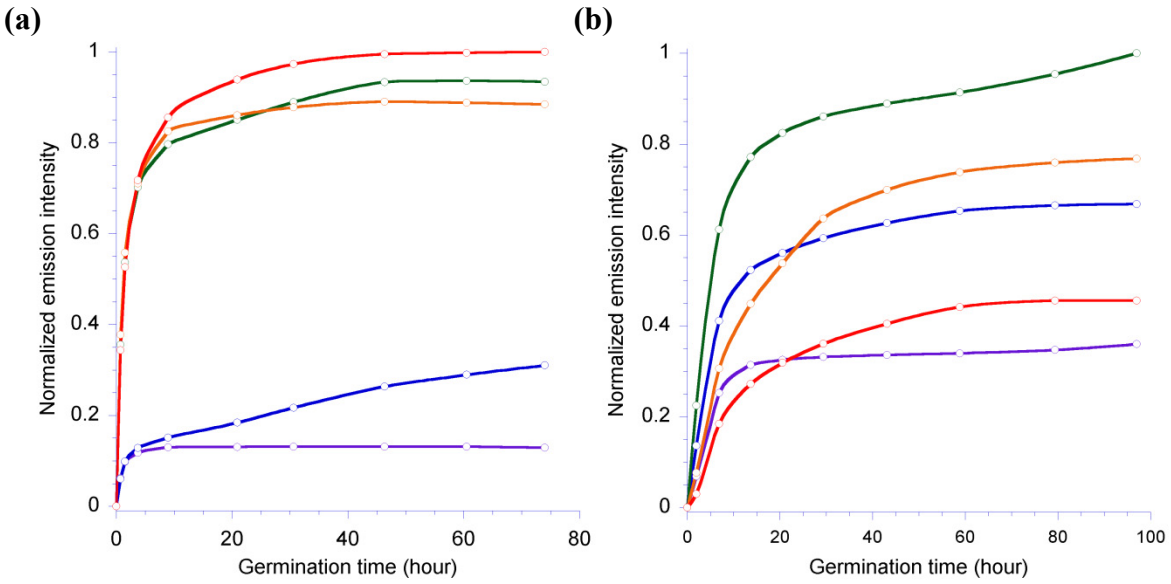

Figure 7.2 | Germination study of mesophilic endospores and psychrophilic endospores. The spores were germinated using 50 mM L-alanine without heat activation. The degree of germination was monitored by the release of DPA measured with a fluorimeter using the Tb-DPA luminescence assay. Plots represent different germination temperatures. Color designation: purple: 4°C, blue: 12°C, green: 22°C, orange: 30°C, red: 37°C. **(a)** Mesophilic *B. atrophaeus* endospores germinated fastest at 37°C.; **(b)** psychrophilic *B. longisporus* germinated fastest at 22°C.

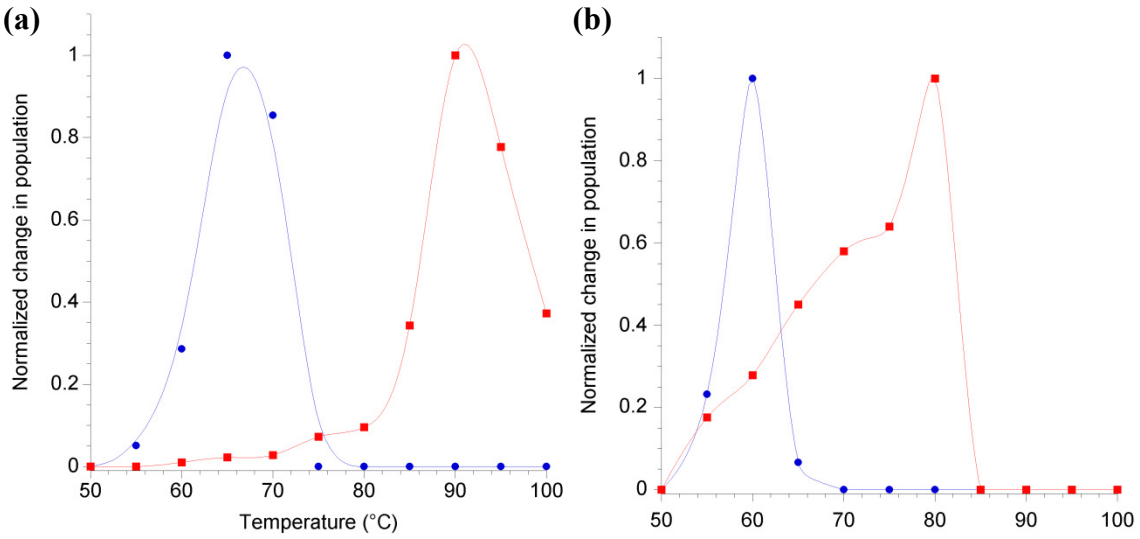

Figure 7.3 | Determination of optimal heat shock temperature in screening endospores from a mixed population of spores and vegetative cells. Y axis represents the normalized absolute change in cfu population. Blue plots represent the heat kill curve of vegetative cells and the red plots represent the kill curve of endospores. **(a)** The optimal heat shock temperature for mesophilic *B. atrophaeus* is 80°C; **(b)** the optimal heat shock temperature for psychrophilic *B. longisporus* is 70°C.

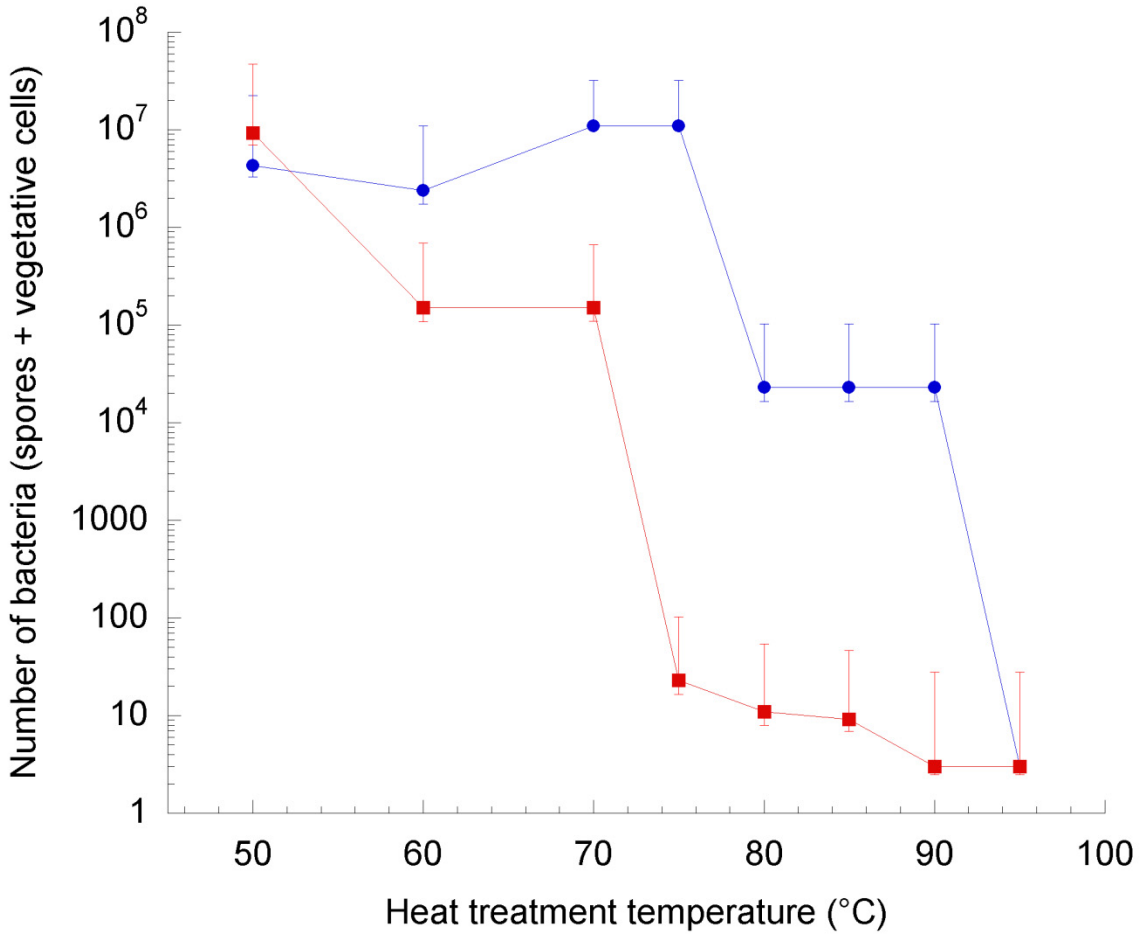

Figure 7.4 | Kill curve of *Bacillus* endospores. Blue plot represents mesophilic *B. atrophaeus* endospores and red plots represents psychrophilic *B. longisporus*. Initial inoculum consists ~10^7 cells with endospores and vegetative cells in 1:1 ratio.

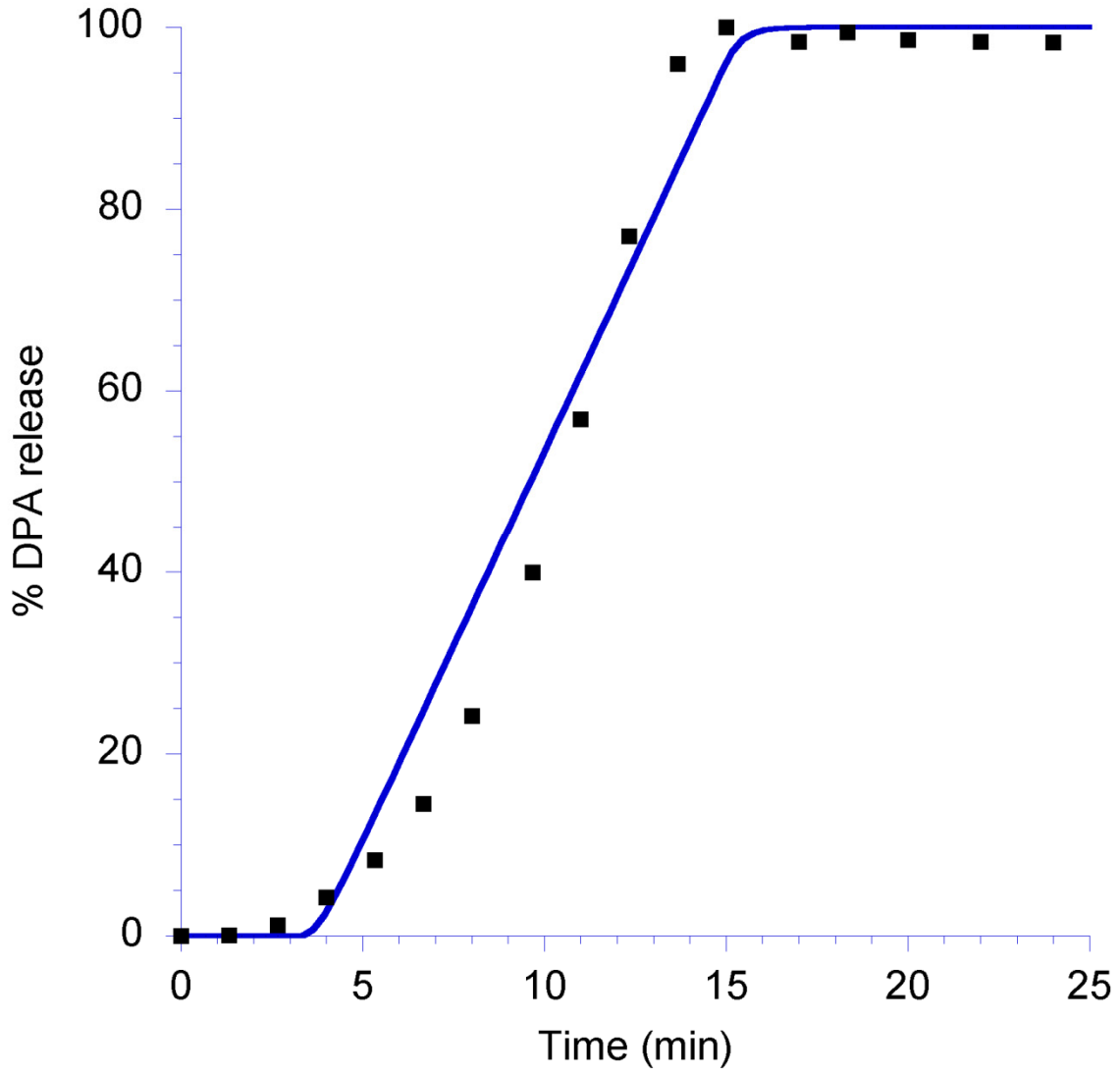

Figure 7.5 | Single endospore germination of *B. subtilis* and its predicted time curves predicted corresponding to a rectangular pulse approximation

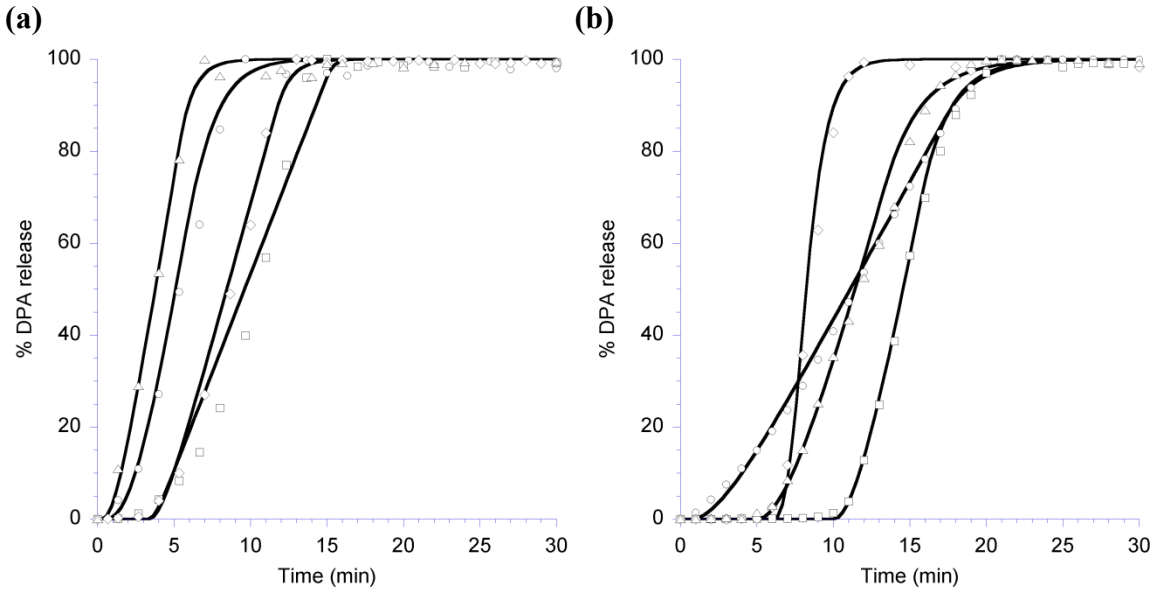

Figure 7.6 | A characteristic single endospore germination and predicted time curves predicted corresponding to a rectangular pulse approximation. Symbol designation: **(a)** circle: *B. atrophaeus*; square: *B. cereus*; diamond: *B. subtilis*; triangle: *G. stearothermophilus;* **(b)** circle: Atacama Desert isolate; square: Lake Vida isolate; diamond: Greenland GISP2 isolate; triangle: permafrost isolate.

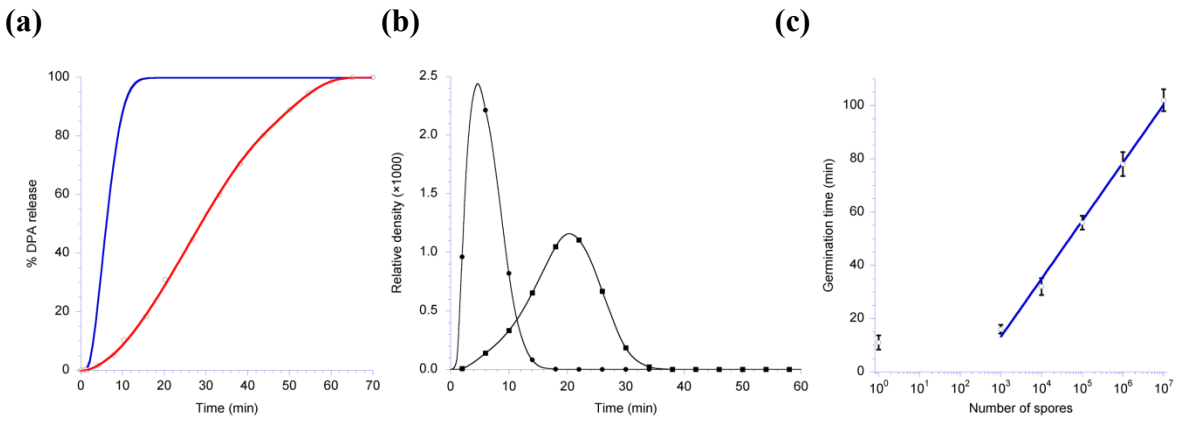

Figure 7.7 | (a) Comparison of a stochastic model derived from microgermination kinetics (blue) and measured macrogermination kinetics of *B. atrophaeus*. **(b)** Correlation of the number of spores with germination time. 10^0 data was obtained using μEVA while the rest of the data are obtained using spectroEVA. **(c)** The plot with circle points represent the τ distribution and the plot with rectangular points represents the microlag distribution of *B. atrophaeus* endospores.

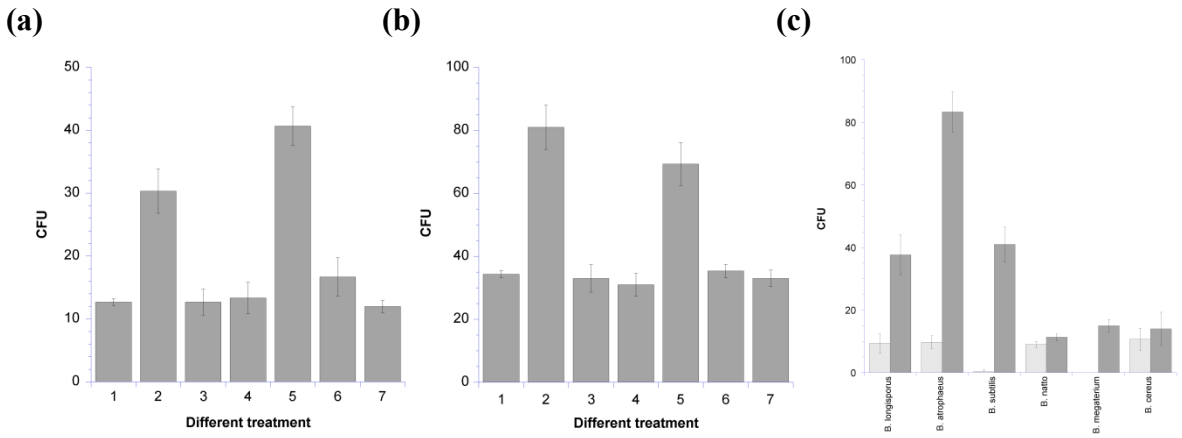

Figure 7.8 | The effect of pre-incubation of endospores to increase culturable counts. The effect of seven germinants on **(a)** *B. atrophaeus*. **(b)** environmental soil sample. The seven germinants are (1) calcium picolinate, (2) calcium dipicolinate, (3) calcium chloride, (4) sodium dipicolinate, (5) L-alanine, (6) AGFK, and (7) water control. **(c)** The use of calcium dipicolinate during pre-incubation of different Bacillus endospores prior to plating. Shaded bar represents the CFU obtained without germinant pre-incubation and the solid bar represents the data with germinant pre-incubation.

Property	*B. longisporus*	*B. psychrodurans*	JPL soil #1	JPL soil #2	Lake Vida #1	Lake Vida #2
Spore shape	Oval	oval	Round	Round	Round	Round
Location of forespore	Apical	Central	Apical	Apical	Middle	Polar
# spores/cell	1	1	1	1	1	2
Sporulation %	75%	75%	85%	80%	75%	75%
Colony	Mucoid, yellow	Dry, brown	Mucoid, orange	Mucoid, yellow	Mucoid, orange	Mucoid, orange
Hydrophobicity	0	0	0.20	0	0	0
Core density	1.30 ± 0.08	1.25 ± 0.08	1.35 ± 0.04	1.31 ± 0.11	1.28 ± 0.05	1.28 ± 0.06
Growth at 30°C	X	X	X	X	X	X
Heat shock temperature	70°C	65°C	60°C	65°C	60°C	60°C
Optimal germination temp.	22°C	22°C	22°C	12°C	22°C	12°C

Table 7.1 | Psychrophilic endospore properties.

	B. atrophaeus	*B. cereus*	*B. subtilis*	*G. stearothermophilus*
$\lambda_A(sec^{-1})$	0.015	0.7	0.7	0.7
$\lambda_B(sec^{-1})$	0.013	0.04	0.018	0.018
t_0 (sec)	20	200	200	20
a (sec)	300	700	500	300

	Atacama	Lake Vida	GISP2	permafrost
$\lambda_A(sec^{-1})$	0.7	0.7	0.022	0.7
$\lambda_B(sec^{-1})$	0.008	0.009	0.02	0.007
t_0 (sec)	40	600	360	300
a (sec)	1000	340	100	500

Table 7.2 | Germination parameters and lab-strain and environmental-strain endospores

CHAPTER 8: ENDOSPORES IN COLD BIOSPHERE

8.1 Abstract

Bacterial endospores entombed in polar ices, suspended in frozen lakes and embedded in permafrost present an opportunity to investigate the most durable form of life in the ideal media for maintaining long-term viability. However, little is known about the bacterial spore distribution and viability in these frigid biospheres. We have determined the concentration of endospores capable of germination in a depth transect of Greenland ice core, corresponding to an ages from 295 to 110,000 years, and in Antarctic Lake Vida using two complementary endospore viability assays (EVA). They are based on bulk spectroscopic analysis (i.e., spectroEVA), and direct microscopic enumeration (i.e., μEVA). Both assays detect dipicolinic acid (DPA) release during L-alanine induced germination *via* terbium ion (Tb^{3+})-DPA luminescence. In addition, DNA analysis and culture-based methods were conduced to characterize the microbial diversity. Anaerobic culturability was up to 11 cfu mL^{-1} of melted ice after 6 months of incubation at room temperature on solid media. *Bacillus* spore-forming species have been isolated in the brine water from Lake Vida. We hypothesize the longevity of life based on extrapolation of our exponential decay trend of endospores viability along a depth profile of the

Greenland ice cores. Studying these extreme polar habitats on Earth gleans invaluable information on the search for extinct or extant life on icy biospheres such as Mars and Europa.

8.2 Introduction

Approximately 75% of Earth's biosphere is cold and covered by oceans at temperatures below 5°C[1]. More than 70% of Earth's freshwater occurs as ice and a large portion of the soil ecosystem exists as permafrost. These permanently frigid habitats are unique repositories of microbes frozen at various points in the geologic past. A diversity of viable microorganisms, including fungi, bacteria and archaea have been isolated from glacial ice up to 400,000 years old and permafrost up to 3 million years old, originating from many geographical locales[2-10]. Formation of the remarkably resistant and dormant endospores in genera such as *Bacillus*, *Clostridium*, and *Sporosarcina* is observed as a response to nutrient-poor and cold environmental conditions. Research on endospores as the most resistant life form in these permanently cold environments provides insight into how microbial life endured the ice ages during Paleoproterozoic and Neoproterozoic[11], and the validity of the Snowball Earth Hypothesis. This is synergistic with the search for past or present life on the polar regions of Mars, Europa and the moons of Jupiter and Saturn[12-17].

The extent to which organisms can survive extended periods of metabolic inactivity in ice cores is one of the key questions in the exobiological study of life in extreme environments. Viable bacteria have been cultured from 110,000-year-old Greenland ice cores, but the relationship between the age of the bacteria and the age of the sediment remains controversial. In this study, we analyze the germination property of endospores embedded in GISP2 ice core samples collected from several sites in Greenland. We have shown that even during long exposures to low temperatures (-10°C to -15°C), the bacterial cells in permafrost are not completely dormant, but continue to metabolize and at least partially control the extent of amino acid racemization.

Endospores (i.e., bacterial spores) are dormant structures formed by *Bacillus*, *Clostridium*, and several other genera in the Firmicutes phylum[18] that are highly resistant to chemical, physical, and radiation sterilization processes[19]. Their structure is highly unique and very different from the structure of normal vegetative bacterial cells to survive extended periods of adverse environments. Because of their metabolic dormancy, bacterial spores do not require any nutrients or energy sources to persist[20]. In fact, *Bacillus subtilis* spores have survived for six years in space while exposed to high vacuum, temperature extremes, and intense solar and galactic radiation[21]. This has led to the suggestion that endospores are the most likely to

survive an interplanetary lithopanspermic journey[19,22-24]. If endospore formers were present in an early warm and wet Martian environment, they may currently be surviving in the subsurface ice/permafrost. Certain extreme environments on Earth are considered close approximations to those found on Mars or Europa. Antarctic ice sheets and underground lakes, for example, have been treated as models for these planetary systems[25,26].

Endospores exhibit remarkable longevity, with reports ranging from thousands[19,23,27-29] to one quarter of a billion years[30,31], although it is difficult to rule out contamination in these most ancient samples[32]. The extent to which endospores can survive extended periods of metabolic inactivity in ice cores, frozen brine and permafrost is one of the key questions in the exobiological study of life in extreme environments. Ice cores, as an environment with low and more or less constant temperature, is the region where remnants of life or even dormant forms of life would be preserved for the longest time. Viable bacteria have been cultured from 110,000-year-old Greenland ice cores, but the relationship between the age of the bacteria and the age of the sediment remains controversial. The transition from a water-rich past to the present Mars implies that endospores might have undergone a terminal hyper-saline frozen niche that resembled the Lake Vida habitat. Considering that ice is an excellent storage medium for preserving endospore

viability, we are interested in answering the overarching questions—how well can the most durable form of life (i.e., endospores) survive in an extreme medium (i.e., Lake Vida frozen brine) and how long endospores remain viable in an ideal storage medium (i.e., ice)?

The ice sheets of Greenland and Lake Vida in Antarctica are considered suitable sites for the study of longevity of microbial cells at low temperature[33,34]. GISP2 (Greenland Ice Sheet Project 2) is an international collaborative project that lasted from 1993 to 1998 to drill and collect ice cores from different depths along the 3053.44 m ice. Lake Vida is located in the McMurdo Dry Valley in Antarctica. This endorheic lake has been isolated from outside world by a layer of non glacial icecap. The briny water is 7 times more saline than sea water and remains unfrozen at -10°C. Only a few studies have been carried out on bacterial communities within ice cores and the population of bacterial spores in these communities has never been directly assessed. However, bacterial spore formers have been isolated from various ice core environments[35-40].

Permafrost in defined to be soils at or below the freezing point of water for two or more years. Over 20% of the terrestrial soil ecosystems consist of alpine and glacier permafrost. Permafrost is one of the extreme habitats on Earth, characterized by permanently subzero temperatures, high salinity, low water activity and low rate

of nutrient and metabolite transfer. Extremophiles residing and thriving in this habitat are composed of a great diversity of microorganisms, including halophiles, psychrophiles and spore-forming bacteria. Formation of the remarkably resistant and dormant endospores in genera such as *Bacillus*, *Clostridium*, and *Sporosarcina*. is generally regarded as a response to nutrient-poor and adverse environmental conditions. So far, most of the endospore studies on permafrost habitats are constituted by culture-based techniques. In this study, we demonstrated the integration of culture-based and non-culture-based techniques to assess the viable bacterial endospore population in a permafrost sample. Dipicolinic acid was measured from endospores as a proxy for endospore viability in an effort to determine the longest dormancy period demonstrable for one of the most resilient Earth microorganisms and the survival strategies under martian-like extraterrestrial conditions including dehydration, freezing, starvation and salinity, for exobiology exploration.

Microbial communities from permafrost have been described as "a community of survivors.[41]" This "starvation-survival style" is the normal physiological state of microbial communities within permafrost, contributed by cold temperature, desiccation and starvation[42] that are coincidentally the driving forces for sporulation. Endospores have been widely found in permafrost all over the world[14,41,43,44]. As one

of the most resistant form of life on Earth, endospores present themselves as time capsule preserving geological history, as well as the ideal surviving candidate in other analogous extraterrestrial environments from the perspective of astrobiology.

In the GISP2 ice core experiment, we ultimately aim to determine the longevity of bacterial spores embedded in ices by measuring the viable fraction of endospores as a function of ice core age. Toward this end, we have developed two complementary endospore viability assays (EVA) capable of quantifying the number of endospores capable of germination[45,46], where the ability to germinate serves as an indicator for viability. These viability assays are based on bulk spectroscopic analysis (i.e., spectroEVA), and direct microscopic enumeration (i.e., μEVA). Both assays detect the release of dipicolinic acid (DPA), a unique chemical marker found only in endospores[47], during L-alanine induced germination. The process of endospore germination can be initiated on the timescale of minutes by the addition of trigger molecules such as L-alanine, L-asparagine, or glucose[47-51]. During the first stage of germination, most of the DPA is released from the core of the endospore into solution[47,52,53].

Specifically, in μEVA experiments, the Tb^{3+}-DPA luminescence halos that form as DPA is released into Tb^{3+}-containing media under UV excitation are enumerated in a microscope field of view. SpectroEVA experiments quantify

germinating endospore concentrations by comparison of Tb^{3+}-DPA luminescence intensities to a standard curve. In addition, the total number of endospores in a sample can be determined with spectroEVA experiments by inducing total DPA release through spore rupture by autoclaving, which in combination with the germinating spore count allows the computation of the viable fraction of endospores.

In the permafrost study, we focus on developing culture-dependent and culture-independent methods to detect endospores embedded in permafrost. Permafrost can be any soil or rock which has remained frozen for two consecutive winters and the intervening summer. The matrix is usually highly complex and presents difficulty in detecting the resident endospores. Apart from the previously-reported μEVA, we have used phase-contrast microscopy, SYBR® Gold, Live/Dead *BacLight* viability, 5-cyano-2,3-diotolyl tetrazolium chloride (CTC) staining[54], ATP luciferin-luciferase and terbium-dipicolinate (Tb-DPA) luminescence assays to study microorganisms in permafrost. Different property and processes associated with endospore, including phase property, germination, DPA content, ATP synthesis, outgrowth and respiration, are all used as proxy for assessing viability. Among these methods, the use of CTC is a novel method to detect respiring endospores in permafrost. Because of their bright red fluorescence

(emission maximum = 602 nm), actively respiring endospores were readily distinguishable from abiotic particles and other background substances, which typically fluoresced at shorted wavelengths.

Here we report the first application of μEVA and spectroEVA to determine the germinating and total endospore concentrations in Greenland (GISP2) ice cores, Antarctic Lake Vida brine water, and polar permafrost.

8.3 Materials and Methods

8.3.1 Materials

Deionized water (18.2 MΩ/cm) was obtained from an ultrafilter system (Water Pro PS, LabConco, Kansas City, MO). Terbium (III) chloride hexahydrate-(99.999%), dipicolinic acid (99%) (2,6-pyridinedicarboxylic acid, DPA), and L-alanine were obtained from Aldrich (Milwaukee, WI), and were used without further purification. Agarose for culturing experiments was obtained from MacConnell Research (San Diego, CA). Agarose for μEVA experiments was obtained from Invitrogen (Carlbad, CA). All utensils were either prepackaged one-use only or glassware was kilned at 500°C for 4 hours for sterilization and removal of biomolecules such as DNA, RNA and DPA. All media and utensils were pre-chilled to 4°C before use. All aerobic procedure, unless otherwise specified, was carried out inside a biohazard safety

cabinet (Sterilgard III Advance, The Baker Company, Sanford, ME) on a cold aluminum plate. Anaerobic procedure was carried out in an anaerobic chamber with using bench-top chiller and ice for temperature control.

8.3.2 Validation of ice core decontamination protocol

The ice core was received as a gift from the Greenland Ice Sheet Project (GISP 2) and corresponded to 11 depths from 1566 to 2804 m. We have made synthetic ice core sections (a cylinder 5 cm in diameter and 15 cm in length), consisting of frozen suspensions of 10^4 *B. atrophaeus* endospores in the interior, and 10^5 *B. megaterium* endospores smeared on the exterior surfaces. The colonies of these two endospores can easily be distinguished by color. We compared and evaluated the effectiveness of decontamination protocols previously reported[55,56] (Figure 8.1).

8.3.3 GISP2 ice core handling

The GISP2 ice cores, arranged in ascending depth order (ID# G2-271, depth 93.96–94.21 m, age 295 years; MCA.02 # 1566, depth 1565.75-1566.00 m, age 10,000 years; MCA.02 #1923, depth 1922-1922.25 m, age 20,000 years; MCA.02 #2096, depth 2095.75-2096.00 m, age 30,000 years; MCA.02 #2253, depth 2252.10-2252.35 m, age 40,000 years; MCA.02 #2429, depth 2428.00-2428.25 m,

age 50,000 years; MCA.02 #2517, depth 2516.75-2517.00 m, age 60,000 years; MCA.02 #2593, depth 2592.31-2592.56 m, age 70,000 years; MCA.02 #2657, depth 2656.20-2656.45 m, age 80,000 years; MCA.02 #2703, depth 2702.11-2702.36 m, age 90,000 years; MCA.02 #2746, depth 2745.65-2745.90 m, age 100,000 years; MCA.02 #2804, depth 2803.65-2803.90 m, age 110,000 years), were obtained from the National Ice Core Laboratory (NICL) and stored at -80°C. In preparation for decontamination, the ice core temperature was ramped to 0°C *via* storage first at -25°C for eight hours, followed by two hours at 0°C. Temperature equilibration of the ice core was necessary to prevent the decontamination solutions from freezing onto the outside of the ice core.

Decontamination was carried out under aseptic conditions, as illustrated in Figure 8.2. The core sections were then placed on an aluminum block (pre-chilled at -80 °C freezer and disinfected by bleach). A heat-sterilized saw was used to cut the core into half. One half underwent the decontamination process and the remaining portion was stored at -80 °C for future processing. A beaker containing 1600 mL of cold (4°C) 6.25% sodium hypochlorite solution and 3 beakers containing 1600 mL of cold (4°C) sterile distilled water (18.2 MΩ, < 1 ppb TOC, DNase-free and RNase-free) were prepared. The ice core was submerged in the NaOCl solution for 10 s and then rinsed with sterile water 3 times, each with 10 s, and finally placed in

another beaker for melting at room temperature inside a biohazard cabinet hood aseptically.

Before melting, 1/10 of the meltwater was reserved for culturing. The remaining meltwater was vacuum filtered through a 45 mm 0.1 μm membrane filter (Nucleopre Track-etch membrane, Sterlitech Corporation, Kent, WA) backed with a 0.45 μm Supor backing filter. The meltwater was analyzed with 24 hours by culturing. The filter(s) was/were resuspended in 5 mL of the original cold filtrate. The suspension and filter(s) were vortexed for 5 minutes, with 1-min chilling increment in between to prevent cells from overheating. The membrane filter(s) was/were removed from the suspension and stored in -20°C freezer for clone library analysis. The concentrated suspension was used for subsequent endospore viability assays, microscopy and ATP analyses.

After melting, the ice core sample (~400 mL) was vacuum filtered through 0.2 μm filters (Nucleopore Track-Etch Membrane, Sterlitech Corporation, Kent, WA) and resuspended in 3 mL of cold, sterile water, resulting in a concentration factor of 145. Of this volume, 1 mL was used for spectroEVA, 1 mL for μEVA, 1 mL for DAPI stain fluorescence microscopy. These aliquots were sufficient to reproduce all measurements in triplicate.

8.3.4 Permafrost handling

The permafrost decontamination protocol was developed based on previous reports on the sources of contamination on permafrost[57,58]. The permafrost sample was moved from -80°C to -20°C overnight for gradual warming. A cold (-20°C) aluminum plate was used as a workbench to keep the sample and hood cold. The permafrost sample consisted of a compact ball of silty and claylike soil particles. The frozen spherical soil sample was fractured in a hood with a sterile knife and scalpel and only internal fragments are taken by forceps aseptically for analysis. 3 layers of surface soils were scrapped off in series. The excavated sample was then weighted in a 50 mL centrifuge tube quickly lest water evaporation affected the final weight (Figure 8.3). 1:5 ratio of 50 mM sodium pyrophosphate with 0.1% Tween-80 is added into the tube. The suspension was vortexed for 5 min and sonicated for 2 min. To prevent overheating, samples were put on ice during sonication, and between vortexing and sonication the samples were cooled on ice for at least 1 min. The suspension was centrifuged at 200 g for 20 min to separate the silty permafrost particles and microbial cells. The supernatant was aliquoted into 3 vials (1) without heat treatment; (2) heat shocked at 60°C for 15 min and (3)

heat-shocked at 80°C for 15 min. Culture-based and culture-independent analysis tests were carried out on these permafrost extracts.

8.3.5 Ice core analysis using spectroEVA

For shallow ice cores, SpectroEVA experiments were performed as previously described[46]. Endospore suspensions for spectroEVA experiments were prepared to a final volume of 3 mL and contained 100 mM L-alanine and 1 μM $TbCl_3$, unbuffered, at pH 6.2. Tb-DPA luminescence excitation (λ_{ex} = 250 – 360 nm, λ_{em} = 544 nm) and emission (λ_{ex} = 278 nm, λ_{em} = 515 - 580 nm) spectra were recorded at room temperature with a fluorimeter (Fluorolog 3-τ system, Jobin Yvon, Edison, NJ, FL-1089). Emission intensities were calibrated with respect to an external Tb-DPA luminescence standard solution. Luminescence intensities were quantified by integrating the area under the 544-nm emission peak with a baseline subtraction. To correlate intensity to endospore concentrations, a calibration curve was established for 1 μM Tb^{3+} over the range of 10^3 – 10^7 spores mL^{-1}. From this, the corresponding limit of detection was calculated to be 1000 spores mL^{-1} of a preconcentrated sample.

Several different sample holders have been explored to determine the concentration of DPA spectroscopically to maximize the final concentration factor

and decrease the background fluorescence. Initially, disposable methacrylate cuvettes have been used. To determine the concentration of germinating endospores in a sample, 50 μL of 1 M L-alanine was added to 450 μL of the concentrated ice core sample. This solution was then placed in a 37°C water bath for 16 h to promote germination. To determine the total endospore concentration, a parallel aliquot of the concentrated solution was autoclaved at 124°C for 20 min. Following either germination or autoclaving, 300 μL of 10 μM Tb^{3+} and 2550 μL of deionized water were added to 150 μL of each solution, which were analyzed using fluorescence spectroscopy. The integrated intensities were converted into germinating endospore concentrations or total endospore concentrations, respectively, by comparison to the standard curve. The endospore concentrations were then divided by the dilution factor of 7.25 to account for the pre-concentration of the ice core and obtain the germinating endospore and total endospore concentrations in the dilute, native ice core.

For deeper and old ice cores, the protocol has been modified and optimized to analyze the much lower concentrations of embedded endospores. The use of a 250-μL quartz microcuvette and 50-μL micro-cuvette called Fluorovette (ALine, Redondo Beach, CA) have been explored to minimize the sample volume. The endospore suspension was prepared in 300 μL containing 100 mM L-alanine and 1

μM $TbCl_3$ at pH 6.0.The pH of the autoclaved sample was adjusted accordingly with 1 N HCl with respect to the reference. Steady-state emission and excitation spectra were taken as described before with a Fluorolog-3 FL-1089 model. Phosphorescence spectra were obtained by coupling a Spex 19340 phosphorimeter module to the Fluorolog-3 instrument; the excitation and emission slits were set at 10 nm. All spectra were corrected for lamp fluctuations and photomultiplier tube response. Quartz micro-cuvettes (Starna Cell) were used for minimal dilution factor.

The anaerobic version of spectro-EVA has also be employed on the deeper ice cores with a change in the germinant used. Sodium bicarbonate has been used as an activator to germinate anaerobic endospores.

8.3.6 Ice core analysis using μEVA

μEVA experiments were performed as previously described[45]. Briefly, a time-gated microscopy technique was used to count individual endospores in a microscope field of view. The contrast in the image is generated by the formation of the long-lived and brightly luminescent Tb-DPA complex as DPA is released during the germination process. DPA release is observed as a spreading halo originated from each endospore during germination, where DPA molecules bind with Tb^{3+} that has

been added into the surrounding matrix. The germinating endospores manifest as bright spots in the field of view that grow in intensity over a period of 3-5 minutes.

Specifically, a 300 μL aliquot of the concentrated sample was filtered through a 9 mm spot of a 25 mm 0.2 μm pore size black polycarbonate filter (#110656 Whatman, Florham Park, NJ), backed with a 0.45 μm pore size cellulose membrane (#140618 Whatman, Florham Park, NJ), using a conventional membrane filtration apparatus. The filter was transferred aseptically to 1.5% agarose doped with 100 μM $TbCl_3$ and 10 mM L-alanine, contained in a 9 mm silicone well (Molecular Probes, Eugene, OR) on a quartz slide. A 15 mm × 15 mm piece of 0.5 mm thick polydimethylsiloxane (PDMS) was placed on top of the agarose to prevent evaporation and aerial contamination, and the sample was analyzed using time-resolved fluorescence microscopy.

Endospores were filtered and concentrated onto the surface of a membrane filter. The particles were transferred onto Tb^{3+}- and L-alanine-doped agarose by streaking the membrane filter across the agarose surface. The L-alanine within the agarose triggers any endospores present to germinate and release DPA. A piece of 4.5 μm thick polydimethylsiloxane (PDMS) film was placed on top of the agarose to prevent aerial contamination, minimize water loss and DPA diffusion across the agarose substrate. Images were taken with a time-gated microscope, which consists

of a pulse xenon flashlamp, a stereoscopic microscope (1 mm × 0.8 mm field of view at 63× magnification), mounted with a time-gated camera (Photonics Imaging System, UK). The timing of gating is governed by the xenon flashlamp, which serves as the master oscillator at 300 Hz. After a delay of 100 μs after the lamp flash, the CCD camera begins integration of single photons. Over a germination course of 30 minutes, formation of miniature luminescence spots could be observed under time-gated microscopy, which was indicative of the localized formation of Tb-DPA due to DPA release during endospore germination. Background fluorescence and autofluorescence were minimized because of time gating, rendering a dark background. Characteristic germination time course allows unambiguous assignment of germinating endospores.

8.3.7 Ice core cultivation

For the shallow ice core, the growth medium consisted of 1/100th R2A (Difco) dissolved into distilled water and solidified with 0.8% agarose. Freshly melted sample water was plated onto a total of 7 plates with three replicates of 200 μL and 4 replicates of 100 μL. The plates were wrapped in Parafilm to prevent desiccation, placed at 4°C in the dark and monitored biweekly for growth for 147 days.

For the deeper ice cores, $^{1}/_{10}$ R2A was used for the cultivation of aerobic bacteria. Two solid media, MM2 and $^{1}/_{10}$ R2A, were used for the growth of anaerobic microbial communities. MM2 consisted of basal salts, trace elements, vitamin solution, and different substrate supplements to enrich for different groups of microorganisms at 7°C and at room temperature. MM2, as described by Ferrara Guerrero *et al.*[59], was designed for enrichment of fermentative bacteria and for methanogens. The Petri dishes were sealed inside GasPaks to provide an anaerobic environment. 3-tube MPN series method was applied in the aerobic culture and 2 MPN series dilutions was used in the anaerobic culture. The anaerobically prepared media (50 mL in 125-mL bottles) were overgassed with N_2, inoculated from the melted ice (~1:200 dilution). For each depth, solid agar plates were prepared in duplicate, and the aerobic and anaerobic plates and tubes were incubated with appropriate controls at 7 °C and room temperature. Results reported are based on solid agar cultures after ~6 months of incubation at room temperature.

In addition, a system of 5 enrichment media was prepared using filtered-sterilized ice core filtrate, mineral and vitamin supplements, 1 mM calcium dipicolinate as the basal medium, namely (1) full strength R2B for heterotrophic bacteria, (2) B_{10} medium for ferric-reducing bacteria, (3) Butlin's broth supplemented with agar (1.5%) for sulfate-reducing bacteria, (4) nitrate broth

supplemented with agar (1.5%) for nitrifying bacteria, (5) N-deficient combined broth for diazotrophic bacteria[60]. The agar plates were prepared at 5 different pHs (3, 5, 7, 9, 11) and incubated at 7°C and 22°C. Calcium dipicolinate was added for facilitating spore germination and hence subsequent outgrowth and colony formation

8.3.8 Lake Vida Cultivation

Various cultivation methods were used, spread plating, most probable number, fluid thioglycollate culture and multiplex 24-well microtiter plate for isolation of *Bacillus* endospores. The medium consisted of 12.5 g of NaCl, 2 g of K_2HPO_4, 1.25 g of KH_2PO_4, 0.5 g of $MgSO_4 \cdot 7H_2O$, 0.125 g of $CaCl_2 \cdot 2H_2O$, 0.05 g of $MnSO_4 \cdot H_2O$, 2.5 g KNO_3 and 2.5 g of yeast extract in 1 liter of water. 0.2-µm filter sterilized Wolfe's mineral (0.5%) and vitamin (0.5%) solutions (ATCC) were added aseptically to the sterile medium at 60°C. The basal medium was made from 1/5 of the autoclaved actual brine water sample, incubated at different temperatures, different pHs and different salinity with and without urea.

8.3.9 Permafrost cultivation

Heterotrophic plate counts were prepared by spread plate 100 µL aliquots of 10^{-3}, 10^{-4}, and 10^{-5} serial dilutions of samples on 1/2 TSA agar (Becton, Dickson and Company, Sparks, MD), supplemented with 0.1 M sucrose and 10% sodium chloride, as well as on 1/5 R2A with cycloheximide (50 µg mL^{-1}). Plates were incubated at ambient temperature for up to 20 days and 7°C for up to 2 months. All plating was performed in quadruplicate and results are reported as mean counts with standard error. Colonies were streaked for isolation on fresh medium of the same type from which they were isolated and incubated at their specific growth temperature. Plates were incubated aerobically and anaerobically inside GasPaks.

A MPN technique was used to enumerate viable bacteria. Three replicate 10-fold dilutions of sediment samples in the medium broth consisting of 1/5 TSB with 0.1 M sucrose and 10% sodium chloride were prepared. MPN tubes were incubated for 2 months aerobically under ambient temperature and at 7°C. Tubes were score positive on the basis of ATP production by the firefly luciferin-luciferase bioluminescence assay.

8.3.10 Permafrost metabolic study

In the augmentation experiment, the permafrost extract was incubated in a low nutrient bath (final concentration of 1/10 TSB and 10 mM L-alanine) at ambient temperature for 1 week with agitation and full aeration. The ATP level, DPA level and respiration rate were monitored during the course of growth.

ATP was measured by the microluminometer NHD Model 3550i (New Horizon Diagnostics). A sample suspension was transferred to the Filtravette^{TM} (0.45 μm), four drops of somatic cell releasing agent were added. The mixture was pushed though the Filtravette by a positive pressure device. Four more drops of somatic cell releasing agent were added and pressure filtered to ensure the removal of interfering substances, free ATP, and somatic cell ATP. The Filtravette was then placed into the drawer slide of the microluminometer. Two drops of bacterial releasing agent were added into the Filtravette to extract the microbial ATP. Immediately after the addition of the bacterial releasing agent, 50 μL of luciferin-luciferase reagent was added and mixed by aspirating the fluid up and down three times. The drawer slide was closed immediately. Light emission was measured with integration with 10 seconds. ATP was reported as relative light units (RLUs), taken directly from the luminometer's digital readout.

DPA measurement is equivalent to the measurement of germination propensity. 1.5 mL of extract was pipetted into methylcrylate cuvettes at each time interval. 1.5 mL of 50 μM $TbCl_3$ supplemented with 10 mM aluminum chloride buffered with 10 mM sodium acetate to pH 5.5 was added. The luminescence intensity was measured using the following home made spectrometer: the spectrometer consists of a 24 W pulsed xenon flashlamp (FWHM ~5 μs and tailing out to ~50 μs), a photomultiplier tube (Hamamatsu R6353P, Bridgewater, NJ), 2 concave aluminum mirrors and 2 bandpass filters. Pulsed excitation light at 10 Hz was focused on samples with a concave aluminum turning mirror and band-limited by an interference filter (50% pass bandwidth 255–280 nm, 23% maximum transmittance). Luminescence from the sample traversed through a bandpass filter (50% pass bandwidth 538–553 nm, 70% maximum transmittance) and another concave aluminum mirror to enter the PMT. The filter set was chosen to overlap with the excitation and emission spectra of Tb-DPA. Time gating was achieved by a delayed detection of the sample luminescence after each flash, according to a chosen delay time. Throughout all measurements in this study, the PMT was operated at 950 V, photocathode aperture set to be 15 mm × 10 mm, delay and integration time was 100 μs and 2 ms, respectively. The entire assembly was shielded from ambient light using a black anodized aluminum enclosure. The spectrometer was custom constructed by Jobin

Yvon, Edison NJ. Cuvettes and tape matrix were measured at a distance of 15 mm from the spectrometer.

CTC was used to test the respiratory activity during germination and growth. Reduction of CTC was used to evaluate the respiratory potential of freshly isolated endospores. Dehydrogenase activity in bacterial respiration was measured with this dye, which has the ability to produce a red fluorescent molecule (formazan) when reduced. A stock solution of 50 mM CTC was prepared in sterile ultra-filtered water. 90 µL TSB and 10 µL CTC stock solution (final concentration of 5 mM) were incubated for an additional 2 hours at 37°C in the dark. The stained samples were loaded on a filtration apparatus and pumped through a 0.22-µm nucleopore polycarbonate filter. The filters were mounted on a slide and observed under 100× oil immersion objective.

8.3.11 Fluorescence microscopy

The DNA-intercalating fluorescent dye, SYBR Gold (Molecular Probes, Invitrogen) was used to determine the number of total cells by epifluorescence microscopy. To dislodge cells from sediment particles, the protocol described by Epstein and Rossel was modified[61]. Aliquots of fixed sediment samples were mixed with 0.2-µm filter-sterilized and autoclaved water. The samples were sonicated three times for 1

min at the lowest setting with a microtip. Aliquots of the sonicated sediment samples or fixed pure cultures were diluted in 5 mL of particles free PBS and stained with SYBR Gold (1 μg of SYBR Gold mL^{-1} of PBS). After 10 min of staining, the cells were concentrated by filtration onto black polycarbonate filters (pore size 0.2 μm; Nuclepore). The membrane filters were mounted with immersion oil. Epifluorescence microscopy was performed with a Nikon Optiplex microscope. For each filter no fewer than 400 cells were counted in at least 10 microscopic fields.

The LIVE/DEAD® *BacLight*™ kit (Molecular Probes, Invitrogen) was employed to assess the viability of permafrost vegetative bacterial communities. Phase contrast microscopy was performed to determine the total number of endospores present. Endospores are not stainable but they can be observed as phase-bright oval bodies under phase contrast optics. Malachite green staining was performed to identify the presence of endospores. Endospores would be stained green while the rest would be stained red.

Direct cell counts were obtained as previously described[62], with the exception of using a 3.7% formaldehyde fixative and 2 μg mL^{-1} of 4',6-diamidino-2-phenylindole (DAPI) stain. One hundred microliters of the DAPI stock solution (1 mg mL^{-1}) were added to 1 ml of sample which was stained for 8-10 min and then filtered through a black 0.2 μm Nucleopore black polycarbonate filter.

For staining with acridine orange 40 µl of stock solution (0.5 mg mL^{-1}, dissolved in PBS) were added to 1 ml of sample, stained for 2 min and further tested as the DAPI-stained sample. Filters were mounted with immersion oil before the cover slip was placed on top. DAPI binds strongly to DNA for total bacterial enumeration. The counts were enumerated by IP-Lab imaging processing software (Becton Dickinson). Segmented particles were included in the count if they ranged from 0.06 to 0.5 μm^2, which corresponds to a sphere with a radius ranging from 0.14 to 0.4 µm. This lower size limit also corresponds to the volume, 0.01 μm^3, of the smallest know free living bacterial cell, *Pelagibacter ubique.* The apparently high counts could be due to non cell particles that were able to take up the DAPI stain.

8.3.12 Phase contrast microscopy

Spores appear as phase bright bodies under microscope and thus TSU can be obtained. Epifluorescence microscopy was performed with a Nikon Optiplex microscope. For each filter no fewer than 400 cells were counted in at least 10 microscopic fields. Deposit on agarose for easy enumeration. Spore films were prepared by drying 50 µL of a suitably diluted suspension of spores spread out over a circular area of about 1.5 cm in diameter. When dry, the monolayer of cells formed a smear of endospores. Due to the low number of counts, the entire smear

was counted. Approximately 100 fields of views were examined using 60× pH3 phase contrast objective. Endospore appeared as bright thick-wall round/oval bodies, and vegetative cell appeared as phase dark. Spore size was determined using the following equation:

$$\mathbf{V} = \left(\frac{\mathbf{d^2\pi}}{\mathbf{4}}\right)(\mathbf{L} - \mathbf{d}) + \left(\frac{\mathbf{d^3\pi}}{\mathbf{6}}\right)$$

8.3.13 Method of Schaeffer and Fulton

The Schaeffer and Fulton method in staining endospores were modified as follows: A smear of 20 µL of Lake Vida brine was prepared, air dried and heat fixed on a microscope slide. The smear was covered with a piece of blotting paper soaked with malachite green, and then placed over a boiling water bath for 5 min. The overlying blotting paper was kept moist by constant introduction of malachite. The slide was then cooled down and washed with deionized water until no residual green stain was left. The slide was placed in a staining jar with safranin for 2 min, and then rinsed until no residual red stain was left. The entire smear was examined using 100× oil immersion objective in which endospores were stained light green found/oval bodies and vegetative were stained red. This method is not quantitative due to unknown number of cells being washed out during the staining procedure. 3 slides

were prepared and counted. This method is, however, a definitive qualitative method and can set the lower boundary for endospore count.

8.3.14 Flow cytometry

Staining of 500 µL samples from the melted ice with propidium iodide (PI) and SYTO-9 was according to the instructions of the LIVE/DEAD *BacLight* bacterial viability kit (Molecular Probes, Eugene, OR), and samples were examined under a Nikon Optiplex microscope with a 100× objective. Flow cytometry analysis was carried out with a FACSCalibur flow cytometer (Beckton Dickinson Immunocytometry Systems, San Jose, CA) equipped with an air-cooled argon ion laser emitting 15 mW of blue light at 488 nm and with a standard filter setup. Live/Dead BacLight viability kit is used to stain live cells green with SYTO-9 and dead cells red with propidium iodide. The green and red fluorescence were collected using a 530 ± 30 nm bandpass filter (FL1 channel); the red fluorescence emitted from PI was collected by a 650 ± 13 nm bandpass filter (FL3 channel). All analyses were performed at low flow-rate setting (~12 µL min^{-1}) while the count was lower than 1000 events/s. Data were analyzed in software. Control samples as well as 1µm europium fluorescent beads (Bead concentration = 1.25 x 10^8 mL^{-1}) were used for the instrument calibration (voltage of the detector and threshold) and for checking the

instrument sensitivity over time. Cells were discriminated from background using a double threshold set on both side scatter (SSC) and forward scatter (FSC). A dual dot plot of FSC vs. SSC in combination with a one parameter histogram representing the green fluorescence (FL1) was used to back gate cells and distinguish them from the background.

8.4 Results

In this section, we will describe the first successful application of two novel endospore viability assays (i.e., spectroEVA and μEVA) on Greenland ice cores. Parallel determination of both germination-capable and total endospore concentrations allows us to calculate the fraction of germination-capable endospores in a given sample. Since germination is an indicator of viability, we call this the viable fraction. Ultimately, we measure the viable fraction as a function of ice core age to determine the viability decay and corresponding longevity of endospores embedded in ices. The spectroEVA and μEVA experimental results reported here represent the first step towards addressing the endospore longevity question. First, we will review the data on the first ice core (295 years) that we analyzed and then proceed to the other deeper and more challenging depths, followed by preliminary characterization experiments of Lake Vida and polar permafrost.

8.4.1 Validation of ice core decontamination protocol

The outside of ice cores was associated with contaminants originated from such as drilling fluids, transport, handling and cutting. The outer surfaces of the ice cores had to be effectively removed and decontaminated in specimen authentication. We carried out the validation based on two criteria, the first was to ensure that contaminants are completely eliminated from outer layers; the second was to protect organisms inside the ice cores during decontamination and melting of the ice. Among the liquid sterilants (sodium hypochlorite, calcium hypochlorite, ethanol, hydrogen peroxide) used, sodium hypochlorite in the form of Chlorox (6.25% active ingredient) was the most effective, assuring completing elimination of all outer *B. megaterium* endospores and preservation of the inner *B. atrophaeus* endospores (Figure 8.1).

8.4.2 Ice core SpectroEVA

Different SpectroEVA procedures and data analyses were applied to the shallow depth (94 m) and deeper depths ($\geqq$1566 m) because of the difference in postulated endospore concentrations. SpectroEVA results are presented in two parts here.

Figure 8.4 illustrates a comparison of the excitation spectrum between a 94 m Greenland ice core and the excitation spectrum of 1 μM DPA with 10 μM Tb^{3+}. The excitation spectrum of the ice core concentrate clearly showed Tb-DPA complex formation, indicating the presence of endospores. The slight differences in shapes between the excitation spectra arise due to the presence of impurities in the ice core; however, the maxima of the DPA vibrational progressions clearly aligned. Control negative experiments did not manifest excitation spectra similar to the Tb-DPA complex. This evidence supports our claim that DPA was extracted from the ice cores and was the source of the increased Tb^{3+} luminescence intensity. From this, and the fact that endospores are the only source of DPA in a natural environment[47], we conclude that SpectroEVA was able to detect and quantify endospores within the GISP2 ice core.

After the germination process in the ice core sample was complete, the germination-capable endospore concentration was determined to be 295 ± 19 spores mL^{-1} for the native ice core. After autoclaving the ice core sample, the total endospore concentration was determined to be 369 ± 36 spores mL^{-1}. From these two values, we calculated a viability ratio of 0.80 ± 0.09.

Figure 8.5 illustrates an excitation spectrum of a 1566 m deep ice core section. The green spectra represented the excitation spectra of 1 μM DPA with 5 μM $TbCl_3$

in water (solid line) and native ice core filtrate with 0.1 μm membrane filter (dotted line). The filtrate was shown to slightly broaden the characteristic Tb-DPA characteristic dual-peak spectroscopic handle. Endospore spectra were compared with the dotted DPA reference. The blue, orange and pink plots represented the DPA content by autoclaving, induced aerobic germination and induced anaerobic germination of the ice core sample, respectively. The control negative sample, shown in black, did not manifest any spectral similarity to the Tb-DPA complex. A DPA reference and standard curve was created for each specific ice core due to heterogeneity of background fluorescence observed in the meltwater filtrate.

In the DPA calibration curve, adding interferring chemicals would only result in a general broadening and up-shifting of the entire excitation spectrum. Only in the presence of DPA that the excitation peaks at 271 and 279 nm could be observed. The robustness of the Tb-DPA binding was also stressed in other literature. Pure DPA demonstrated background absorption at wavelengths beyond the range of 260 and 300 nm. So, we performed a deconvolution on the spectra assuming supposition of x molar ratio of DPA that contributed to the dual-peak pattern and y molar ratio of interferring background fluorescence that contributed to the general broadening and up-shifting of the spectrum. DPA reference and the deconvolved sample spectra were compared with a point-to-point matching algorithm. Similarity was assessed based on

an Euclidean cosine squared correlation coefficient[63]. 0.9 was chosen as the threshold correlation coefficient. In the case of the ice core sample shown in Figure 8.5, the total endospore and aerobic germination endospore spectra were shown correlated with the DPA reference, while the anaerobic germination spectrum was classified as uncorrelated. The total endospore concentration was calculated to be 136 ± 26 spores mL^{-1} and germination-capable aerobic endospore concentration was calculated to be 29 ± 9 spores mL^{-1} after deconvolution and linear regression with the standard curve. The viability ratio was determined to be 0.23 ± 0.11.

SpectroEVA experiments rely on a standard curve to relate measured Tb-DPA intensities to an equivalent endospore concentration. The standard curve for the 94 m sample was generated using *B. atrophaeus* (ATCC 9372) endospores assuming that endospores within an ice core contained an average DPA content per spore equivalent to that of the *B. atrophaeus* spores. For the rest of the deeper samples, the standard curve was created using *B. longisporus*, a psychrophilic strain, in each specific ice core filtrate due to heterogeneity of background fluorescence. *B. atrophaeus* contained 0.208 fmol DPA $spore^{-1}$. And *B. longisporus* contained 0.992 fmol DPA $spore^{-1}$.

8.4.3 Ice core μEVA

Figure 8.6 shows a representative μEVA image of germinated endospores and corresponding germination time course plots of 10 endospores. DPA release during germination resulted in bright luminescent spots due to Tb-DPA complex formation with the Tb^{3+} that was present in the surrounding agarose medium. While individual endospores, with reported sizes between 0.8 and 4 μm, could hardly be spatially resolved with a stereoscopic microscope, the intense Tb-DPA luminescence emanating from the location of germinating endospores enabled rapid enumeration. From μEVA experiments, we determined that 27 ± 3 spores mL^{-1} in the 94 m sample germinated under experimental conditions. Germination-capable endospores were detected in all depths except the core sections at 2517 m and 2804 m. The number of spores was approximately two orders of magnitude lower than the measurable at 94 m underground. Control negatives experiments contained background counts that were at least 3 orders of magnitude lower than those obtained from ice core samples.

Our data showed that individual endospores in the GISP2 ice core released detectable amounts of DPA within the first 10 minutes. Our observed germination time course data are consistent with microgermination times previously reported [64-66]. For reference, we overlaid the germination time courses of ice core endospores

with (1) a pure *B. atrophaeus* spore suspension, and (2) an environmental surface swab from our laboratory.

8.4.4 Ice core microscopy and flow cytometry

The 93 m sample was the clearest among all the depths, with a cell concentration of $7.0 \times 10^3 \pm 6.7 \times 10^2$ cells mL^{-1}. This ice core sample was visibly clear and cell count preparations showed very little sand or debris. Cell concentration of the rest of the ice cores ranged from 2.1×10^4 to 8.3×10^6 cells mL^{-1} showing correlation with the degree of meltwater turbidity of specific depths. For instance, the depths that corresponded to ages 20,000, 30,000 and 40,000 years, which took twice as much time to filter, contained the highest cell counts. An increased number of microorganisms was found associated with a high degree of fine grain sediments in the silty layer at the bottom portion of the GISP2 ice cores[67]. Although DAPI staining is generally specific for DNA, occasionally larger particles that are obviously not cells are stained. Therefore, this count may be a slight overestimate as some cell-sized particles (approximately 1 μm), which are not as easily distinguished from actual cells, may have been included in the count. Staining with the fluorescent DNA-binding dyes SYTO-9 and PI allowed the accessibility of bacterial DNA and the status of the cytoplasmic membrane to be assessed. Using the

Live/Dead *BacLight* viability kit, the live to dead cells ratio was approximately 10^{-3} (Figure 8.7). Both flow cytometry and epifluorescence revealed a predominately PI-stained red cell bodies. Phase contrast microscopy revealed approximately 10^2 to 10^3 phase-bright bodies mL^{-1} of the native ice core. Most of the cells were small, with sizes 1 μm or below. Detailed counts are shown in Table 8.2.

8.4.5 Ice core cultivation

Culturing attempts yielded two colonies in the 93 m deep sample after applying 1 mL of fresh ice core meltwater to 1/100 R2A. These colonies only became visible as pinpoints after 147 days at 4°C corresponding to a concentration of 2 cfu mL^{-1} in the native ice core. For the deeper ice cores, both aerobic and anaerobic culturing were practiced. No colonies were observed in the spread plating culture on either 1/10 R2A medium, B_{10} medium, Butlin's medium, nitrate medium, or N-deficient medium supplemented with native ice core meltwater at different pHs 3, 5, 7, 9, 11 at 7°C and 22°C after 6 months of incubation. Aerobic MPN tubes were still under incubation and would be tested for growth by ATP assay. Anaerobic spread plating yielded 0 to 11 cfu mL^{-1}, some of which were heat-shock survivors, on both 1/10 R2A and MM2 media.

8.4.6 Lake Vida analysis

The method described for examining endospore abundance in ice cores[46,68] was not applicable to Lake Vida brine water. Interference from background fluorescence masked the spectral characteristics of DPA. Pre-concentration was impossible because the lake water was highly turbid. A modified ethyl extraction protocol successfully extracted detectable quantities of DPA from the lake water[69,70]. Figure 8.8 shows an overlay of the excitation spectra of DPA references and endospore suspensions. The green spectra represented the excitation spectra of 1 μM DPA with 5 μM $TbCl_3$ in water (solid line) and native filtered Lake Vida water with 0.2 μm membrane filter (dotted line). The filtrate was shown to slightly broaden and elevate the spectrum from 300 – 360 nm, due to presence of unknown interference particulates that fluoresced green in the UV range. The characteristic Tb-DPA characteristic dual-peak spectroscopic handle could still be observed. Endospore spectra were compared with the dotted DPA reference. The blue, orange and pink plots represented the DPA content by autoclaving, induced aerobic germination and induced anaerobic germination of the brine water sample, respectively. The control negative, shown in black, did not manifest any spectral similarity to the Tb-DPA complex. Using a deconvolution, point-to-point matching algorithm and Euclidean cosine squared correlation coefficient method, it was determined that the total endospore and

germination-capable aerobic endospore populations were 4800 ± 800 spores mL^{-1} and 1600 ± 230 spores mL^{-1}, respectively. The excitation spectrum derived from germination-capable anaerobic endospores elicited a broad band across 270-280 nm and therefore lacked similarity with the DPA reference. μEVA experiment revealed a concentration of 0.80 ± 0.24 spores mL^{-1} of germination-capable aerobic endospores.

Cultivation attempt on various media yielded a total culturable count of 0.5 cells mL^{-1} and 0.1 heat-shock survivors mL^{-1} of native lake water (heat shocked at 65°C). Growth was observed in cultures incubated at 7°C and 22°C with distinct differences in morphologies. Colonies obtained from low-temperature cultures in general exhibited bright colors, e.g., orange, red and pink, while those from room-temperature cultures were usually brown in color. Most of the isolates were halotolerant and were recovered from medium with NaCl concentration of >5%. Majority of the isolates were obtained from alkaline media (pH 9 and 11) supplemented with urea. Subsequent sporulation attempt resulted in an endospore-forming species that harbored two endospores per mother cell (Figure 8.9). DPA was detected from a sporulating culture of this species.

A spore size distribution histogram (Figure 8.10) was observed using phase contrast microscopy. Spores remaining after being washed in the malachite green staining protocol were determined to be 5% of the original population. Malachite

green staining revealed a concentration of 196 ± 58 spores mL^{-1} and phase contrast microscopy revealed $1.9 \times 10^4 \pm 2.7 \times 10^3$ spores mL^{-1} of the native Lake Vida brine water. The spore size calculated by phase contrast microscopy was 10%-15% larger than that by malachite green staining. The size discrepancy is due to the presence of phase ring, which obscures the accurate determination of an endospore appearing as a phase bright body under phase contrast microscopy.

8.4.7 Permafrost analysis

After incubation of about 4 months, colonies started to show up takes time to grow. Sub-culture did not take as much as to grow under low temperature. Inoculum has been heat-shocked and therefore colonies isolated should presumably by spore-forming species. DNA analysis revealed the presence of spore-forming species. After 2 weeks of incubation, aerobically, we have obtained 8.7×10^2 cfu g^{-1} on minimal TSA plates selecting for halophiles; and 6.7×10^2 cfu g^{-1} on minimal R2A selecting for heterotrophic bacteria at 7°C. At room temperature, we obtained 3.8×10^3 cfu g^{-1} on TSA plates and 1.3×10^2 on R2A plates. It showed the presence of both aerobic mesophilic and psychrophilic halophiles and heterotrophs vegetative bacteria. Anaerobic culture yielded no growth on TSA; 1.3×10^2 cfu g^{-1} and 4.3×10^2 cfu g^{-1} on R2A plates at 7°C and room temperature, respectively. No anaerobic halophiles were recovered but some heterotrophic counts were obtained. MPN enumeration yield

comparable results with spread plate counting. Conventional endospore selection process involves heating at 80°C for 15 minutes. It has, however, been reported that psychrophilic endospores has a lower heat tolerance. Therefore two different heat-shock temperatures were used to experiment the heat resistance of any present endospores. We have chosen a heat-shock treatment at 80°C and 60°C for 15 minutes on the permafrost sample, respectively. We have only obtained approximately 10^2 cfu g^{-1} and 10^2 mpn g^{-1} for the 60°C-treated sample incubated aerobically at room temperature on TSA plates and in TSB. The rest of the heat-shocked samples yielded unobservable growth after one month of incubation. The permafrost under analysis contained a very low culturable aerobic mesophilic bacterial endospore population which is susceptible to 80°C of heat treatment. All negative controls showed negative growth (Table 8.1).

A DPA-spike standard curve could not be established with the ethyl acetate extraction method because of the high background interference. Spectro-EVA approach failed but μEVA identified 8.3 ± 3.3 spores g^{-1} of native permafrost. Figure 8.11 shows time-lapse images of spore germination time courses. Endospores were induced to germinate at room temperature on an agarose substrate fortified with 50 mM L-alanine and covered with PDMS. The germination timecourse of the predominant endospore in the permafrost had a sigmoidal kinetics of DPA release.

SYBR-Gold staining of permafrost yielded a total number of vegetative cells of 3.57×10^6 cells g^{-1} (n = 24). *BacLight* viability staining yielded a live SYTO-9 count of 4.07×10^5 cells g^{-1} and a dead PI count of 3.47×10^6 cells g^{-1}. Phase contrast microscopy gave a total endospores count of 3.96×10^3 spores g^{-1}. μEVA gave a germinable endospore population of 8.33×10^0 spores g^{-1} (Figure 8.12). Of the total 3.57×10^6 cells g^{-1} in the permafrost sample, 11.40% were stained live by SYTO-9 and the live to dead ratio of vegetative cells was found to be 11.73%. Total and germinable endospores constituted 0.11% and 0.0002% of the total microbial population. Compared with the cultivation results, approximately 0.1% of the vegetative cells were culturable; ~0.01% of the total endospores was culturable and ~0.002% of the total endospores was germinable.

At the beginning of incubation with CTC (*t = 0*), no red signal (CTC-positive cells) was detected for the heat-shock permafrost sample. However, after 6 hours of incubation, some endospores demonstrated respiration and some red signal was observed at the center of endospores. The red signal appeared as round, oval and small at this time. After 2 days of incubation, the red signal became more apparent and the stained endospores looked bigger than the previous ones. In addition, some stained elongated cells forms could be observed. Some endospores should have undergone germination and outgrowth to become vegetative cells again. After 7

days in incubation, a huge increase in cell numbers and size were noticed. The red-stained cells have characteristic morphologies of vegetative cells in oval and filamentous shapes (Figure 8.13). It showed that the vegetative bacteria have undergone multiplication. Positive reduction reaction was not observed in the control sample.

The levels of ATP and DPA of permafrost samples were monitored over 7 days upon exposure to nutrients (1/2 TSB and 10 mM L-alanine). Figure 8.14 shows the respective ATP and DPA timecourses. ATP levels rose in both the non-heat-shock and heat-shock samples at 60°C, indicating the presence of metabolic processes. No ATP was released when the sample was subjected to 80°C for 15 minutes. This is probably due to the inactivation power of heat at this temperature. Insignificant levels of DPA were detected in any of the three cases due to low number of endospores present in the permafrost. It was anticipated to be close to, or not lower than, the limit of detection of the instrument. Moreover, any released DPA *via* endospore germination would be used up as energy in the growth broth. Therefore, no observable changes were noticed in DPA level.

8.5 Discussion

The dormancy of endospores, combined with their resistance, enables them to last for extreme periods of time. Numerous reports have documented the isolation of viable spores from environmental samples such as dried soil in herbarium collections, paleosols, ancient lake sediments, permafrost soils, ice cores and old cans of meat. These samples ranged in age from several decades to thousands of years[28,71-75].

To better understand constraints on bacteria at extremely low temperatures in ice, we describe here the adaptation of methods previously developed for the imaging of mesophilic endospores. Endospore viability assessment, using the Tb-DPA luminescence assay, time-gated microscopy and image analysis were applied to Greenland ice core. Abundances of aerobic, anaerobic, total, viable, germinable, culturable were also determined from samples melted at 0°C using Tb-DPA luminescence assay and DNA intercalating dyes. Following a vertical transect of 11 depths in Greenland ice cores, we observed a decrease in both bacterial viability and abundance with increasing age. Germinable endospores were found in all ice core samples (295 years and 10,000 to 110,000 years), but on average less than 1 endospore/mL of the original ice. Percentage of viable cells ranged between >0.1% based on germination assay and total epifluorescence

enumeration. Endospore viability was significantly correlated ($p < 0.001$), indicating that viability assessment by μEVA is a good probe for endospore enumeration in ice cores. Our results expand the spectrum of information available on bacteria in ice cores on a scale relevant to the organism and provide insight into characteristics of frozen microbial habitats on Earth and perhaps elsewhere in the universe. Viable bacteria have been recovered from Greenland ice cores over 100,000 years old. Although there is not much doubt about the presence of microorganisms and other biotic materials in ice cores, the microorganisms or their DNA could survive in a viable or amplifiable form in ice for centuries or millennia is not universally accepted. We concentrated our efforts on spore-forming bacteria, because, as with other types of microorganisms, spore-forming bacteria respond to stressful environmental conditions by producing a resistant structure, dormant endospores. Most of these structures have extremely thick cell walls, some with another layer of exosporium. The microbial composition of ancient ice core samples from Greenland was examined through culture and culture-independent approaches. The culturable and non culturable microorganisms found in the ice cores provide a prototype for possible life on the cryogenic planets of the solar system.

8.5.1 Comparison of spectroEVA and μEVA at 295 m depth

Our measurements of this GISP ice core yielded 295 ± 19 spores/mL using spectroEVA and 27 ± 3 spores/mL using μEVA. This discrepancy is presumably due to differences in DPA content between environmental samples and lab strain *B. atrophaeus*, which may give rise to an overcount in spectroEVA experiments. In addition, agglomeration of more than one endospore per dust particle will lead to an undercount in μEVA experiments, but not in spectroEVA experiments. These two factors may constructively combine to account for the discrepancy; for example, a three-fold difference in DPA content combined with an agglomeration rate of three endospores per particle results in an order of magnitude difference between the two measurements. Comparison of the two methods using laboratory *B. atrophaeus* gave a linear correlation as given by equation (1).

$$\text{Spores/mL (}\mu\text{EVA)} = 1.6 \times \text{Spores/mL (spectroEVA)} \quad (1)$$

8.5.2 Viability assessment at 295 m depth

The definition of viability of microorganisms is neither simple nor straightforward[76,77]. Endospores that give rise to colonies on growth media are clearly viable, but culture based approaches generally miss more than 99% of the viable-but-not-culturable cells found in the environment[78-80]. Similarly, the

conditions we provide for germination will not work for all endospores in a given sample (e.g., superdormant endospores). In addition, endospores that germinate are not necessarily viable since the molecular machinery for subsequent metabolic activity and reproduction may be damaged.

Quantification of the true viable biomass of an environmental sample, defined as cells that have the capability of metabolic activity and reproduction is currently not experimentally accessible since all experimental methods used to determine viability each have their own intrinsic biases and limitations. Due to the well-documented difficulty of obtaining growth of environmental cells under laboratory conditions we contend that our method of measuring endospore germination gives an easy and reliable measurement of viability. We have demonstrated that DPA release can be observed using EVA, based on bulk spectroscopic analysis and direct microscopic enumeration. Rather than requiring full outgrowth before enumeration, we probe for viability much earlier, during stage I germination when DPA is released and water begins to enter the core. Germination and colony formation assays are complementary in that they set experimentally tractable upper and lower bounds for the viable endospore population. For a given population of endospores, a subset will germinate and a subset of the population capable of germination will form colonies. We have previously demonstrated the

reproducible correlation of germination-capable populations to culturable populations[46], and we contend that germination is a good indicator of endospore viability. In this study, we define the viable fraction as the ratio of germination-capable and total endospore concentrations, and we investigate the longevity of endospores by looking at their total population, viability, germinability as well as the culturable fractions, as shown in the Venn diagram (Figure 8.15).

Both the germinable and culturable counts are very low in our study. One of the reasons may be non optimal germination conditions for psychrophilic spores. Another experiment performed by our group has demonstrated that psychrophilic spores do not respond to conventional germinants, such as L-alanine and arginine, glucose, etc. A more thorough study should be carried out to characterize the germination kinetics of psychrophilic spores.

8.5.3 Toward endospore longevity experiments

The experimental results presented above clearly demonstrate the utility of spectro- and μEVA experiments to determine germinating and total endospore concentrations in Greenland ice cores. The particular Greenland ice core sample used in this investigation was obtained from a depth of ~94 m and is estimated to be 295 years old. As we obtain additional allocations of ice cores from increasingly

older layers, we will be able to evaluate the viability decay of endospores in ices. In the case that the initial viable fraction (V_i) at the time of deposition is constant across various age samples, and decays exponentially with time (t) at a rate (k), we would expect to observe a viable fraction decay (V) following equation (2).

$$V = V_i e^{-kt} \quad (2)$$

Regarding the underlying assumption that V_i is constant for samples from all depths, we acknowledge that the initial viable fraction (V_i) for a given sample will depend on the spore-forming species, sporulation conditions, and exposure to environmental conditions prior to deposition. However, given a large enough population sampled per experiment, we contend that the average V_i will not vary with ice core depth, thus enabling the viability decay experiment. Another assumption in the interpretation of putative viability decay data in terms of endospore longevity is that the spores are lying dormant while embedded in the ice core. While this assumption is generally well accepted, we note that bacteria have been found to be metabolically active in Arctic Sea ices down to -20 °C[81,82] found no evidence of a minimum metabolic threshold and estimated 10 cellular carbon turnovers per billion years at -40°C. Rejuvenation of endospore populations through germination, repair, and sporulation cycles on the time scale of endospore longevity would yield viability depth data that are flat.

In microbiology, the definition of viability is often plagued with the presence of microbes existing in a viable-but-not-germinable state. This phenomenon is made more complicated when studying microbes residing in extreme environments because of the low culturability of extremophiles and the abundance of endospores. Endospores are ubiquitous in most extreme environments on Earth. Despite the broad application of culture-independent techniques for the analysis of endospores in a wide range of these extreme habitats, little information is available on their viability because of 3 major problems: (1) endospores exhibited very low or null metabolism, making metabolic and microcalorimetric assays impossible; (2) endospores escape from fluorescence staining because their spore coat is high unsusceptible to most types of staining without a rigorous pre-treatment process; (3) the resistant spore coat poses a challenge to extract DNA via cell lysis and therefore endospores tend to escape from molecular biology methods. Even if they are lysed, their DNA content is usually much lower than that of vegetative cells; (4) the difficulty in differentiating methods. All in all, endospore viability assignment is a very challenging task in extreme environments.

In this study, the viability of endospores inhabiting GISP2 ice cores, Lake Vida and permafrost were analyzed by a combination of experiments in terms of culturability, germinability and microscopic total cell counts. Based on our

observables in terms of culturability, germinability and total cell counts from microscopy, four different viability ratios were proposed to assess the long-debated viability dilemma in microbiology from different perspectives.

Viability ratios are defined by the following 4 equations.

$$\text{Viability ratio 1 } (V_1) = \frac{\text{Germinating spore equivalents measured by spectroEVA}}{\text{Total spore equivalents measured by spectroEVA}}$$

$$\text{Viability ratio 2 } (V_2) = \frac{\text{Germinating spore units measured by } \mu\text{EVA}}{\text{Phase bright bodies measured by phase contrast microscopy}}$$

$$\text{Viability ratio 3 } (V_3) = \frac{\text{Cell bodies stained by SYTO} - 9 \text{ (live stain) measured by flow cytometry and fluorescence microscopy}}{\text{Cell bodies stained by SYTO} - 9 + \text{Cell bodies stained by PI (dead stain) measured by flow cytometry and microscopy}}$$

$$\text{Viability ratio 4 } (V_4) = \frac{\text{Colony forming units measured by spread plating}}{\text{Cell bodies stained by DAPI measured by fluorescence microscopy}}$$

Figure 8.16 shows the fits to the viability curves with the following 4 equations. Viability ratio 1 is fitted by a logarithmic plot with $R^2 = 0.7643$. Viability ratio 2 is fitted by an exponential plot with $R^2 = 0.9774$. Viability ratio 3 is fitted by a logistic / sigmoidal plot with $R^2 = 0.9954$. Viability ratio 4 is fitted by an exponential plot with $R^2 = 0.9997$. The data are shown in Table 8.3.

$$V_1 = 0.71 - 0.25\log(t)$$

$$V_2 = 4.77e^{-1.01\times10^{-4}\cdot t}$$

$$V_3 = \frac{1}{1 - e^t} 4.77e^{-0.10t}$$

$$V_4 = 400e^{-3.24\times10^{-7}\cdot t}$$

Viability ratio 1 utilizes spectroEVA to characterize the total number of endospores *via* autoclave and number of germinable endospores *via* induced germination using a Tb-DPA luminescence assay. The amount of DPA measured was correlated to the number of endospores by a standard calibration curve, similar to the method described by Shafaat & Ponce with slight modifications[46]. We have observed a correlation between total DPA content and spore size given the same sporulation condition. In addition, spore size was found to be affected by the origin and species of endospores. Therefore, instead of using laboratory-grown mesophilic *B. atrophaeus* endospores, we have adopted *B. longisporus* as the model microorganism to establish the reference standard curve. *B. longisporus* was a psychrophilic microorganism and contained a DPA content similar to psychrophilic endospores isolated from Lake Vida. *B. longisporus* endospores were expected to bear more resemblance to the endospores embedded in GISP2 ice cores and help us obtain a more accurate result.

Viability ratio 2 determined endospore viability by direct enumeration under two types of microscopies. The viable portion was determined by enumerating germinable endospores using μEVA. The total number of endospores was

enumerated by counting phase-bright bodies under phase contrast microscopy. While performing phase contrast microscopy on environmental samples was often plagued with phase-bright cell-like lipid inclusions and particulate matters, the ice core extract was relatively clear to enable accurate assignment of endospores. Viability ratio 2 could be fitted with an exponential decaying curve with a high coefficient of determination, suggesting a gradual loss of endospore viability with increase in age.

The reported ageing phenomenon of endospores had a direct effect on viability and germination propensity[83-85]. When stored at low temperature for extended periods of time in the laboratory, endospores demonstrated a decrease in viability and an increase in germination propensity, which was analogous to our decaying fits observed in viability ratios 1 and 2. It was hypothesized that windborne endospores deposited on the ice cores were encased into sedimentary layers and stored in a dormant state. Endospores found in the environment usually exhibit a more inert response to germination induction. Our observation was on the contrary because native ice core endospores had germination rates comparable to those of laboratory endospores, suggesting an enhanced propensity to germinate.

Viability ratio 3 switched gear to study the viability of vegetative cells by examining the integrity of the cell membrane. The Live/Dead *BacLight* bacterial

viability was used. It consists of the green SYTO-9 and red PI. SYTO 9 stained both live and dead vegetative bacteria but PI only penetrated bacteria with damaged membranes. Therefore healthy and live vegetative cells were stained green and dead cells were stained red. The proportion of green and red stained cell bodies was quantified by a combination of flow cytometry and epifluorescence microscopy. Endospores were precluded from measurement because of their unstainable cell coat. Except for a ~50% viability ratio at 295 m depth, the rest of the samples elicited a sigmoidal fit, with higher viability towards deeper depths. While it might sound counterintuitive, we postulated that the membrane-compromised cells were susceptible to remain intact physiologically at times of analysis. The cellular materials disintegrated and the cell ceased to exist in the form of an intact body during the course of preservation or during the melting, filtration and staining processes. And the rate of membrane susceptibility was positively corrected to depths. At lower depths, fewer “dead” cells remained intact enough to be stained and therefore the ratio of live to dead vegetative cells increased with increasing age. To avoid underestimation of ultra small cells (i.e., < 1 μm), we have also enumerated the samples using a 100× objective under epifluorescence to compare with the flow cytometry results. No significant differences were observed in the measurement of viability ratio.

Viability ratio 4 addressed the VBNC phenomenon in ice cores by looking at the colony-forming units normalized by the total cell counts by DAPI staining. Apart from a culturability ratio of 10^{-4} at the shallow depth at 295m, all the other depths recorded ratios approximately equal to 10^{-6}. That meant about 1 out of 1 million cells could be recovered on agar plate. This low culturable ratio was consistent with cultivation studies in other extreme environments on Earth. The replication pathway was damaged over hundreds of thousands of years.

These are preliminary results based on analysis on ice cores from 10,000 to 110,000 years of age. More data will be collected on ice cores from different depths to test our hypothesis. Bacterial endospore is among one of the most interesting extremophiles due to its resistance, ubiquity and longevity. And GISP2 ice core offers a sedimentary time capsule in which ancient genetic materials; endospores and biological remnants of the past can be retrieved. A thorough μEVA study of the viability of endospores at each depth will give us with a unique window to understand analogous extreme environments in other celestial bodies, such as Martian permafrost, ice on the Jovian moon Europa, lunar ice and other frozen planetary bodies, and evaluate the possibility of interplanetary microbial transfer *via impact ejecta*[86] by determining the maximum period of time of that dormant endospores can retain viability.

8.5.4 Our results in the context of literature reports

Our results fall within the range of reported microbial abundance values in glacial ice meltwater, 10^0 to 10^4 viable microbes per milliliter of ice core meltwater[4,6,9,87-91]. Miteva and colleagues found spore formers among the isolates acquired from GISP2 3,043 m, a visibly silty layer, which had a total microbial concentration of 1 to 9 × 10^7 cells/mL[36-38]. However, they note that spore formers were not dominant in their culture collection. Spore-forming bacteria have also been isolated from 750,000 year old Guliya ice[35] and from a Malan Glacier ice core (0-102m)[39,40]. While spore formers have been previously isolated from deep ice cores, no studies have been previously undertaken to determine the abundance of the endospores themselves in these systems. Our DAPI stained fluorescence enumeration in correlation with spectroEVA data suggest that endospores are ~10% of the total bacterial population in this GISP2 sample. This is the first study that assesses the ratio of spore formers to the total bacteria population in any ice core sample.

The age of ice cores from Vostok Station increases with increasing depth with 2,750 m, corresponding to an age of ~240,000 years. The microorganism distribution as a function of depth (1,500 to 2,750 m) was examined for both viable and total number of cells using radioactive carbon consumption and direct microscopic enumeration, respectively[92]. This data corroborated their earlier finding

that viability, as assessed by cfu mL^{-1}, decreased with increasing depth from 0 to 2,400 m. It was also noted that in all layers below 500 m only spore forming bacteria were able to form colonies[2]. Overall the authors showed a decreasing probability of finding viable microorganisms with increasing depth. A unique attribute of the spectroEVA measurement is that both the viable and total endospore concentrations can be measured. This enables us to calculate the viable fraction of endospores within a given sample. Considering that the total concentrations of microorganisms vary over several orders of magnitude, the viable fraction is the relevant measurement to glean viability decays from ice cores.

8.5.5 Insights from Lake Vida analysis

Lake Vida presents a greater than GISP2 ice cores in determining the concentration of DPA using Spectro-EVA because of background interference and the quenching of fluorescence. So, prior to spectro-EVA analysis, a DPA extraction protocol based on ethyl acetate phase separation has been performed. Using this method, the dual-peak spectral characteristics of DPA can be observed in the excitation spectrum with an improved Euclidean cosine squared correlation coefficient from 0.45 to 0.84. This is the first application of Tb-DPA luminescence assay on the analysis of Lake Vida brine water. We have isolated a spore-forming isolate from Lake Vida which

contained 2 endospores per sporulating mother cell, which hinted at other evolutionary roles of endospores. Endospores considered as only a stage in the life cycle for the microorganisms to survive through unfavorable environments. The cell would have died if it did not undergo sporulation without a role in reproduction. Endospore formation has long been suggested to be an autogamic process. During sporulation, a diploid phase was observed in our isolate and it might confer a genetic advantage upon the microorganism, representing a primitive form of recombination and segregation. Producing a large number of offspring in times of unfavorable conditions is not an evolutionarily competitive strategy. But it would be advantageous to the spore-forming bacteria if genetic differences are observed in the two spores. Further studies on this species will glean us useful information on the reproduction mechanism of endospores.

8.5.6 Insights from permafrost analysis

Plate count is the only method to assess bacterial endospore viability in routine microbiological analysis. Although culturing is an easy way to verify the multiplicative growth capacity of endospores, colony formation requires several hours, and its efficiency is highly debatable due to the VBNC state. In this study, we aim to complement traditional culturing with a variety of culture-independent

methods to evaluate viability of endospores as well as other psychrophilic and halophilic microorganisms entombed in the permafrost matrix.

The conventional heat-shock temperature 80°C was shown to be too high to screen for endospores. In this experiment, all endospores were inactivated at 80°C as all cultivation, μEVA, CTC staining, and ATP assay were reported negative. We have chosen a lower temperature 60°C to kill off vegetative cells and screen for endospores. In the CTC respiratory experiment, we have observed a gradual staining of red cells over time. The surviving endospores were undergoing respiration, which reduced CTC via electron transport activity for form a fluorescent and insoluble CTC-formazan. It accumulates intracellularly and reflected transition of the shape of the cells. In the first 24 hours of incubation, the stained cells all shared an endospore-like morphology – oval and small. As time progressed, the stained cells grew in size and transitioned from oval to filamentous and rod shaped, resembling vegetative cells. After 7 days of incubation, a huge increase in the cell number was observed, which was consistent with the corresponding increase in ATP level measured separately. Dormant endospores were not stainable by fluorescent dyes, but after addition of combinations of L-alanine and TSB, endospores quickly became stainable by fluorescent markers and DNA-binding dyes. This indicated

activation of lytic enzymes and an increase in permeability of the spore membranes, both of which are events in the process of spore germination.

We conclude the application of a suite of comprehensive endospore detection methodologies in permafrost. The mechanisms that preserve endospore viability at subzero temperature, and in highly halophilic permafrost with water phase near zero on Earth probably also extend to environments beyond the planet Earth, such as the frozen subsurface environments that may house past or extinct life in Mars and Europa[43,44,93]. Recent data from the Mars Global Surveyor mission suggest the possibility of permafrost or perhaps liquid water under the Martian surface[13]. The results in this study shed light for the development of future exobiological life-detection technologies.

8.6. Conclusion

Both spectro- and μEVA methods are sensitive enough to determine the trace endospore concentrations capable of germination in Greenland GISP2 ice cores. In addition, spectroEVA was used to determine the viable fraction (i.e., the fraction of endospores capable of germination under experimental conditions) by quantifying both germination-capable and total endospore concentrations. Since spectro- and μEVA assays require germination for detection, these assays can be

completed on the timescale of minutes for μEVA and hours for spectroEVA experiments. This is in marked contrast to the months of incubation required for colony formation. We have also described the application of a combination of culture-based and culture-independent assays on endospores in extreme cold biospheres on Earth, including GISP2 (Green Ice Sheet Project 2) ice cores, Antarctic underground frozen brine Lake Vida, and polar permafrost. Apart from the Tb-DPA luminescence assays, a lot of other methods such as metabolic dyes, bioluminescence and flow cytometry are explored to determine viability of the resident microbes. 4 different viability ratios have been obtained independently based on different measurables in terms of culturability, germinability and total microscopy counts to characterize the microbial abundance and viability in each of these cold habitats. In particular, a transect of 12 depths extending from 295 to 110,000 years old have been analyzed to shed light on the longevity of the most resistant life form, i.e., endospores, in the best storage repository on Earth.

The proof-of-principle experiments reported here will enable us to measure endospore viability decays in ice cores. Strong experimental evidence of endospore longevity greater than 10^5 or 10^6 years would be a milestone in microbiology. A precedent that life can be stored in a viable form on a geological timescale would have profound implications in astrobiology. In particular, extreme longevity of

endospores would imply that microbial life on an early warm and wet Mars might remain dormant, but viable, in subterranean ice to this day.

8.7 References

1. Cavicchioli, R. Cold-adapted archaea. *Nature Reviews Microbiology* **4**, 331-343 (2006).
2. Abyzov, S.S., in *Antarctic Microbiology*, edited by EI Friedmann (Wiley-Liss, Inc., New York, NY, 1993), pp. 265-295.
3. Castello, J.D. *et al*. Detection of tomato mosaic tobamovirus RNA in ancient glacial ice. *Polar Biology* **22**, 207-212 (1999).
4. Catranis, C. and Starmer, W.T. Microorganisms entrapped in glacial ice. *Antarctic Journal of the United States* **26**, 234-236 (1991).
5. Christner, B.C., Mosley-Thompson, E., Thompson, L.G., and Reeve, J.N. Isolation of bacteria and 16S rDNAs from Lake Vostok accretion ice. *Environmental Microbiology* **3**, 570-577 (2001).
6. Christner, B.C. Recovery and identification of viable bacteria immured in glacial ice. *Icarus* **144**, 479-485 (2000).
7. Dmitriev, V.V. *et al*. Yeasts in late Pleistocene-early Pleistocene Siberian permafrost. *Cryosphere of the Earth* **1**, 67-70 (1997).
8. Karl, D.M. *et al*. Microorganisms in the accreted ice of Lake Vostok, Antarctica. *Science* **286**, 2144-2147 (1999).
9. Ma, L.J., Rogers, S.O., Catranis, C.M., and Starmer, W.T. Detection and characterization of ancient fungi entrapped in glacial ice. *Mycologia* **92**, 286-295 (2000).
10. Priscu, J.C. *et al*. Geomicrobiology of subglacial ice above Lake Vostok, Antarctica. *Science* **286**, 2141-2144 (1999).
11. Vincent, W.F., Rae, R., Laurion, I., Howard-Williams, C., and Priscu, J.C. Transparency of Antarctic ice-covered lakes to solar UV radiation. *Limnology And Oceanography* **43**, 618-624 (1998).
12. Thomas, D.N. and Dieckmann, G.S. Antarctic sea ice - a habitat for extremophiles. *Science* **295**, 641 (2002).
13. Malin, M.C. and Edgett, K.S. Evidence for recent groundwater seepage and surface runoff on Mars. *Science* **288**, 2330-2335 (2000).
14. Steven, B., Léveillé, R., Pollard, W.H., and Whyte, L.G. Microbial ecology and biodiversity in permafrost. *Extremophiles* **10**, 259-267 (2006).
15. Link, L.S., Jakosky, B.M., and Thyne, G.D. Biological potential of low-temperature aqueous environments on Mars. *International Journal of Astrobiology* **4**, 155-164 (2005).
16. Schulze-Makuch, D. *et al*. Scenarios for the evolution of life on Mars. *Journal of Geophysical Research-Planets* **110** (2005).
17. Jakosky, B.M., Nealson, K.H., Bakermans, C., Ley, R.E., and Mellon, M.T. Subfreezing activity of microorganisms and the potential habitability of Mars' polar regions. *Astrobiology* **3**, 343-350 (2003).
18. Onyenwoke, R.U., Brill, J.A., Farahi, K., and Wiegel, J. Sporulation genes in members of the low G+C Gram-type-positive phylogenetic branch (Firmicutes). *Arch. Microbiol.* **182**, 182-192 (2004).

19. Nicholson, W.L., Munakata, N., Horneck, G., Melosh, H.J., and Setlow, P. Resistance of Bacillus endospores to extreme terrestrial and extraterrestrial environments. *Microbiol. Mol. Biol. Rev.* **64**, 548-572 (2000).
20. Keynan, A., Evenchik, Z., Gould, G.W., and Hurst, A. The Bacterial Spore. *Vol* **2**, 1?8 (1983).
21. Horneck, G., Bucker, H., and Reitz, G. Long-term survival of bacterial spores in space. *Adv. Space Res.* **14 (10)**, 41-45 (1994).
22. Hoch, J.A. and Losick, R. Panspermia, Spores and the *Bacillus subtilis* genome. *Nature* **390**, 237-238 (1997).
23. Kennedy, M.J., Reader, S.L., and Swierczynski, L.M. Preservation records of microorganisms - evidence of the tenacity of life. *Microbiol-UK* **140**, 2513-2529 (1994).
24. Parsons, P. Dusting off panspermia. *Nature* **383**, 221-222 (1996).
25. Horneck, G. The microbial world and the case for Mars. *Planet. Space. Sci.* **48**, 1053-1063 (2000).
26. Abyzov, S.S. *et al*. Antarctic ice sheet as an object for methodological problems of exobiology. *Adv. Space Res.* **23**, 371-376 (1999).
27. Gest, H., Mandelstam, J. Longevity of microorganisms in natural environments. *Microbiol. Sci.* **4**, 69-71 (1987).
28. Potts, M. Desiccation Tolerance of Prokaryotes. *Microbiol. Rev.* **58**, 755-805 (1994).
29. Sneath, P.H. Longevity of micro-organisms. *Nature* **195**, 643-646 (1962).
30. Cano, R.J. and Borucki, M.K. Revival and Identification of Bacterial-Spores in 25-Million- Year-Old to 40-Million-Year-Old Dominican Amber. *Science* **268**, 1060-1064 (1995).
31. Vreeland, R.H., Rosenzweig, W.D., and Powers, D.W. Isolation of a 250 million-year-old halotolerant bacterium from a primary salt crystal. *Nature* **407**, 897-900 (2000).
32. Willerslev, E., Hansen, A.J., and Poinar, H.N. Isolation of nucleic acids and cultures from fossil ice and permafrost. *Trends Ecol. Evol.* **19**, 141-147 (2004).
33. Lozina-Lozinski, L., (Nauka, Leningrad, 1972), pp. 288.
34. Llano, G., presented at the Proceeding of the Colloquium on Conservation Problems in Antarctica, Lawrence, Kansas, 1972 (unpublished).
35. Christner, B.C., Mosley-Thompson, E., Thompson, L.G., and Reeve, J.N. Bacterial recovery from ancient glacial ice. *Environ. Microbiol.* **5**, 433-436 (2003).
36. Miteva, V.I. and Brenchley, J.E. Detection and isolation of ultrasmall microorganisms from a 120,000-year-old Greenland glacier ice core. *Appl. Environ. Microbiol.* **71**, 7806-7818 (2005).
37. Miteva, V.I., Sheridan, P.P., and Brenchley, J.E. Phylogenetic and physiological diversity of microorganisms isolated from a deep Greenland glacier ice core. *Appl. Environ. Microbiol.* **70**, 202-213 (2004).
38. Sheridan, P.P., Miteva, V.I., and Brenchley, J.E. Phylogenetic analysis of anaerobic psychrophilic enrichment cultures obtained from a Greenland glacier ice core. *Appl. Environ. Microbiol.* **69**, 2153-2160 (2003).
39. Zhang, X.J., Yao, T.D., Ma, X.J., and Wang, N.L. Microorganisms in a high altitude glacier ice in Tibet. *Folia Microbiol.* **47**, 241-245 (2002).
40. Zhang, X.J., Yao, T.D., Ma, X.J., and Wang, N.L. Analysis of the characteristics of microorganisms packed in the ice core of Malan glacier, Tibet, China. *Sci. China Ser. D.* **44**, 369-374 (2001).
41. Friedmann, E.I., in *Viable Microorganisms in Permafrost*, edited by D. A. Gilichinsky (Russian Academy of Science, Pushchino, Russia, 1994), pp. 21-26.
42. Morita, R.Y., *Bacteria in Oligotrophic Environments: Starvation-Survival Lifestyle*. (Chapman & Hall, New York, 1997).
43. Gilichinsky, D. *et al*. Biodiversity of cryopegs in permafrost. *FEMS Microbiology Ecology* **53**, 117-128 (2005).

44. Rivkina, E. *et al*. Microbial life in permafrost. *Advances in Space Research* **33**, 1215-1221 (2004).
45. Yung, P.T., Kempf, M.J., and Ponce, A., presented at the IEEE Aerospace Conference, Big Sky, Montana, 2006 (unpublished).
46. Shafaat, H.S. and Ponce, A. Applications of a rapid endospore viability assay for monitoring UV inactivation and characterizing Arctic ice cores. *Applied and Environmental Microbiology* **72**, 6808-6814 (2006).
47. Gould, G.W. and Hurst, A., *The Bacterial Spore*. (Academic Press, New York, 1969).
48. Hills, G.M. Chemical Factors In The Germination Of Spore-Bearing Aerobes - The Effect Of Yeast Extract On The Germination Of Bacillus-Anthracis And Its Replacement By Adenosine. *Biochem. J.* **45**, 353-362 (1949).
49. Hills, G.M. Chemical Factors In The Germination Of Spore-Bearing Aerobes - The Effects Of Amino-Acids On The Germination Of Bacillus-Anthracis, With Some Observations On The Relation Of Optical Form To Biological Activity. *Biochem. J.* **45**, 363-370 (1949).
50. Hills, G.M. Chemical Factors In The Germination Of Spore-Bearing Aerobes - Observations On The Influence Of Species, Strain And Conditions Of Growth. *J. Gen. Microbiol.* **4**, 38-47 (1950).
51. Setlow, P. Spore germination. *Curr. Opin. Microbiol.* **6**, 550-556 (2003).
52. Sacks, L.E. Chemical germination of native and cation-exchanged bacterial-spores with trifluoperazine. *Appl. Environ. Microbiol.* **56**, 1185-1187 (1990).
53. Woese, C. and Morowitz, H.J. Kinetics of the release of dipicolinic acid from spores of Bacillus subtilis. *J. Bacteriol.* **76**, 81-83 (1958).
54. Hurwitz, S.J. and McCarthy, T.J. 2, 3, 5-Triphenyltetrazolium chloride as a novel tool in germicide dynamics. *Journal of Pharmaceutical Sciences* **75**, 912-916 (1986).
55. Rogers, S.O. *et al*. Comparisons of protocols for decontamination of environmental ice samples for biological and molecular examinations. *Appl. Environ. Microbiol.* **70**, 2540-2544 (2004).
56. Christner, B.C., Mikucki, J.A., Foreman, C.M., Denson, J., and Priscu, J.C. Glacial ice cores: A model system for developing extraterrestrial decontamination protocols. *Icarus* **174**, 572-584 (2005).
57. Juck, D.F. *et al*. Utilization of fluorescent microspheres and a green fluorescent protein-marked strain for assessment of microbiological contamination of permafrost and ground ice core samples from the Canadian High Arctic. *Applied and Environmental Microbiology* **71**, 1035 (2005).
58. Smith, H.D. and McKay, C.P. Drilling in ancient permafrost on Mars for evidence of a second genesis of life. *Planetary and Space Science* **53**, 1302-1308 (2005).
59. Ferrara-Guerrero, M.J., Marty, D.G., and Bianchi, A., in *Handbook of Methods in Aquatic Microbial Ecology*, edited by P. Kemp (Lewis Publishers, Boca Raton, FL, 1993), pp. 9-19.
60. Knowles, R. and Barraquio, W.L., in *Methods of Soil Analysis, Part 2. Microbiological and Biochemical Properties* (Madison, WI, 1994), pp. 179-197.
61. Epstein, S.S. and Rossel, J. Enumeration of sandy sediment bacteria: Search for optimal protocol. *Marine Ecology Progress Series. Oldendorf* **117**, 289-298 (1995).
62. Turley, C.M., in *Handbook of Methods in Aquatic Microbial Ecology* edited by P.F. Kemp, Sherr, B.F., Sherr, E.B. and Cole, J.J. (Lewis Publishers, Boca Raton, 1993), pp. 143-147.
63. Li, J., Hibbert, D.B., Fuller, S., and Vaughn, G. A comparative study of point-to-point algorithms for matching spectra. *Chemometrics and Intelligent Laboratory Systems* **82**, 50-58 (2006).
64. Hashimoto, T., Frieben, W.R., and Conti, S.F. Microgermination of *Bacillus cereus* spores. *J. Bacteriol.* **100**, 1385-1392 (1969).
65. Hashimoto, T., Frieben, W.R., and Conti, S.F. Germination of single bacterial spores. *J. Bacteriol.* **98**, 1011-1020 (1969).

66. Vary, J.C. and Halvorson, H.O. Kinetics of germination of *Bacillus* spores. *J. Bacteriol.* **89**, 1340-1347 (1965).
67. Sheridan, P.P. Phylogenetic analysis of anaerobic psychrophilic enrichment cultures obtained from a Greenland glacier ice core. *Applied and environmental microbiology* **69**, 2153 (2003).
68. Yung, P.T., Shafaat, H.S., Connon, S.A., and Ponce, A. Quantification of viable endospores from a Greenland ice core. *FEMS Microbiology Ecology* **59**, 300-306 (2007).
69. Warth, A.D. Liquid chromatographic determination of dipicolinic acid from bacterial spores. *Applied and Environmental Microbiology* **38**, 1029-1033 (1979).
70. Fichtel, J., Koster, J., Rullkotter, J., and Sass, H. Spore dipicolinic acid contents used for estimating the number of endospores in sediments. *FEMS Microbiology Ecology* **61**, 522-532 (2007).
71. Gest, H., Mandelstam, J. Longevity of microorganisms in natural environments. *Microbiological Science* **4**, 69-71 (1987).
72. Nicholson, W.L., in *Bacterial Spore Formers: Probiotics and Emerging Applications*, edited by E. Ricca, A. O. Henriques, and S. M. Cutting (Horizon Scientific, Norfolk, UK, 2004), pp. 1-15.
73. Parkes, R.J. and Wellsbury, P., in *Microbial Diversity and Bioprospecting*, edited by A. T. Bull (ASM Press, 2004), Vol. 1000, pp. 67.
74. Parkes, R.J. A case of bacterial immortality? *Nature* **407**, 897-900 (2000).
75. Sussman, A.S., in *The Bacterial Spore*, edited by G. W. Gould and A. Hurst (Academic Press, London, England, 1969), Vol. 1, pp. 1-38.
76. Colwell, R.R. and Grimes, D.J. eds., *Nonculturable Microorganisms in the Environment*. (ASM Press, Washington, DC, 2000).
77. Roszak, D.B. and Colwell, R.R. Survival Strategies of Bacteria in the Natural-Environment. *Microbiol. Rev.* **51**, 365-379 (1987).
78. Amann, R.I., Ludwig, W., and Schleifer, K.H. Phylogenetic Identification and in-Situ Detection of Individual Microbial-Cells without Cultivation. *Microbiol. Rev.* **59**, 143-169 (1995).
79. Jones, J.G. Effect of Environmental-Factors on Estimated Viable and Total Populations of Planktonic Bacteria in Lakes and Experimental Enclosures. *Freshwater Biol.* **7**, 67-91 (1977).
80. Torsvik, V., Goksoyr, J., and Daae, F.L. High Diversity in DNA of Soil Bacteria. *Appl. Environ. Microbiol.* **56**, 782-787 (1990).
81. Junge, K., Eicken, H., and Deming, J.W. Bacterial activity at -2 to -20 degrees C in Arctic wintertime sea ice. *Appl. Environ. Microbiol.* **70**, 550-557 (2004).
82. Price, P.B. and Sowers, T. Temperature dependence of metabolic rates for microbial growth, maintenance, and survival. *Proc. Natl. Acad. Sci. U.S.A.* **101**, 4631-4636 (2004).
83. Powell, J.F. Factors affecting the germination of thick suspensions of *Bacillus subtilis* spores in L-alanine solution. *Journal of General Microbiology* **4**, 330-339 (1950).
84. Keynan, A. and Evenchik, Z., in *The Bacterial Spore*, edited by G. W. Gould and A. Hurst (Academic Press, London, England, 1969), Vol. 1, pp. 359-396.
85. Murty, G.G.K. and Halvorson, H.O. Effect of duration of heating, L-alanine and spore concentration on the oxidation of glucose by spores of *Bacillus cereus* var. *terminalis*. *Journal of Bacteriology* **73**, 235 (1957).
86. Mileikowsky, C. *et al*. Natural transfer of viable microbes in space 1. From Mars to Earth and Earth to Mars. *Icarus* **145**, 391-427 (2000).
87. Abyzov, S.S., Mitskevich, I.N., and Poglazova, M.N. Microflora of the deep glacier horizons of Central Antarctica. *Microbiology* **67**, 451-458 (1998).
88. Gruber, S. and Jaenicke, R. Biological microparticles in the Hans Tausen ice cap, North Greenland. *Meddelelser om Groland Geoscience* **39**, 161-163 (2001).

89. Li, W.H., Fraser, S.E., and Meade, T.J. A calcium-sensitive magnetic resonance imaging contrast agent. *Journal of the American Chemical Society* **121**, 1413-1414 (1999).
90. Sharp, M. *et al*. Widespread bacterial populations at glacier beds and their relationship to rock weathering and carbon cycling. *Geology* **27**, 107-110 (1999).
91. Skidmore, M.L., Foght, J.M., and Sharp, M.J. Microbial life beneath a high Arctic glacier. *Applied And Environmental Microbiology* **66**, 3214-3220 (2000).
92. Abyzov, S.S. *et al*. Antarctic ice sheet as a model in search of life on other planets. *Adv. Space Res.* **22**, 363-368 (1998).
93. Gilichinsky, D., Rivkina, E., Shcherbakova, V., Laurinavichuis, K., and Tiedje, J. Supercooled water brines within permafrost - An unknown ecological niche for microorganisms: A model for astrobiology. *Astrobiology* **3**, 331-341 (2003).

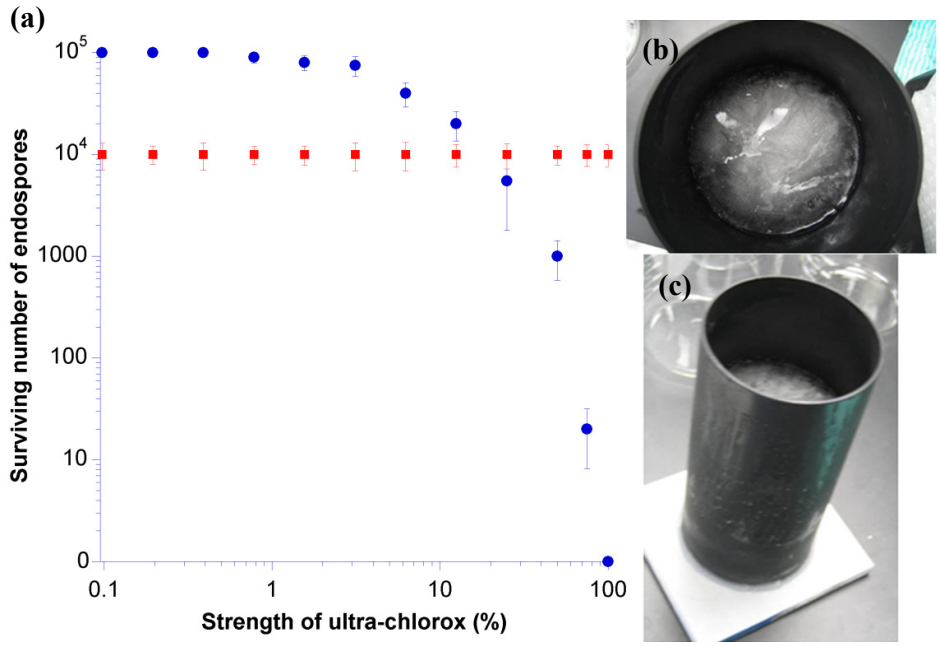

Figure 8.1 | **(a)** Validation of ice core decontamination protocol by using a fabricated ice core in **(b)** and **(c)** with 10^5 *B. atrophaeus* endospores (blue) smeared on the surface and 10^4 *B. megaterium* endospores (red) embedded and frozen with the ice. These two species were chosen due to their distinctive difference in colony morphology. When the concentration of ultra-chlorox (6.25% sodium hypochlorite) increased, a corresponding decrease in the number surface *B. atrophaeus* endospores was measured. At full strength (100%), all of the surface endospores were either removed or inactivated while the number of endospores in the ice core interior remained constant.

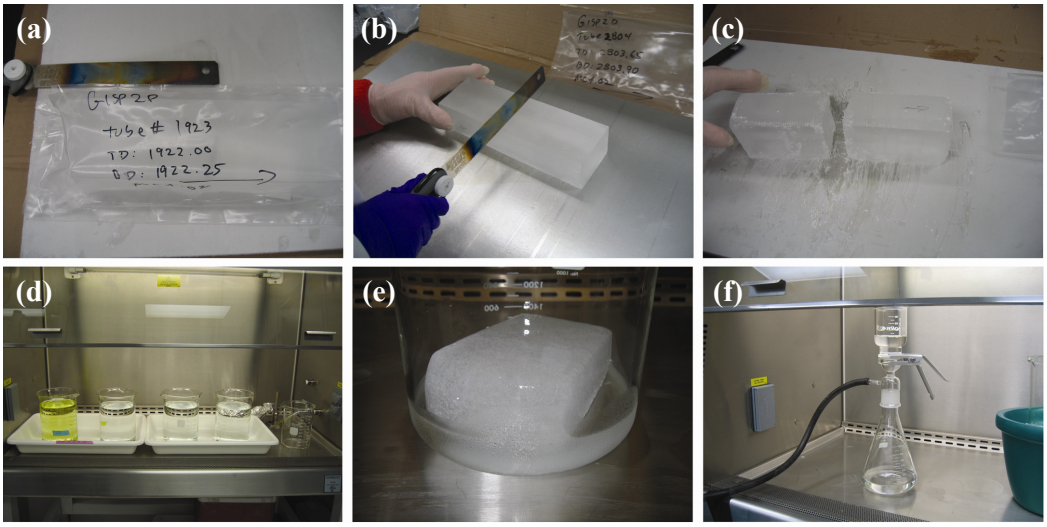

Figure 8.2 | Ice core handling procedure. Ice cores were obtained form the National Ice Core Laboratory and stored in -80°C freezer before use. **(a)** A cylinder of ice core, wrapped in sterile packaging, was placed on top of a chilled aluminum plate as a cold operating bench. **(b, c)** A heat-sterilized saw was used to cut the core into two halves for duplicate analysis. **(d)** The cut ice core was decontaminated by a 10-s dipping in full-strength ultra-chlorox, followed by 3 sequential 10-s rinses in filter-sterilized ultrapure water. **(e)** The decontaminated ice core was allowed to melt under room temperature inside a biohazard safety cabinet. **(f)** The ice core meltwater was filtered and concentrated on 0.1-µm polycarbonate membrane filter for spectroscopic and microscopic analyses.

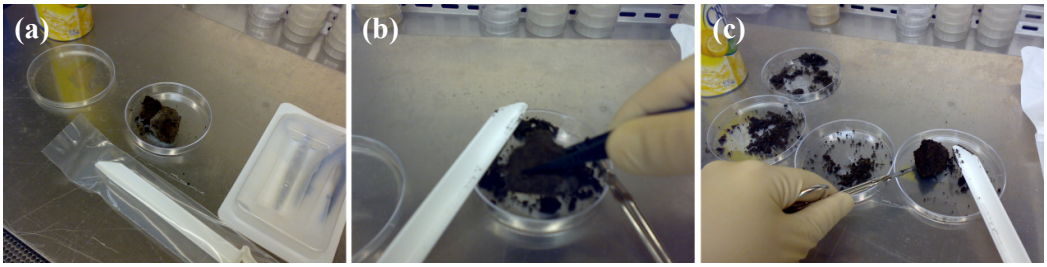

Figure 8.3 | Permafrost decontamination procedure. **(a)** All procedure was carried out in a class I biohazard safety cabinet. A cold (-20°C) aluminum plate was used as a workbench to keep sample cold. All utensils were packaged sterile and DNA-free. **(b)** The frozen sample was fractured with a sterile knife and scoop. Only the internal pristine fragments were taken by sterile forceps for analysis. **(c)** 3 layers of surface soils were scrapped off and discarded serially. The excavated sample was then weighted, extracted and analyzed subsequently.

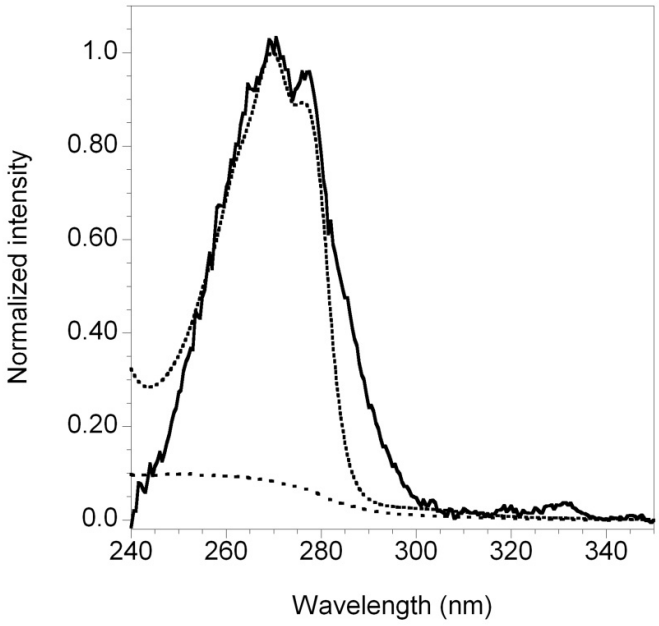

Figure 8.4 | ——— Excitation spectrum of ice core concentrate with 1 μM Tb^{3+}, monitoring emission intensity at 543 nm; ····· Excitation spectrum of 1 μM DPA with 10 μM Tb^{3+}; - - - Negative control for ice core with 1 μM Tb^{3+}.

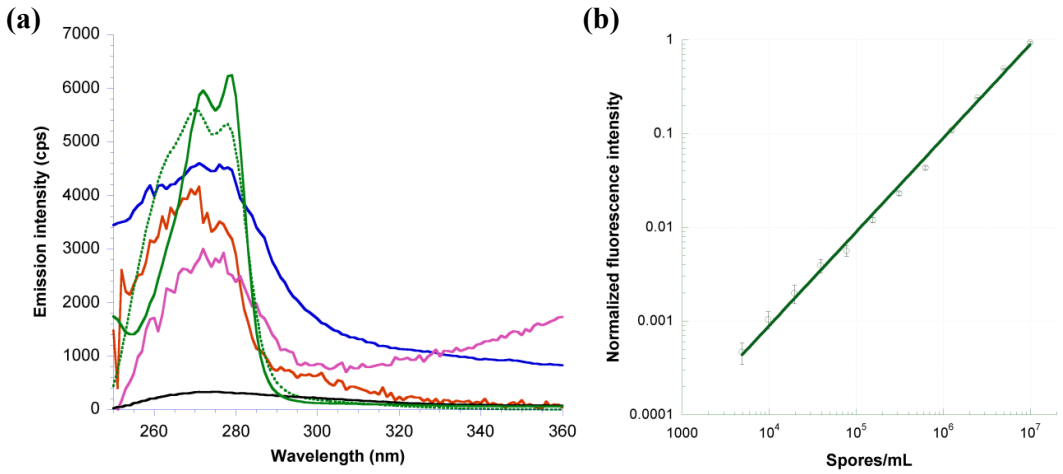

Figure 8.5 | **(a)** Excitation spectra of GISP2 ice core concentrate measured in 10 µM $TbCl_3$ following the spectro-EVA protocol, monitoring emission intensity at 544 nm. Here are the color assignments: autoclaved sample (plot in solid blue); sample induced to aerobic germination (plot in solid orange); sample induced to anaerobic germination (plot in solid pink); 1 µM DPA (plot in solid green); 100 µM DPA in filter-sterilized ice core meltwater (plot in dotted green) and the negative control brine water control (plot in black). **(b)** Calibration curve obtained by autoclaving *B. atrophaeus* in filter-sterilized ice core meltwater.

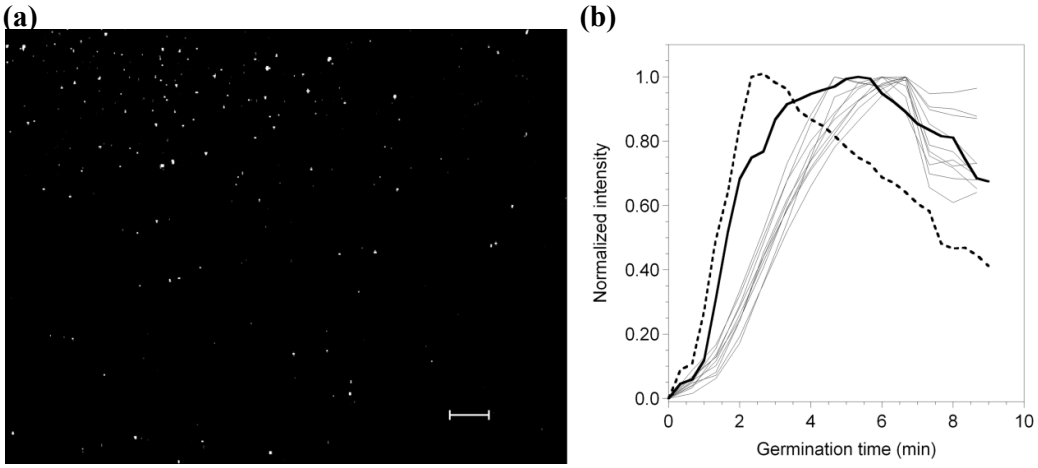

Figure 8.6 | **(a)** μEVA image showing germinated endospores in the ice core sample. It was taken after 10 minutes of germination. **(b)** Corresponding time course plots of germinating spores. 10 overlays from image of ice core sample (fine solid line); *B. atrophaeus* ATCC 9372, broken line; unidentified spore species from a surface swab of our laboratory, bold solid line.

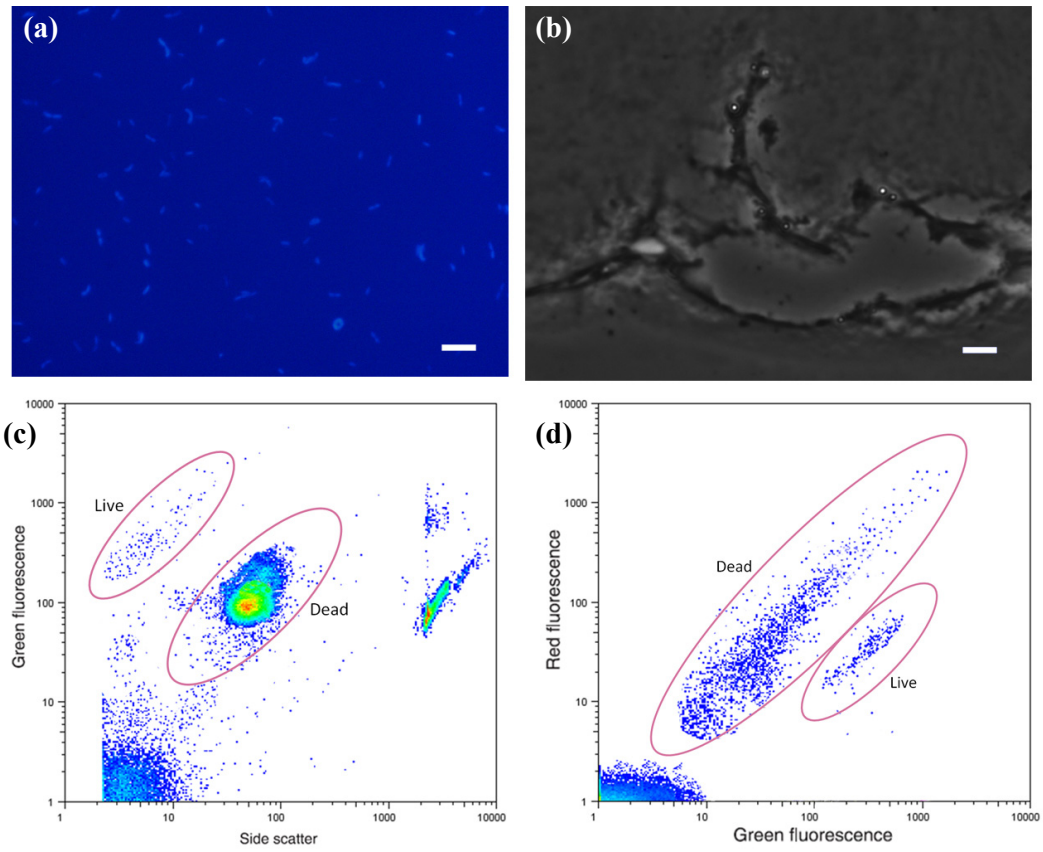

Figure 8.7 | **(a)** DAPI stain of an anaerobic enrichment culture of the GISP2 ice cores. Scale bar, 10 µm. **(b)** Phase contrast micrograph of the ice core meltwater. Endospores appear as phase bright bodies. Scale bar, 10 µm. **(c, d)** Flow cytometry of the ice core meltwater. Live cells stained by SYTO-9 appeared as green and dead cells stained by PI appeared as red, detected by different channels of the flow cytometry. 1 µm europium fluorescent beads were included (shown on the right region of **(c)**) for enumeration.

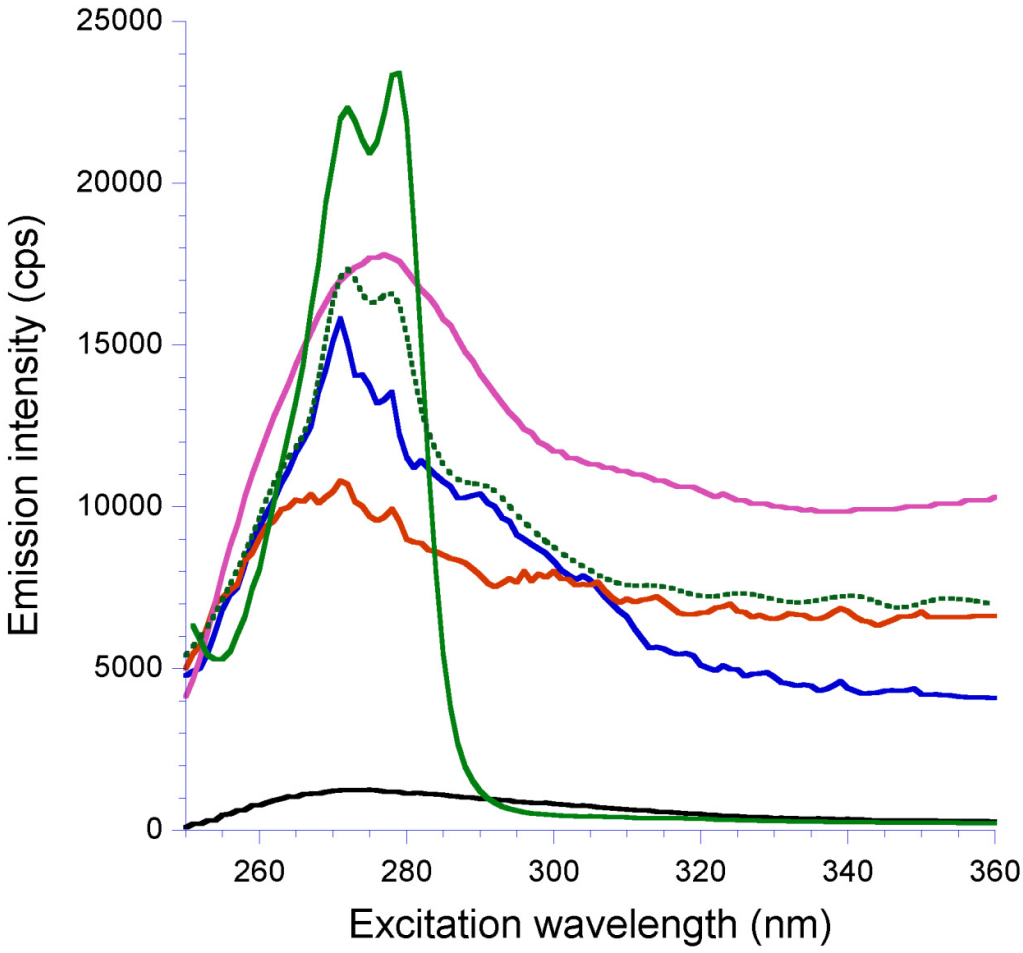

Figure 8.8 | Excitation spectra of Lake Vida concentrate measured in 10 µM $TbCl_3$ following the spectro-EVA protocol, monitoring emission intensity at 544 nm. Here are the color assignments: autoclaved sample (plot in solid blue); sample induced to aerobic germination (plot in solid orange); sample induced to anaerobic germination (plot in solid pink); 1 µM DPA (plot in solid green); 100 µM DPA in filter-sterilized Lake Vida brine water (plot in dotted green) and the negative control brine water control (plot in black).

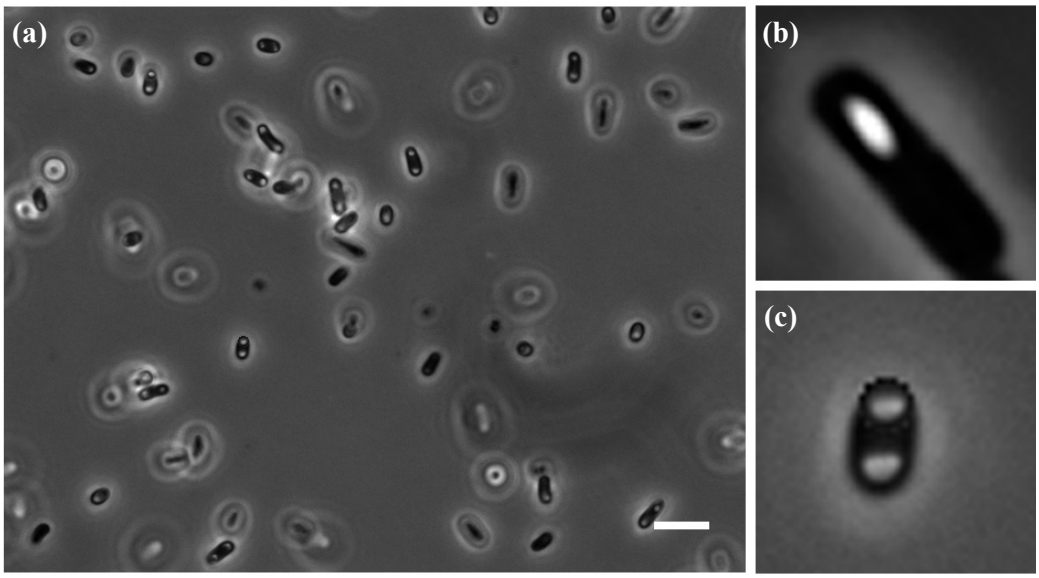

Figure 8.9 | **(a)** Phase contrast micrograph of an aerobic subculture of Lake Vida that was isolated from pH 3 minimal agar supplemented with urea and 5% NaCl. This endospore-forming bacterium elicited two endospores during sporulation. DPA has been detected from this bacterium. **(b)** A *Bacillus subtilis* 168 mother cell undergoing sporulation to produce one endospore. **(c)** Mother cell of the Lake Vida isolate undergoing sporulation, producing two endospores.

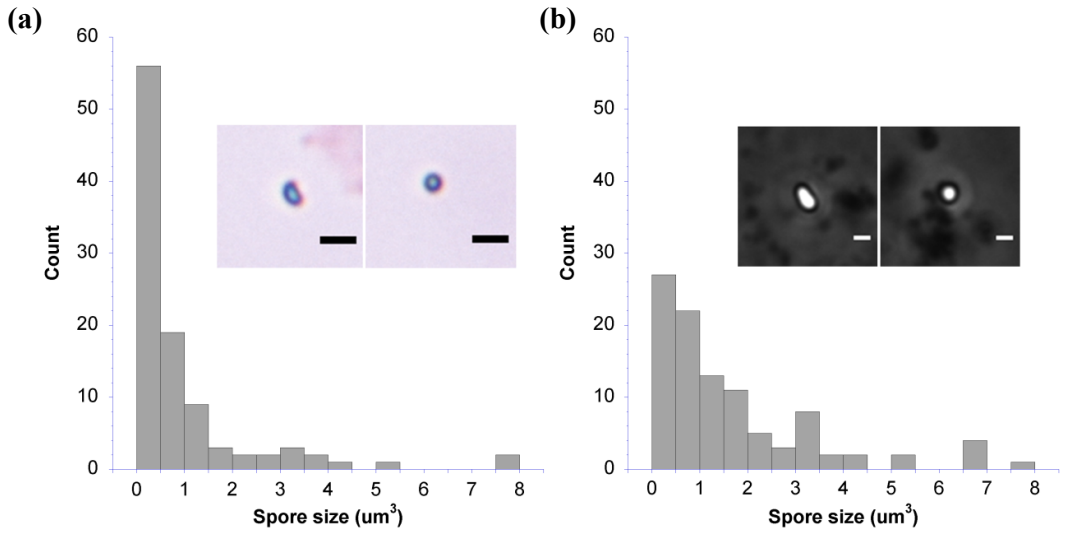

Figure 8.10 | Size distribution of 100 endospores found in the brine water of Lake Vida **(a)** using malachite green staining and **(b)** under phase contrast microscopy. The majority of the endospores are round or oval shaped. Scale bar, 1 µm. Endospore sizes are Poisson distributed. Malachite green stained endospores in general show a smaller size when they are observed under phase contrast microscopy. This size discrepancy is due to presence of phase ring, which obscures the accurate determination of size.

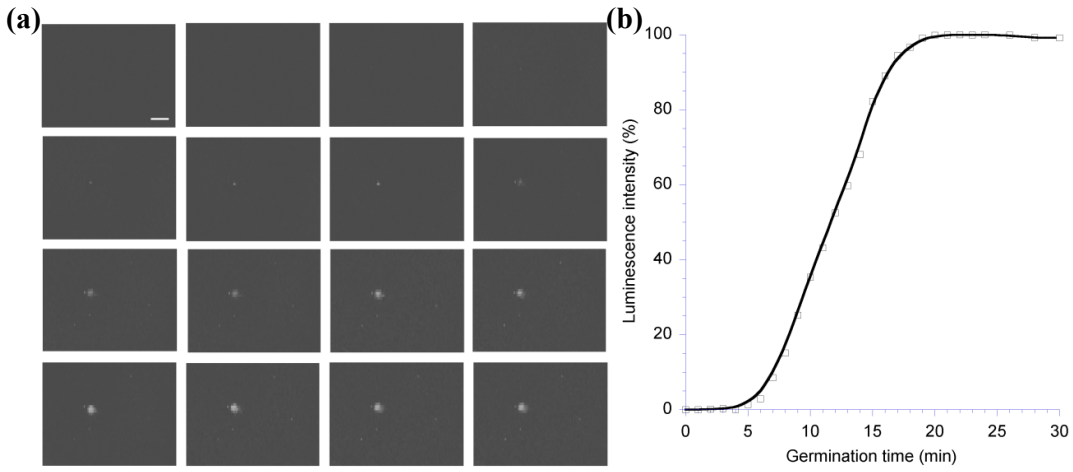

Figure 8.11 | **(a)** Germination timecourse pictures of endospores embedded in permafrost. Endospores were induced to germinate at room temperature on an agarose substrate fortified with 50 mM L-alanine and covered with a piece of PDMS. Successive pictures are separated by 90 s. Scale bar, 10 µm. **(b)** Germination timecourse represented in a scatter plot. Notice the sigmoidal shape.

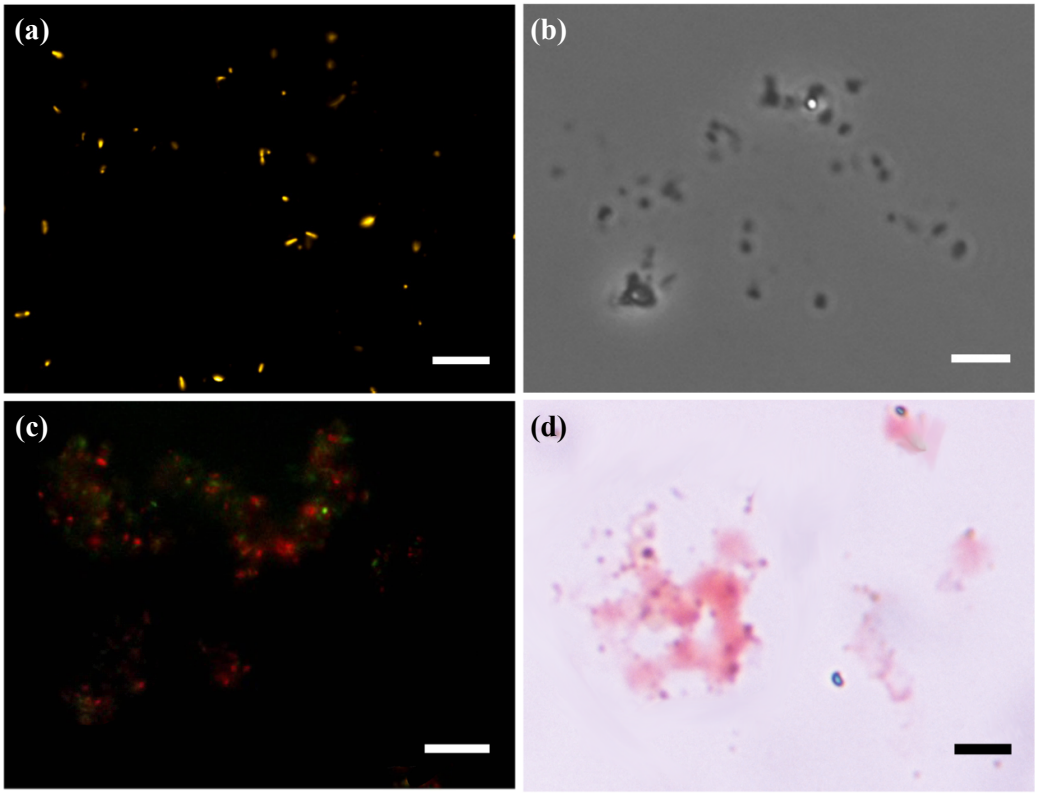

Figure 8.12 | Staining micrographs of permafrost samples. Scale bar, 10 µm. **(a)**. SYBR Gold staining epifluorescence microscopy. All cells, except endospores, were stained gold by this DNA-intercalating dye. **(b)** Phase contrast microscopy. Endospores appear as distinct phase-bright oval bodies. **(c)** Live/Dead *BacLight* viability staining. Dead cells were stained red and live cells were stained green by propidium iodide and SYTO-9, respectively. **(d)** Malachite green staining bright-field microscopy. Dead cells and cell debris were stained red while endospores were stained green.

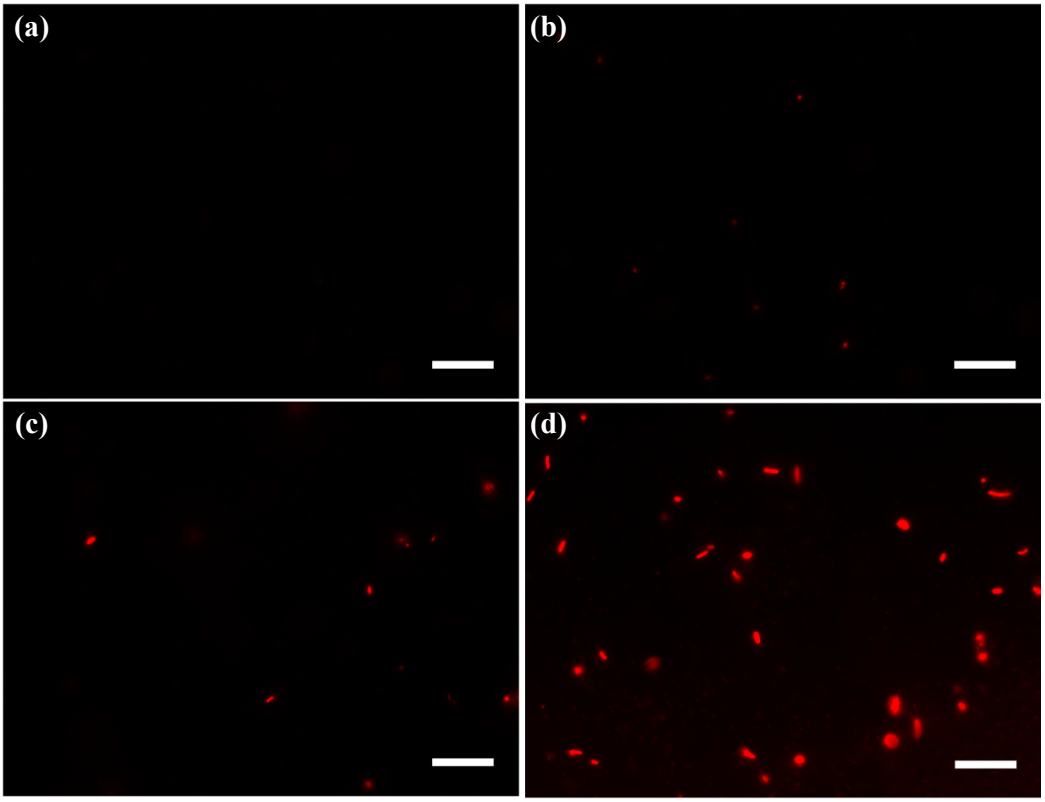

Figure 8.13 | Tetrazolium chloride staining of permafrost sample. The suspension was heat shocked at 60°C for 15 minutes to inactivate all vegetative cells, selecting for bacterial endospores. The micrographs show heat-shocked permafrost after a certain incubation time with nutrient augmentation - 1/10 TSB and 10 mM L-alanine at ambient temperature. Scale bar, 10 µm. **(a)** 0 hour of incubation; **(b)** 6 hours of incubation; **(c)** 48 hours of incubation; **(d)** 7 days of incubation.

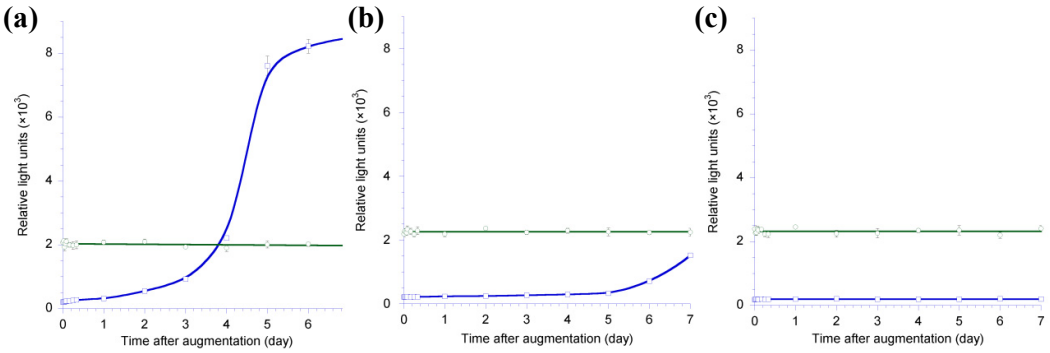

Figure 8.14 | Monitoring of ATP and DPA levels of permafrost samples over 7 days upon exposure to nutrients (1/10 TSB and 10 mM L-alanine). The blue fit represents ATP level and green fit represents DPA level. **(a)** Non-heat shock; **(b)** heat shock at 60°C for 15 minutes; **(c)** heat shock at 80°C for 15 minutes.

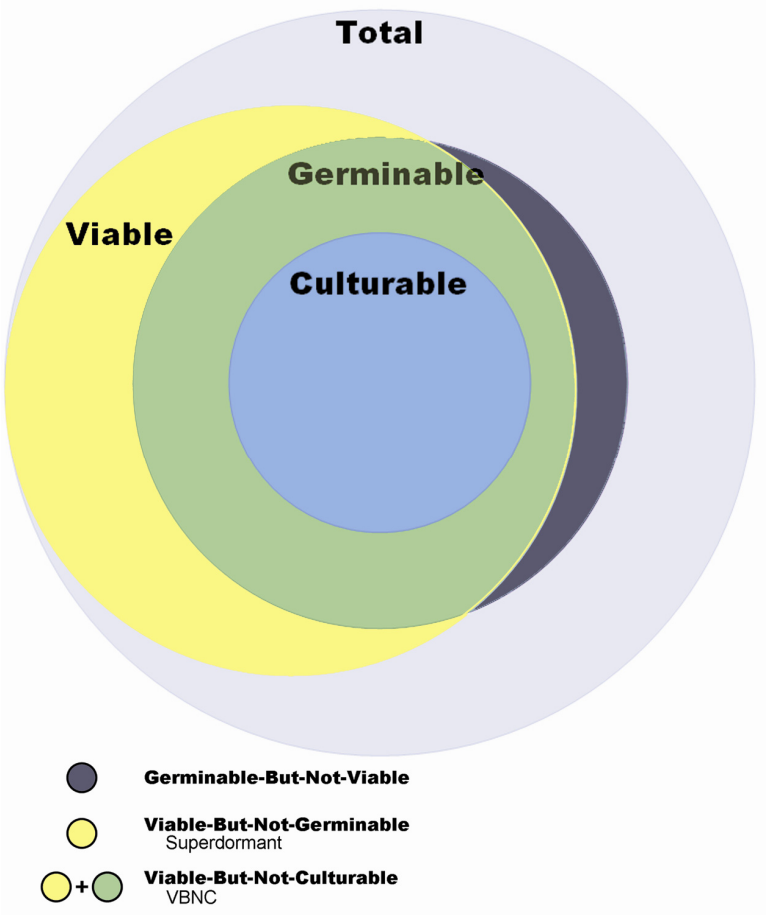

Figure 8.15 | Various endospore populations expressed in a Venn diagram. Labeled circles represent *total* endospore population (e.g., as counted with phase contrast microscopy), *germinable* endospore population (e.g., as measured by EVA, or phase transition from bright to dark), *culturable* endospore population (e.g., as CFU counted on agar growth plate) and *viable* endospore population (i.e., defined as the proportion of endospores capable of metabolic activity). The indicated overlapping regions illustrate *germinable-but-not-viable*, *viable-but-not-germinable* (i.e., superdormant), and *viable-but-not-culturable* (VBNC) endospore populations. Relative area varies with species/environment and is not quantitative.

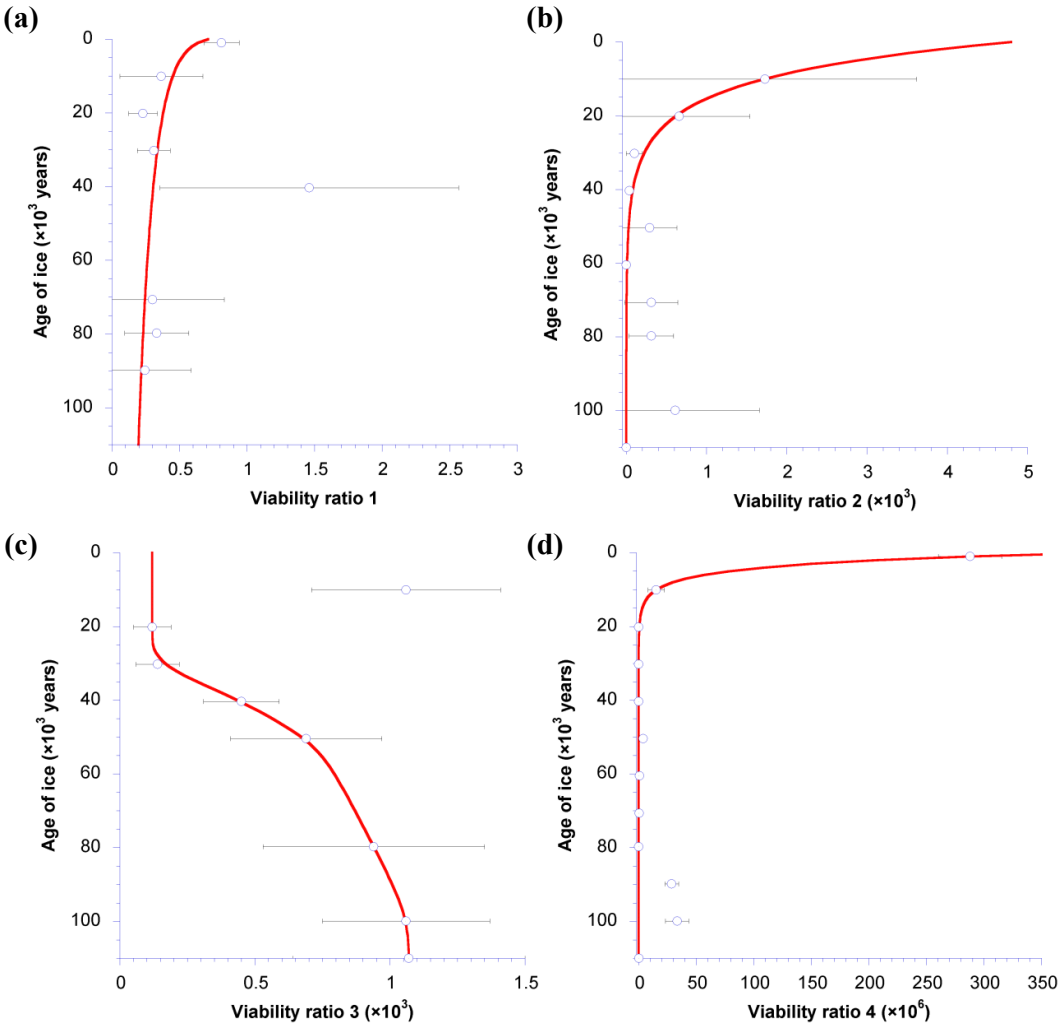

Figure 8.16 | Viability plots of the ice cores samples along a depth transect. Definitions of the 4 different viability ratios are stated previously. **(a)** Viability ratio 1 shows a logarithmic decaying trend of the proportion of germinable endospores with increasing age. One outlying data point at age 40,000 is neglected in obtaining the fit. **(b)** Viability ratio 2 shows an exponential decaying trend of the proportion of germinable endospores with increasing age. **(c)** Viability ratio 3 shows an increasing correlation of cells stained by SYTO-9 with ice age in a sigmoidal fashion. One

outlying data point at age 10,000 has been removed. **(d)** Viability ratio 4 shows an exponential decaying trend of the number of culturable bacteria with increasing age.

	Aerobic						*Anaerobic*			
	1/2 TSA		1/5 R2A		1/2 TSB		1/2 TSA		1/5 R2A	
	7°C	20°C	7°C	20°C	7°C	20°C	7°C	20°C	7°C	20°C
Non-HS	8.7×10^{2}	3.8×10^{3}	6.7×10^{1}	4.9×10^{2}	6.0×10^{2}	4.1×10^{3}	0	0	1.3×10^{2}	4.3×10^{2}
HS@60°C	0	6.7×10^{1}	0	0	0	3.2×10^{1}	0	0	0	0
HS@80°C	0	0	0	0	0	0	0	0	0	0

Table 8.1 | Summary data of permafrost analysis. **(a)** Aerobic and anaerobic cultivation results on permafrost samples subjected to different heat shock treatments. **(b)** Various staining and microscopy techniques were used to characterize viability of the sample. All the units are expressed in terms of observed cell-like bodies per gram of permafrost.

Site locations	Description of samples	Depth below surface (m)	Age ($\times 10^3$ years)	Spectro-EVA (total spores mL^{-1})	Spectro-EVA (germinable spores mL^{-1})	µEVA (germinable spores mL^{-1})	Phase contrast microscopy (spores mL^{-1})	Cultivation[ii] (cells mL^{-1})	Fluorescence microscopy (cells mL^{-1})
Greenland	Ice	93	0.295	369 ± 36	295 ± 19	27 ± 3	ND	2.00	$7.0 \times 10^3 \pm 6.7 \times 10^2$
Greenland	Ice	1566	10	59.0 ± 29.9	12.4 ±7.2	0.15 ± 0.05	85 ± 13	0.25	$2.1 \times 10^4 \pm 9.8 \times 10^3$
Greenland	Ice	1923	20	135.5 ± 25.6	28.5 ± 8.5	0.50 ± 0.19	746 ± 131	0	$1.6 \times 10^6 \pm 6.6 \times 10^5$
Greenland	Ice	2096	30	38.3 ± 16.9	37.5 ± 17.5	0.15 ± 0.04	1424 ± 332	0	$5.5 \times 10^6 \pm 2.9 \times 10^6$
Greenland	Ice	2253	40	207.0 ± 56.8	57.3 ± 7.6	0.18 ± 0.06	4490 ± 656	0	$2.8 \times 10^6 \pm 1.0 \times 10^6$
Greenland	Ice	2429	50	139.1 ± 61.1	< LOD	0.29 ± 0.10	1008 ± 176	6.50	$1.7 \times 10^6 \pm 2.8 \times 10^5$
Greenland	Ice	2517	60	42.9 ± 38.6	12.8 ±3.3	0	2520 ± 593	5.50	$8.3 \times 10^6 \pm 2.6 \times 10^6$
Greenland	Ice	2593	70	40.2 ±18.5	9.0 ± 3.4	0.08 ± 0.03	263 ± 73	0.40	$9.9 \times 10^5 \pm 2.7 \times 10^5$
Greenland	Ice	2657	80	17.7 ± 2.5	3.5 ± 5.4	0.06 ± 0.02	198 ± 35	0	$2.2 \times 10^5 \pm 7.9 \times 10^4$
Greenland	Ice	2703	90	< LOD	< LOD	0.44 ± 0.12	121 ± 37	8.50	$3.1 \times 10^5 \pm 6.5 \times 10^4$
Greenland	Ice	2746	100	< LOD	< LOD	0.15 ± 0.08	252 ± 50	1.00	$3.3 \times 10^4 \pm 1.0 \times 10^4$
Greenland	Ice	2804	110	< LOD	< LOD	0	117 ± 23	0.40	$1.5 \times 10^6 \pm 5.2 \times 10^5$
Lake Vida	Brine water	N/A	~10	4800 ± 800	1600 ± 230	0.80 ± 0.24	$1.9 \times 10^4 \pm 2.7 \times 10^3$	0.50	$3.8 \times 10^7 \pm 1.2 \times 10^7$
Lake Vida	Filter[i]	N/A	~10	< LOD	< LOD	0.60 ± 0.20	ND	0	ND
Arctic region	Permafrost	NI	NI	ND	ND	8.33 ± 3.33	$4.0 \times 10^3 \pm 1.7 \times 10^3$	100	$3.6 \times 10^6 \pm 1.3 \times 10^6$

Table 8.2 | Summary of GISP2 and Lake Vida results using culture-based and culture-independent methods. [i] Lake Vida brine water sample was pre-concentrated on 18-mm anodisc filters. [ii] Cultivable counts here refers to a lumped sum of aerobic and anaerobic non-heat shock spread plates. (< LOD = below limit of detection; ND = not determined, NI = no information)

Site locations	Description of samples	Depth below surface (m)	Age ($\times 10^3$ years)	Viability ratio 1[i]	Viability ratio 2[ii]	Viability ratio 3[iii]	Viability ratio 4[iv]
Greenland	Ice	93	0.295	81.2% ± 13.1%	ND	ND	$2.88 \times 10^{-4} \pm 2.76 \times 10^{-5}$
Greenland	Ice	1566	10	36.5% ± 30.7%	0.173% ± 0.189%	0.106% ±0.035%	$1.52 \times 10^{-5} \pm 7.10 \times 10^{-6}$
Greenland	Ice	1923	20	23.0% ± 10.6%	0.066% ± 0.088%	0.012% ±0.007%	0
Greenland	Ice	2096	30	31.0% ± 12.2%	0.010% ± 0.010%	0.014% ±0.008%	0
Greenland	Ice	2253	40	146% ± 110.6%	0.004% ± 0.004%	0.045% ± 0.014%	0
Greenland	Ice	2429	50	< LOD	0.029% ± 0.034%	0.069% ± 0.028%	$3.93 \times 10^{-6} \pm 6.47 \times 10^{-7}$
Greenland	Ice	2517	60	30.0% ± 53.2%	0	ND	$7.35 \times 10^{-7} \pm 2.30 \times 10^{-7}$
Greenland	Ice	2593	70	33.2% ± 23.8%	0.031% ± 0.033%	ND	$4.37 \times 10^{-7} \pm 1.19 \times 10^{-7}$
Greenland	Ice	2657	80	24.5% ± 34.0%	0.031% ± 0.028%	0.094% ± 0.041%	0
Greenland	Ice	2703	90	< LOD	36.3% ± 0.189%	ND	$2.87 \times 10^{-5} \pm 6.01 \times 10^{-6}$
Greenland	Ice	2746	100	< LOD	0.061% ± 0.105%	0.106% ± 0.031%	$3.34 \times 10^{-5} \pm 1.01 \times 10^{-5}$
Greenland	Ice	2804	110	< LOD	0	0.107% ± 0.043%	$3.03 \times 10^{-7} \pm 1.05 \times 10^{-7}$
Lake Vida	Brine water	N/A	~10	35.1% ± 10.6%	0.004% ± 0.002%	0.004% ±0.003%	$1.46 \times 10^{-8} \pm 4.62 \times 10^{-9}$
Lake Vida	Filter	N/A	~10	< LOD	ND	ND	ND
Arctic region	Permafrost	NI	NI	ND	0.297% ± 0.210%	12.84% ± 7.47%	$3.20 \times 10^{-3} \pm 1.15 \times 10^{-3}$

Table 8.3 | Summary of viability ratios calculated based on different observables.

[i] Viability ratio 1 = germinating spore equivalents divided by total spore equivalents determined by spectro-EVA; [ii] Viability ratio 2 = germinating spore units determined by μEVA divided by total number of spore determined by phase contrast microscopy; [iiii] Viability ratio 3 = live cells stained by SYTO-9 in *BacLight* viability kit divided by dead cell stained by PI in *BacLight* viability kit determined using a combination of flow cytometry and fluorescence microscopy; [iv] Viability ratio 4 = number of culturable cells divided by total number of cells stained by DAPI or SYPRO Gold observed using fluorescence microscopy.

CHAPTER 9: ENDOSPORES IN HYPER-ARID BIOSPHERE

9.1 Abstract

Bacterial endospores are one of the hardiest life forms on Earth, renowned for their omnipresence in extreme environments, including polar ices, permafrost, and deserts. This chapter is devoted to the study of endospores in hyper-arid environments on Earth as terrestrial model to Mars. The Atacama Desert in Chile serves as the perfect model system because it is the driest desert on Earth. Previous studies have reported a near-sterile state in the soils. My research group has been on a sampling expedition to the Atacama Desert for 10 days in September 2007 to carry out a series of *in situ* and sample return analyses with the goal to study the microbial diversity, abundance and the response of the effect of water on the native microbes. New culture-independent methods, such as phospholipid fatty acid and total organic carbon analyses were performed on the desert soils along with terbium-dipicolinic acid based assays. Significant differences in culturability and germinability were obtained along a depth profile in a soil pit corresponding to ages approximately equal to 25000 and 35000 years ago based on radioactive carbon dating. A spike in microbial response was also observed when sterile water was added into otherwise-sterile desert soils. Endospore isolates obtained from the Atacama Desert were compared with laboratory strains and other environmental isolates as an effort to investigate the long-debated ecological role of endospores in a particular environment. Comparative studies were made on sporulation, outgrowth, germination kinetics, morphology, dipicolinic acid content, thermal and UV resistances. Environmental strains generally exhibited higher resistance and are less responsive to

conventional chemical germinants. In particular, we assess the feasibility of using the abundance and viability of endospore as proxies to study the ecosystem in Atacama.

9.2 Introduction

The Atacama Desert in Northern Chile is the driest place on Earth. This is a cold desert with a hyperarid habitat. The average annual air temperature is -5°C to 45°C, depending upon elevation and distance from the sea. The annual precipitation is less than 1 mm. Some of the weather stations in the Atacama Desert have never received any rainfall records. The cold water brought from Antarctica along the Chilean coast creates a phenomenon called the temperature inversion in which cold air is below a ceiling of warm air, preventing water evaporation and formation of clouds. Also, the desert is in the rain shadow of the Andes on the west and Chilean Coast Range on the north, within the dry subtropical climate belt[1,2]. Owing to the combined effects of these physical factors, the Atacama Desert has been devoid of water for over 150 million years[3-5]. The upper soil layers are dry and weathered. The soil environment precludes any downward infiltration. For this reason, the possibility of penetration of model microorganisms into the soil subsurface is precluded, making it a very good model to assess the dry limit of life, effect of water on microbial abundance and preservation of organic material along a depth transect of soil.

The study of environmental endospores has gained wider popularity. An increased understanding of the interactions between the environment and the dormant life form provides insight into microflora. Until relatively recently, conventional cultivation techniques has been the primary tool for the study of environmental endospores.

Nevertheless, endospore viability is still the one often-neglected topic. μEVA has been developed as a time-gated luminescence microscopy technique to assess the viability of endospores. Indigenous microflora of most environments develop in spatially organized gradients according to physicochemical driving forces[6]. Microbial population is organized either horizontally or vertically along these gradients. Endospores follow suit under different environments. For example, dormant endospores can remain viable for long periods of time and may thus accumulate in deep sea sediments, ice cores, and desert soils as a function of stratification age. The quantitative distribution of endospores will be an interesting subject to study.

When vegetative cells of *Bacillus* species are confronted with low nutrient, the bacteria can initiate the process of sporulation, in which the growing cells differentiate into dormant spores[7]. Spores do not metabolize at a detectable level and are highly resistant to several perturbations, such as heat and exposure to UV and gamma radiation[8-10]. They exhibit longevity with reports ranging from thousands up to half a billion years[11-13]. Arid desert is one of the best repositories for life on Earth because of minimal biological degradation of dead remains. Bacteria have been entombed desiccated in these environments for a long time. Endospores are one of the survivors due their remarkable resistance. Understanding constraints on microbial populations in extreme environments is of great interest in the context of Earth analogs for possible extraterrestrial habitats. Hyper-arid and oxidizing environemnts, such as the Atacama Desert, are good analogs of environments on Mars and the Jovian moon Europa.

Two conditions stressful to soilborne bacteria are carbon starvation and low water activity. Water is indispensable in for bacterial activities. Water activity (a_w) is defined as the measure of how efficiently the water present can take part in a chemical reaction[14]. There is a direct correlation between water activity and microbial activity in a soil habitat[15-18]. Low water activity in soil is generally related to a low matric potential (retention of free water molecules by water-insoluble soil colloids) but also to low osmotic potential (retention of free water molecules by water-dissolved substances such as electrolytes or organic compounds). Low water activity represent a typical stress conditions in soils. The availability of water for physiological processes decreases as the water potential is lowered. Although the wetting and drying effects on soil processes have been studied for decades[19-21], we report the first *in situ* study for endospore metabolism and germination response to water augmentation in a hyperarid region.

We also evaluate the ecological role of endospores by comparing the endospore-forming isolates from the Atacama Desert with other laboratory-stain mesophilic, thermophilic and psychrophilic isolates. Life cycle of an endospore-forming bacterium consists of a vegetative cell and an endospore stage. Sporulation produces resting endospores in preparation for environmental changes or extremes. In the presence of water and nutrients, endospores may germinate and reengage in the vegetative cycle. Three indicators are associated with the course of germination, namely dipicolinic acid (DPA) release (germination stage I), water uptake (germination stage I), and onset of ATP production (germination stage II). We employ optical density measurement, terbium-DPA (Tb-DPA) luminescence assay and ATP luciferin-luciferase assay to monitor each of these events, respectively. A mathematical model is formulated to

describe germination based on DPA released, which will be helpful for understanding the underlying germination kinetics and eventually help detecting spores based on induced germination.

For over 80 years it has been known that there is a large discrepancy between the number of bacterial colonies that form on solid media when soil is used as an inoculum and the total number of bacterial cells actually present in that same soil. This discrepancy has limited our understanding of the species diversity of soil bacterial communities. In the past decade, this limitation has been partially overcome through the application of molecular ecological techniques.

Based mostly on bulk measurements from homogenized soil samples, microbial communities have been found to exist and possibly even maintain their activity in the Atacama Desert, Chile, but the actual distribution and metabolic activity of the organisms under *in situ* conditions has not been demonstrated due to the lack of adequate technologies. Extracting microorganisms in soils through suspending in buffer, subsequently by vortexing and sonication, destroys the micro-environments within the soil matrix.

Here we report the first successful extraction of DPA and measurement of germinable endospores from the soils in the most arid zone of the Atacama Desert, the Yungay area. We focused on two primary Yungay sample collection sites, which we call sites A and E. Site A is the location of a past effort to extract DNA from the soils of this region, which did not yield detectable concentrations of DNA[22]. Site E is 5 km northeast of Site A, and is the location of prior investigations that focused on soil chemistry, identification of cultured isolates and DNA extraction[23,24]. We also determined

phospholipid fatty acid (PLFA), total organic carbon (TOC), culturable microbial populations, anion concentrations, soil reduction potential (E_h), conductivity (eC), and water activity for surface and subsurface samples. In addition, we measured the change in microbial abundance along a depth transect in a soil pit to investigate endospore viability and the long-term preservation of organic materials in an arid environment.

In this study, we first of all build upon various endospore detection assays that have been developed, together with germination models, airborne endospore models, sporulation protocols for psychrophilic and thermophilic endospores and a lot of different ideas to develop instruments for field work. We first tested the new instruments and field protocols in the local Mojave Desert for the proof of principles. Next, we went on an expedition to the Atacama Desert to test out our new field-customized assays and instruments. Finally, we compared the bacterial isolates that we obtained from the desert with laboratory endospore strains to study the ecological role of endospores in different environments and various temperature extremes.

Next, we aim to compare properties of spores isolated from soils, including isolates from Atacama Desert, with laboratory strain spores. Germination kinetics will be emphasized in the pursuit to devise an optimal germination conditions for spores inhabiting in each of the different biotic extremes. Psychrophilic and thermophilic spores are prepared to study both cold and hot habitats. In particular, Atacama Desert is considered one of the most extreme places on Earth. It is the driest desert. It has been reported to contain near sterile soils with only trace organic carbon and nitrogen content and these conditions have existed for at least several millions years.

After that, we screened endospores of isolated spore-forming bacteria from a

growing collection of spacecraft and associated environmental isolates for resistance to UV irradiation at 254 nm (UV_{254}). In order to examine the biocidal effects of direct UV irradiation predicted for Mars, UV_{254}-resistant spores were exposed to simulated Martian UV irradiation. The effects of UVA, UVA+B (280 to 400 nm), UVC (200 to 280 nm), and total UV irradiation (200 to 400 nm) on the survival of microorganisms at intensities expected to strike the surface of equatorial Mars were examined.

9.3 Methods

9.3.1 Materials

Terbium (III) chloride hexahydrate (99.999%), L-alanine, D-alanine, dipicolinic acid (99%; 2,6-pyridinedicarboxylic acid), L-asparagine, L-glucose, L-fructose, potassium chloride were all purchased from Sigma Aldrich (Milwaukee, WI) and were used as received. ATP luciferin and luciferase mix were purchased from Promega. n-hexadecane was purchased from TGI American. Bacteria were counted by spreading plating on tryptic soy agar (Difco, Sparks, MD). An endospore suspension of *Bacillus atrophaeus* (ATCC 9372) was purchased from Raven Biological Laboratories (Omaha, NE) and stored at 4°C before use. Other lab-strain *Bacillus* endospores used in this study include *B. atrophaeus* (ATCC 9372), *B. subtilis 168*, *B. subtilis natto*, *B. cereus*, *B. licheniformis*, *B. megaterium* and *B. pumilis*. All solutions were prepared in 18.2 MΩ-cm deionized water (Elga, UltraPure Lab) and 0.2-µm filter sterilized.

9.3.2 Soil sampling

All utensils were either packaged sterile or pre-treated at 240°C overnight. The sampling sites were approached downwind, and gloves and masks worn to reduce the chance of contamination. Care was taken to minimize contamination of the experimental sites by reducing foot traffic to designated paths and areas. Soil samples were collected by spoons and scoops aseptically into sterile Whirl-Paks with the collector wearing masks, apron, and sterile gloves collected when facing the wind[25]. The rhizosphere domain is defined as extending approximately 5 cm from the root surface in all directions. Some root nodules were collected together with soils. Sieving, homogenizing and sample handling took place in a station in Yungay. After some on-field preliminary experiments (culturing, ATP measurements, DPA measurements), the soil samples were sealed in amber jars to protect from sunlight and moisture, transported in coolers with ice packs/dry ice or placed in dry shipper dewars for transport back for laboratory analysis.

9.3.3 Air sampling

Air sampling was carried out in places with minimal human activity using a SAS sampler. The air sampler was positioned 20 cm above the ground and orientated such that the left arm always faced the windward side and the right arm faced the leeward side. The stainless steel receptacle part was disinfected by alcohol swabs in between each sampling. 100 L of air was collected 3 times (i.e., total of 6 samples) onto 1/10 R2A. 3 plates were incubated aerobically and the other 3 were sealed and incubated inside GasPaks anaerobically at room temperatures. Passive air sampling was also carried by placing fallout plates on the ground next to the air sampler site, 3 facing upward and 3 mounted 20 cm upside down. The fallout plates were composed of a substrate made of

polydimethylsiloxane (PDMS) instead of nutrient agar lest all the moisture would be evaporated under the dry weather. After exposure for various amount of time, the piece of PDMS was peeled off and plated on top of 1/10 R2A for aerobic incubation.

9.3.4 Resistance experiment

10^6 endospores of two laboratory strains (*B. subtilis*, *B. pumilis*) and two Atacama isolates from previous trip (*B. subtilis* and *B. pumilis*) were inoculated and sandwiched between two pieces of 2 × 2 inch polydimethylsiloxane (PDMS). The PDMS pieces were exposed to solar UV irradiation for various amount of time before separating and plated on full strength TSA for enumerating the surviving population. The effective UV dosage was measured by a radiometer discounted by the percent transmittance of the PDMS.

9.3.5 Water augmentation experiment

The water augmentation experiment was done in the Yungay region of the Atacama Desert, Chile, approximately 10 kilometers northeast of the Yungay Experimental Station operated by the University of Antofagasta. 10 Stainless steel 306 rings (60 mm height × 49 mm ID, highly polished) were aseptically entrenched halfway into the soil and 200 mL of sterile deionized water was added over the surface enclosed in each ring simulating a rain event of approximately 27 mm. 2 rings were sampled each day for a total of 5 days. Water activity was measured. Microbial activity was measured by ATP luciferin-luciferase assay, Tb-DPA luminescence assay and direct plate counts. Samples were also analyzed of the anion content, carbon 14 dating and total organic carbon 2 weeks after sample return.

Upon sample return, the same water augmentation experiment was repeated under simulated laboratory conditions. The amount of soil and augmented were the same. Atacama soil sample and kilned soil sample were placed inside beakers exposed to sterile air inside a level-1 biohazard safety cabinet for 5 days.

9.3.6 Measure of soil water activity, pH, E_H, eC and temperature in field

Most of the instrumentation and procedure were outlined in Connon *et al*[23]. Briefly, water activity was measured by a field compatible water activity meter (Decagon, Pullman, WA). Soil hydrogen ion activity (pH), redox potential (E_H), redox (E_H) and conductivity (eC) were performed in the field on a 1:5 solids:deionized water suspension. An IQ150 Handheld pH/mV/temperature meter (I.Q. Scientific Instruments) or similar was used to measure pH and redox potential. Soil conductivity was measured in triplicate with an Orion 4-cell conductivity probe model 125A+ (Thermo Electron, Beverly, MA) or similar and calibrated using two traceable conductivity calibration solutions, 1413 μS cm^{-1} and 12.9 mS cm^{-1} (Cole Palmer, Vernon Hills, IL). Soil samples were analyzed for anion composition by anion exchange chromatograph (AEC) and total organic carbon (TOC). AEC was performed following the protocols of the EPA's Method 300.0 and TOC followed a modified version of a Lloyd Kahn Method by Datachem Labs (Salt Lake City, UT). A field compatible Pawkit water activity meter (Decagon, Pullman, WA) was calibrated using standards of 6.0 M NaCl (a_w = 0.76) and 13.41 M LiCl (a_w = 0.25). Following calibration, a thin layer of homogenized soil was placed along the bottom of a disposable sample cup and placed in the instrument for measurement.

9.3.7 Anion exchange chromatography

Anion exchange chromatography was performed by Datachem Labs (Salt Lake City, UT) using a Dionex Model DX 320 ion chromatograph following the protocols of EPA Method 300.0.

9.3.8 Total organic carbon (TOC) measurement

Total organic carbon analysis was performed by Datachem Labs using a LECO CHN-1000 Elemental Analyzer following a modified version of a Lloyd Kahn Method[26,27]. The limit of detection (LOD) was 200 mg g^{-1} and the limit of quantification (LOQ) was 1000 mg g^{-1}.

9.3.9 Phospholipid fatty acid (PLFA) analysis

PLFA analyses on 50 g soil samples were performed by Microbial Insights (Knoxville, Tenn.) using a modified method of Bligh and Dyer was used to extract microbial lipids[28-30], which were analyzed by gas chromatography-mass spectrometry. The limit of detection (LOD) is 50 and the limit of quantification (LOQ) is 150 pmol of PLFA. PLFA cell equivalent biomass was estimated from the total concentration of ester-linked phospholipid fatty acids in the samples[31]. The conversion factor for obtaining cell equivalents is 2×10^4 cells $pmol^{-1}$ of PLFA, which gives limits for LOD and LOQ of 2×10^4 and 6×10^4 cell equivalents $gram^{-1}$, respectively, in a 50 g sample. A control sample of Atacama soil was brought up to 485°C in a kiln for 4 h to pyrolize all PLFA before submission to Microbial Insights for analysis.

9.3.10 Radioactive carbon dating

Radiocarbon dating was performed on the deep profile top and bottom samples by β Analytics. The unsieved soil samples were acid-washed prior to an AMS-standard delivery analysis.

9.3.11 Cell extraction from soils

Two different soil extraction procedures were used in this study: (I) a quick method used for field work and culture-based analyses conducted in the laboratory and; (II) a multi-step method for microscopy, spectroscopy and cytometry analyses conducted in the laboratory.

Extraction method I was used in times of limited availability of instruments. The goal was to maximize the recovery of microorganisms, rather than obtaining a suspension with minimal turbidity. 30 mL of autoclaved phosphate-buffered saline (PBS) with 10 mM sodium pyrophosphate and 0.1% Tween-80 was added to 15 g of soil in a 50-mL centrifuge tube. The tube was vortexed at maximum speed for 5 min, with intervening 1-min cooling in ice (when in laboratory) or water (when on the field). The tube was then allowed to sediment for 20 – 40 min until a clear layer of supernatant was visible. The supernatant was aliquoted into heat shock and non-heat shock portions. Heat shock treatment was carried out in a water bath at 80°C for 15 min, followed by immediate chilling in ice or water. A parallel control tube was set up attached with a data-logging thermocouple (Fluke Corp., Everett, WA) to ensure the accuracy of temperature.

Extraction method II aims to obtain a maximum dispersion of soil microbes while obtaining a final clear suspension with a minimum of soil particles. 15 mL of 0.2-μm

filter-sterilized PBS with 10 mM sodium pyrophosphate and 0.1% Tween-80 was added to 30 g of soil in a sterile 50-mL centrifuge tube. The tube was vortexed at maximum speed for 5 min, followed by 2 min of sonication (B-15 Brandon, Danbury, CT), intercepted with 1-min cooling in ice. Cells were extracted using a buoyant density by the nonionic Nycodenz® (Accurate Chemical and Scientific Corp., Westbury, NY) density gradient centrifugation (10,000 × g, 1.3 g mL^{-1}). Cells were collected in a layer on top of a visible cushion, and the suspension (final volume = 10 mL) was subsequently aliquoted into halves for heat-shock treatment outlined as above.

Extraction method II yields a higher microbial recovery rate and a cleaner suspension than method I, but, it entails lots of preparatory time and effort. To optimize productivity, extraction method I was used in cultivation assays which are immune to interference and extraction method II was primarily used in interference-sensitive assays.

9.3.12 Cultivation

Aerobic and anaerobic spread plating of samples from sites A, E and augmentation samples were performed on the field in the Atacama Desert. The rest of the cultivation experiments were conducted in the laboratory within 2 weeks from sample collection. A combination of cultivation techniques were used, namely spread plating, most probable number, fluid thioglycollate culturing and multiplex 24-well microtiter plate for isolation and enrichment of rare endospore-forming species (please see Chapter 7). 6 aerobic solid media and 4 anaerobic solid media were used. Aerobic media included (1) full strength R2A, (2) 1/10 R2A supplemented with Wolfe's micronutrient solution (0.05%) (ATCC, Manassas,VA) and cycloheximide (20 μg mL^{-1}) as a fungal inhibitor, (3) salt agar[32]

($CaSO_4$ 0.3 g L^{-1}, NaCl 0.3 g L^{-1}, $MgCO_3$ 0.1 g L^{-1}, KNO_3 0.1 g L^{-1}, $(NH_4)_2HPO_4$ 0.1 g L^{-1}, $FeCl_3$ 0.01 g L^{-1}, agar 15 g L^{-1}, Wolfe's micronutrient solution, 0.05% and cycloheximide 20 μg mL^{-1}, pH adjusted by 0.1 N NaOH to 7.6), (4) Actinomycetes isolation agar (nutrient agar 0.6 g L^{-1}, agar 15 g L^{-1}, novobiocin 50 μg mL^{-1}, cycloheximide 20 μg mL^{-1}), (5) Frankiae isolation agar (KH_2PO_4 1.0 g L^{-1}, $MgSO_4 \cdot 7H_2O$ 0.1 g L^{-1}, $CaCl_2 \cdot 2H_2O$ 0.01 g L^{-1}, sodium propionate 1.2 g L^{-1}, agar 15 g L^{-1}, $FeSO_4 \cdot$ EDTA 0.18%, Wolfe's micronutrient solution, 0.05% and cycloheximide 20 μg mL^{-1}, pH adjusted by 0.1 N NaOH to 7.6). (6) The neutralized acid soil extract agar[33] was prepared using the actual Atacama soil. 25 g of soil was extracted with 100 mL of 0.1 N H_2SO_4. It was then neutralized with 1.0 N NaOH. 15 g L^{-1} agar and water was added to fill up to 1 L. 0.2-μm filter sterilized Wolfe's micronutrient solution (0.05%) was added to the autoclaved media cooled down to 60°C. 1/10 R2A, salt agar and soil agar plates were also incubated anaerobically. MM2 was the other anaerobic media designed for isolating *Clostridium*, which consisted of 0.5 g of KH_2PO_4, 0.4 g of NaCl, 0.16 g of NH_4Cl, 0.05 g of $MgCl_2 \cdot 6H_2O$, 0.01 g of $CaCl_2 \cdot 2H_2O$, 7.5 g of $NaHCO_3$, and 0. 01 mg of resazurin per liter and 0.05% of Wolfe's micronutrient solution, with pH adjusted to 7.0 using HCl. 100 μL of soil extract (extraction method I) was inoculated and spread onto the agar surface by a disposable spreader. All incubations were carried out at room temperature (22°C) with heat-shock and non heat-shock samples in triplicate. Anaerobic plates were sealed inside GasPaks (BD Diagnostic Systems, Franklin Lakes, NJ). Plate counts were made as soon as colonies were macroscopically viable.

Aerobic fluid thioglycollate medium, modified by glucose (10 mM L^{-1}) and cycloheximide (20 μg mL^{-1}), was prepared and dispensed into screw-capped test tubes

(100 × 16 mm). 0.2 mL of soil extract (extraction method I) was inoculated into 4.8 mL of fluid thioglycollate medium. Tubes were incubated at room temperature to assess the proportion of aerobic, microaerophilic and anaerobic bacteria.

In the most probable number (MPN) technique, 10-fold dilutions of 50 μL soil extract (extraction method I) in 200-μL medium broth consisting of 1/5 R2B and cycloheximide (20 μg mL^{-1}) were prepared in 96-well microtiter plates. MPN was carried out across 5 orders of magnitude in triplicate. The plates were incubated for 3 months aerobically under room temperature. Anaerobic MPN was conducted inside an anaerobic chamber with an atmosphere supplied with nitrogen and hydrogen. Wells were scored positive on the basis of the presence of ATP measured by the firefly luciferin-luciferase bioluminescence assay. MPN samples were incubated for about 2 months until the number of positive tubes was constant. MPNs were calculated using standard probability charts[34].

A 24-well microtiter plate method was developed to provide specific isolation and enrichment media for maximum recovery of endospore-forming bacteria. The following media were all minimal growth media. The 24 media consisted of (1) neutralized acid fertile soil extract agar; (2) neutralized acid desert soil extract agar; (3) neutralized acid rhizosphere soil extract agar; (4) 1/10 R2A adjusted to pH 3.0; (5) 1/10 R2A adjusted to pH 11.0; (6) yeast extraction with biotin; (7) 10% NaCl; (8) lysozyme; (9) nalidixic acid; (10) NH_4SO_4 and 5% urea; (11) novobiocin (25 μg mL^{-1}); (12) *Sporolactobacillus* isolation medium; (13) *Sporosarcina halophila* isolation medium and (14) *Sporosarcina ureae* isolation medium. Each of the respective chemical was added as the sole carbon and nitrogen source in a minimal medium, namely (15) trimethylamine, (16) benzoate,

(17) nitrate, (18) citrate, (19) propionate, (20) arginine, (21) allantoin, (22) succinate, (23) urea and (24) control. Once growth was observed, colonies were re-streaked onto a more nutrient-rich media for isolation.

S. halophila isolation medium consisted of 5.0 g of peptone, 3.0 g of meat extract, 30.0 g of NaCl, 5.0 g of $MgCl_2$, 15.0 g of agar in 1 L of water, with pH adjusted to 7.5. The soil suspension was treated with ethanol, 50% (v/v) for 1 hour to kill vegetative bacterial cells. After 3 days of incubation at 3°C, mainly pigmented (yellow, orange, or pink) colonies of various sizes of *Bacillus* species will have developed. *S. ureae* isolation medium consisted of 30.0 g of L-asparagine $\cdot H_2O$, 3.4 g of KCl, 0.25 g of K_2HPO_4, 0.2 g of $(NH)_2SO_4$, 0.05 g of $MgSO_4 \cdot 7H_2O$, 2.5 mg of $FeSO_4 \cdot 7H_2O$, 0.25 mg of $MnCl_2 \cdot 4H_2O$, 1 mg of biotin, 5 mg of L-cysteine in 1 L of water, adjusted to pH 8.7 with1 M NaOH and supplemented with NaCl to a final concentration of 50 mM Na^+. *Sporolactobacillus* isolation medium consisted of 10.0 g of glucose, 10.0 g of polypeptone, 10.0 of yeast extract, 0.027 g of sodium citrate, 0.5 g of KH_2PO_4, 0.5 g of K_2HPO_4, 0.3 g of $MgSO_4 \cdot 7H_2O$, 0.01 g of NaCl, 10 mg of $MnSO_4 \cdot 5H_2O$, 1.0 mg of $CuSO_4 \cdot 5H_2O$, 1.0 mg of $CoC_2 \cdot 6H_2O$, 1.0 mg of $FeSO_4 \cdot 7H_2O$, 100 mL soil extract and 900 distilled water. Soil extract was prepared by autoclaving 100 g of soil mixed with 200 mL distilled water for 20 min at 130°C. The mixture was centrifuged to obtain a clear supernatant.

9.3.13 µEVA

200 µL of soil extract (extraction method II) was filtered onto 1.5-mm^2 spots using a 96-well micro-sample filtration manifold (Schleicher & Schuell, Keene, NH). Details of

the procedure are outlined in previous chapters[35]. The filtered particles were transferred onto Tb^{3+}- and L-alanine-doped agarose by streaking the membrane filter across the agarose surface. A piece of polydimethylsiloxane (PDMS) of 20-µm thickness was placed on top of the agarose to prevent aerial contamination, minimize water loss and DPA diffusion across the agarose substrate. Images were taken with a time-gated microscope, which consists of a pulsed xenon flashlamp (Perkin-Elmer, Waltham, MA), and a Nikon SMZ800 stereoscopic microscope (1 mm × 0.8 mm field of view at 63× magnification), mounted with a time-gated camera system (Photonics Imaging System, UK). The xenon flashlamp operated at a frequency of 300 Hz. After a 100-µs delay after the lamp pulse, the CCD camera began collecting and integrating photons for 2 ms. Time-lapse images were recorded for 60 min to capture the endospore germination timecourse. Germination was carried out at 30°C on top of a heated microscope stage. Each sample was analyzed in triplicate with 8 fields of view.

9.3.14 SpectroEVA

For the determination of DPA in soil samples, 2.0 g of freeze-dried sediment was weighed into 10mL glass ampoules and suspended in 5 mL of 0.5 M HCl for extraction of DPA. Standard addition was used for quantification, taking into account background and possible quenching of terbium dipicolinate fluorescence, but also potential loss of DA during extraction. Therefore, five additional samples were spiked with different amounts of DPA by suspending the sediment aliquots in standard solutions with defined DPA concentrations. DPA standard solutions (in the concentration range from 100 nmol L^{-1} to 2 mmol L^{-1}, corresponding to 0.25–5.0 nmol DPA g^{-1} sediment) were also prepared

in 0.5M HCl. For release of DPA from endospores in the sediment, samples were autoclaved and filtered as described for the spore suspensions. Because of the high background fluorescence, presumably caused by humic material in the sediment, DPA had to be extracted from the filtrate. After cooling, the samples were transferred to 40mL centrifugation tubes, and the glass ampoules were rinsed with 5 mL of 0.5 M HCl to quantitatively transfer DPA. The pH was checked and adjusted to 0.5 by adding HCl (35%), if necessary. The aqueous solution was extracted three times with 20 mL of ethyl acetate. In each extraction step, the sample was vortexed for about 1 min and centrifuged (4000 g, 10 min, 15°C), and the added ethyl acetate was removed with a disposable pipette. The three ethyl acetate phases obtained were transferred into the same 100-mL round-bottomed flask. The solvent was evaporated, and the extract was redissolved in 5mL of sodium acetate buffer (1 mol L^{-1}, pH 5.6) and subsequently washed with diethyl ether (10 mL) and ethyl acetate (5 mL). To the sodium acetate fraction containing the DPA, 100 mL of an AlCl3 solution (2 mmol L^{-1}) was added to minimize quenching of terbium dipicolinate fluorescence by phosphate-containing substances[36]. As organophosphates, e.g., NAD, have been shown reduce terbium dipicolinate fluorescence, presumably by complexation of terbium[37], addition of Al^{3+} was expected to saturate the Tb^{3+}-binding sites and reduce this effect. After addition of $AlCl_3$, the samples were passed through a 0.2 mm cellulose acetate filter.

For fluorescence measurements, 3 mL of the filtrate was transferred to a 3.5mL quartz cuvette. First, emission spectra of the samples without addition of terbium were recorded to obtain background spectra for baseline correction. For the fluorimetric detection of DPA, 30 mL of a 1 mmol L^{-1} $TbCl_3$ solution was added, and the samples

were mixed in the quartz cuvette by pipetting up and down several times before measurement. To check for extraction efficiency, the residues of the diethyl ether and ethyl acetate washing fractions were also dissolved in sodium acetate buffer and subjected to fluorimetric detection of DPA as described above.

9.3.15 Extraction of DPA

DPA can be extracted with ethyl acetate from the aqueous phase after adjustment of the solution to pH 1.8[38]. However, our own experience from experiments with internal DPA standards showed that the samples had to be acidified to as low as pH 0.5, which was achieved by resuspending the sediment in 0.5 M hydrochloric acid prior to autoclaving. Extraction efficiency is strongly influenced by pH. Therefore, it can be necessary to adjust the pH after autoclaving, particularly if carbonate-rich sediments are being analyzed. Three times extraction with twice the volume of ethyl acetate at pH 0.5 generally resulted in an extraction efficiency of more than 96%. Further purification was achieved by redissolving the extract in 5 mL of sodium acetate buffer (pH 5.6) and then washing with diethyl ether and ethyl acetate. At this pH, a loss of DPA caused by the washing procedure was not observed.

Spore suspensions were extracted immediately after determination of spore counts to avoid possible alteration of DPA content due to germination of spores and possible subsequent microbial degradation of DPA. For extraction of DPA from endospores, 5mL volumes of endospore suspension (with at least 10^8 spores mL^{-1}, necessary for quantification of DPA *via* HPLC) were placed into autoclavable 15 mL polypropylene tubes with screw caps (Sarstedt, Germany) and autoclaved at 136°C for 45 min to

completely release DPA from endospores[39]. Impermeability of the tubes was confirmed by weighing all samples before and after autoclaving. After cooling, the samples were centrifuged (4000 g, 5 min, 15°C), and the supernatant was sterile-filtered (0.2 mm pores, cellulose acetate) to remove spore debris.

9.3.16 ATP measurement

ATP was assay from soil extracts using a portable luminometer (New Horizon Diagnostics). The ATP luciferin-luciferase was kept cold at 4°C until reconstitution with buffer before use. The instrument was calibrated using reagent blanks and ATP standards for initialization. 1000 µL of the soil extract was added into a disposable test device with a permeable membrane filter disc, called Filtravette, equipped with a cell concentrator. 4 drops of somatic cell releasing agent were added to the Filtravette. The fluid was filtered through the filter disc by applying positive pressure on top, thereby concentrating target analytes and removing interfering substances. The filter retentate was further washed with 4 more drops of somatic cell releasing agent and then 2 drops of bacterial cell releasing agent. 50 µL of reconstituted luciferin-luciferase reagent was added to the Filtravette immediately before bioluminescence reading was taken with the luminometer. Light intensity would be integrated for 10 seconds and measured by a hand-held microluminometer (model 3550i, New Horizon Diagnostics). Triplicate measurements were made to determine the number of vegetative cells. To assay for the number of bacterial endospores, the previously heat-shocked soil extract was aliquoted into 3 tubes with an equal volume of 1/10 TSB and 50 mM L-alanine. The same ATP assay was applied after 24 hours of incubation at 37°C.

9.3.17 Microscopic enumeration

The DNA-intercalating fluorescent dye, SYPRO® gold (Molecular Probes, Invitrogen) was used to determine the number of total cells by epifluorescence microscopy. To dislodge cells from soil particles, the protocol described by Epstein and Rossel was modified[40]. Aliquots of fixed sediment samples were mixed with 0.2-μm filter-sterilized and autoclaved water. The samples were sonicated three times for 1 min at the lowest setting with a microtip. Aliquots of the sonicated soil samples or fixed pure cultures were diluted in 5 mL of particles-free PBS and stained with SYBR-GOLD (1 μg of SYBR-GOLD per mL of PBS). After 10 min of staining, the cells were concentrated by filtration onto black polycarbonate filters (pore size , 0.2 μm; Nuclepore). The membrane filters were mounted with immersion oil. Epifluorescence microscopy was performed with a Nikon Optiplex microscope. For each filter no fewer than 400 cells were counted in at least 10 microscopic fields.

The LIVE/DEAD *BacLight* kit (Molecular Probes, Invitrogen) was employed to assess the viability of vegetative bacterial communities. Phase contrast microscopy was performed to determine the total number of endospores present. Endospores are not stainable but they can be observed as phase-bright oval bodies under phase contrast optics. Malachite green staining was performed to identify the presence of endospores. Endospores would be stained green while the rest would be stained red.

Metabolically active bacteria were enumerated using the fluorescent reagent 5-cyano-2, 3-ditoyl tetrazolium chloride (CTC). CTC was used a final concentration of 5 mM in 3-h incubations at 37°C to determine concentrations of actively respiring cells for total and metabolically active cells[41]. CTC was used to test the respiratory activity during

germination and growth. Reduction of CTC was used to evaluate the respiratory potential of freshly isolated endospores. Dehydrogenase activity in bacterial respiration was measured with this dye, which has the ability to produce a red fluorescent molecule (formazan) when reduced. A stock solution of 50 mM CTC was prepared in sterile ultra-filtered water. 90 µL TSB and 10 µL CTC stock solution (final concentration of 5 mM) were incubated for an additional 2 hours at 37°C in the dark. The stained samples were loaded on a filtration apparatus and pumped through a 0.22-µm nucleopore polycarbonate filter. The filters were mounted on a slide and observed under a 100× oil immersion objective.

9.3.18 Ecology study and strain identification

Bacterial spores were isolated on Rodac plates from the Atacama Desert in 2005. They were stored in darkness at 4°C for 9 months before study. Thermophilic and psychrophilic endospores were isolated from soils in Jet Propulsion Laboratory, Pasadena, CA. Soil samples were collected with sterile metal scoops and dispersed in 0.1% sodium pyrophosphate with 0.01% Tween-80 in a ratio of 1 g soil to 10 mL solution. The soil slurry was vortexed at maximum speed for 5 minutes and then let settled down for 30 minutes when clear sedimentation was observed. The supernatant was extracted and heat shocked at 80°C for 15 minutes to select for endospores, following by plating and isolation on TSA. Thermophilic and psychrophilic endospores were selected by incubating cultures at 60°C and 7°C, respectively. DNA amplifications were performed in a reaction containing ~50 ng of pure culture genomic DNA, 2.5 U of Taq DNA polymerase (Applied Biosystems), 5 µL of 10× PCR buffer, 2.5 mM $MgCl_2$, 200 µM

each deoxynucleotide triphosphate, 150 ng μL^{-1}, 1 μM each forward and reverse primers, and sterile water to a total volume of 50 μL. Reaction mixtures were irradiated with ultraviolet light for 5 min at 254 nm (1000 J/m^2) before the addition of template and Taq DNA polymerase to eliminate potential contamination[42]. All negative controls with water instead of DNA template were tested.

9.3.19 Sporulation

Spores were prepared in 2 x SG sporulation agar[43]. All ingredients were obtained from Sigma unless otherwise stated. 16.0 g nutrient broth (Difco), 2.0 g KCl, 0.5 g $MgSO_4$ and 16.0 g agar in 1 litre of water were suspended in water with pH adjusted to 7.0. The medium was autoclaved and let cool down. 1.0 ml 1 M $Ca(NO_3)_2$; 1.0 ml 1 M $MnCl_2 \cdot 4H_2O$, 1.0 ml 0.001 M $FeSO_4$ and 2.0 ml 5% L-glucose (w/v) were freshly made, filter-sterilized and added after cooling of the media. Vegetative bacteria in exponential growth phase were inoculated onto agar plates. Thermophilic spores were incubated at 60°C for 10 days, mesophilic spores were incubated at 37°C for 10 days; and psychrophilic spores were prepared using the protocol outlined in Chapter 7. Percent sporulation was monitored by observing phase-brightness under a phase contrast microscope (Nikon). Spores and cells were collected by adding 5 mL of sterile deionized water into each agar plate and cell scrappers. The resultant suspension was sonicated for 5 minutes (Branson) and then washed 4 times at 13,200 rpm for 20 minutes. Lysozyme (50 μg mL^{-1}) was added and the suspension was incubated at 30°C for 2 hours. Subsequent washing (6-12 times) using sterile deionized water performed until the suspension was more than 95% spores. The spore suspension was then stored in water at

4°C in the dark. Psychrophilic endospores were prepared in the way outlined in Chapter 7.

9.3.20 Spore size measurement

Cell volume is calculated from simple length and width measurements and the application of simple geometrical formula under a phase contrast microscope. Transmission electron microscope was performed at the imaging center at Caltech. Spore counts were determined by phase contrast microscopy using a hemocytometer counting chamber. At least 24 randomly chosen squares with about 100 cells were counted. Suspensions were diluted to an appropriate spore density of about 10^8 spores mL^{-1}. For volume determination, the shape of the endospores was approximated as a cylinder with hemispherical ends. Volume (V) was calculated from the length (l) and width (w) of the spores using the following formula[44,45]:

$$V = \frac{w^2\pi}{4}(l - w) + \frac{w^3\pi}{6}.$$

This formula can be used for rod-shaped as well as coccoid spores, as for cocci the term (l–w) becomes zero. For calculation of spore volume, the length and width of at least 100 spores were determined. Associated errors were estimated by consideration of error propagation on the basis of SDs of length and width measurements.

9.3.21 Hydrophobicity

Spore surface hydrophobicity is measured using a modified BATH assay by Rosenberg *et al.*[46] Spores are suspended in 100 µL of water with an initial A_{660} around 0.4 to 0.5. 10 µL of n-hexadecane (MP Biomedicals, Solon, OH) is added. The mixture is vortexed for

1 minute and then let settle for 15 minutes before pipetting out the organic hydrocarbon layer. Absorbance measurements are done on the aqueous layer using a NanoDrop spectrophotometer. Percent hydrophobicity is calculated by $100 - (A_{600\ after} / A_{600before}) \times 100$.

9.3.22 Germination

DPA measurement is equivalent to the measurement of germination propensity. 1.5 mL of extract was pipetted into methylcrylate cuvettes at each time interval. 1.5 mL of 50 μM $TbCl_3$ supplemented with 10 mM aluminum chloride buffered with 10 mM sodium acetate to pH 5.5 was added. The luminescence intensity was measured using the following home-made spectrometer: the spectrometer consists of a 24 W pulsed xenon flashlamp (FWHM ~5 μs and tailing out to ~50 μs), a photomultiplier tube (Hamamatsu R6353P, Bridgewater, NJ), 2 concave aluminum mirrors and 2 bandpass filters. Pulsed excitation light at 10Hz was focused on samples with a concave aluminum turning mirror and band-limited by an interference filter (50% pass bandwidth 255–280 nm, 23% maximum transmittance). Luminescence from the sample traversed through a bandpass filter (50% pass bandwidth 538–553 nm, 70% maximum transmittance) and another concave aluminum mirror to enter the PMT. The filter set was chosen to overlap with the excitation and emission spectra of Tb-DPA. Time gating was achieved by a delayed detection of the sample luminescence after each flash, according to a chosen delay time. Throughout all measurements in this study, the PMT was operated at 950 V, photocathode aperture set to be 15 mm × 10 mm, delay and integration time was 100 μs and 2 ms, respectively. The entire assembly was shielded from ambient light using a

black anodized aluminum enclosure. The spectrometer was custom constructed by Jobin Yvon, Edison NJ. Cuvettes and tape matrix were measured at a distance of 15 mm from the spectrometer.

9.3.23 UV inactivation

A low-pressure handheld mercury arc UV lamp (model UVG-11; UVP) was placed over a sample, and the UV flux at the surface of the spore suspension was measured using a UVX digital radiometer (UVP). The exposure time required to produce 1,000 J m^{-2} of energy at the sample surface was determined to be 167 s at 600 μW cm^{-2}. The spore suspension was placed in an uncovered 100 mm glass Petri dish containing a magnetic stir bar and was exposed to UV_{254} irradiation under sterile conditions. In a qualitative screening analysis, strains surviving 1,000 J m^{-2} irradiation were selected for quantitative lethal dose curve analysis. Samples (100 μL) were removed after specific periods of time, serially diluted, and plated on TSA. The dose at which 90% of the spores were inactivated (LD_{90}) was >200 J m^{-2}.

Spores resistant to UV_{254} irradiation were exposed to UVA (315 to 400 nm), UVA+B (280 to 400 nm), or total UV (200 to 400 nm) at a simulated Mars constant level of total solar irradiance of 590 W m^{-2} (190 nm to 3 μm) using an X-25 solar simulator (Spectrolab) equipped with a xenon arc lamp located at the Environmental Test Laboratory, JPL. The intensity of UV irradiation was approximately 10% of the intensity of the full spectrum (59.0 W m^{-2}). The total level of irradiance in these simulations matched the actual Mars constant level of solar irradiance, 590 W m^{-2}.[47-49] The intensity of the irradiation was constantly adjusted by fine-tuning the lamp power to

achieve ±5% variability, as indicated by an Optronics Laboratories OL754 spectroradiometer. The various bandwidths were generated by using Corning glass (UVA) or plastic Petri dish lids (UVA+B; Fisher Scientific) as filters in front of the sample cuvettes. The lethal doses were calculated for each strain in order to estimate LD_{50}, LD_{90}, and LD_{100} UV dosages. LD_{100} was defined as the UV dose at which no cultivable spores were recovered using the procedures described here.

9.4 Results & Discussion

Understanding the boundary conditions for survival in extreme environments and subsequent revival with water will aid the NASA effort for preparing to search for life on Mars. Bacterial spores are highly resistant to both dehydration and high temperatures and, for this reason; endospore-forming bacteria are extremely common in soils. Exospores produced by micro fungi and Actinomycetes are generally considered to be a means of dispersal rather than of survival. There is strong evidence, however, that exospores are of significantly greater resistance to desiccation. It is also possible that exospores are able to respond faster to an improvement in conditions than surviving but stressed bacterial cells.

The Atacama Desert serves as a proving ground for future life detection instrumentation, and characterizing the environmental microbiology will provide an important context for data sets to be obtained by future instruments slated for flight. Finally, understanding which phylogenetic groups and species of microorganisms are most likely to grow in Mars special regions will aid in establishing planetary protection requirements to help prevent forward contamination. We have performed a series of culture-based and culture-independent methods to analyze the microbial, in particular endospore,

abundance and diversity, along with measurements of PLFA, TOC, anion concentrations, soil reduction potential, conductivity, temperature and water potential for surface (0-20 mm) and subsurface (20 – 200 mm) samples from Site A, Site E and other interesting locations. A list of all sample collection sites are tabulated in Table 9.1. The corresponding microbiological results are shown in Table 9.2. In this results section, we will focus on (1) Site A & E characterization, (2) water augmentation experiment, (3) air sampling, (4) depth profile and (5) other interesting sites.

9.4.1 Spatial and temporal heterogeneity in Site A and Site E

Hyper-arid and highly oxidizing soil in Atacama Desert, the habitat predominantly studied to date as a proxy for extraterrestrial life, differs from other extreme environments on Earth, such as permafrost, deep-sea hydrothermal vent, ice cores, in its absence of culturable bacteria and zero water activity, which precludes metabolism of all types of bacteria. The total organic carbon content varies from 0.05% to 0.1% in the soil. The pH is acidic. The redox potential (Eh) of the investigated samples varied from +260 to +480. The water activity recorded ranged from 0.01 to 0.08 during the day and peaked at 0.52 in the early predawn hours, which is also below the lowest reported a_w for microbial growth. The total organic carbon content was between 880 and 1700 μg g^{-1}, which was around the borderline of the limit of quantitation (1000 μg g^{-1}). Most desert soils contain significantly more organic carbon. For example, the TOC for samples obtained from the Mojave in Eureka Valley, California was 7,000 μg g^{-1}. There were no significant differences in water activity, soil chemistry and TOC levels between surface and subsurface samples from sites A and E.

Navarro-Gonzalez *et al.* has report in the *Science* journal in 2003 that site A is a near-sterile region with no recoverable DNA and extremely low culturable counts[22]. And my research group has investigated the soil chemistry and microbial diversity in site in previous trips to Atacama. So, it will be interesting to track the temporal change in microbial counts. Normal soil contains around $10^7 – 10^8$ culturable bacteria per gram and normal desert soil contain around 10^4 culturable bacteria per gram. However, in the Atacama Desert, we have observed a very low count from 0 to about 400 vegetative cells per gram. And the recovery of spores is even lower. Top means the surface 3-6 cm layer of soil. SUB means the 12-cm layer underneath the surface. While commonly used medium, R2A, recover only a low number of bacteria, the 2 media that I used, namely salt agar and soil agar, are much better in recovering soil-borne bacteria. Salt agar is made to mimic the salt concentration in Atacama Desert soil; and the soil agar is made directly from the native soil. The nutrient level in these two media was kept very low to give microorganisms enough time to recover; otherwise too much nutrient will simply kill them instantly. Soil extract plated on rich media, such as full strength R2A, resulted in fewer colonies than 1/10 R2A (Figure 9.1). The rapid increase in nutrient availability was considered stressful to bacteria[50]. Although PLFA analysis has suggested the presence of large relative numbers of Actinobacteria, no colonies were observed in the Actinomycetes isolation media, suggesting most of them were either dead or nonculturable. Total microbial counts on spread plates ranged from 10^2 to 10^3 cfg g^{-1}. Heat shock survivor counts were between 0 and 1 cfu g^{-1}, indicating 0.1% to 1% of the culturable soilborne microorganisms were endospores. However, incubation in a liquid medium using the MPN number for enumerated resulted in cell counts that were 1 – 2

orders of magnitude more. This may suggest that water was more amiable to the microbes. Using paired *t*-test, no significant difference was observed between the surface (0 – 20 mm) and subsurface samples (20 – 200 mm), between site A and site E.

Patchiness is a fundamental attribute of soil ecosystem Presence of patchiness and importance in maintaining bacterial diversity[51-54]. In order to quantify microbial abundance over an area, one needs to interpolate values between sampling sites. In doing so, one may be able to identify hot spots or high residence numbers. Mapping can be done using conventional geostatistical methods such as construction of a variogram to model the correlation that exists as a function of distance between stations to calculate predicted values for locations in an area. The heterogeneity of soilborne bacteria can be thought of discontinuities in space and time (i.e., patchiness). Zhou *et al.* observed that soils which were saturated with water had both fewer bacterial taxa and a more uneven distribution of bacteria taxa than unsaturated soils[54]. They suggested that this difference was the result of patchiness in the unsaturated soil (i.e., the lack of water reduced migration between soil particles), which allowed the coexistence of a larger number of bacterial taxa and produced a more uniform community composition. Complexity in environmental conditions can vary at multiple spatial scales and could potentially influence bacterial diversity. Microscale heterogeneity (e.g., at the scale of a soil particle) can be very high and potentially allows for high microbial diversity in a relatively small area. For example, within a single soil particle, oxygen concentrations can range from 21% to 0% over only a few millimeters[55].

Some interesting observations can be observed when compared this dataset with the previous 2 trips in 2003 and 2005. The culturable biomass in 2003 were determined to

range from 2×10^2 to 5×10^3 cfu g^{-1} and the heat shock survivors were around 10^1 - 10^2 cfu g^{-1}. While we have comparable total cell counts, the 2007 heat shock survivor counts were lower by at least an order of magnitude. Other than patchiness and slight differences in the extraction protocol, a plausible reason may be the difference in effect heat shock temperature. In 2003, heat shock was performed inside a small air incubator at 80°C for 15 minutes on agar plates inoculated with soil extract. A later study found out that the effective temperature experienced by the microbes was merely around 60°C. Our current heat-shock protocol involves heating soil slurry contained in tubes inside a 80°C water bath with a large heat capacity for 15 min. Yet, most of the heat-shock survivors recovered from the 2003 trip were found to be spore-forming species. In addition, bacteria isolated from the Atacama Desert have exhibited resemblance to psychrophilic counterparts in terms of germination behavior, DPA content, heat tolerance and hydrophobicity. These bacteria also demonstrated preference to grow in liquid media than solid plates, suggesting their hydrophilic origin. We postulate that the endospores residing in the Atacama Desert soils have a cold origin, possibly brought by wind from Antarctica. This hypothesis will be tested in the coming sections.

The 2005 data, however, showed extremely low counts. 7 months prior to the 2005 sampling, there was a rare rainfall even accounting for 20 mm of precipitation in these areas. We have a hypothesis that transient water revived dormant life forms but the subsequent harsh environment killed them immediately. The top layer (0 – 200 mm) of the Atacama Desert soils represented a dynamic contributed not by microbial activities but the action of wind. Since the perennial low water activity in the hyperarid area did not support any microbial activities, the resident microbes were brought in by the action of

wind from neighboring areas, including Antarctica, giving rise to the psychrophile-like bacteria in Atacama.

9.4.2 Water augmentation

The availability of water (often expressed as water activity, a_w) is of major importance to microorganisms as to other forms of life. Fluctuations in the osmolarity of the environment immediately surrounding an organism are the source of considerable stress and there must be a strategy to permit growth and survival[56]. Growth requires the maintenance of positive turgor pressure; the pressure differential between the internal osmotic pressure and that of the environment. The Atacama Desert is permanently arid and select a specialized microflora. This requires survival rather than growth and microorganisms produce a variety of desiccation-resistant bodies including endospores and exospores, many of which can persist for extended periods of time. Coccal-shaped are more resistant than rod shaped and drying out of an environment can change the balance of the population after rehydration.

A water augmentation experiment was carried out to mimic the effect of rainfall by adding sterile water into different patches of soil, confined by these stainless steel rings. We had added 200 mL of water into each of the 15 rings, simulating a 26 mm rainfall. We added water at day 0 and sampled a set of 3 rings per day for a total of 5 days. Upon addition of water, we noticed a spike in microbial activity, germination propensity of endospores, and an increased in culturable counts, which quickly died off within the next 2 days. Water activity was monitored and undisturbed soils were sampled on a daily basis. The level of nutrients, associated with these changes, the anion composition, total organic

carbon and PLFA were also measured before and after water augmentation. Microbial activity as measured by ATP luciferase assay increased sharply after the addition of water and rapidly decreased to background levels as the soil dried (Figure 9.2). Soil water activity correlated with microbial activity and endospore germination on the first day after addition of water. Non-augmented soil did not exhibit any measurable microbial activity or endospore germination. All these experiments were performed on the field. To verify our results, an analogous experiment was conducted under simulated laboratory conditions. A similar trend was observed in the culturable, metabolizable and germinable results with a slight shift in time (Figure 9.3), which may be due to the age of soil, and differences in environmental factors. But the bottom line is that we still observed a bloom in microbial activity after water addition. This finding is in favor of our hypothesis that water revives microorganisms in the soil but they are killed subsequently.

Kieft *et al.* used a chloroform-fumigation biomass assay to study a similar water augmentation effect on dry soils[19]. They have reported a sharp pulse of respiration during the first 2 days, followed by a gradual decline to background or control rates of soil, similar to what we have observed. But caution has to be taken in analyzing our *in situ* data collected in the desert because we did not decouple the microbial response to wetting effect from other effects such as increase solute diffusion or increased microbial mobility. We repeated the same experiment under simulated arid condition by drying the same soil and control kilned soil. The slight difference between the two analyses increases our confidence in the authenticity of our *in situ* data.

Adenosine 5'-triphosphate (ATP), the central molecule of bioenergetic reactions, occurs in all terrestrial microorganisms. In this study, we try to develop a way to measure

ATP in soil. This procedure is based on the use of the firefly luciferin-luciferase bioluminescence reaction. The amount of light emitted is proportional to the amount of ATP. Efficient extraction of ATP from soils requires reagents which will lyze cells, disrupt other organic complexes and release ATP chemically bound to soil, but will not destroy luciferase activity in the time required for measuring the peak luminescence intensity.

9.4.3 Air sampling

Following the previous hypothesis that deposition of airborne endospores is the source of soilborne microorganisms, we have carried out an active and passive air sampling to study the interaction of microbial exchange between the air and surface, in relation to the various environmental factors such as UV irradiation, relative humidity, temperature and wind velocity. Airborne transport of microbes was more prevalent during the night than daytime, as reflected by active and passive air sampling results. Almost nil culturable counts were recorded during the day using the SAS air sampler, while nighttime sampling gave an airborne bacterial concentration between 0.1 and 0.5 cfu L^{-1} (Figure 9.4). This is consistent with the fall-out plate results in which 0 microbial deposition rate was recorded during the day but 0.01 cfu hr^{-1} was recorded during the night. The higher relative humidity, absence of UV radiation and higher wind speed at night may have contributed to these observations. Since the absence of water in the Atacama Desert does not allow microbial activity, most of the resident bacteria are likely brought by winds from the neighboring environments taking place during the night. During the day, UV radiation inactivates all microbes exposed to the sun, particularly the microbes traveling

in the air. Airborne microbes have been reported to possess a lower resistance to stressors than bacteria attached to surfaces. This fits into our hypothesis of the aerial dispersal of endospores *via* wind[57]. In fact, the intercontinental transfer of endospores has been reported in the literature[58]. This model may also shed light on the scenario in Mars, whereby the cosmic and UV radiations sterilize all exposed surfaces. Subsurface microbes, if there are any, may be aerosolized at night by winds to colonize different niches of Mars.

9.4.4 Depth profile

The Atacama Desert has remained stable and arid for the past 150 Ma, containing a sedimentary record of deposition from Late Jurassic to present days. The upper soil layers are dry and weathered, precluding any downward infiltration. The possibility of penetration of microorganisms into the soil subsurface is highly unlikely. For this reason, we hypothesize that airborne endospores from the past deposited on the soil surface were entombed into sedimentary layers in a dormant form due to the continual low water activity. And the bacteria along this depth transect will exhibit a trends reflecting their survival strategy, longevity and the dry limit of dormancy. In this experiment, following a vertical transect of 6 depths in a soil pit from 80 cm to 220 cm underneath the surface soil, we have determined he biomass in terms of colonies, germinable counts, TOC and PLFA contents. Culturable counts were obtained using spread plating and MPN methods. Similar the sites A and E, the bacteria elicited preferences in growing in the liquid media than the solid plates. Actinobacteria constituted around 20% of the culturable biomass, which ranged from $10^1 – 5 \times 10^2$ cfu g^{-1}. A slight increase in CFU was observed along the

depth profile (Figure 9.5). μEVA has successfully recovered 110 – 15 spores g^{-1}, following a decreasing trend toward deeper samples (Figure 9.6).

Phospholipid fatty acid (PLFA) is a measure of viable biomass in soil. Normally, once a bacterium dies, its PLFA content will be rapidly degraded by other bacteria. However, the soil water activity rarely rises above the metabolic activity. So, in the absence of metabolic activities, PLFA may be preserved on the timescales of chemical oxidation. So, a lot of the PLFA is presumably derived from dead bacteria accumulated for thousands and millions of years. Both TOC and PLFA analyses showed an increasing trend of total biomass along the depth transect. At 217 cm underneath the surface, a total organic carbon of 34500 mg kg^{-1} of soil was measured and a PLFA content corresponding to 92000 cell g^{-1} was measured. In addition to nitrate, composite analyses of the soil pit indicate substantial amounts of chloride and sulfate[59,60]. The age of the soil samples were estimated by carbon 14 dating. The measured radiocarbon age of the bottom sample as 35080 ± 320 BP and the top sample was 25640 ± 180 BP. The 13C to 12C ratio was -27.3 for both cases. These results suggest that the organics and dead remnants of microbes were preserved over years, presumable due to aerial deposition of microbes. Some intact plant root remains were discovered towards the bottom of the soil pit, indicating a minimal biological degradation and preservation of ancient organics in the hyperarid region.

9.4.5 Determination of DPA by terbium dipicolinate fluorescence assay

Hindle and Hall reported the limit of detection of the Tb-DPA luminescence assay to be 2 nM[61], which is theoretically equivalent to 10^5 spores g^{-1} soils. By optimizing the protocol,

we are able to detect 200 nM of DPA within the limit of quantitation, corresponding to 10^4 spores g^{-1} soils. The Atacama Desert soils, however, contained a much lower concentration of soilborne endospores. In addition to this, potential interference and quenching effect by humic substances in the soils makes spectroscopic detection of DPA an even more challenging task. So, prior to spectro-EVA analysis, a DPA extraction protocol based on ethyl acetate phase separation has been performed. Using this method, the dual-peak spectral characteristics of DPA can be observed in the excitation spectrum with an improved Euclidean cosine squared correlation coefficient from 0.23 to 0.80. This is the first application of Tb-DPA luminescence assay on the analysis of soil samples (Figure 9.7).

9.4.6 Other interesting sampling locations

In general, 2 sampling strategies were employed in this study. One was the sampling along transects of certain interesting characteristics (depth profile and Ponce Hill water runoff). In the depth profile sampling, zigzag sampling along the depth transect was performed. The unit of sampling distance is the distance underneath the ground level in the soil pit depth transect along which the depth profile samples were taken. If the sampling distance was too large, potentially useful information about the distribution of the depth would be lost. If it was too small, successive samples would be correlated, in which case it would be difficult to determine the confidence interval for the microbial abundance estimate. The second was sampling in special isolated sites, such as site A, site E, the rhizosphere and copper mine soils, and ground water. Random sampling was carried out in this case. Therefore, herein, the sampling sites were chosen to allow the

unbiased reconstruction of an original distribution field. Figure 9.8 shows a comparison of heat-shock culturable and germinable endospores quantified by μEVA across all the sampling sites in Atacama.

Most aerobic endospore-formers are saprophytes widely distributed in the natural environment. Based on μEVA and cultivation experiments, endospores constitute approximately 40% of the total heterotrophic biomass in the Atacama Desert, eliciting a large degree of heterogeneity. We would like to reconstruct the distribution field of endospores in the Atacama Desert. Patchiness is a fundamental attribute of ecosystem and geostatistical tools were used to help with the sampling strategies. The soil contains a considerable quantity of organic matter as well as mineral constituents accumulated for thousands of years because the low water activity does not support any microbial decomposition. The autochthonous microflora of the soil is always present in significant numbers, irrespective of the nutrient status. In contrast, the allochthonous microflora is dependent on a periodic increase in nutrient status and, under normal conditions, is present only in very small numbers or present as either exospores or endospores. Response to a local increase in nutrient level is rapid and colonization of organic material by allochthonous microorganisms can occur immediately.

The rhizosphere is the region of soil immediately surrounding the root hairs of plants together with the surface of the roots themselves. In the rhizosphere region, which effectively extends a few millimeters from the surface of each root, microorganisms are directly influenced by the biochemical activities of the plant. Some bacteria are able to live in ores containing high metal concentrations. These endospores are highly tolerant of high concentrations of metals. An unusual relationship occurs between

penicillin-producing fungi and *B. cereus* in areas containing high metal concentrations. Penicillin-producing fungi are highly resistant as a consequence of the breakdown of penicillin into the metal-complexing substance penicillamine. *B. cereus* is not inherently resistant to metals but is highly penicillin resistant and is able to use the fungal defense mechanism against metal toxicity.

9.4.7 Ecological Study

It has been reported that sporulation condition will, to a certain extent, affect spore properties[62]. So, we have adopted a very close sporulation protocol among all the spores, except for differences in sporulation temperatures for thermophilic and psychrophilic spores. We have also picked the properties that are reported to be invariant to sporulation conditions, namely DPA content per unit volume, spore size and hydrophobicity[63,64]. Size of some small spores ($<0.5\ \mu m^3$) from Atacama Desert remain small after 1 generation and sporulation. Similarities are observed between spores isolated from Atacama Desert and psychrophilic spores. Neither the spore nor vegetative form is hydrophobic. Both of them have high DPA per unit volume ratios. DPA is one of the contributory factors for UV resistance. It has a very high molar absorption coefficient in the UV wavelength and therefore acts as an effective UV shield for spores. Psychrophilic bacteria are usually more UV resistant and it makes sense for them to have a spore core more densely packed with DPA. In addition, Atacama Desert is a place with intense solar radiation. In the 1960s, Cameron has found psychrophilic bacteria, but no thermophilic bacteria, in Atacama Desert[65,66]. The fact that Atacama spores behave close to psychrophilic spores may suggest the presence of cold-living spores in the desert. Though counterintuitive, this

hypothesis will be tested in our future trip to Atacama Desert.

A total of 18 spore-forming species were studied in this case (Table 9.3). All negative controls with water instead of DNA template showed no amplification. We have also tested several of the reagents we used and confirmed that there was no contamination. The results of PCR were reproducible. Figure 9.9 shows the hydrophobicity of the different species. Insights into properties of endospores residing in extreme habitats are of great importance in the exobiological life detection technological development. We tested endospores from several *Bacillus* strains isolated from the Atacama Desert for their endospore properties, heat, UV, oxygen plasma resistance, germination kinetics and compared these characteristics with the laboratory *Bacillus* strains. Endospores from the Atacama Desert showed a large variation in heat resistance, UV resistance. Most of the isolates were less sensitive than the laboratory strains to the germinants tested. A clear link between DPA content and degree of resistance cannot be established.

9.4.8 Germination model

A germination model based on optical density drop has long been proposed by McCormick in the 1960s[67]. In this study, we have formulated a parallel mathematical model based on DPA released measured by Tb-DPA luminescence assay. Experiments show that OD_{600} measurement correlate very well with Tb-DPA luminescence measurement in monitoring the initial germination timecourse of various types of mesophilic lab-strain spores. Both assays measure the events taking place in the stage I of germination. As a control experiment, the firefly luciferin-luciferase assay has been employed simultaneously. A delayed release of ATP has been observed. This is

consistent with the germination timecourse because ATP synthesis occurs in the second stage of germination. D-alanine has also been used to study its inhibitory effect on L-alanine and AGFK-induced germination.

Table 9.4 lists the germination parameters and some other properties of all 18 species of spore-forming bacteria. Figure 9.10 shows the modeling the L-alanine induced germination kinetics based on Chapter 7. For instance, Lab-strain *B. cereus* demonstrated no lag period and finished germination in less than 60 min, giving a mircrolag period, t_0 = 0 min, germination time, α = 1 min, and transition probabilities λ_a = 0.6 min^{-1} and λ_b = 0.08 min^{-1}. Another Lab-strain *B. atrophaeus* endospores demonstrated a lag period before a synchronous germination event, giving t_0 = 4 min, α = 8 min, λ_a = 0.4 min^{-1} and λ_b = 0.10 min^{-1}. *B. pumilus XJU-3* endospores isolated from the Atacama reaching plateau after 24 hours. The parameters are t_0 = 260 min, α = 850 min, λ_a = 0.4 min^{-1} and λ_b = 0.008 min^{-1}. All endospores demonstrated sigmoidal kinetics in the exception that one of the Atacama isolate had a biphasic sigmoidal kinetics. In general, the microlag period and rate of germination of environmental spores were longer than their lab strain counterparts. This delayed response to germinants presents a strategic advantage of environmental spores. Commitment to germination is an irreversible process and it means the concomitant loss of resistance. This property prevents environmental endospores from responding to transient favorable conditions.

9.4.9 Germinability and culturability between lab strains and environmental strains

One of the driving forces behind this project is to examine differences between laboratory strain and environmental strain endospores. Some of the current methods that we have

developed involve fluorimetric determination of dipicolinic acid (DPA), a spore core-specific compound, after reaction with terbium chloride. The concentration of DPA in natural samples is converted into endospore numbers using lab-strain pure cultures such as *B. atrophaeus* as standards. This assumption only holds when the DPA content of environmental endospores and laboratory growth endospores are comparable. In this study, we carried out a systematic study comparing these endospores.

High temperature environments are widely distributed and of many different types. The best known are probably hot springs, geysers and surrounding sulfur-containing soils. Equivalent hydrothermal environemnts, such as vents and seamounts (underwater volcanoes), have also received considerable recent attention. Thermophilic bacteria are defined as microorganisms having an optimum growth temperature in excess of 45°C. The psychrophiles, or the cold loving organisms, are on the other side of the temperature scale from the thermophiles. Psychrophiles are organisms that have optimum growth at temperatures of approximately 15°C, a maximum growth temperature of about 20°C and a minimum of 0°C or lower[68]. They live in cold soils and water and even in sea ice.

In this study, the effect of L-alanine has been explored as a universal germinant for *Bacillus* endospores. On the other hand, D-alanine will be examined as an inhibitor for germination[69]. Different chemical germinants such as inosine and AGFK were found to facilitate the germination of certain species. For instance, *B. cereus* endospores germinated much better in L-alanine with the presence of inosine. *B. megaterium* endospores germinated best in the presence of AGFK only.

It has been well established that bacterial spore properties are affected by the conditions during sporulation. In most studies, spores are routinely produced from

fortified agar or rich liquid media, which results in heterogeneous sporulation conditions for the individual cells[70]. This prevents careful analysis of the metabolism during growth and sporulation. Recent studies describing the effect of sporulation conditions on spore properties involved modulation of sporulation temperature[71-73] or compared spores produced from different media[74-76] and under different environmental conditions[77]. The two strains of *B. subtilis* used in this study were germinated under the same conditions to minimize sources of variation. Most of the properties are similar except for their aerosolization property. The bacterial strain isolated from Mojave Desert is more susceptible to aerosolization.

Germination timecourse was monitored by looking at optical density drop, DPA release and ATP release simultaneously using *B. atrophaeus* spores. A complementary kinetics pattern was observed between OD_{600} drop and Tb-DPA intensity increase, which presumably illustrates the course of events taking place during germination stage I. Water influxes into the spore, displacing DPA and other exudates out of the spore, thus leading to a loss in refractility, i.e., a drop in optical density. ATP is being synthesized afterwards entering germination stage II, which is illustrated as a delayed curve in the graph.

A 50% decrease in A_{660} correspond to 99% germination as observed under phase-contrast microscopy. Laboratory strains responded well to all of the germinants tested. Heat inactivation enhanced the germination response, by increasing the specific germination rate and decreasing the germination lag time. The only strains showed highly variable responses; 5 strains did not respond to any of the germinants; 6 strains showed responded only the combination of L-alanine and inosine, and four strains showed

response to L-alanine as a single germinant. Heat activation resulted in efficient germination of twelve out of fifteen isolates.

Although DPA has long been implicated in spore resistance to wet heat and spore stability, definitive evidence on the role of this abundant molecule in spore properties has generally been lacking[78]. A clear link between germination capacity and heat resistance cannot be found. Several strains with a relatively high D-value had a low colony forming capacity, which may be due to a low germination capacity. However, when these strains were tested in a germination assay, no clear correlation between germination capacity and colony forming capacity was apparent.

9.4.10 Role of DPA on spore resistance

While the exact role of Ca-DPA is still unclear, it is highly implicated in the resistance and stability of endospores[78,79]. Mutant endospores lacking Ca-DPA demonstrated instability and elevated germination propensity without the need of heat activation[78-80]. One plausible role of Ca-DPA in spore resistance is the lowering of core water content, thereby protecting DNA integrity from UV irradiation and other deleterious agents[78,79,81-84], as well as the proteins from thermal denaturation[79,85].

Large variation in spore DPA levels is well observed in the literature as a result of differences in species, sporulation conditions and the heterogeneity of endospores[62,78,79,82,85-89]. Non-definitive and sometimes controversial dependence of heat resistance of endospores on their DPA content has been reported by Church *et al.*[82,90,91] In this study, we measured the DPA content and density in thermophilic, mesophilic and psychrophilic endospores from laboratory cultures and from the environment and

correlate with their thermal and UV resistances. Figure 9.11 show a plot of DPA density vs. spore volume. Isolates from the Atacama Desert exhibited the greatest degree of variation among other environmental isolates. One of them has a size of 8.5 μm^3 while have a normal DPA density of around 0.2 fmol μm^3. Some of the Atacama isolates, however, exhibited a small size, ~ 0.5 – 1 μm^3 packed with a high density of DPA, from 0.8 -1.2 fmol μm^{-3}. This phenomenon is similar to the psychrophilic spores, which also packed a high density of DPA (~ 1.0 fmol μm^{-3}). Other mesophilic and thermophilic lab-strains and environmental strains elicited very little variations in terms of volume and DPA density, with the exception of the large volume of *B. megaterium*. Resistance plots Figure 9.12 shows one of the thermal and UV resistance plots. Figure 9.13 shows the correlation of DPA density with thermal D-values and UV D-values. In the thermal inactivation, no significant differences are observed between lab-strain and environmental-strain endospores. It is driven, to a larger extent, by the intrinsic growth temperature of the endospores. For instance, thermophilic endospores have D-values over 50 min and psychrophilic endospores have D-values less than 5 min. A higher DPA density suggests a higher UV resistance, but this correlation is not apparent. A lot of factors contribute to the UV resistance of endospores, namely the small acid soluble proteins, spore coat, degree of core hydration.

9.4.11 Inheritance of properties in spores

It has been indicated that DPA content as well as volume might be affected by growth conditions[62]. In contrast to this, a more detailed study on the spore size distribution of *Bacillus* species by Carrera *et al.* showed that the choice of medium seems to have a

relatively small impact on spore volume[64]. Also, temperature does not seem to affect the DPA content of spores, as B. subtilis spores prepared at temperatures from 22 to 48°C by Melly *et al.* (2002) contained almost identical amounts of DPA (variations < 10%)[72]. In this study, all endospores were prepared in the same way, with the exception of some of the psychrophilic species. Because of their slow growth and sporulation rate, active aeration was applied and germination inhibitors, such as D-alanine, was added to synchronize sporulation and enhance the spore yield. We have observed that spore size and DPA density were the two properties that were carried along generations as long as an ample supply of calcium and manganese ions were provided during sporulation, consistent with other reported findings.

9.5 Conclusion

Bacterial spores are dormant structures formed during the resting stage in the life cycle of genera such as *Bacillus* and *Clostridium*. They are formed within vegetative cells during sporulation, which is frequently triggered in response to adverse changes in the environment. The spore DNA is protected from the environment by a surrounding spore coat comprised of calcium ions, DPA and protein layers. DPA is a unique chemical marker found only in bacterial spores and can be released from the core into the surrounding by inducing germination (e.g., with L-alanine[92,93]) or physical lysing (e.g., autoclaving, microwave[94]).

When DPA binds with Tb^{3+}, highly selective DPA-to-Tb^{3+} binding triggers bright green luminescence when viewed under UV light, featuring an interchelate energy transfer from DPA to the resonance energy level of Tb^{3+}. DPA has a high molar

extinction coefficient and can transfer the excitation energy to terbium effectively, thus enhancing the emission luminescence by more than 20,000 times. Lifetime gating is enabled due to the long luminescent lifetime ($\tau \sim 1$ ms) of Tb^{3+}, which effectively removes all background fluorescence (i.e., interferent fluorophores with nanosecond lifetimes), thus rendering the background intensity for measuring silent. Terbium dipicolinate photoluminescence assay was first proposed by Sacks. After several iterations of improvements, it is by far the most sensitive assay in DPA detection. The limit of detection has been further pushed down over the years, from 1.2×10^5 spores mL^{-1} (1998), 10^4 spores mL^{-1} (1999) to 1100 spores mL^{-1} (2004).

Endospore-forming bacteria are subject to stress as a result of changes in environmental conditions. Stress factors are typically unfavorable temperature, pH value, nutrient supply, water availability, and the like. Members of microbial populations can, within limits, adapt (habituate) to changing environmental parameters and changes over protracted periods may have relatively limited effects. All bacteria, however, have a point at which exogenous nutrients can no longer be obtained and are thus effectively exhausted. At this point cells may enter a dormant, abiotic state that permits them to survive for long periods without reproduction, development and repair[95]. In arid habitats, bacteria may enter a state of anhydrobiosis as a survival strategy to tolerate extreme desiccation, where cells cease to metabolize. During this state, cells are considered to be nonculturable. It also seems likely that in some situations at least true dormancy is preceded by a "nutritionally opportunistic" state in which endogenous metabolism is sufficient to maintain the ability of the cell to respond very rapidly to nutrient availability. A low level of endogenous metabolism, together with a low maintenance energy

requirement, would therefore appear to be of considerable importance not only in determining the capacity of micro-organisms to survive, but also in responding rapidly to the advent of more favorable conditions.

Spore germination is an essential step to endospores. Most of our knowledge of germination is based on studies on the derivatives of the *B. subtilis* 168 laboratory strain of *B. subtilis*. In the present study we provide a comprehensive comparison of the germination capacity of spores from naturally occurring *Bacillus* isolates. As anticipated, we observed a large variation in heat resistance and germination capacities among different strains, and more than half of the isolates were more resistant than the lab strains. Such variability in heat resistance among *Bacillus* isolates has been reported before[96-98].

We found large differences in germination capacity. Spore germination in response to nutrients is initiated by the binding of germinants to germination receptors. An important factor affecting the germination response was the age of the spores. Prolonged storage enhanced germination, a phenomenon that is known as ageing activation[99]. Therefore, care should be taken to make sure that all the spore-batches have approximately the same age, when performing comparative analyses. Furthermore, in some cases inconsistency and variability was observed in the germination response of spores from the same batch measured at the same time. Such findings were reported previously[100], and may be avoided by measuring germination parameters other than the decrease in absorbance.

Overall, many of the environmental isolates germinated relatively poorly without heat activation. Nevertheless, we clearly showed that after heat activation and with a strong germinant, all of the strains demonstrated various degrees of germinations, albeit

in a few cases to a relatively small extent. Apart from nutrient germinants, cationic surfactants such as dodecylamine[101-103] were studied. Furthermore, ammonia may be included in the mixture, as it has been reported that ammonia can stimulate germination of *B. cereus* spores without the need for heat activation[104].

L-alanine is a common, though not universal, germinant for aerobic bacterial spores[103,105,106]. It is, however, not true in the case of anaerobic and environmental spores. For instance, spores of *C. sporogenes* require the addition of sodium bicarbonate as a potentiator for germination. None of the thermophilic or psychrophilic spores germinate well in the presence of L-alanine only. Combination of L-alanine and AGFK results in a higher percentage of germination measured by the Tb-DPA luminescence assay in most of the mesophilic lab-strain spores and spores from Atacama Desert. Spores of *B. cereus* respond poorly to the germinants provided probably because inosine is missing. Inosine has been reported to be important for *B. cereus* germination but it adds interference to the Tb-DPA excitation spectrum. In future experiments, apart from germinant combination, heat activation and temperature should also be explored to optimize spore germination. Effective germination for psychrophilic spores will be very helpful in the investigation of germinable spores in the Atacama Desert soils.

The results of our study in the Atacama Desert have interesting implications concerning spatial, temporal distribution of microbes, long-term preservation of organics in arid environment, microbial response to water and viability of endospores in the Atacama Desert. The aim of the research reported here was to determine the effect of a hyper-arid environment on the distribution, viability, prevalence, interactions and persistence of the most resistant living organism on Earth, bacterial endospores.

Endospores were isolated and recovered in media prepared under different nutrients and environments. In most cases, bacteria did not manifest themselves as colony forming units, but appear by producing ATP, releasing DPA and could be stained by metabolic dyes. The water augmentation experiment demonstrates a way in which native soilborne microorganisms interact with their environment. *In situ* activities of a mixed population of vegetative cells and endospores were assessed to extrapolate the role of water in the most hyper-arid regions on Earth. Our data indicate the aerial transfer of microbes during the night in the Atacama Desert. We have been able to isolate and characterize endospores from the hyper-acid Atacama Desert, there are, however, challenges to scrutinize their ecological role. Thermophilic and psychrophilic, as well as mesophilic spore-forming bacteria, have been isolated from the hyper-arid habitat. Although they serve as excellent experimental materials for use in probing the basis of particular temperature dependence, we still have a paucity of information about what activities these endospores carry out in their native habitat. In conclusion, study of endospores from environments with temperature extremes gleans valuable information for optimizing spore detection protocols in extreme environments on Earth.

9.6 References

1. Rech, J.A., Currie, B.S., Michalski, G., and Cowan, A.M. Neogene climate change and uplift in the Atacama Desert, Chile. *Geology* **34**, 761-764 (2006).
2. Houston, J. and Hartley, A.J. The central andean west-slope rainshadow and its potential contribution to the origin of hyper-aridity in the Atacama desert. *International Journal of Climatology* **23**, 1453-1464 (2003).
3. Hartley, A.J., Chong, G., Houston, J., and Mather, A.E. 150 million years of climatic stability: evidence from the Atacama Desert, northern Chile. *Journal of the Geological Society* **162**, 421-424 (2005).
4. Rech, J.A., Quade, J., and Hart, W.S. Isotopic evidence for the source of Ca and S in soil gypsum, anhydrite and calcite in the Atacama Desert, Chile. *Geochimica et Cosmochimica Acta* **67**, 575-586 (2003).

5. Clarke, J.D.A. Antiquity of aridity in the Chilean Atacama Desert. *Geomorphology* **73**, 101-114 (2006).
6. Keith, S.M., Russ, M.A., Macfarlane, G.T., and Herbert, R.A. The ecology and physiology of anaerobic bacteria isolated from Tay estuary sediments. *Proceedings of the Royal Society of Edinburgh* **92B**, 323-333 (1987).
7. Gould, G.W. and Hurst, A., *The Bacterial Spore*. (Academic Press, New York, 1969).
8. Nicholson, W.L., Munakata, N., Horneck, G., Melosh, H.J., and Setlow, P. Resistance of *Bacillus* endospores to extreme terrestrial and extraterrestrial environments. *Microbiology and Molecular Biology Reviews* **64**, 548-572 (2000).
9. Setlow, P. Mechanisms which contribute to the long term survival of spores of bacillus species. *Journal of Applied Bacteriology* **76**, 49S-60S (1994).
10. Setlow, P. Resistance of bacterial spores. *Bacterial Stress Response ed. Storz, G., Hengge-Aronis, R.*, 217-230 (2000).
11. Cano, R. Characterizing ancient bacteria. *Analytical Chemistry* **68**, A609-A611 (1996).
12. Cano, R.J. and Borucki, M.K. Revival and identification of bacterial spores in 25-million-year-old to 40-million-year-old Dominican amber. *Science* **268**, 1060-1064 (1995).
13. Vreeland, R.H., Rosenzweig, W.D., and Powers, D.W. Isolation of a 250 million-year-old halotolerant bacterium from a primary salt crystal. *Nature* **407**, 897-900 (2000).
14. van Elsas, J.D., Jansson, J.K., and Trevors, J.T., *Modern Soil Microbiology*. (CRC Press, 2006).
15. Skopp, J., Jawson, M.D., and Doran, J.W. Steady-state aerobic microbial activity as a function of soil water content. *Soil Science Society of America Journal* **54**, 1619 (1990).
16. Orchard, V.A. and Cook, F.J. Relationship between soil respiration and soil moisture. *Soil Biology and Biochemistry* **15**, 447-453 (1983).
17. van Loosdrecht, M.C., Lyklema, J., Norde, W., and Zehnder, A.J. Influence of interfaces on microbial activity. *Microbiological Reviews* **54**, 75 (1990).
18. Davidson, E.C.A., Belk, E., and Boone, R.D. Soil water content and temperature as independent or confounded factors controlling soil respiration in a temperate mixed hardwood forest. *Global Change Biology* **4**, 217-227 (1998).
19. Kieft, T.L., Soroker, E., and Firestone, M.K. Microbial biomass response to a rapid increase in water potential when dry soil is wetted. *Soil Biology and Biochemistry* **19**, 119-126 (1987).
20. Stevenson, I.L. Some observations on the microbial activity in remoistened air-dried soils. *Plant and Soil* **8**, 170-182 (1956).
21. Birch, H.F. The effect of soil drying on humus decomposition and nitrogen availability. *Plant and Soil* **10**, 9-31 (1958).
22. Navarro-Gonzalez, R. *et al*. Mars-like soils in the Atacama Desert, Chile, and the dry limit of microbial life. *Science* **302**, 1018-1021 (2003).
23. Connon, S.A. and Connon, S.A. Bacterial diversity in hyperarid Atacama Desert soils. *Journal of geophysical research* **112**, G04S17 (2007).
24. Lester, E.D., Satomi, M., and Ponce, A. Microflora of extreme arid Atacama Desert soils. *Soil Biology and Biochemistry* **39**, 704-708 (2007).
25. Cameron, R.E., Blank, G.B., and Gensel, D.R. Sampling and handling of desert soils. *JPL Technical Report* **32-908**, 1-42 (1966).
26. Kahn, L., 1988.
27. Kahn, L. Lloyd Kahn Method, Determination of Total Organic Carbon in Sediment. *U.S. Environmental Protection Agency Standard Operating Procedure* (1988).
28. White, D.C., Davis, W.M., Nickels, J.S., King, J.D., and Bobbie, R.J., *Determination of the sedimentary microbial biomass by extractible lipid phosphate*. (Springer-Verlag, 1979).

29. White, D.C., in *Methodology for Biomass Determinations and Microbial Activities in Sediments*, edited by C. D. Litchfield and P. L. Seyfreid (American Society for Testing and Materials, Philadelphia, PA., 1979), Vol. ASTM STP 673, pp. 87-103.
30. Bligh, E.G. and Dyer, W.J. A rapid method of total lipid extraction and purification. *Canadian Journal of Biochemistry and Physiology* **37**, 911-917 (1959).
31. White, D.C. and Ringelberg, D.B., in *The Microbiology of the Terrestrial Deep Subsurface*, edited by P. S. Amy and D. L. Haldeman (CRC Press, New York, NY, 1997), pp. 119-136.
32. Cameron, R.E. Abundance of microflora in soils of desert regions. *NASA Technical Report* **32**, 1-16 (1969).
33. Cameron, R.E., Gensel, D.R., and Blank, G.B. Soil studies - desert microflora. XII. Abundance of microflora in soil samples from the Chile Atacama Desert. *JPL Space Programs Summary* **IV**, 140-147 (1966).
34. Eaton, A.D., Clesceri, L.S., Greenberg, A.E., and Franson, M.A.H., *Standard Methods for the Examination of Water and Wastewater*. (American Public Health Association, Washington, D.C., 1999).
35. Yung, P.T., Kempf, M.J., and Ponce, A., presented at the IEEE Aerospace Conference, Big Sky, Montana, 2006 (unpublished).
36. Fell, N.F., Pellegrino, P.M., and Gillespie, J.B. Mitigating phosphate interference in bacterial endospore detection by Tb dipicolinate photoluminescence. *Analytica Chimica ACTA* **426**, 43-50 (2001).
37. Pellegrino, P.M., Fell, N.F., Rosen, D.L., and Gillespie, J.B. Bacterial endospore detection using terbium dipicolinate photoluminescence in the presence of chemical and biological materials. *Analytical Chemistry* **70**, 1755-1760 (1998).
38. Warth, A.D. Liquid chromatographic determination of dipicolinic acid from bacterial spores. *Applied and Environmental Microbiology* **38**, 1029-1033 (1979).
39. Shafaat, H.S. and Ponce, A. Applications of a rapid endospore viability assay for monitoring UV inactivation and characterizing Arctic ice cores. *Applied and Environmental Microbiology* **72**, 6808-6814 (2006).
40. Epstein, S.S. and Rossel, J. Enumeration of sandy sediment bacteria: Search for optimal protocol. *Marine Ecology Progress Series. Oldendorf* **117**, 289-298 (1995).
41. Hurwitz, S.J. and McCarthy, T.J. 2, 3, 5-Triphenyltetrazolium chloride as a novel tool in germicide dynamics. *Journal of Pharmaceutical Sciences* **75**, 912-916 (1986).
42. Sarkar, G. and Sommer, S.S. Parameters affecting susceptibility of PCR contamination to UV inactivation. *Biotechniques* **10**, 590-594 (1991).
43. Nicholson, W. and Setlow, P., in *Molecular Biology Methods for Bacillus*, edited by S. M. Cutting (John Wiley and Sons, Sussex, England, 1990), pp. 391-450.
44. Norland, S., Heldal, M., and Tumyr, O. On the relation between dry matter and volume of bacteria. *Microbial Ecology* **13**, 95-101 (1987).
45. Loferer-Krossbacher, M., Klima, J., and Psenner, R. Determination of bacterial cell dry mass by transmission electron microscopy and densitometric image analysis. *Applied and Environmental Microbiology* **64**, 688 (1998).
46. Rosenberg, M., Gutnick, D., and Rosenberg, E. Adherence of bacteria to hydrocarbons: A simple method for measuring cell-surface hydrophobicity. *FEMS Microbiology Letters* **9**, 29-33 (1980).
47. Schuerger, A.C., Richards, J.T., Newcombe, D.A., and Venkateswaran, K. Rapid inactivation of seven *Bacillus spp*. under simulated Mars UV irradiation. *Icarus* **181**, 52-62 (2006).
48. Newcombe, D.A. *et al*. Survival of spacecraft-associated microorganisms under simulated Martian UV Irradiation. *Applied and Environmental Microbiology* **71**, 8147 (2005).
49. Nicholson, W.L., Schuerger, A.C., and Setlow, P. The solar UV environment and bacterial spore UV resistance: considerations for Earth-to-Mars transport by natural processes and

human spaceflight. *Mutation Research-Fundamental and Molecular Mechanisms of Mutagenesis* **571**, 249-264 (2005).
50. Christner, B.C. Recovery and identification of viable bacteria immured in glacial ice. *Icarus* **144**, 479-485 (2000).
51. Korona, R., Nakatsu, C.H., Forney, L.J., and Lenski, R.E. Evidence for multiple adaptive peaks from populations of bacteria evolving in a structured habitat. *Proceedings of the National Academy of Sciences of the United States of America* **91**, 9037-9041 (1994).
52. Rainey, P.B., Buckling, A., Kassen, R., and Travisano, M. The emergence and maintenance of diversity: insights from experimental bacterial populations. *Trends in Ecology & Evolution* **15**, 243-247 (2000).
53. Treves, D.S., Xia, B., Zhou, J., and Tiedje, J.M. A two-species test of the hypothesis that spatial isolation influences microbial diversity in soil. *Microbial Ecology* **45**, 20-28 (2003).
54. Zhou, J. *et al*. Spatial and resource factors influencing high microbial diversity in soil. *Applied and Environmental Microbiology* **68**, 326 (2002).
55. Madigan, M.T., Martinko, J.M., and Parker, J., *Brock Biology of Microorganisms*. (Prentice Hall, Upper Saddle River, NJ, 2000).
56. Booth, I.R., Cairney, J., Sutherland, L., and Higgins, C.F. Enteric bacteria and osmotic stress: an integrated homeostatic system. *Journal of Applied Microbiology* **65**, 35-49 (1988).
57. Gammack, S.M., Paterson, E., Kemp, J.S., Cresser, M.S., and Killham, K. Factors affecting the movement of microorganisms in soils. *Soil Biochemistry* **7**, 263-305 (1992).
58. Close, R.C., Moar, N.T., Tomlinson, A.I., and Lowe, A.D. Aerial dispersal of biological material from Australia to New Zealand. *International Journal of Biometeorology* **22**, 1-19 (1978).
59. Ericksen, G.E. The Chilean Nitrate Deposits. *American Scientist* **71**, 366-374 (1983).
60. Ericksen, G.E., in *Geological Survey Professional Paper 1188* (US Government Printing Office, Washington DC, 1981), pp. 1-37.
61. Hindle, A.A. and Hall, E.A.H. Dipicolinic acid (DPA) assay revisited and appraised for spore detection. *Analyst* **124**, 1599-1604 (1999).
62. Hitchins, A.D., Greene, R.A., and Slepecky, R.A. Effect of carbon source on size and associated properties of *Bacillus megaterium* spores. *Journal of Bacteriology* **110**, 392 (1972).
63. Wiencek, K.M., Klapes, N.A., and Foegeding, P.M. Hydrophobicity of *Bacillus* and *Clostridium* spores. *Applied and Environmental Microbiology* **56**, 2600-2605 (1990).
64. Carrera, M., Zandomeni, R.O., Fitzgibbon, J., and Sagripanti, J.L. Difference between the spore sizes of *Bacillus anthracis* and other *Bacillus* species. *Journal of Applied Microbiology* **102**, 303-312 (2007).
65. Cameron, R.E. and Blank, G.B. Soil studies - microflora of desert regions. VIII. Distribution and abundance of desert microflora. *JPL Space Programs Summary* **IV**, 193-202 (1965).
66. Cameron, R.E. and Gensel, D.R.e.a. Soil studies - desert microflora. XII. Abundance of microflora in soil samples from the Chile Atacama Desert. *National Aeronautics and Space Administration, Jet Propulsion Laboratory* **Pasadena, CA**, 140-147 (1966).
67. McCormick, N.G. Kinetics of spore germination. *Journal of Applied Bacteriology* **89**, 1180-1185 (1965).
68. Morita, R.Y. Psychrophilic bacteria. *Bacteriological Reviews* **39**, 144-167 (1975).
69. Hills, G.M. Chemical factors in the germination of spore-bearing aerobes - observations on the influence of species, strain and conditions of growth. *Journal of General Microbiology* **4**, 38-47 (1950).
70. Rose, R. *et al*. Comparison of the properties of *Bacillus subtilis* spores made in liquid or on agar plates. *Journal of Applied Microbiology* (2007).

71. Atrih, A. and Foster, S.J. Analysis of the role of bacterial endospore cortex structure in resistance properties and demonstration of its conservation amongst species. *Journal of Applied Microbiology* **91**, 364-372 (2001).
72. Melly, E. *et al*. Analysis of the properties of spores *of Bacillus subtilis* prepared at different temperatures. *Journal of Applied Microbiology* **92**, 1105-1115 (2002).
73. Palop, A., Manas, P., and Condon, S. Sporulation temperature and heat resistance of *Bacillus* spores: a review. *Journal of Food Safety* **19**, 57-72 (1999).
74. Hornstra, L.M., de Vries, Y.P., de Vos, W.M., and Abee, T. Influence of sporulation medium composition on transcription of ger operons and the germination response of spores of *Bacillus cereus* ATCC 14579. *Applied and Environmental Microbiology* **72**, 3746-3749 (2006).
75. Cazemier, A.E., Wagenaars, S.F.M., and ter Steeg, P.F. Effect of sporulation and recovery medium on the heat resistance and amount of injury of spores from spoilage bacilli. *Journal of Applied Microbiology* **90**, 761-770 (2001).
76. Mazas, M., Gonzalez, I., Lopez, M., Gonzalez, J., and Sarmiento, R.M. Effects of sporulation media and strain on thermal resistance of *Bacillus cereus* spores. *International Journal of Food Science and Technology* **30**, 71-78 (1995).
77. Baweja, R.B. *et al*. Properties of *Bacillus anthracis* spores prepared under various environmental conditions. *Archives of Microbiology* **189**, 71-79 (2008).
78. Setlow, B., Atluri, S., Kitchel, R., Koziol-Dube, K., and Setlow, P. Role of dipicolinic acid in resistance and stability of spores of *Bacillus subtilis* with or without DNA-protective α/β-type small acid-soluble proteins. *Journal of Bacteriology* **188**, 3740-3747 (2006).
79. Paidhungat, M., Setlow, B., Driks, A., and Setlow, P. Characterization of spores of *Bacillus subtilis* which lack dipicolinic acid. *Journal of Bacteriology* **182**, 5505-5512 (2000).
80. Setlow, P. Spore germination. *Current Opinion in Microbiology* **6**, 550-556 (2003).
81. Berg, P.E. and Grecz, N. Relationship of dipicolinic acid content in spores of *Bacillus cereus* to ultraviolet and gamma radiation resistance. *Journal of Bacteriology* **103**, 517-519 (1970).
82. Church, B.D. and Halvorson, H. Dependence of the heat resistance of bacterial endospores on their dipicolinic acid content. *Nature* **183**, 124-125 (1959).
83. Slieman, T.A. and Nicholson, W.L. Role of dipicolinic acid in survival of *Bacillus subtilis* spores exposed to artificial and solar UV radiation. *Applied and Environmental Microbiology* **67**, 1274-1279 (2001).
84. Yamazaki, K., Kawai, Y., Inoue, N., and Shinano, H. Influence of sporulation medium and divalent ions on the heat resistance of *Alicyclobacillus acidoterrestris* spores. *Letters in Applied Microbiology* **25**, 153-156 (1997).
85. Gerhardt, P. and Marquis, R.E., in *Regulation of Prokaryotic Development*, edited by I. Smith, R. A. Slepecky, and P. Setlow (American Society for Microbiology, Washington, D.C., 1989), pp. 43-63.
86. Murrell, W.G., in *The Bacterial Spore*, edited by G. W. Gould (Academic Press, New York, 1969), pp. 245-270.
87. Huang, S. *et al*. Levels of Ca^{2+}-dipicolinic acid in individual *Bacillus* spores determined using microfluidic Raman tweezers. *Journal of Bacteriology* **189**, 4681-4687 (2007).
88. Brehm-Stecher, B.F. and Johnson, E.A. Single-cell microbiology: Tools, technologies, and applications. *Microbiology and Molecular Biology Reviews* **68**, 538 (2004).
89. Dubnau, D. and Losick, R. Bistability in bacteria. *Molecular Microbiology* **61**, 564-572 (2006).
90. Mallidis, C.G. and Scholefield, J. The release of dipicolinic acid during heating and its relation to the heat destruction of *Bacillus stearothermophilus* spores. *Journal of Applied Microbiology* **59**, 479-486 (1985).

91. Mallidis, C.G. and Scholefield, J. Relation of the heat resistance of bacterial spores to chemical composition and structure. I. Relation to core components. *Journal of Applied Bacteriology* **62**, 65-69 (1987).
92. Foster, S.J. and Johnstone, K. Pulling the trigger: the mechanism of bacterial spore germination. *Molecular Microbiology* **4**, 137-141 (1990).
93. Johnstone, K. The trigger mechanism of spore germination. *Journal of Applied Bacteriology* **76**, 17S-24S (1994).
94. Vaid, A. and Bishop, A.H. The destruction by microwave radiation of bacterial endospores and amplification of the released DNA. *Journal of Applied Microbiology* **85**, 115-122 (1998).
95. Kaprelyants, A.S., Gottschal, J.C., and Kell, D.B. Dormancy in non-sporulating bacteria. *FEMS Microbiology Letters* **104**, 271-286 (1993).
96. Dufrenne, J., Bijwaard, M., te Giffel, M., Beumer, R., and Notermans, S. Characteristics of some psychrotrophic *Bacillus cereus* isolates. *International Journal of Food Microbiology* **27**, 175-183 (1995).
97. Dufrenne, J., Soentoro, P., Tatini, S., Day, T., and Notermans, S. Characteristics of *Bacillus cereus* related to safe food production. *International Journal of Food Microbiology* **23**, 99-109 (1994).
98. Delignette-Muller, M.L. and Rosso, L. Biological variability and exposure assessment. *International Journal of Food Microbiology* **58**, 203-212 (2000).
99. Keynan, A. and Evenchik, Z., in *The Bacterial Spore*, edited by G. W. Gould and A. Hurst (Academic Press, London, England, 1969), Vol. 1, pp. 359-396.
100. Welkos, S.L., Cote, C.K., Rea, K.M., and Gibbs, P.H. A microtiter fluorometric assay to detect the germination of *Bacillus anthracis* spores and the germination inhibitory effects of antibodies. *Journal of Microbiological Methods* **56**, 253-265 (2004).
101. Setlow, B., Cowan, A.E., and Setlow, P. Germination of spores of *Bacillus subtilis* with dodecylamine. *Journal of Applied Microbiology* **95**, 637-648 (2003).
102. Rode, L.J. and Foster, J.W. Germination of bacterial spores with alkyl primary amines. *Journal of Bacteriology* **81**, 768 (1961).
103. Foerster, H.F. and Foster, J.W. Endotrophic calcium strontium and barium spores of *Bacillus megaterium* and *Bacillus cereus*. *Journal of Bacteriology* **91**, 1333-1345 (1966).
104. Preston, R.A. and Douthit, H.A. Stimulation of germination of unactivated *Bacillus cereus* spores by ammonia. *Journal of General Microbiology* **130**, 1041-1050 (1984).
105. Strange, R.E. and Dark, F.A. Cell-wall lytic enzymes at sporulation and spore germination in *Bacillus* species. *Journal of General Microbiology* **17**, 525-537 (1957).
106. Hills, G.M. Chemical factors in the germination of spore-bearing aerobes - the effects of amino acids on the germination of *Bacillus anthracis*, with some observations on the relation of optical form to biological activity. *Biochemical Journal* **45**, 363-370 (1949).

Designation	Site description	GPS coordinates	Sample type	Depth (cm)	Cl^-, µg/g	F^-, µg/g	SO_4^{2-}, µg/g	NO_3^-, µg/g	PO_4^{3-}, µg/g
A1	Site A – surface 1	S 24° 04.147’ W 069° 51.866’	Soil	0 – 2	68.7	15.5	3050	60.2	3.65
A2	Site A – surface 2								
A3	Site A – surface 3								
A4	Site A – subsurface 1			2 – 20	102	7.45	8160	23.1	< LOD
A5	Site A – subsurface 2								
A6	Site A – subsurface 3								
E1	Site E – surface 1	S 24° 00.685’ W 069° 52.013’	Soil	0 – 2	859	13.3	11400	319	< LOD
E2	Site E – surface 2								
E3	Site E – surface 3								
E4	Site E – subsurface 1			2 – 20	24.4	8.89	8280	15.7	0.807
E5	Site E – subsurface 2								
E6	Site E – subsurface 3								
D1	Depth profile 1, bottom	S 24° 06.102’ W 070° 01.096’	Soil	214	3850	< LOD	11000	1420	< LOD
D2	Depth profile 2			189	ND	ND	ND	ND	ND
D3	Depth profile 3			163	2440	< LOD	9850	1010	< LOD
D4	Depth profile 4			139	ND	ND	ND	ND	ND
D5	Depth profile 5			115	ND	ND	ND	ND	ND
D6	Depth profile 6, top			88	5150	19.3	4200	2730	< LOD

Designation	Site description	Temperature, °C	pH	eH, mV	eC, µS/cm	Water activity, a_w
A1	Site A – surface 1					
A2	Site A – surface 2	36.3	5.97	60.5	2373	0.01
A3	Site A – surface 3					
A4	Site A – subsurface 1					
A5	Site A – subsurface 2	23.5	6.92	5.3	2740	0.06
A6	Site A – subsurface 3					
E1	Site E – surface 1					
E2	Site E – surface 2	25.1	5.89	65	2710	0.10
E3	Site E – surface 3					
E4	Site E – subsurface 1					
E5	Site E – subsurface 2	19.7	6.73	15.5	2360	0.07
E6	Site E – subsurface 3					
D1	Depth profile 1, bottom	14.8	8.14	-68.2	7.12	0.37
D2	Depth profile 2	34.2	ND	ND	ND	0.20
D3	Depth profile 3	15.7	8.19	-71.8	5883	0.20
D4	Depth profile 4	23.9	ND	ND	ND	0.30
D5	Depth profile 5	20.0	8.72	-103.2	2177	0.25
D6	Depth profile 6, top	20.8	8.67	-98.7	9120	0.25

Designation	Site description	GPS coordinates	Sample type	Depth (cm)	Cl^-, µg/g	F^-, µg/g	SO_4^{2-}, µg/g	NO_3^-, µg/g	PO_4^{3-}, µg/g
M1	Mine pit 1			117 m					
M2	Mine pit 2	S 24° 16.002’	Soil	467 m	ND	ND	ND	ND	ND
M3	Mine pit 3	W 069° 04.433’	Water	467 m					
M4	Mine pit 4		Mud	467 m					
H1	Hill 1	S 24° 02.566’ W 069° 37.750’		0 – 20	638	2.55	3390	5.65	< LOD
H2	Hill 2		Soil	0 – 20					
H3	Hill 3	S 24° 04.267’ W 069° 37.885’		0 – 20	ND	ND	ND	ND	ND
H4	Hill 4			0 – 20					
X1	Pre-augmentation	S 24° 04.147’		0 – 20	78	9.67	10600	22.4	< LOD
X2	Post-augmentation	W 069° 51.866’		0 – 20	44.6	< LOD	15700	20.7	22.7
X3	Hydrocyclone	S 24° 06.033’ W 070° 00.051’	Soil	0 – 20	2.95	0.592	171	1.13	0.23
X4	Plant rhizosphere	S 24° 03.596’ W 069° 49.825’		20 – 40	ND	ND	ND	ND	ND

Designation	Site description	Temperature, °C	pH	eH, mV	eC, µS/cm	Water activity, a_w
M1	Mine pit 1	10.0	4.89	121.0	1655	0.37
M2	Mine pit 2	10.1	5.27	105.6	719	1.01
M3	Mine pit 3	18.6	3.53	206.3	30867	ND
M4	Mine pit 4	19.7	ND	ND	ND	ND
H1	Hill 1	37.0	7.48	-29.4	127.3	0.07
H2	Hill 2					
H3	Hill 3	33.9	7.15	-7.0	1045	0.01
H4	Hill 4					
X1	Pre-augmentation	ND	ND	ND	ND	0.01
X2	Post-augmentation	ND	ND	ND	ND	Time-varying[i]
X3	Hydrocyclone	26.1	ND	ND	ND	0.025
X4	Plant rhizosphere	26.5	ND	ND	ND	0.19

Table 9.1 | List of collected samples in the Atacama Desert. [i] Water activity of the post-augmentation sample was measured on a daily basis for a total of 5 days. The values are reported in subsequent figures.

Sample	Non heat shock						Heat shock					
	1/10 R2A cfu/g	Salt agar cfu/g	Soil agar cfu/g	Actinobacteria agar, cfu/g	1/5 TSB mpn/g	Germinable spore/g	1/10 R2A cfu/g	Salt agar cfu/g	Soil agar cfu/g	Actinobacteria agar, cfu/g	1/5 TSB mpn/g	Germinable spore/g
A1	10.0	33.3	453	0	38.0	6.7	0	0	0.67	0	0	ND
A2	46.7	0	0	0	1537	0	0	20	0	0	0	ND
A3	0	460	820	0	232	0	0	0	0.33	0	0	ND
A4	33.3	113	33.3	0	375	13.8	0	0	0.33	0	0	ND
A5	80.0	133	227	0	> 40,000	14.2	0	0	0	0	1537	ND
A6	20.0	33.3	227	0	4900	1.7	0	0	0	0	3600	ND
E1	0	0	0	0	0	0	6.67	107	2	0	0	ND
E2	13.3	26.7	13.3	0	38.0	0.8	0	0	12	0	38.0	ND
E3	0	80	33.3	0	38.0	0.8	26.7	40	13.7	0	14.4	ND
E4	10.0	13.3	767	33.3	1537	0	0	33.3	7	0	59.2	ND
E5	0	6.67	60	0	182	1.3	0	46.7	0	0	103	ND
E6	20.0	0	180	0	3600	3.3	0	0	0	1013	82.4	ND
D1	13.3	33.3	0	0	114	109.6	3.7	353	240	100	114	ND
D2	6.67	0	0	0	7622	118.3	293	520	313	50	38.0	ND
D3	6.67	0	0	0	3600	112.1	393	460	400	46.7	> 40,000	ND
D4	0	0	0	0	> 40,000	75.4	86.7	40	60	0	1011	ND
D5	0	0	0	0	82.4	52.5	26.7	0	60	0	> 40,000	ND
D6	20	0	0	0	2089	16.3	33.3	6.67	6.67	40	14.4	ND

Sample	Non heat shock						Heat shock					
	1/10 R2A cfu/g	Salt agar cfu/g	Soil agar cfu/g	Actinobacteria agar, cfu/g	1/5 TSB mpn/g	Germinable spore/g	1/10 R2A cfu/g	Salt agar cfu/g	Soil agar cfu/g	Actinobacteria agar, cfu/g	1/5 TSB mpn/g	Germinable spore/g
M1	0	0	0	0	724	0	0	0	0	0	> 40,000	ND
M2	0	0	0	0	375	0	0	0	0	0	> 40,000	ND
M3	0	6.67	0	0	> 40,000	15.8	0	0	0	0	> 40,000	ND
M4	0	0	0	0	300	8.3	0	0	0	0	182	ND
H1	0	53.3	253	0	14.4	3.3	0	0	0	0	0	ND
H2	0	53.3	33.3	0	724	3.8	0	0	0	0	114	ND
H3	0	0	0	0	38.0	1.7	0	0	13.3	0	38.0	ND
H4	0	0	66.7	0	724	0.8	0	0	0	0	25.2	ND
X1	0	0	0	0	29.2	0	0	0	0	0	0	ND
X2	0	6.67	13.3	0	1537	0.8	6.67	0	13.3	6.67	4900	ND
X3	0	2260	1540	0	> 40,000	15	0	6.67	0	0	> 40,000	ND
X4	0	113	0	0	4900	4.6	0	147	40	0	82.3	ND

Sample	TOC, μg/g	PLFA, cells/g	Percent of total PLFA						Carbon dating, BP
			TerBrSats	Monos	BrMonos	MidBrSats	Nsats	polyenoics	
A1									
A2	1700	2.89×10^6	36.96	44.57	0.00	3.90	14.15	0.42	ND
A3									
A4									
A5	880	1.02×10^6	31.06	54.20	0.00	0.26	13.83	0.64	ND
A6									
E1									
E2	1100	1.55×10^6	29.03	54.07	0.00	3.20	13.23	0.46	ND
E3									
E4									
E5	1200	4.19×10^6	21.49	63.75	0.33	1.82	12.35	0.25	ND
E6									
D1	3400	9.81×10^4	0.00	74.84	0.00	0.00	25.16	0.00	35040 ± 320
D2	ND	3.57×10^4	0.00	37.76	0.00	0.00	62.25	0.00	ND
D3	2700	2.25×10^4	0.00	35.05	0.00	0.00	64.95	0.00	ND
D4	ND	2.06×10^4	0.00	49.87	0.00	0.00	50.13	0.00	ND
D5	ND	2.14×10^4	0.00	33.95	0.00	10.17	55.89	0.00	ND
D6	1500	1.55×10^4	0.00	17.66	0.00	0.00	82.34	0.00	25600 ± 180

Sample			Percent of total PLFA						
	TOC, μg/g	PLFA, cells/g	TerBrSats	Monos	BrMonos	MidBrSats	Nsats	polyenoics	Carbon dating, BP
M1 M2 M3 M4	ND	ND	ND	ND	ND	ND	ND	ND	ND
H1 H2 H3 H4	< LOD	6.09×10^4	17.2	40.18	0.00	7.52	35.11	0.00	ND
X1	870	0	0	0	0	0	0	0	ND
X2	750	2.89×10^6	28.36	52.70	0.00	0.10	18.81	0.00	ND
X3	< TOC	3.93×10^5	13.17	63.70	0.00	3.10	19.56	0.47	ND
X4	ND	ND	ND	ND	ND	ND	ND	ND	ND

Table 9.2 | Microbiological results of the Atacama Desert. ND = not determined.

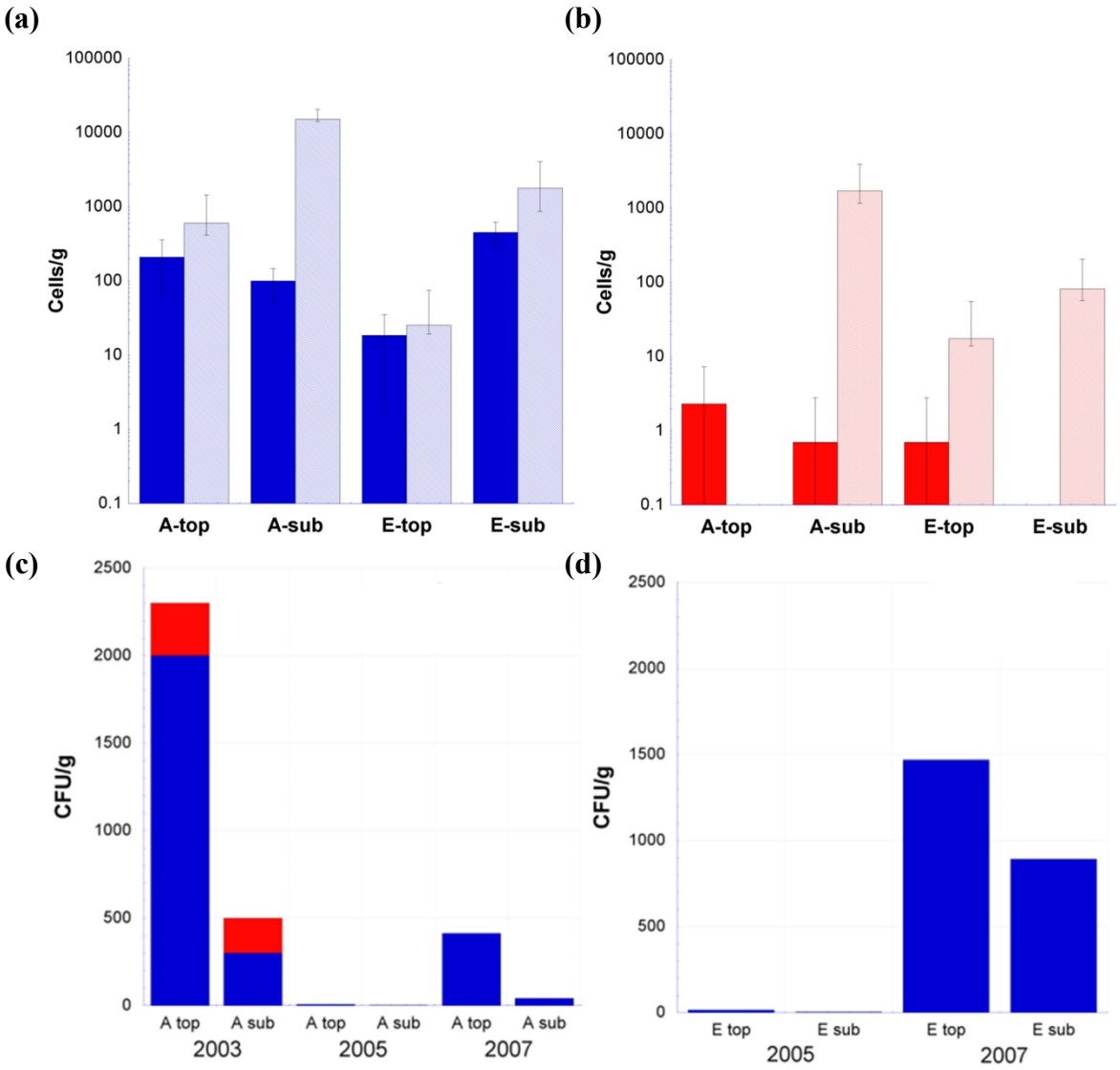

Figure 9.1 | Culture-based results on two sites (A and E) in the Atacama Desert. The designation *top* corresponds to the 3-cm layer closest to the soil surface; *sub* corresponds to the 12-cm subsurface layer. Solid color refers to spread plating results (a combination of 5 different aerobic media) and shaded color refers to the most probable number (MPN) results on the **(a)** non heat shock results and **(b)** heat shock results in sites A & E. Comparisons are made with previous sampling expeditions to **(c)** site A and **(d)** site E. Only full-strength spread plating on R2A are compared in these two cases. Blue color designates the non heat shock results and red color designates the heat shock results.

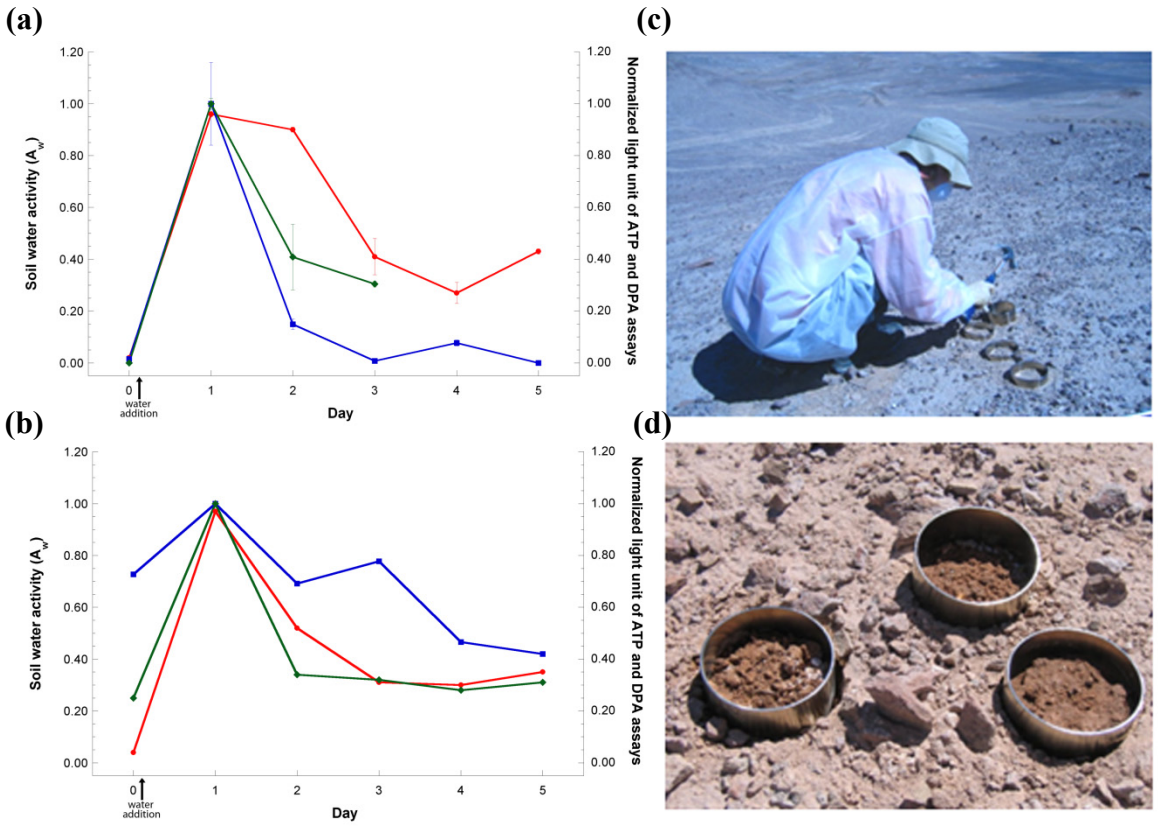

Figure 9.2 | Soilborne microbial change in response to water augmentation in Atacama Desert soils. Timecourses of microbial activity in terms of ATP (red plots), endospore germination propensity in terms of DPA (green plots) and soil water activity (blue plots) were measured with Atacama Desert soil after a simulated 27-mm rain event conducted (**a)** *in situ* in the Atacama Desert and **(b)** under dry and sterile laboratory conditions in a biohazard safety cabinet. **(c)** A researcher carried out the water augmentation experiment wearing gloves, mask and gown facing windward to minimize contamination. **(d)** Stainless steel rings were entrenched halfway into the soil to confine a specified amount of soil for water addition. Notice the color change.

(a)

	cfu g^{-1}		mpn g^{-1}		germinable spores g^{-1}
	non-HS	HS	non-HS	HS	non-HS
in situ					
Pre-augmentation	0.0	0.0	29.2	0.0	0.0
Post-augmentation	6.7 (9.4)	6.7 (9.4)	1537.3	4899.2	0.8 (0.9)
lab					
Pre-augmentation	6.7 (9.4)	0.0	59.2	0.0	1.3 (1.1)
Post-augmentation	28.0 (25.5)	8.0 (6.9)	723.6	1537.3	2.2 (1.5)

(b)

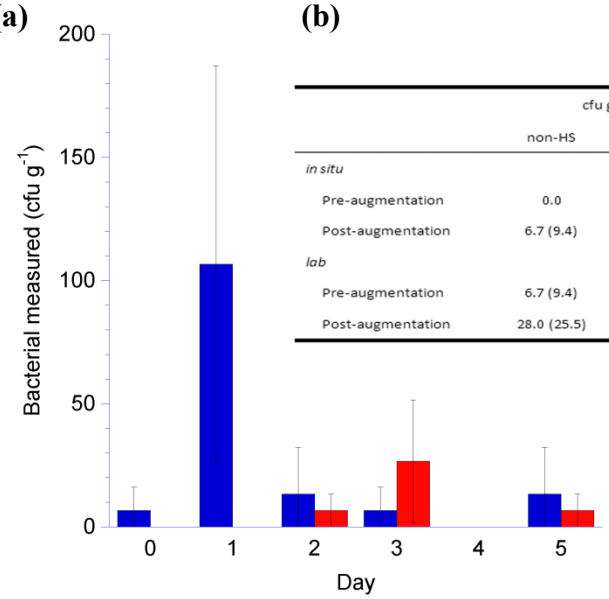

Figure 9.3 | **(a)** The table shows the water augmentation results obtained using culture-based spread plating and MPN methods, as well as the culture-independent µEVA. Numbers in brackets represent the standard deviation based on 12 plates for cfu enumeration and 24 field of views for germinable spore enumeration. The confidence interval associated with the MPN method is not shown for brevity. Only non-heat shock results were obtained using µEVA because this assay probes for the presence of endospores only. Water augmentation performed on 500°C-kilned soil samples under laboratory conditions showed negative results in all of the analyses. **(b)** Changes in the number of culturable bacteria (non heat shock, blue bars; heat shock, red bars) before and after water augmentation preformed under laboratory conditions. Error bars represent 95% confidence interval.

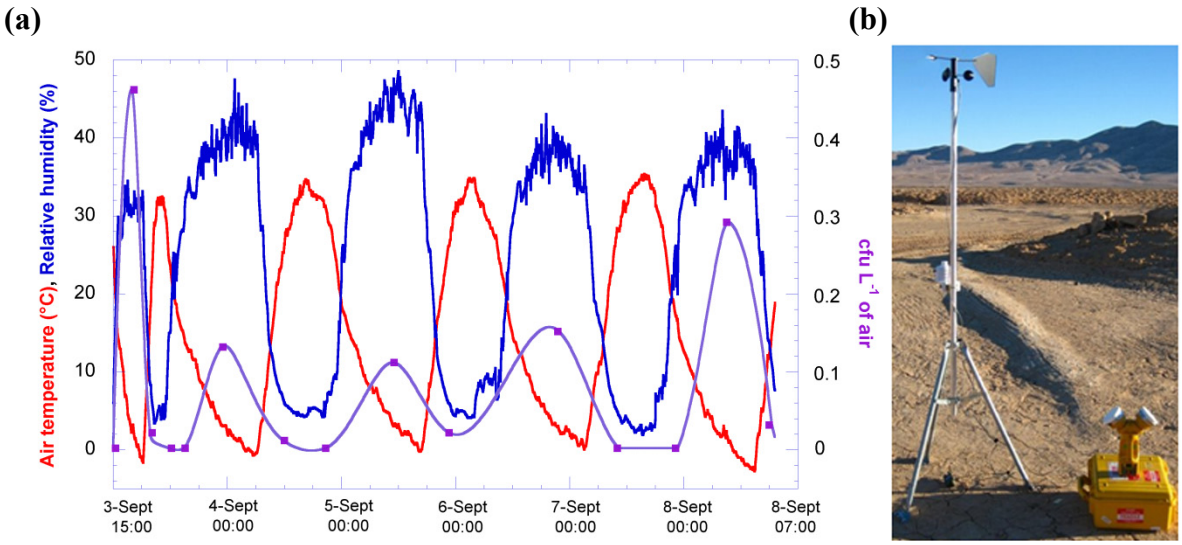

Figure 9.4 | Weather monitoring and air sampling in the Atacama Desert. **(a)** Blue plot represents relative humidity and red plot represents the air temperature taken every 15 min using a portable weather station. Purple plot represents the air sampling results collected by the SAS air sampler in terms in cfu L^{-1} of air on 1/10 R2A incubated aerobically under room temperature. **(b)** Configuration of the weather station and SAS air sampler in the desert.

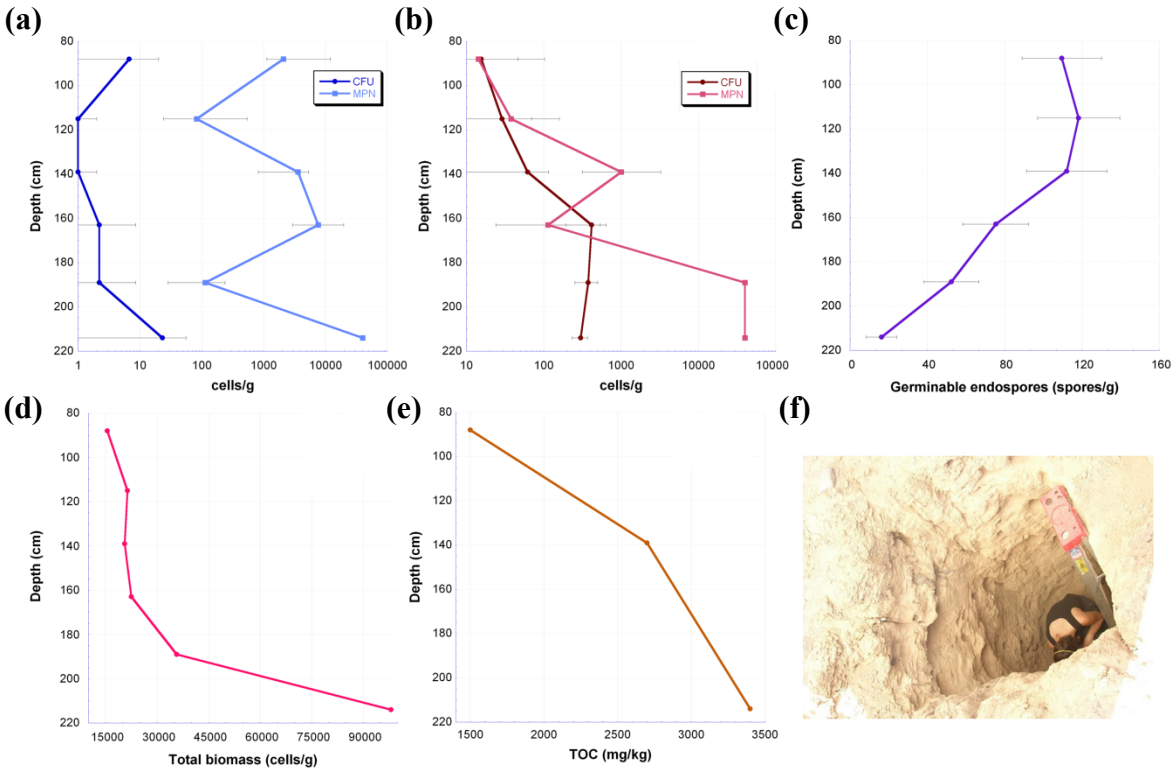

Figure 9.5 | Microbial numbers along a transect of depth profile in a soil pit in the Atacama Desert. Culturable counts were obtained using spread plating and MPN methods on **(a)** non-heat shock and **(b)** heat shock samples. Culture independent methods were also employed, namely **(c)** μEVA, **(d)** phospholipid fatty acid analysis and **(e)** total organic carbon analysis, as different proxies for microbial abundance. Error bars show the 95% confidence interval (n = 12 for CFU enumeration, n = 3 for MPN and n = 24 fields of view for μEVA). **(f)** Picture of the soil pit where which the depth profile data were measured.

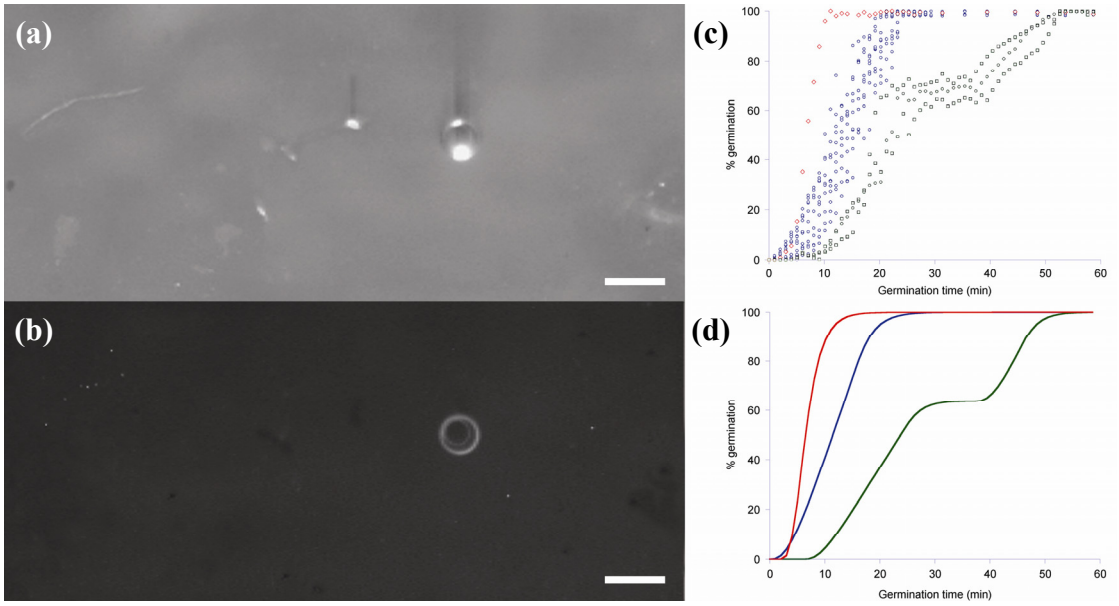

Figure 9.6 | µEVA results on the Atacama soil extract. Left panel shows an **(a)** ungated and **(b)** time-gated micrograph. Scale bar, 100 µm. Some of the dirt and lint in the ungated picture disappear in the gated image. Germinating endospores, manifested as bright spots, in the gated image exhibit luminescence timecourses depicted in **(c)**. The timecourses of germinating endospores from the Atacama Desert broadly fall into 3 patterns, as modeled mechanistically in **(d)** by parametrizing the microlag period, micro-germination time and transition probabilities into hypothetical triggering states during endospore germination. Although the bubble still exists in the time-gated image, it can easily be differentiated from endospores by examining its intensity profile over time.

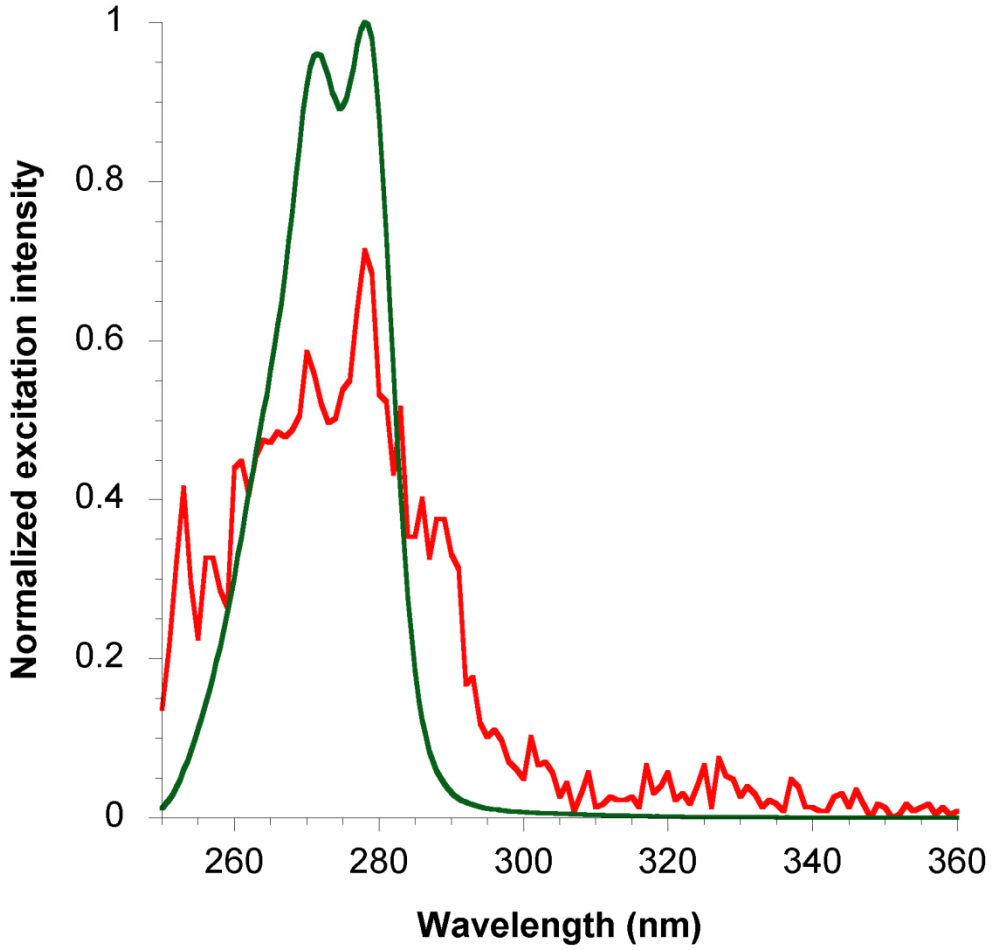

Figure 9.7 | Qualitative determination of DPA from Atacama soil samples using SpectroEVA. After autoclave of soil slurry, DPA was extracted with ethyl acetate from the aqueous phase after adjustment of the suspension to pH 1.8 (Warth, 1979). Green plot shows a pure 1 µM Tb-DPA reference excitation spectrum. The red plot shows the excitation spectrum of soil extract (equivalent to 50 g of Atacama soil) with 100 µM $TbCl_3$ measured with a phosphorimeter with a 50-µs delay.

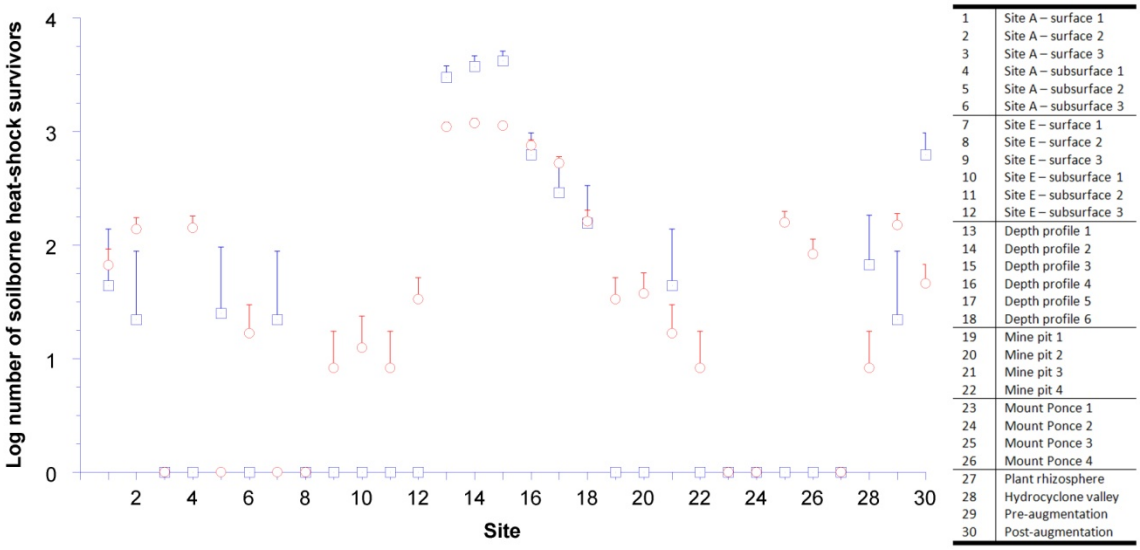

Figure 9.8 | Comparison of spread plating (blue) and μEVA (red) over 30 different heat shocked Atacama Desert soil samples. Only the upper bounds of the 95% confidence interval are shown for clarity reason because of the disproportionately extended lower bounds due to the logarithmic y-axis.

Designation	Species	Source	Growth temperature (°C)	Sporulation temperature (°C)	Sporulation %	Germination temperature (°C)
A1	*Bacillus subtilis HDYM-34*	Atacama Desert, Chile	30	30	95%	37
A2	*B. pumilis XJU-3*	Atacama Desert, Chile	30	30	70%	37
A3	*B. pumilis JH-4*	Atacama Desert, Chile	30	30	70%	37
A4	*B. amyloliquefaciens*	Atacama Desert, Chile	37	30	70%	37
A5	*B. vallismortis*	Atacama Desert, Chile	37	30	90%	37
B1	*B. atrophaeus*	Raven Biological Lab.	37	30	Purchased as spores	37
B2	*B. atrophaeus*	ATCC	37	30	99%	37
B3	*B. subtilis* 168	ATCC	30	30	99%	37
B4	*B. subtilis natto*	Isolated from spore powder	37	30	95%	37
B5	*B. cereus*	Raven Biological Lab.	30	30	Purchased as spores	37
B6	*B. megaterium*	ATCC	30	30	95%	37
B7	*B. licheniformis*	ATCC	37	30	99%	37
B8	*B. pumilis*	ATCC	37	30	70%	37
C1	*Geobacillus stearothermophilus*	Autoclave spore strip	55	50	60%	65
C2	*G. tropicalis*	JPL soil	55	50	80%	65
C3	*G. thermodenitrificans*	JPL soil	60	50	65%	65
D1	*B. longisporus*	DSMZ	15	7	70%	22
D2	*B. simplex*	JPL soil	12	7	70%	22

Table 9.3 | Species for ecology study. ATCC standards for American Type Culture and Collection. DSMZ stands for German Collection of Microorganisms and Cell Cultures. JPL stands for Jet Propulsion Laboratory.

Designation	Spore size (μm^3)	DPA content ($fmol/\mu m^2$)	Hydrophobicity	Heat Resistance D_{90}-value (min)	UV resistance D-value (min)	Micro-lag, t_0 (min)	Germination time, α (min)	Transition probability 1, λ_s	Transition probability 2, λ_c	% germinable	% culturable (without activation)	% culturable (with activation)	% Viable-cut-not-culturable
A1	2.26	0.270	0.0	19.1	27.3	0	30	0.6	0.08	89.7	13.4	31.2	58.5
A2	8.41	0.155	29.5	24.9	28.5	260	850	0.4	0.008	76.0	20.7	50.5	25.5
A3	0.39	1.158	0.0	14.5	23.9	200	760	0.4	0.008	79.6	21.5	49.1	30.5
A4	0.68	0.840	0.0	25.6	36.7	20	1020	0.4	0.004	88.1	41.5	88.8	-0.7
A5	2.69	0.178	0.0	14.0	15.1	0	40	0.6	0.08	68.8	18.7	61.5	7.3
B1	2.06	0.101	28.9	26.6	23.5	5	23	0.5	0.05	81.9	27.4	83.2	-1.3
B2	2.38	0.171	59.2	4.7	22.5	4	8	0.4	0.10	96.8	9.35	71.2	25.6
B3	1.93	0.192	10.6	25.2	23.8	0	1	0.6	0.10	34.8	3.75	45.7	-10.9
B4	2.00	0.326	8.6	23.2	32.5	1	3	0.6	0.25	95.6	50.9	98.5	-2.9
B5	2.18	0.127	86.7	15.0	14.2	0	1	0.6	0.08	41.3	20.9	61.1	-19.8
B6	5.01	0.166	9.0	12.4	28.2	3	15	0.6	0.06	96.1	23.8	100	-3.9
B7	1.59	0.301	13.8	7.0	8.8	1	16	0.6	0.20	58.3	5.19	33.3	25.0
B8	1.40	0.174	86.0	5.1	46.5	3	6	0.6	0.4	79.1	3.90	18.5	60.6
C1	3.01	0.267	7.8	68.2	13.8	5	2	0.6	0.03	33.3	11.3	22.5	10.8
C2	2.59	0.310	36.1	58.2	16.4	20	25	0.6	0.04	22.8	4.87	13.4	9.4
C3	1.84	0.309	15.0	53.8	20.9	35	42	0.6	0.04	19.5	1.80	11.2	98.3
D1	1.52	0.992	0.0	1.2	34.2	10	520	0.4	0.01	58.2	37.0	45.5	12.7
D2	2.01	0.926	0.0	3.3	29.7	230	1020	0.4	0.008	8.48	2.54	2.35	6.13

Table 9.4 | Data of the different thermophilic, mesophilic, psychrophilic laboratory and environmental strain endospores. In the germination section, the best germinant combination was used in the modeling and calculation of percent germinable. A combination of L-alanine and AGFK was usually the best germinant, and sometimes AGFK itself worked optimally for *B. megaterium* endospores and L-alanine plus inosine worked optimally for *B. cereus* and psychrophilic endospores.

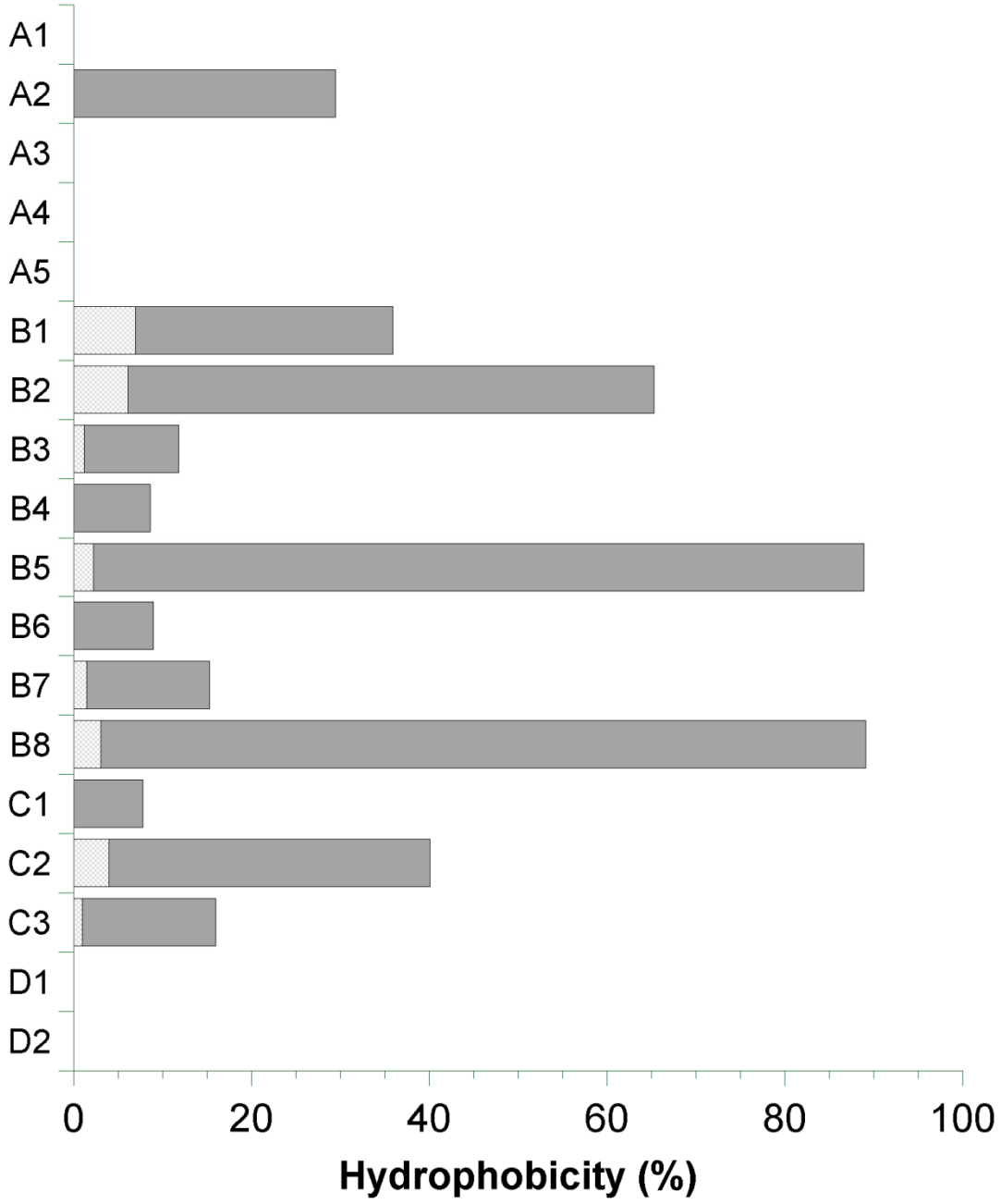

Figure 9.9 | Measurement of hydrophobicity. Solid bars represent hydrophobicity of endospores and the shaded empty bars represent that of vegetative cells.

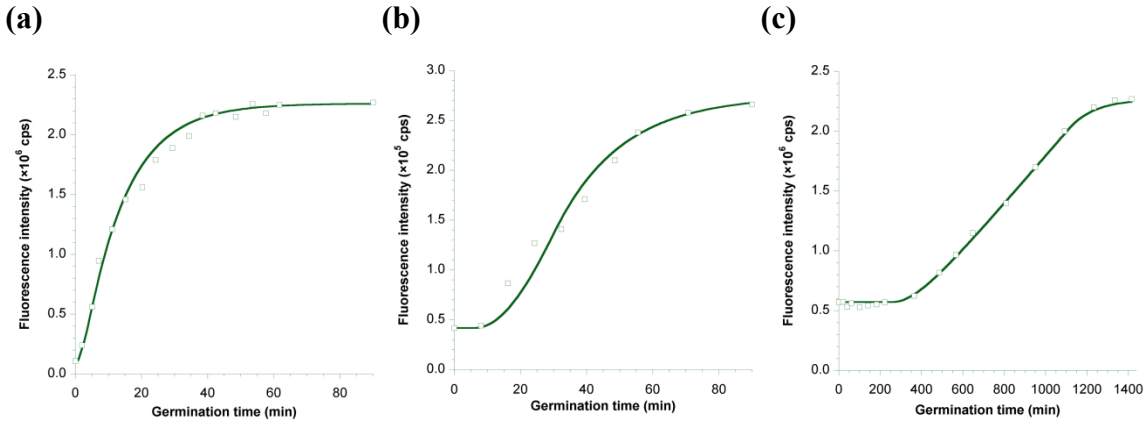

Figure 9.10 | Kinetics of L-alanine-induced endospore germination. **(a)** Lab-strain *B. cereus* demonstrated no lag period and finished germination in less than 60 min, giving t_0 = 0 min, α = 1 min, λ_a = 0.6 min^{-1} and λ_b = 0.08 min^{-1}. **(b)** Lab-strain *B. atrophaeus* endospores demonstrated a lag period before a synchronous germination event, giving t_0 = 4 min, α = 8 min, λ_a = 0.4 min^{-1} and λ_b = 0.10 min^{-1}. **(c)** *B. pumilus XJU-3* endospores isolated from the Atacama Desert UV demonstrated a prolonged course of germination reaching plateau after 24 hours. The parameters are t_0 = 260 min, α = 850 min, λ_a = 0.4 min^{-1} and λ_b = 0.008 min^{-1}.

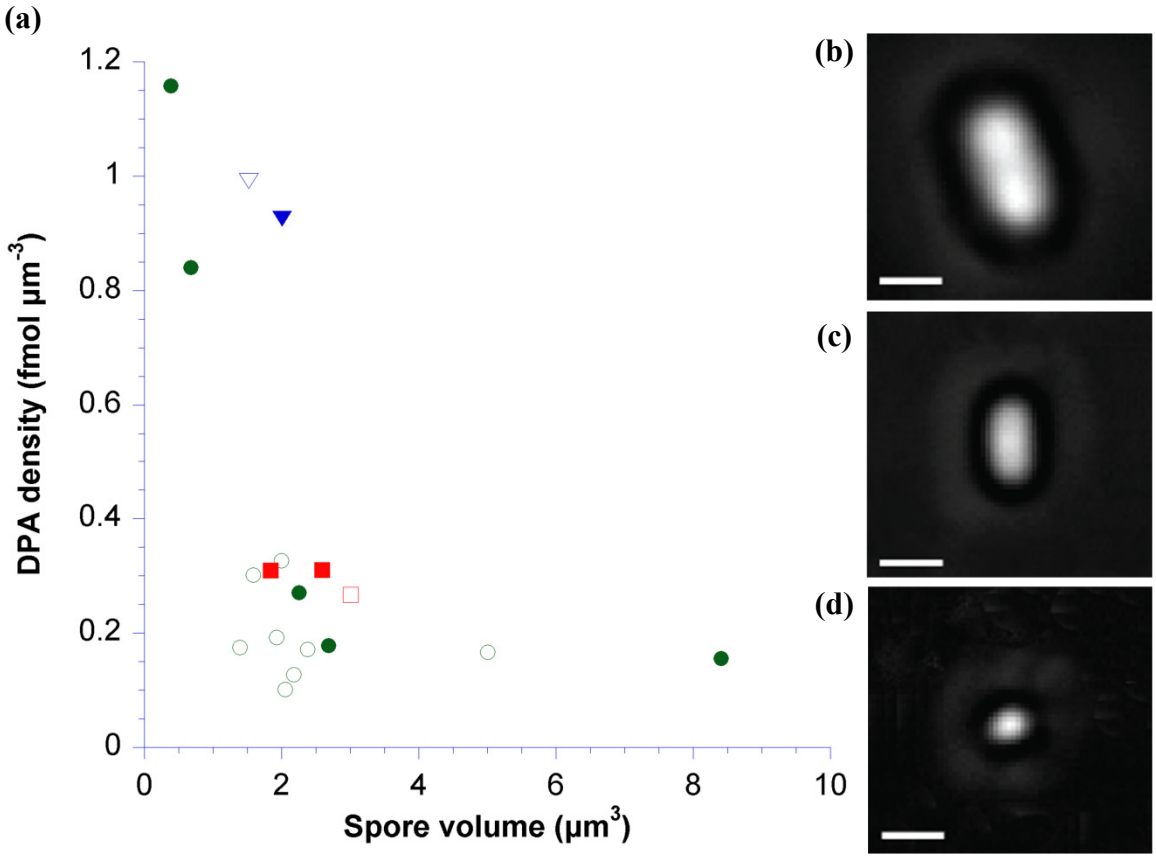

Figure 9.11 | **(a)** DPA density vs. spore volume plot. Solid data points represent environmental strains and empty data points represent laboratory-grown strains. Thermophiles are represented in red, mesophiles in green and psychrophiles in blue. Phase contrast image of the endospores of **(b)** *B. amyloquedaciens* isolated from Atacama Desert; **(c)** lab-strain *B. subtilis* 168; and **(d)** *B. pumilus* XJU-3 isolated from Atacama Desert. Scale bar, 1 µm.

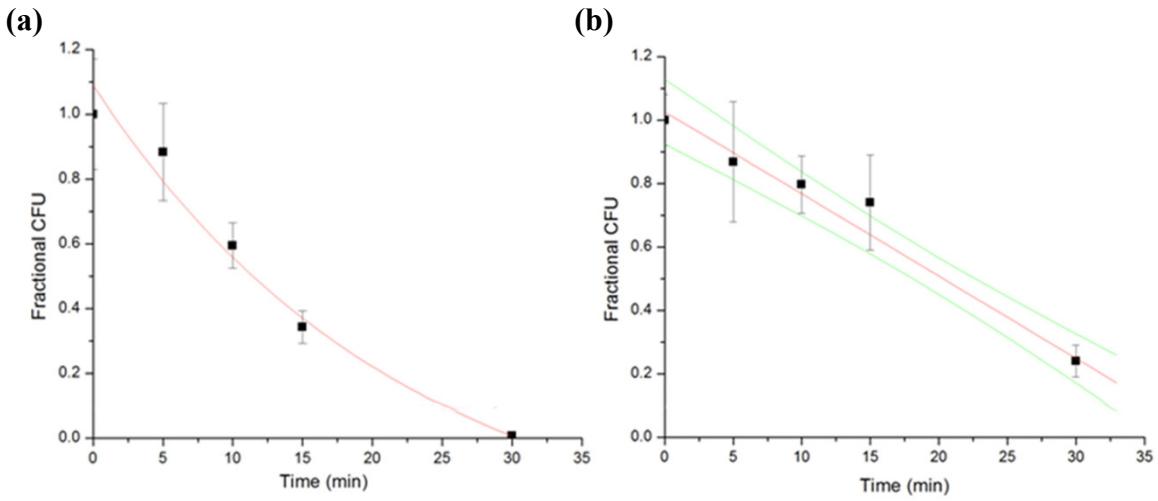

Figure 9.12 | **(a)** UV inactivation (22.9 μW cm^{-2} @ 254 nm) of *B. amyloliquefaciens* endospores isolated from the Atacama Desert. D-value is determined to be 25.1 min. **(b)** 90°C-wet heat inactivation of *B. subtilis* HDYM-34 endospores isolated from the Atacama Desert. D-value is calculated as 35.8 min.

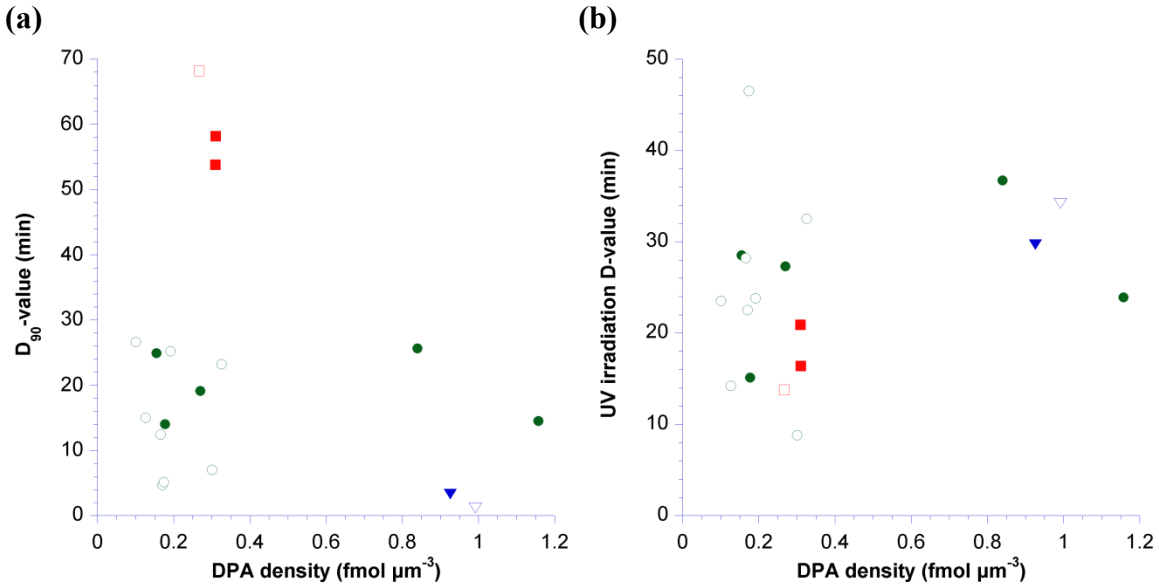

Figure 9.13 | Solid data points represent environmental strains and empty data points represent laboratory-grown strains. Thermophiles are represented in red, mesophiles in green and psychrophiles in blue. **(a)** Correlation of DPA density and D-values of heat inactivation at 90°C. **(b)** Correlation of DPA density and D-values of UV inactivation at 22.9 µW cm^{-2} @ 254 nm.

CHAPTER 10: CONCLUSION

Ever since endospores had been discovered independently by Cohn, Koch and Tyndall in the latter part of the 19th century[1-4], their extreme resistance and hardy structure have fascinated the field of microbiology. They are one of the most differentiated and evolutionary capable living organisms on Earth. They are omnipresent and omnipotent, integrating survival capabilities from halophiles, mesophiles, psychrophiles, thermophiles, etc. They inhabit the air, soil, deep-sea sediments, permafrost and ice cores. They are the airborne carrier agent for anthrax attack and bio-insecticide. They determine the expiration dates in pasteurized products. They can remain dormant in soil and amber for millions of years before waking up and germinate back to vegetative form. They are even postulated to have traveled billions of light years from other planets to the Earth *via* meteorites.

The multifaceted world of endospores has been explored in this thesis project. It is not difficult at this point of our study to reach the conclusion that while each of the individual habitats for endospores are different, endospores themselves are highly conserved in terms of their sporulation, germination and outgrowth properties, varying to some extent.

I conclude this thesis by assessing the capacity of endospores in fulfilling the roles of acting as surrogate for total biomass in a closed system, reflecting key

environmental variables and providing early warning signs of an anticipated stressor. The assessment has been carried out comprehensively from sampling in the air, validating bioburden level on surfaces and ecological systems in extreme habitats. Sharing a concerted similarity, spacecraft air, spacecraft surfaces and extreme environments are all good examples of a closed system. The air inside a space station or spacecraft is no doubt a closed system. Spacecraft hardware has to be assembled in highly controlled clean rooms in designated facilities. And we can also find closed systems in environmental extremes such as the ice cores in which the microbes are frozen, and the subsurface soil habitat the Atacama Desert where the absence of moisture makes dormant life forms undisturbed. Endospores have been found to be a good and reliable biological indicator to suit the aforementioned roles because (1) they are responsive to indicate impending changes in key changes in the ecosystem, e.g., they react to the presence of water and nutrients; (2) they are ubiquitous in almost all terrestrial environments; (3) they can readily be monitored continuously by the technology developed in our lab over a wide range of environments; (4) the detection technology is highly specific to endospores because of the uniqueness of DPA in the natural environment; (5) the detection technology is an automated and cost-effective approach; (6) the detection principle is highly versatile and can be amenable to be integrated into comprehensive monitoring systems. In conclusion, an

effective germination-based endospore detection tool has been developed to complement the current cultivation and nucleic acid approaches to answer basic questions in microbiology, ecology and astrobiology.

10.1 Development of Automated Bacillus Spore Viability Instrumentation for Sterilization Validation, Biodefense and Astrobiology

Previously, a luminescence time-gated microscopy technique called Rapid *Bacillus* Spore[1] Viability Assay (Rapid BSVA) was developed and validated in Dr. Ponce's laboratory. Rapid BSVA enables the enumeration of single germinable *Bacillus* spores in less than an hour. The method is based on direct counting of individual endospores under a time-gated microscope, where the image contrast is generated by a highly luminescent complex that forms between dipicolinic acid (DPA) released *via* spore germination and terbium ions previously doped into the substrate. The highly luminescent and long-lived terbium dipicolinate complex, acting as an intrinsic luminescence probe for each endospore, can be resolved spatially and temporally under pulsed UV excitation. Currently, Rapid BSVA consists of a bench-top instrument. Under NPP funding, I will develop a second generation prototype of Rapid BSVA by miniaturizing the bench-top instrument into a portable,

[1] In this document, references to spores denote bacterial spores/endospores.

high-throughput and automated device that will find application in (1) monitoring the efficiency of post anthrax attack decontamination, (2) quantifying germinable spore population in spacecraft assembly facilities, (3) astrobiology by evaluating germinability of the most durable form of life in the most extreme environments (e.g., Atacama Desert, Chile), and (4) the effect of spore injury and repair on germination system subjected to different inactivation regimens.

10.1.1 Statement of problem

Currently, the effectiveness of a sterilization regime is monitored by spores in the form of biological indicators, frequently requiring incubation periods in excess of 48 hours for a detectable level of colony formation[5]. In hospitals and spacecraft assembly facilities, such a long quarantine period is undesirable due to the high cost of having devices inactive and the possibility of secondary contamination. The shorter the analysis time, the faster the processed devices can be returned to use with a higher degree of confidence in sterility and fidelity of life detection. In particular, inhalational anthrax is curable if antibiotics are given promptly after infection[6]. A rapid, automated and high-throughput spore-detection method thus grants precious time for emergency management to mitigate catastrophic anthrax attack by appropriate medical care and timely decontamination. Rapid BSVA has therefore been

developed to address the aforementioned issues.

10.1.2 Background and relevancy to previous work

Endospores are highly differentiated cell types in the life cycle of sporeforming genera of *Bacillus* and *Clostridium*. They are formed within vegetative cells during sporulation, which is frequently triggered in response to adverse environments, such as starvation and desiccation. Spore DNA is protected from the environment by a surrounding spore coat comprised of calcium ions, dipicolinic acid (DPA) and protein layers. DPA was first discovered in spores by Powell in 1953[7]. It is present in the protoplast of spores and constitutes 5% - 15% of the dry weight. DPA is synthesized during sporulation and is a unique chemical found only in bacterial spores and amounts to a high local concentration of 1 molar, thereby serving as a confirmatory biomarker for spores. With no detectable metabolism, bacterial spores are ubiquitous in environmental extremes, such as freezing, boiling, pressure and desiccation. Once favorable conditions return, spores undergo germination and outgrowth to return to vegetative cells that can actively multiply to cause food spoilage, contaminations, diseases, etc.

Sterilization has been known since historic times as a cleansing and purifying agent. In 1832 William Henry found that contaminated garments treated with

pressurized steam could be worn with impunity by others; Louis Pasteur also used a pressure vessel with safety valve for contagion inactivation. Their work laid the foundation for the sterilization efforts nowadays, such as autoclave, radiation and ethylene oxide. Although the concept of sterility is simple and straightforward, the verification of a sterile state is very complex. The inability of a sterility test to detect low levels of contamination with a reasonable number of samples has been recognized since early 1970s[8]. Validation of sterilization is a critically important topic on planetary protection, homeland security and health care.

Dr. Adrian Ponce's research team at JPL pioneers in spore detection methodologies ranging from traditional cultivation, to molecular biology methods and novel techniques such as DPA-triggered terbium luminescence assay[9-14]. As a graduate student, I am part of the team in the development and implementation of anthrax smoke detector, endospore viability assay, and the 1st generation Rapid BSVA in the past 4 years[15]. With this proposed work, I would like to apply my experience gained on my thesis with that of my bioengineering graduate curriculum to build a portable, high-throughput and automated 2nd generation Rapid BSVA instrument to investigate spore viability in extreme environments, and to perform on-site sterility assessments (e.g., spacecraft assembly facilities).

10.1.3 General methodology and procedures to be followed

Currently, Rapid BSVA involves a 3-step procedure: swab-rinse, sample preparation and imaging. First, spores are collected by sterile cotton applicators from surfaces, resuspended into water, subsequently filtered, concentrated and immobilized onto membrane filters. Spore-laden filters are placed on top of a germination agarose substrate comprised of terbium and L-alanine as a spore germinant. When triggered by L-alanine, spores germinate and release ~10^8 DPA molecules. Individual spores, or more specifically the resultant Tb-DPA luminescence halos surrounding the germinated spore bodies, are imaged with a time-gated microscope, with a distinct intensity profile from minutes to an hour based on characteristic germination kinetics of the species. Figure 10.11 shows the working principle of the assay[16,17]. Each of these bright spots is assigned as a germinable spore unit (GSU), in analogous with colony-forming unit (CFU).

DPA acts as a light-harvesting antenna to transfer the energy to Tb^{3+} in the proximity upon UV excitation. Luminescence can be observed due to energy transfer from the lowest-lying DPA triplet excited state to the emissive $^5D_4$ state of Tb^{3+}. Significant luminescence enhancement can be observed because of the large energy gap between the Tb^{3+} ground state and emissive states (20,500 cm^{-1}). In addition, terbium dipicolinate (Tb-DPA) is characterized by a long millisecond luminescence

lifetime[18-21]. Therefore, a microsecond time gating can effectively eliminate background interference, whose lifetimes are usually on the order of 1-10 nanoseconds[22].

10.1.4 Proposed work

Task 1 - Design and test an automated, field portable and high-throughput Rapid BSVA instrument

The current Rapid BSVA is a benchtop instrument consisting of bulky components such as a xenon flashlamp and stereoscopic microscope. Figure 10.2 illustrates the design for the next generation instrument, which is automated, field portable and able to handle parallel sample processing. The excitation light source will be miniaturized using solid-state, deep UV LEDs, and the microscope will be reduced to a focusing objective for magnification and piezoelectric actuators for focusing. The LED controller will serve as the master oscillator that controls the overall repetition rate of data acquisition. The camera will be synchronized with the LED pulses *via* a control box that is triggered by TTL-inputs from the LED control system. The entire assembly will be put inside a light-tight enclosure. To enable high sample throughput, we will employ a 96-well assay plate that will be mounted on a 3D stage, such that each well can be assayed in series. Each reading of germinable spores by instrument

will require less than 20 seconds, thus enabling 96 wells to be read out in approximately 30 minutes.

Spore germination on agarose surface follows the reported micro-germination kinetics[23,24]. DPA released from single *B. atrophaeus* and *B. subtilis* spores manifest as individual bright spots in 15 minutes under time-gated microscopy due to local formation of Tb-DPA (figure 10.3). Current image analysis is done in ImageJ based on simple image segmentation and thresholding. The 2nd generation will switch to Matlab to handle the large number of images. Assignment of germinable spores will be based on intensity and size using a neural network system. Adaptive thresholding will be applied to segment pixels that are 3 times brighter than the background with a characteristic rising intensity. Each bright spot must exhibit a continuous rising intensity over the course of germination in order to register a spore count. This criterion will reduce the probability of false positives. The 8-connected adjacent pixels will be analyzed to screen for spore clumps. The number of spores present will be calculated by dividing the squared sum of neighboring pixel brightness by the mean brightness of an individual spore determined empirically. This will be done in a recursive way until all of the pixels are counted and marked. Hardware control and image analysis will be executed using LabVIEW.

Task 2 - Construct spore biological indicator modules for high-throughput monitoring of spore inactivation

In the event of a biological attack, we envision that spore biological indicator modules be distributed to witness the effectiveness of a sterilization regimen applied for building restoration (e.g., vaporized hydrogen peroxide, ethylene oxide, or chlorine dioxide). Each module contains a PDMS strip with 4 spots, 3 spots loaded with 10^7 CFU of spores and 1 control negative spot. After distributing 24 individual modules in the contaminated environment (e.g., in drawers, HVAC units, cabinets, etc.) and following the sterilization procedure, the modules can be collected and readily assembled into 96-spot array. The array can be constructed by linking modules as shown in figure 10.4.

The 96-spot array is then inverted and placed onto a 96-well fixture. This presses the spores against the Tb/L-alanine doped agarose and triggers the germination process for any surviving, germinable spores. The spore-laden PDMS is then secured into place with two clips that allows the removal of the biological indicator array minus the PDMS strips. After 10 minutes of germination, the 96-well assay plate is ready for analysis by the Rapid BSVA reader.

Task 3 - Employ high-throughput Rapid BSVA for analysis of environmental surfaces

sampled with cotton swab method

Stainless steel coupons (2 × 2 in) inoculated with spore populations ranging from 0 to 10^7 spores will be swabbed to remove spores from the surfaces. Spores will be resuspending by sonication and shaking. Extracts from 96 samples will be pipetted, 12 at a time with a multi-pipettor, into a 96-well filtration device (Figure 10.5) and filtered onto a 0.2 μm polycarbonate membrane filter. The membrane filter with 96 filtration spots will then be placed, spore-side up, onto the 96-well assay plate and covered with a PDMS layer. After 20 minutes of germination, the 96-well assay plate is ready for germinable spore analysis by the Rapid BSVA reader. Rapid BSVA will be employed to evaluate the cleanliness of spacecraft assembly facilities.

As a preliminary test, Rapid BSVA yields comparable results as cultivation in evaluating bioburden in a spacecraft assembly facility, with entrance samples showing negative results and floor metal plate samples showing 3.6 germinable endospores cm^{-2} and 1.2 cfu cm^{-2}, respectively. The new prototype will enable parallel processing and expedite the analysis time in order to achieve rapid on-site monitoring of sterility.

Task 4 – Apply Rapid BSVA on samples collected form extreme environments.

One of the scientific goals for the Mars Science Laboratory mission is to assess the biological potential of at least one selected site on Mars. The surface and subsurface

of Mars are characterized by intense UV radiation, presence of oxidizing compounds, absence of water and low temperatures, collectively considered as inhospitable for life as concluded by the Viking mission[25]. Yet the recent discovery of extremophiles thriving in various extreme conditions on Earth has revived the interest in using ecosystems on Earth as model systems for life detection in the past or even present Mars.

By studying the germination characteristics of spores, we can inherently determine the boundary conditions for survival and the longevity of life. We have applied the 1st Rapid BSVA to detect and enumerate spores, the most resilient form of life on Earth, under different extreme conditions, such as the Atacama Desert, Greenland ice cores and Antarctica Lake Vida[26-29]. One limitation is, however, the inability to study in situ spore properties in their native environments. The new portable Rapid BSVA prototype will enable field analysis on extreme environments on Earth and potential future missions looking for trace number of spores on the surface or subsurface of Mars and Europa.

Task 5 - Study spore injury mechanism using high-throughput Rapid BSVA instrument

Spore injury is a temporary damage to spores when they are exposed to physical or chemical treatment[30]. Spore repair is a process by which injured spores revert to their

original state. When placed in growth media incubated at the optimal temperature, untreated spores usually germinate very rapidly, a process to be completed within 30 min. On the other hand, injured spores invariably require longer periods for repair, and for this reason it is prudent to prolong the incubation time well beyond the usual period. This imposes a time constraint to the 1st generation Rapid BSVA because samples are processed serially. Deployment of the 2nd generation device enables high-throughput parallel processing and thus expedites the germination analysis of a large number of samples. Studies on the injury and repair of spore germination system will shed light on the assessment of sterility, which must take into account conditions for repair of injured, but still viable and potentially harmful, bacterial spores[31].

The expression of injury may take many forms but previous research has primarily focused on the loss of ability to form colonies. We have tested the feasibility of measuring the release of DPA as a probe for spore inactivation. The survival curves of various *Bacillus* spores subjected to wet heat, UV and vaporized hydrogen peroxide treatment has been reported in Chapters 5, 6 and by other people[32,33]. On the basis of these observations, we are going to optimize the recovery growth and germination media, determine the repair time and study the differences in the decimal reduction times (D values). We will develop a quantitative model that describes the effect of these inactivating agents on germinability and culturability.

10.1.5 Expected results

Once I have built the automated and high-throughput Rapid BSVA instrument (task 1), I expect to obtain results in the areas of biodefense (task 2), surface hygiene (task 3), spore survival in extreme environments (task 4) and in delineating mechanisms of spore inactivation (task 5). Specifically, I will build and design a miniaturized integrated imaging system described in the previous section capable of analyzing 300 samples/hour with single spore resolution and full automation under a LabVIEW interface. The instrument will firstly be applied in a series of validation tests using different sterilization agents. Spore biological indicator module will be constructed for high-throughput processing. In particular, the instrument will be used to assess the decontamination efficiency of ethylene oxide in a post-anthrax attack cleanup. Second, the instrument will be used to collect data on bioburden measurements on flight hardware surfaces and spacecraft assembly facilities. As outlined in the milestone, this portable 2nd Rapid BSVA unit will also be used to measure *in situ* spore germination characteristics in different extreme environments. The effect of spore injury and repair mechanisms on germination will be investigated and will be useful in understanding the actual effectiveness of different inactivation regimens.

10.1.6 Significance and application

The proposed 2nd generation Rapid BSVA has deliverables synergistic with the goals of NASA research on astrobiology, planetary protection and biodefense. NASA is committed to protecting solar system bodies from contamination by Earth life and to avoid contamination that would obscure the credibility of life detection missions. Stringent standards are imposed in assessing the degree of microbiological contamination of spacecraft hardware and assembly facilities, broadly known as planetary protection. Currently, the major methodology is the counting of viable colony-forming units on various defined media after 3 days, a time frame not in concert with the rigid schedule of spacecraft assembly. Rapid BSVA obviates the need of cultivation by enumerating spores based on germination events, a process that takes 30 minutes to complete. Preliminary results have demonstrated that Rapid BSVA yielded comparable yet more rapid assessment of clean room bioburden than cultivation techniques. The second generation will enable on-site and near real-time measurement.

Rapid BSVA, coupled with the 96-well biological indicator modules, provides a quick and convenient solution to validate various sterilization methods, such as heat, UV, vaporized hydrogen peroxide and ethylene oxide. It can be used in hospitals to ensure utensils are devoid of spores. It is useful in validating the efficiency of post-anthrax attack decontamination. The Rapid BSVA device can also be

incorporated into rovers to be sent to other planets. The assay is fully automated and reagent-free to provide an easy platform to investigate earth-borne spore germination characteristics under outer space conditions.

Spore germination is a process whereby spores change from dormancy to a metabolically active state. The process of spore germination involves a rapid sequence of degradative events. It is through germination and subsequent outgrowth that spores cause food spoilage and toxin formation, which may ultimately give rise to food-borne disease and bioterrorist attack[34]. Furthermore, since resistance properties of spores are concomitantly lost, the mechanism of germination may hold clues to more efficient methods for spore inactivation. Therefore, apart from being scientifically interesting, the process of spore germination is of great importance from the application aspect.

By applying time-resolved luminescence microscopy on bacterial spores, we are able to study spore germination and perform rapid enumeration from a different perspective from the current cultivation methods. We have demonstrated the ability to enumerate single spores within 30 minutes using both lab and environmental strains. Rapid BSVA is a powerful tool for basic science research, environmental microbiology and astrobiology. In particular, it elucidates the behavior of viable endospores because one has the ability to work with smaller sample volumes, shorter

analysis times with higher throughput. Miniaturization and portability has direct relevance to bacterial spore detection in food hygiene and sterility control, as well as great implications in life detection missions. The work proposed here opens up new avenues for exploring the rich biology of bacterial spores and gleans us important information on the longevity of life.

10.2 Development of a Rapid Endospore Detector

This proposal describes the development of a microfluidic device for the rapid detection of viable bacterial endospores by time-gated fluorescence and bioluminescence spectroscopy. Endospores are detected based on a series of unique physiological changes during germination, exemplified by dipicolinic acid release, ATP synthesis, protein degradation and membrane stainability. Total endospore population is determined by monitoring dipicolinic acid release upon electroporation. Sample handling, processing and analyses are all incorporated into a microfluidic circuit to offer the ability to work with smaller reagent volumes, shorter reaction times, and the possibility of parallel operations. Here we propose integrating an entire suite of bacterial endospore detection regimen onto a single chip, which will be deployed and field tested under various extreme environments, such as desert, ice cores and permafrost. The effects of germinants and temperature on viable spore germination

can be studied with full automation and high throughput in less than one hour on the field that closely mimic *in vivo* environment of endospores by coupling spectroscopy with microfluidics.

10.2.1 Statement of problem

Endospore formation is a very successful survival and dispersal strategy. Endospores are found in nearly every conceivable natural habitat on Earth and persist for long times due to their resistance. Therefore, endospores have long been fascinating subjects of investigation for a number of important applications, from sterilization validation, biodefense to astrobiology. Detection of low levels of dormant endospores under various extreme environments presents great challenges to researchers. The current microbiological gold standard is to culture endospores on agar plate, which is lengthy and labor intensive. A limitation of cultivation is the inability to correlate results to *in vivo* endospore behavior because of the difficulty to implement lots of culturing work on the field. This limits the ability to accurately understand endospore dormancy, viability and germination occurring *in vivo*. Here we propose a rapid, automated and handheld device to determine endospore viability from different perspectives, namely germination propensity, metabolic activity, protein degradation and membrane integrity. The lab-on-a-chip design enables portability and on-field

analysis to probe the *in situ* viability state of endospores in their native environments, providing us valuable information in homeland security, food industry and the search for extraterrestrial life.

10.2.2 Background

Bacterial spores, or endospores, are highly specialized structures formed primarily from *Bacillus* and *Clostridium* genera that are designed for the survival of adverse conditions. Spores are metabolically dormant and can withstand harsh physical environments, including ultraviolet (UV) and gamma radiations, extreme (high and low) atmospheric and hydrostatic pressures and desiccation. The remarkable resistance of bacterial spores is highlighted with the examples of spores surviving space travel and multi-million-year spore longevity. The current record for longevity is claimed by isolate 2-9-3, a salt-tolerant organism related to *Bacillus marismortui*, viable spores of which have been isolated from a primary salt crystal 250 million years old. The routine monitoring of bacterial spores is of great interest because some of them may cause food poisoning, diseases, and perhaps more importantly can constitute deadly agents of biowarfare and bioterrorism. Among the numerous biowarfare agents, *B. anthracis*, a spore-forming bacterium causing anthrax, is of the greatest concern. Especially after the anthrax attack in 2001, the rapid detection of

bacteria spores including *B. anthracis* has been a focus area. Bacterial spores are a major nuisance in the food industry, being omnipresent, thus occurring frequently in food ingredients and raw materials. Their high resistance enables survival of food processing treatments designed to inactivate bacteria.

Spore germination is a process whereby spores change from dormancy to a metabolically active state. It can be induced by nutrients or a variety of non-nutrient agents. Nutrient germinants bind to receptors in the spore's inner membrane and this interaction triggers the release of the spore core's huge depot of dipicolinic acid (DPA) and cations, and replacement of these components by water. The spore becomes partially stainable due to degradation of the spore coat and membrane, known as germination stage I. Stage II is marked by the onset of metabolism and macromolecular biosynthesis, giving rise to the production of ATP. Further water influx hydrolyzes and expands the cortex. Germinated spore are fully stainable and there is rapid protein degradation and in the first minutes of spore germination.

Germination process is specific to endospores. And the chemicals associated with germination, dipicolinic acid (DPA) is unique chemical marker found only in endospores[35]. Hence, being able to track germination are synonymous as detecting viable endospores. Toward this end, an endospore viability assay has been developed to quantify the number of total and germinable endospores[13,16,29], where the ability to

germinate serves as an indicator for viability. It determines the total spore population *via* DPA release by spore lysis. Consequently, the proportion of DPA released during germination with respect to the DPA content of the whole spore population provides a measure of the percentage of spores capable of germination. The process of endospore germination can be initiated on the timescale of minutes by the addition of trigger molecules such as L-alanine, L-asparagine, or glucose[34-38]. The firefly luciferin-luciferase assay is used to monitor ATP increase during germination, SYPRO Rose Plus staining is used to track protein degradation during germination and acridine orange is used to monitor stainability upon germination.

To achieve the goal of investigating endospore viability in extreme environments, there are three major tasks in this proposal:

(1) Miniaturize development of an endospore viability assay based on DPA detection;

(2) development of field instrumentation for deployment in extreme environments;

(3) optimize methods of viability assessment of endospores.

The entire suite of endospore detection, namely sample processing, treatment and analyses, are all embedded into a microfluidic platform so that it is portable and can be deployed as a field instrument in extreme environments. Different

spectroscopic techniques are adopted to miniaturize different excitation sources and detectors onto the microfluidic platform. In addition to this, the lab-on-a-chip design enables automated and high-throughput parallel processing of samples. A variety of germinants and temperatures will be tested for optimal germination based on DPA, ATP, membrane integrity and protein degradation, in an effort to characterize *in situ* response of endospores to germination stimuli and consequently a better picture of spore survival in extreme environments.

10.2.3 General methodology

We will design and build a microchannel network to perform on-chip endospore preparation and luminescence detection. Upon germination, characteristic changes associated with DPA, ATP, protein and spore membrane are monitored spectroscopically to determine endospore viability.

Figure 10.6 shows a schematic and time table of the device. An endospore suspension is injected into a heat shock chamber by a syringe pump. The sample will be heat treated at 80℃ for 15 minutes to screen for spores by inactivating the vegetative cells. Some of the heat shocked samples will be directed to the detector chip to establish a baseline for subsequent measurements. The rest of the samples enter either the electroporation chamber for endospore lysis by the pulsed electric

fields, or the germination chip for a 30 min incubation under customizable germinants and temperatures. Lyzed endospore suspension is analyzed at the detector chip to determine the total endospore population based on DPA release. During the 30 min incubation period, 4 timecourse samples will be analyzed to track the physiological changes as a function of germination. Terbium-DPA luminescence assay, firefly luciferin-luciferase bioluminescence assay, SYPRO Rose Plus staining and *BacLight* live/dead viability assay will be employed in the detector chip to study germination of endospores, with details as shown below.

(1) Sample handling, transport, thermal control

(2) Electroporation

(3) Excitation & Emission

(4) Tb-DPA luminescence assay

(5) Firefly luciferin-luciferase bioluminescence assay

(6) SYPRO Rose Plus staining

(7) *BacLight* live/dead viability staining

(1) Fabrication, sample handling and thermal control

Chip layout made by AutoCAD is written onto a glass mask for UV photolithography, through which a mask is further prepared in gold by elelctroplating for synchrotron

radiation lithography. Glass wafer is used as the substrate of a synchrotron radiation-cured polymer mold for replication of the channel pattern to PDMS. Channels are washed sequentially using methanol, water, 1 M NaOH, 0.1 M HCl, 0.1 M NaOH and water. Between runs, channels are rinsed in order with 0.1 M NaOH, water and 20 mM PBS buffer (pH 7.8) to ensure reproducibility. Gated injection mode will be employed for injections and pumping will be provided by peristaltic pumps. Commercial heaters and thermocouples will be manually applied to the back side of the glass chip to control temperature of the heat shock and germination chambers. We will look into the possibility of building microfabricated heaters and detectors within the chambers if more precise temperature control is needed.

(2) Electroporation

Electroporation is a significant increase in the electrical conductivity and permeability of the cell plasma membrane caused by an externally applied electric field. Hamilton and Sale discovered that the application of high electric field pulses at typical field strengths of 10 kV cm^{-1} also affects the viability of bacterial cells[39,40]. We hypothesize that spore coat will be pored or ruptured at high pulsed electrical fields (20-80 kV cm^{-1}). Damage to be spore coat causes inactivation and release of DPA. We hypothesize that method is effective in releasing all the DPA in an endospore population. Therefore, we can determine the total number of spores as a baseline for

assessing viability ratio.

A micro-electroporation flow-through unit can readily be implemented in a microfluidic chip by placing electrodes at the bottom of microchannels perpendicular to the fluid flow. The electrode structure consists of interdigitated gold electrodes with a saw tooth structure to enhance the electric field structure gradient. The microdevice can be operated at more advantageous conditions than conventional systems: small voltages and power consumptions, continuous flow, small sample volume, and negligible heating. By shrinking the inter-electrode distance to a few tens of microns, it is possible to reduce the voltage requirement to a few volts (three orders of magnitude smaller than typical voltages required in a macroscopic apparatus). Consequently, the power consumption becomes six orders of magnitude smaller and heat generation is minimal. A micro-electroporation device will be designed to lyze endospores to determine the total DPA present. The electroporation unit can easily be integrated with other microfluidic devices.

(3) Excitation and Emission

A 4-LED array provides excitation light at selectable wavelengths (280 nm, 320 nm, 470 nm, 530 nm) with half bandwidths lying between 12 and 36 nm. These 4 wavelengths are suitable for exciting DPA, SYPRO Rose Plus, SYTO-9 and propidium iodide, respectively. A microcontroller (BASIC Stamp II, Parallax, Rocklin,

CA) receives commands sent from the host PC through the COM port, then interprets the commands and controls a specific LED to turn on or turn off via MOSFET logic switches. Only one LED that provides maximum emission light is turned on. The LED array will be placed close to the microchannel (at a distance of <1 mm). This simple arrangement and ready coupling to a receiver fiber without additional optics makes for a very rugged and robust fluorescence detector with excellent sensitivity and little need for monochromators to reject the excitation light from the emitted light. A CCD spectrometer detector will provide a fluorescence spectrum for terbium, SYPRO Rose Plus, SYTO-9 and propidium iodide detection. Time-gated circuit will be developed for the fluorescence output of terbium and europium. The LEDs with be coupled to the LabVIEW program that controls the detectors. For ATP measurement, a miniature photomultiplier tube powered with a voltage of -950 V will be mounted to the microfluidic channel. Bioluminescence light is collected by a 20x objective. No filter is used in the optical path. A JFET operational amplifier is used to further amplify and offset the signal and filter the high-frequency noise of the signal from PMT. The PMT current is converted and amplified into a voltage by a picoamperiometer.

(4) Tb-DPA luminescence assay

There is a universal constitute of bacterial spores: dipicolinic acid (DPA). DPA

constitutes %5-15% of the total mass of the spores. Detection of DPA based on the terbium enhanced fluorescence provides a promising low-cost detection method for bacterial spores. DPA can be easily extracted from the spores by treatment with low concentrations of surfactants such as dodecylamine. The dipicolinate ion rapidly chelates various rare earth metals. In particular, the weak native fluorescence of terbium (Tb) ($\lambda_{ex,max}$ = 271, 279 nm) is enhanced more than 20,000 times upon complexation with DPA. In addition, the already long fluorescence lifetime of Tb (III) is further extended upon complexation ($Tb(DPA)_n^{3-2n}$, n = 1-3 τ = 0.6 – 2.0 ms). This permits a time-gated fluorescence detection method, which greatly enhances sensitivity and also improves selectivity over common fluorescent compounds that exhibit much shorter fluorescence lifetimes in the ns range. The signals from scattered lights and short-lived fluorescence from common interferences are excluded.

Without the gated approach, the weak signal of interested is always buried in the signals from scattered lights and short-lived fluorescence. Similar to the scenario when we attempt to see stars in daylight; it is nearly impossible to discriminate between the lights from stars and the light from the sun. Gated detection is like the same observation conducted at night. Without the strong background, the weak signals can readily be observed. This points the way toward an exceptionally sensitive way of fluorescence detection.

(5) Firefly luciferin-luciferase bioluminescence assay

Adenosine 5'triphosphate (ATP) is the primary source of chemical energy and a ubiquitous energy currency in all living organisms. The use of a firefly (*Photuris pyralis*) enzyme to quantify ATP in biological systems was first proposed by McElroy in the 1940s[41,42]. The detection is based on the conversion of chemical energy to light energy during the breakdown of ATP. Firefly luciferase catalyzes the ATP-dependent oxidative decarboxylation of luciferin in the presence of oxygen and magnesium ions into AMP and light. One photon of light is produced per molecule of ATP hydrolyzed when ATP is the limiting component in the reaction[43]. Measurement of ATP is a direct indication of cellular metabolism and is often reckoned as a metric for viability[44,45]. To detect ATP in endospores, first of all, non-microbial ATP is eliminated from the sample using somatic cell releasing agent (Figure 10.7). Bacterial cells are then disrupted using chemicals such as benzalkonium chloride. The ATP released is quantified using the luciferin-luciferase reaction. Hattori *et al.* have achieved a detection limit of 7.7 cfu mL^{-1} using vegetative cells of *Bacillus subtilis*[46]. Promega Corporation also reported a detection limit of 10 cfu mL^{-1} of vegetative *Bacillus cereus*.

Challenges are encountered in the detection of spores using the luciferin/luciferase system. While a vegetative bacterium contains approximately 10^{-17}

mole of ATP per cell[47], dormant spores of a number of *Bacillus* species have no detectable biosynthetic or metabolic activity and contain low levels of ATP[48-50]. Kodaka *et al.* reported that a spore contains about 10^{-21} mole ATP per cell, 4 orders of magnitude lower than that of a vegetative bacterium[51]. Nevertheless, within the first minute of germination, the large depot of 3-phosphoglyceric acid is catabolized into ATP[52]. In additional to this, coat porosity increases after the onset of germination, which permits easy extraction of intracellular ATP[53].

(6) SYPRO Rose Plus staining

There is rapid protein degradation of dormant spore protein in the first minutes of spore germination. 15%-20% of the dormant spore protein is degraded within 20 min of the onset of germination. In *Bacillus*, the degradation products are free amino acids, at least 17 of which are generated. The spore proteins degraded in this early process are a group of up to eight low-molecular weight (6000-11000), acid-soluble proteins located in the spore core.

SYPRO Rose Plus is a europium dye that has a high affinity with proteins. Proteins stained with SYPRO Rose Plus dye have a broad excitation peak at ~350 nm and a luminescence emission maximum at ~610 nm. Europium, another lanthanide element, has a long luminescence emission lifetime, which allows time-resolved measurements that greatly minimize interference from background fluorescence.

Initially, the non-porous spore coat will prevent proteins from binding to the dye. As spore is germinating, its coat is becoming more porous and thus the dye can have access to the proteins inside. The spore proteins are, however, under rapid degradation at the same time and therefore a subsequent decrease in fluorescence intensity will be expected. This characteristic initial increase following by a decrease in fluorescence intensity is a good indication of germination.

(7) BacLight live/dead viability staining

Owing to their tough protein coats made of peptidoglycan and keratin, endospores are highly resistant to normal staining procedures. During germination, spore coat becomes more porous and hence the endospore becomes stainable by conventional DNA-intercalating dyes. Both SYTO-9 and propidium iodide have high affinity towards nucleic acid. SYTO-9 binds all types of cells whereas propidium iodide is only permeable to compromised cell membrane, i.e., dead cells. The ratio of green and red emission provides information on the viability of germinating spores. Integrated fluorescence emission intensities of the green (510-540 nm) and red (620-650 nm) are acquired and the green/red fluorescence ratio is calculated for the viability ratio.

10.2.4 Expected results

Coupling spectroscopy and microfluidics is a powerful tool for elucidating the behavior of viable endospores because one has the ability to work with smaller reagent volumes, shorter reaction times, and greater sensitivity with high throughput. The use of light-emitting diodes, advances in miniaturization and spectrometer design has direct relevance to bacterial spore detection in food hygiene and sterility control, as well as great implications in life detection missions.

The current detection limit for DPA using Tb-DPA luminescence assay in quartz cuvettes with a fluorimeter is 1000 spores mL^{-1}. Since the typical size of an elastomer microfluidic channel is on the order of 50-250 μm wide by 10-20 μm deep, the absorption path length is quite small compared to more conventional cuvette-based absorption spectrometers with interaction lengths 100-1000 times larger. According to the Beer-Lambert Law, the absorbance A is proportional to the concentration of the absorbing material c and the absorption path length l, so that

$$A = \varepsilon c l,$$

where ε is the molar absorptivity. Coupled with time gating, we expect to at least improve the limit of detection down by 2 orders of magnitude down to 10 spores mL^{-1}. Similarly, detection of extracellular proteins using SYPRO Rose Plus can take advantage of time gating and microfluidics architecture to improve the current detection limit. ATP bioluminescence and live/dead viability staining also benefit

from the microfluidics platform by the same token. It can be validated using endospores of *Bacillus atrophaeus* with direct on-chip lysis and germination. The dynamic range is expected to be over 6 orders of magnitude for ATP, with a detection limit down to 100 cells mL^{-1}.

A major hurdle for in situ investigations of biomarkers is the availability of robust and flexible sample-handling systems. Most measurements for biosignatures require that the sample be pretreated in some fashion. Our device also enables *in situ* measurement of endospore germination in the field. In particular, the device can be augmented with air or water samplers for automated sampling and downstream processing and analysis. A wide range of flexibility is associated with this device. The analysis component is customizable and readily amenable to detecting other types of bacteria. It can, in the near future, be incorporated as part of the life detection missions.

Most of the electroporation microdevice research performed so far has focused on analyzing and understanding the electroporation process itself. Integrating electroporation and subsequent analysis of the cell content is still at its early stage of development. This proposal will provide insight on the progressive integration of electroporation, separation and analysis of bacterial cells in the near future and is expected to add further value to the concept of the microfluidic chip.

Electroporation has started to be used in the food processing industry for the pasteurization of liquid foods. The idea is to use pulsed electric field to cause irreversible poration of bacteria and thus rendering them inactive. Reports can be found on electroporation of mammalian and vegetative bacterial cells, but not much on endospores. A side study of this proposal will focus on developing a model on endospore electroporation. It will shed light on assessing and predicting sterilization efficiency of electroporation.

10.2.5 Conclusion

Spore germination is a process whereby spores change from dormancy to a metabolically active state. The process of spore germination involves a rapid sequence of events in which the structure of the spore is degraded. It is through germination and subsequent outgrowth that spores cause food spoilage and potential toxin formation, which may ultimately lead to foodborne disease. Furthermore, because resistance properties of spores are concomitantly lost, the mechanism of germination may hold clues to more efficient methods for spore inactivation. Therefore, apart from being scientifically interesting, the process of spore germination is of great importance from an applied perspective.

We have presented applications of time-resolved fluorescence imaging to study

bioluminescence and mixing within microfluidic devices. We have demonstrated the potential to implement these techniques in conventional wide-field imaging systems. This coupled with the flexibility of soft lithography. Here, we have described one such geometry, which satisfies some of the requirements of an integrated measurement system, in which intelligent analysis of microscopic fluid volumes can be undertaken. We believe that this approach, when optimized sensor arrays are used, can offer similar performance to commercially available spectrophotometers with the opportunity of optically monitoring many fluidic channels at the same time. It shows promise toward the definition of a spectroscopic laboratory on a chip in which either absorption or fluorescence can be measured.

10.3 References

1. Cohn, F. Untersuchungen uber Bacterien. IV. Beitrage zur Biologie der Bacillen. *Beitr. Biol. Pflanz.* **2**, 249-276 (1876).
2. Koch, R. Untersuchungen uber Bakterien V. Die Atiologie der Milzbrandkrankheit, begrundet auf die Entwicklungsgeschichte des *Bacillus anthracis*. *Beitr. Biol. Pflanz.* **2**, 277-310 (1876).
3. Koch, R. Untersuchungen uber Bakterien VI. Verfahren zur Untersuchung, zum Conservieren und Photographieren. *Beitr. Biol. Pflanz.* **2**, 399-434 (1877).
4. Tyndall, J. Further researches on the department and vital persistence of putrefactive and infective organisms from a a physical point of view. *Phil. Trans. Royal Soc.* **167**, 149-206 (1877).
5. Anonymous. NASA standard procedures for the microbiological examination of space hardware, NHB 5340.1D. *Jet Propulsion Laboratory Communication, National Aeronautics and Space Administration* (1980).
6. Tahernia, A.C. Treatment of anthrax in children. *Archives of disease in childhood* **42**, 181-182 (1967).
7. Powell, J.F. Isolation of dipicolinic acid (pyridine-2-6-dicarboxylic acid) from spores of *Bacillus megaterium*. *Biochem. J.* **54**, 210-211 (1953).
8. Bruch, C.W. Levels of sterility: probabilities of survivors vs. biological indicators. *Bull Parenter Drug Association* (1974).
9. Hindle, A.A., Hall, E. A. H. Dipicolinic acid (DPA) assay revisited and appraised for spore detection. *Analyst* **124**, 1599-1604 (1999).

10. Pellegrino, P.M., Fell, N.F., Rosen, D.L., and Gillespie, J.B. Bacterial endospore detection using terbium dipicolinate photoluminescence in the presence of chemical and biological materials. *Anal. Chem.* **70**, 1755-1760 (1998).
11. Rosen, D.L. Bacterial endospore detection using photoluminescence from terbium dipicolinate. *Reviews in Analytical Chemistry* **18**, 1-21 (1999).
12. Sacks, L.E. Chemical germination of native and cation-exchanged bacterial-spores with trifluoperazine. *Appl. Environ. Microbiol.* **56**, 1185-1187 (1990).
13. Shafaat, H.S. and Ponce, A. Applications of a rapid endospore viability assay for monitoring UV inactivation and characterizing Arctic ice cores. *Appl. Environ. Microbiol.* **72**, 6808-6814 (2006).
14. Cable, M.L., Kirby, J.P., Sorasaenee, K., Gray, H.B., and Ponce, A. Bacterial spore detection by [Tb^{3+}(macrocycle)(dipicolinate)] luminescence. *Journal of the American Chemical Society* **129**, 1474-1475 (2007).
15. Yung, P.T., Lester, E.D., Bearman, G., and Ponce, A. An automated front-end monitor for anthrax surveillance systems based on the rapid detection of airborne endospores. *Biotechnology and Bioengineering* **98**, 864-871 (2007).
16. Yung, P.T., Kempf, M.J., and Ponce, A., presented at the IEEE Aerospace Conference, Big Sky, Montana, 2006 (unpublished).
17. Yung, P.T. and Ponce, A. Rapid sterilization assessment by monitoring inactivation of germinable Bacillus endospores. *Nature Methods (submitted)* (2008).
18. Horrocks Jr., W.D. and Sudnick, D. Lanthanide ion luminescence probes of the structure of biological macromolecules. *Accounts of Chemical Research* **14**, 384-392 (1981).
19. Sinha, S., *Systematics and the Properties of the Lanthanides*. (NATO ASI Series 109, 1983).
20. Balzani, V. Supramolecular photochemistry. *Pure Appl. Chem.* **62**, 1099-1102 (1990).
21. Sabbatini, N., Guardigli, M., and Lehn, J.M. Luminescent lanthanide complexes as photochemical supramolecular devices. *Coord. Chem. Rev.* **123**, 201-228 (1993).
22. Lakowicz, J.R., *Principles of Fluorescence Spectroscopy*. (Plenum, New York, 1983).
23. Hashimoto, T., Frieben, W.R., and Conti, S.F. Germination of single bacterial spores. *Journal of Bacteriology* **98**, 1011-1020 (1969).
24. Hashimoto, T., Frieben, W.R., and Conti, S.F. Microgermination of *Bacillus cereus* spores. *Journal of Bacteriology* **100**, 1385-1392 (1969).
25. Margulis, L. *et al*. The Viking mission: Implications for life on Mars. *Journal of Molecular Evolution* **14**, 223-232 (1979).
26. McKay, C.P. *et al*. Temperature and moisture conditions for life in the extreme arid region of the Atacama Desert: Four years of observations including the El Nino of 1997-1998. *Astrobiology* **3**, 393-406 (2003).
27. Doran, P.T. Formation and character of an ancient 19-m ice cover and underlying trapped brine in an "ice-sealed" east Antarctic lake. *Proceedings of the National Academy of Sciences of the United States of America* **100**, 26 (2003).
28. Navarro-Gonzalez, R. *et al*. Mars-like soils in the Atacama Desert, Chile, and the dry limit of microbial life. *Science* **302**, 1018-1021 (2003).
29. Yung, P.T., Shafaat, H.S., Connon, S.A., and Ponce, A. Quantification of viable endospores from a Greenland ice core. *FEMS Microbiology Ecology* **59**, 300-306 (2007).
30. Foegeding, P. and Busta, F. Bacterial spore injury - an update. *Journal of Food Protection* **44** (1981).
31. Hideharu, S. Importance of considering injured microorganisms in sterilization validation. *Biocontrol Science* **11** (2003).
32. Setlow, P., in *Bacterial Stress Response*, edited by G. Storz, Hengge-Aronis, R. (ASM Press, Washington, D.C., 2000), pp. 217-230.
33. Rogers, J.V. *et al*. Decontamination assessment of *Bacillus anthracis*, *Bacillus subtilis*, and *Geobacillus stearothermophilus* spores on indoor surfaces using a hydrogen peroxide gas generator. *Journal of Applied Microbiology* **99**, 739-748 (2005).
34. Setlow, P. Spore germination. *Current Opinion in Microbiology* **6**, 550-556 (2003).
35. Gould, G.W. and Hurst, A., *The Bacterial Spore*. (Academic Press, New York, 1969).

36. Hills, G.M. Chemical factors in the germination of spore-bearing aerobes - the effects of amino acids on the germination of *Bacillus anthracis*, with some observations on the relation of optical form to biological activity. *Biochemical Journal* **45**, 363-370 (1949).
37. Hills, G.M. Chemical factors in the germination of spore-bearing aerobes - the effect of yeast extract on the germination of *Bacillus anthracis* and its replacement by adenosine. *Biochemical Journal* **45**, 353-362 (1949).
38. Hills, G.M. Chemical factors in the germination of spore-bearing aerobes - observations on the influence of species, strain and conditions of growth. *Journal of General Microbiology* **4**, 38-47 (1950).
39. Zhang, Q., Barbosa-Cánovas, G.V., and Swanson, B.G. Engineering aspects of pulsed electric field pasteurization. *Journal of Food Engineering* **25**, 261-281 (1995).
40. Castro, A.J., Barbosa-Cánovas, G.V., and Swanson, B.G. Microbial inactivation of foods by pulsed electric fields. *Journal of Food Processing and Preservation* **17**, 47-73 (1993).
41. McElroy, W.D. The energy source for bioluminescence in an isolated system. *PNAS* **33**, 342-345 (1947).
42. McElroy, W.D. Factors influencing the response of the bioluminescent reaction to ATP. *Archives of Biochemistry* **22**, 420 (1949).
43. Karl, D.D.M. Cellular nucleotide measurements and applications in microbial ecology. *Microbiological reviews* **44**, 739-796 (1980).
44. Chappelle, E.W. and Levin, G.V. Use of the firefly bioluminescence reaction for rapid detection and counting of bacteria. *Biochem. Med* **2**, 41-52 (1968).
45. Thore, A.A., Ansehn, S.S., Lundin, A.A., and Bergman, S.S. Detection of bacteriuria by luciferase assay of adenosine triphosphate. *Journal of clinical microbiology* **1**, 1-8 (1975).
46. Hattori, N.N. *et al*. Enhanced microbial biomass assay using mutant luciferase resistant to benzalkonium chloride. *Analytical biochemistry* **319**, 287-295 (2003).
47. Philip, E.S. A review of bioluminescent ATP techniques in rapid microbiology. *Journal of Bioluminescence and Chemiluminescence* **4**, 375-380 (1989).
48. Church, B.D. and Halvorson, H. Intermediate metabolism of aerobic spores: I. Activation of glucose oxidation in spores of *Bacillus cereus* var *terminalis*. *Journal of Bacteriology* **73**, 470-476 (1957).
49. Setlow, P. and Kornberg, A. Biochemical studies of bacterial sporulation and germination. XXII. Energy metabolism in early stages of germination of *Bacillus megaterium* spores. *Journal of Biological Chemistry* **245**, 3637-3644 (1970).
50. Setlow, P. and Kornberg, A. Biochemical studies of bacterial sporulation and germination. XXIII. Nucleotide metabolism during spore germination. *Journal of Biological Chemistry* **245**, 3645-3652 (1970).
51. Kodaka, H., Fukuda, K., Mizuochi, S., and Horigome, K. Adenosine triphosphate content of microorganisms related with food spoilage. *Japanese Journal of Food Microbiology* **13**, 29-34 (1996).
52. Singh, R.P., Setlow, B., and Setlow, P. Levels of small molecules and enzymes in the mother cell compartment and the forespore of sporulating *Bacillus megaterium*. *Journal of Bacteriology* **130**, 1130-1138 (1977).
53. Santo, L.Y. and Doi, R.H. Ultrastructural analysis during germination and outgrowth of *Bacillus subtilis* spores. *Journal of Bacteriology* **120**, 475-481 (1974).

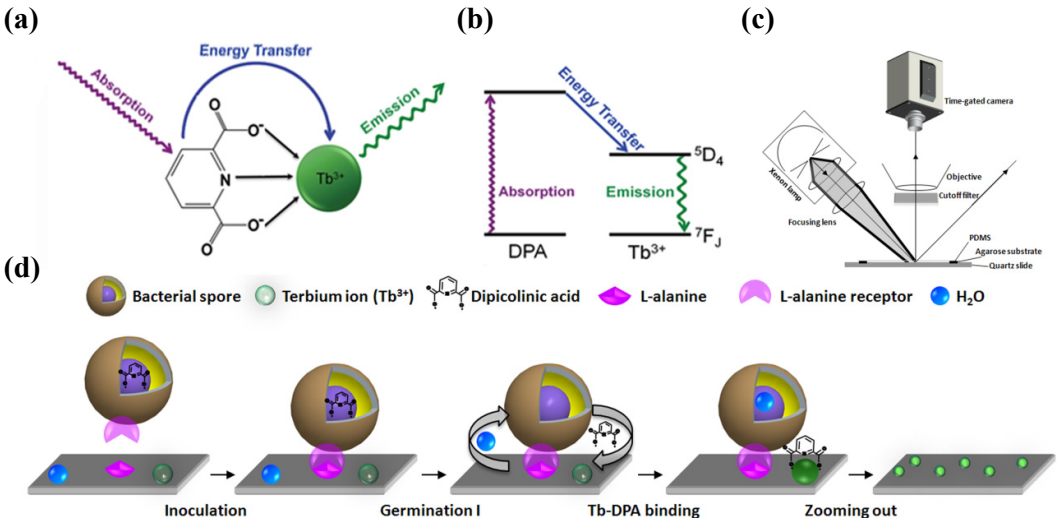

Figure 10.1 | **(a)** Photochemistry of the Tb-DPA assay. DPA acts as a light harvester to transfer UV energy to terbium which exhibit intense green luminescence. **(b)** Jablonski diagram of the photochemistry. **(c)** Experimental setup of the 1st generation Rapid BSVA. The excitation source, xenon flashlamp, was mounted at 45 degrees from the microscope stage. L-alanine and terbium-doped agarose was placed on top of a quartz slide and sandwiched with a piece of PDMS, polydimethylsiloxane. An emission cutoff filter was placed in front of the objective to minimize the excitation light from interferring the results. **(d)** Upon deposition onto the agarose substrate, a spore will be induced to germinate by L-alanine. Water will flux into the spore core and in the same time, Ca-DPA will be displaced out from the spore. DPA released from the spore binds with terbium ions in the agarose to form highly luminescent Tb-DPA complex. This luminescent halo will appear on the proximity of each endospore, enabling the imaging of discrete spots under time-gated microscopy.

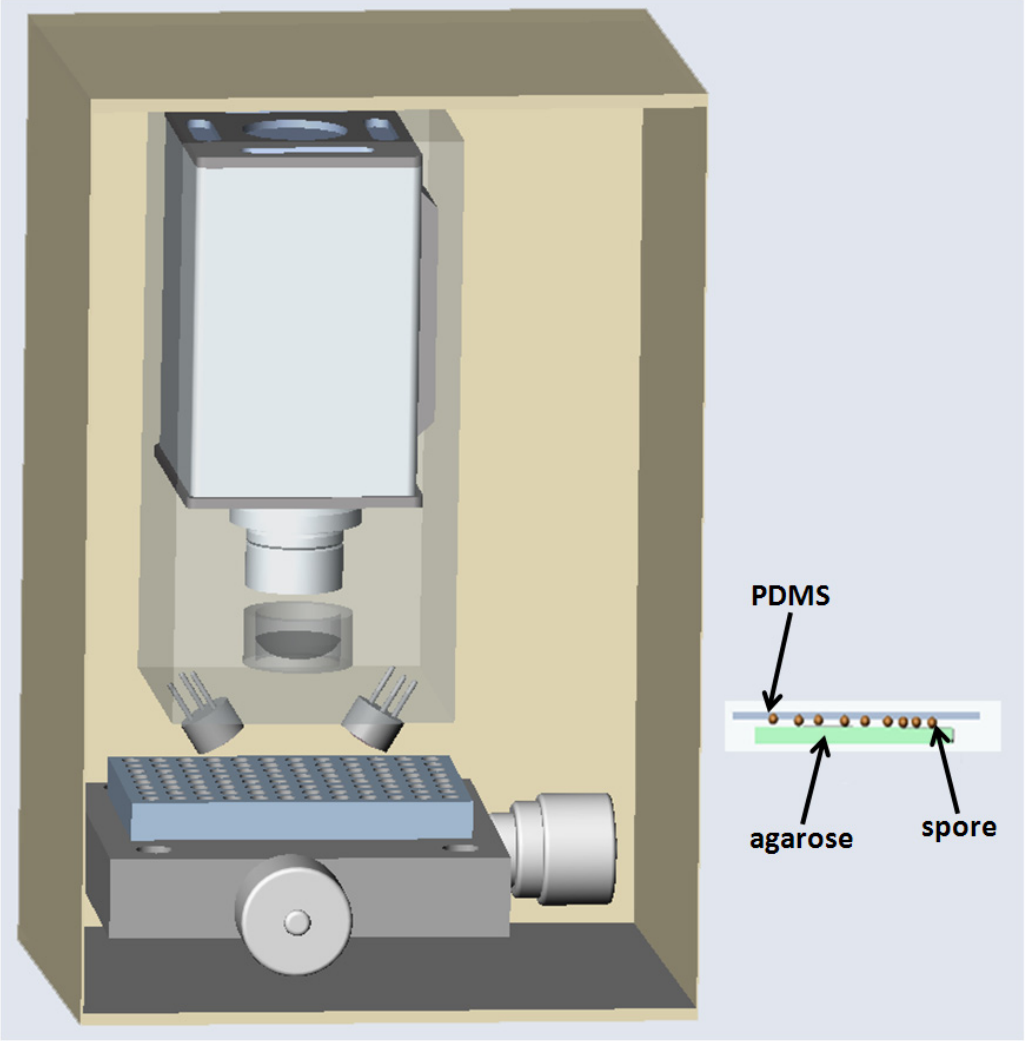

Figure 10.2 | Design of 2nd generation Rapid BSVA.

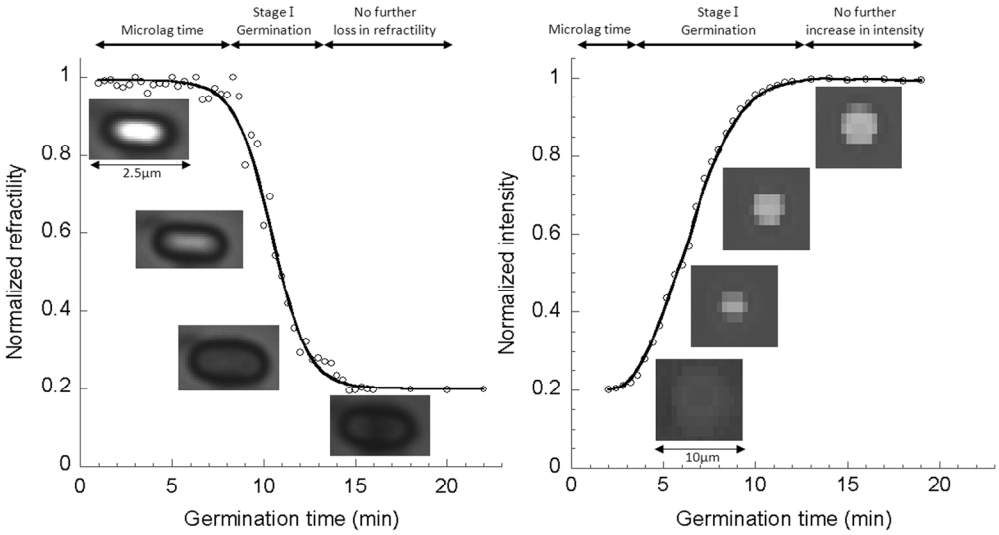

Figure 10.3 | Germination timecourse of a single *B. atrophaeus* spore was monitored by looking at phase darkening as observed under phase contrast microscopy and DPA release under a time-gated microscope.

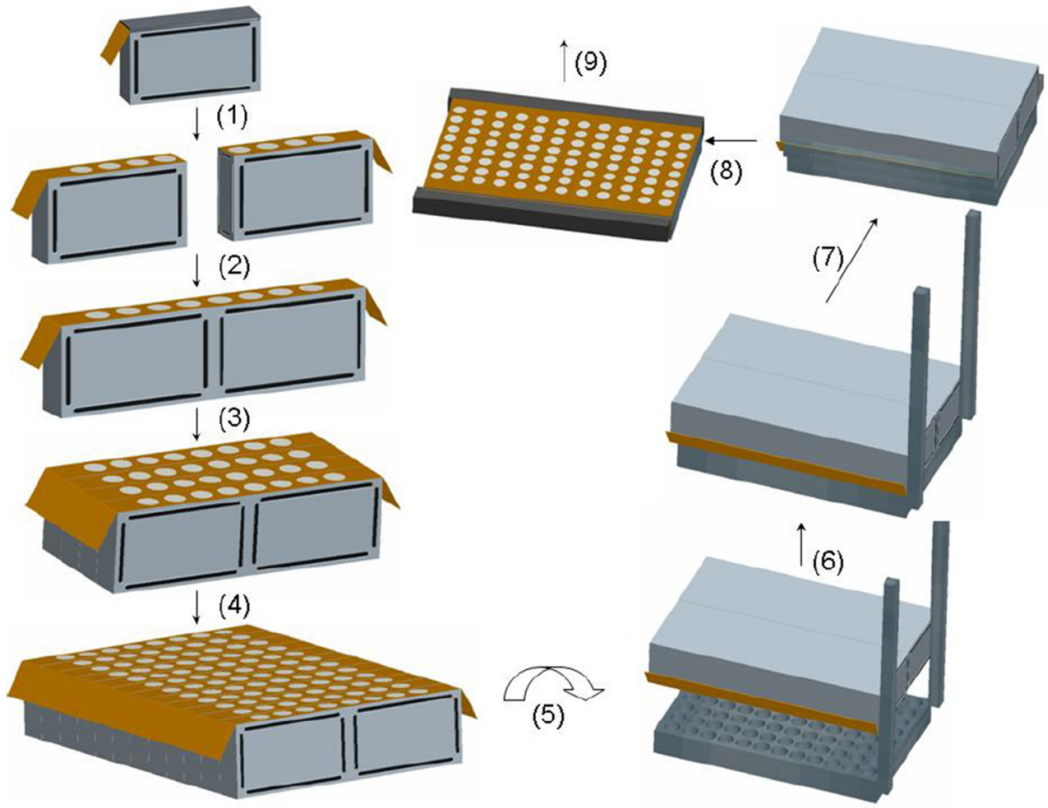

Figure 10.4 | Process for high throughput biological indicator (BI) modules. (1) Remove cover and expose BI module to sterilization regimen, (2-4) assemble modules into 96 array, (5, 6) invert BI array and place onto assay array, (7, 8) lock down levers to attach PDMS spore strips to assay array while removing the BI array, and (9) after 10 minutes of germination perform automated Rapid BSVA analysis.

Figure 10.5 | 96-well filtration unit.

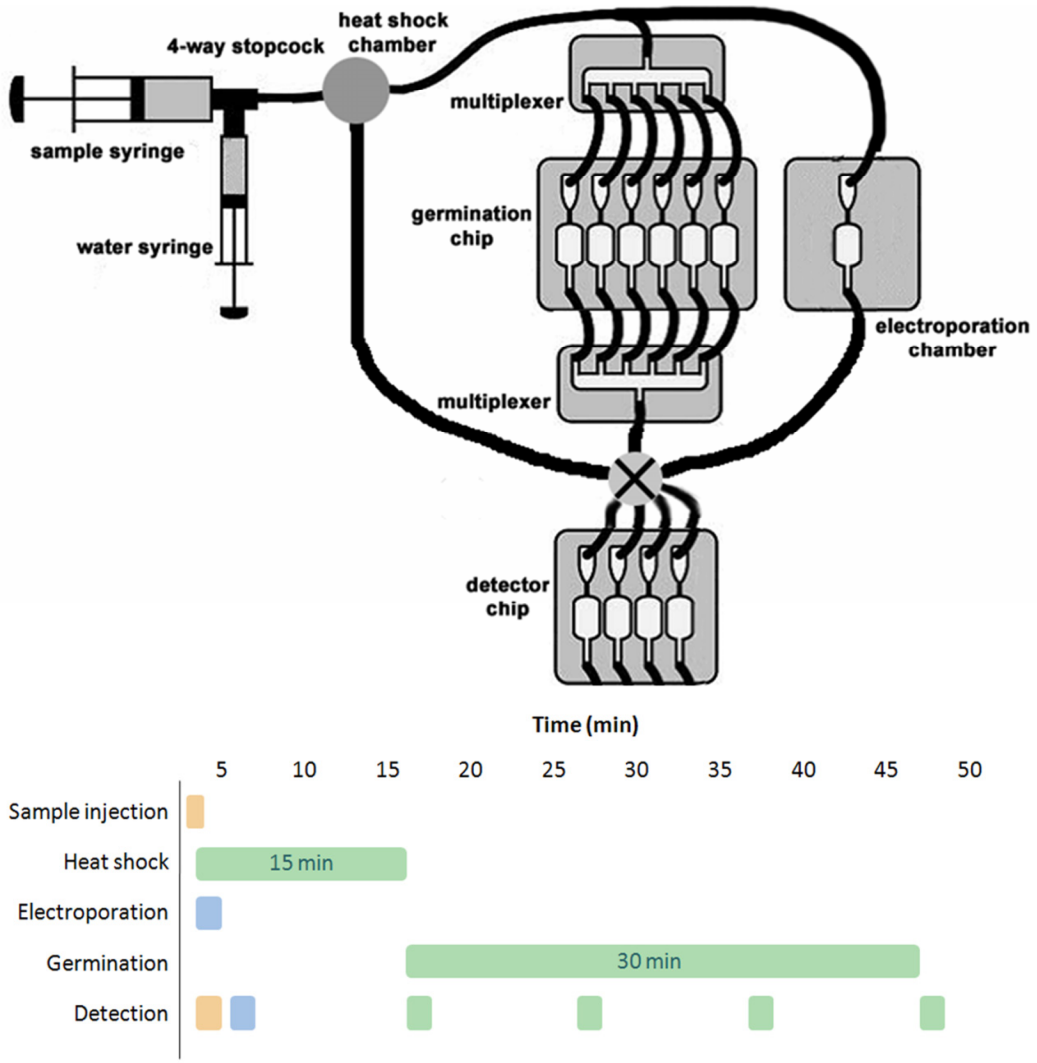

Figure 10.6 | Rapid endospore detector and the time sequence of a standard operation.

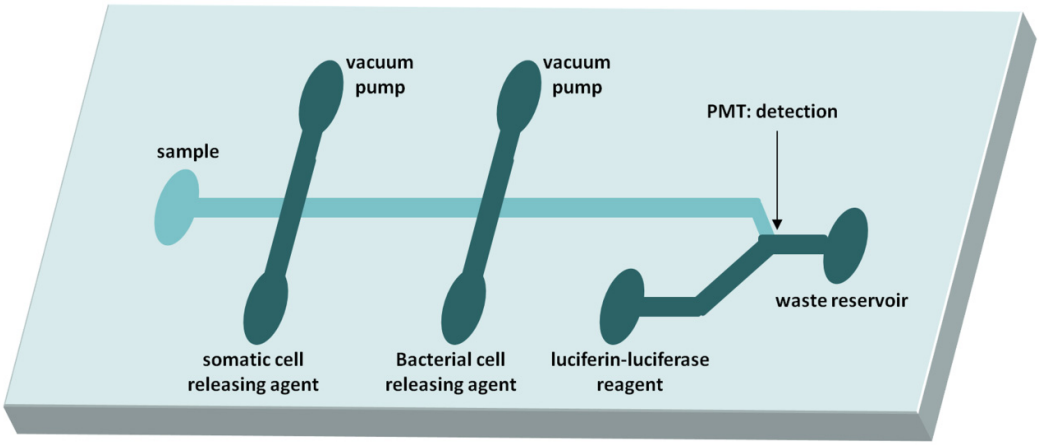

Figure 10.7 | Microfluidic schematic of the ATP luciferin-luciferase assay.